Sh. 69

SAN/1109-8/6

SOLAR PILOT PLANT, PHASE 1
PRELIMINARY DESIGN REPORT

Volume 4. Receiver Subsystem (CDRL Item 2)

May 1, 1977

Work Performed Under Contract No. EY-76-C-03-1109

Honeywell, Incorporated
Energy Resources Center
Minneapolis, Minnesota

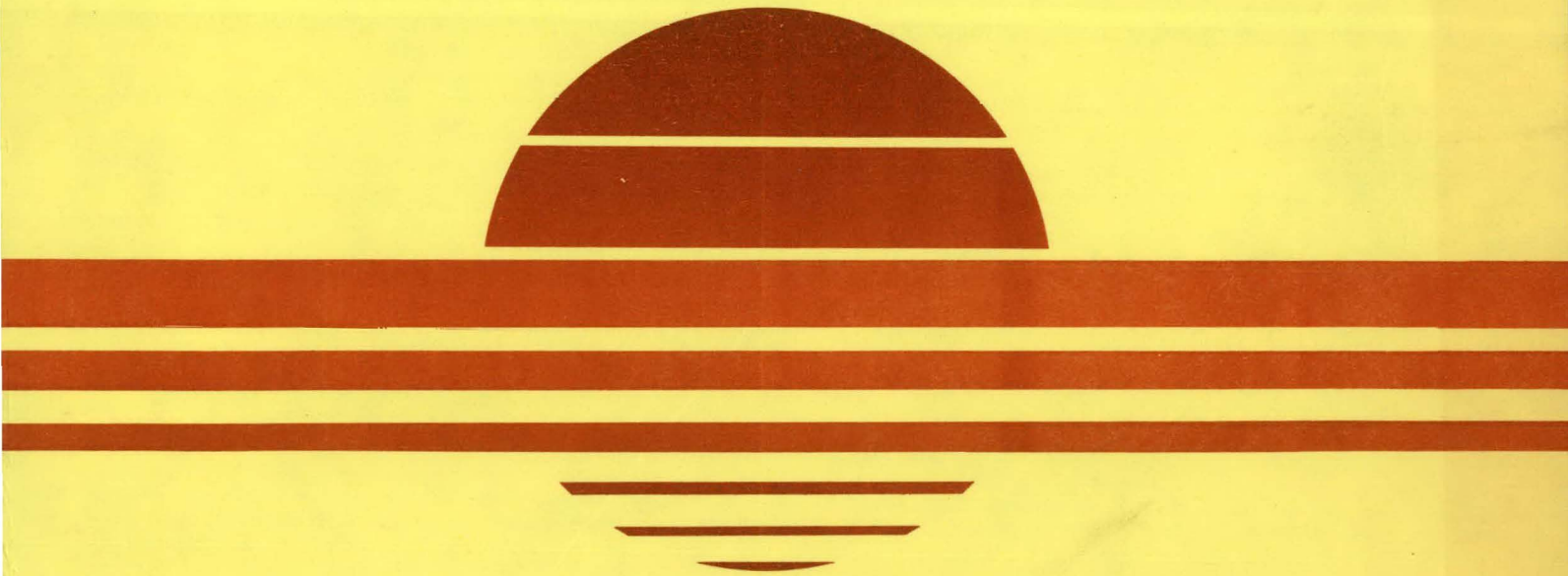

U.S. Department of Energy

Solar Energy

DISCLAIMER

NOTICE

SAN/1109-8/6
Distribution Category UC-59c

Honeywell

ERDA Contract No. E(04-3)-1109

1 May 1977

SOLAR PILOT PLANT
PHASE I

PRELIMINARY DESIGN REPORT

VOLUME IV
RECEIVER SUBSYSTEM

CDRL Item 2

C. J. Bunnell
Contract Administrator

J. C. Powell
Program Manager

Energy Resources Center
2600 RIDGWAY PARKWAY,
MINNEAPOLIS, MINNESOTA 55413

FOREWORD

This is the initial submittal of the Solar Pilot Plant Preliminary Design Report per Contract Data Requirement List Item 2 of ERDA Contract E(04-3)-1109. The report is submitted for review and approval by ERDA. This is Volume IV of seven volumes.

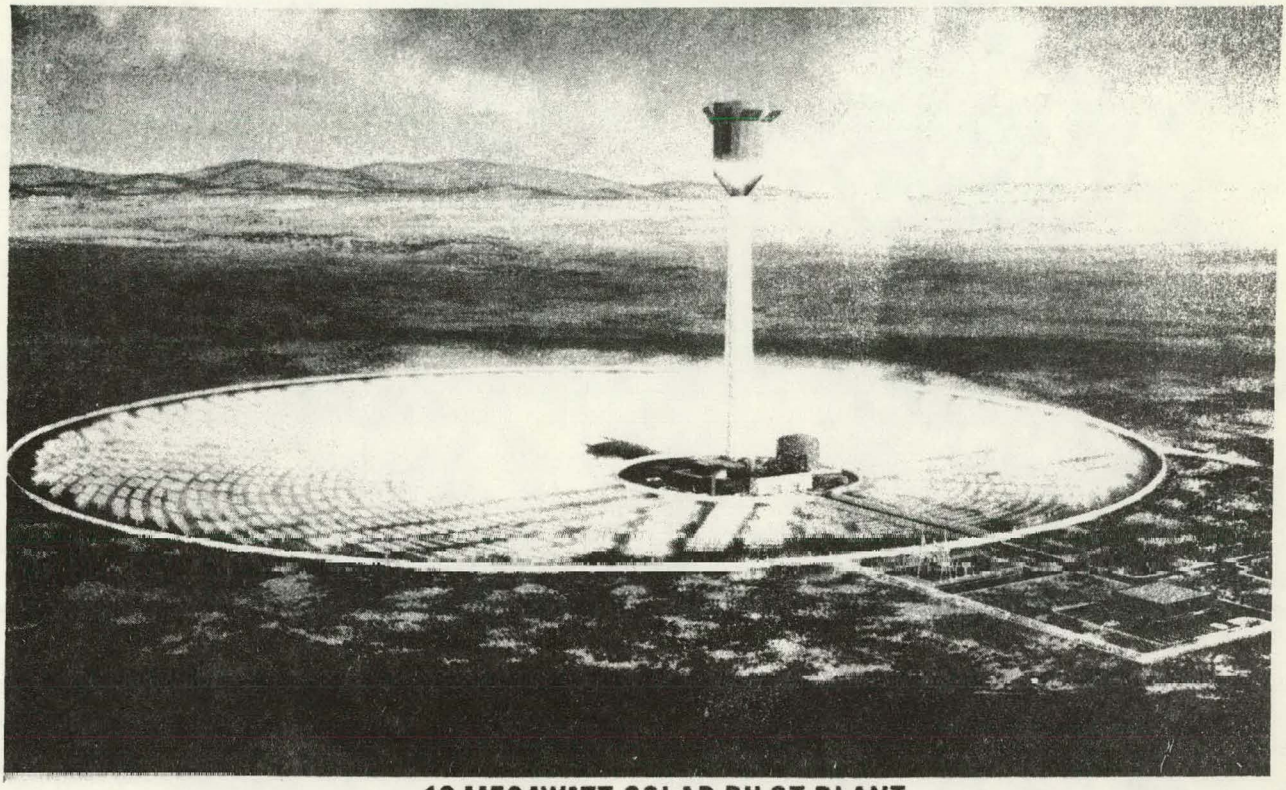

10 MEGAWATT SOLAR PILOT PLANT
ENERGY RESEARCH AND DEVELOPMENT ADMINISTRATION

THIS PAGE

WAS INTENTIONALLY

LEFT BLANK

ABSTRACT

RECEIVER SUBSYSTEM

The Honeywell receiver subsystem design uses well established fossil technology and consists of a cavity receiver housing, a steam generator, a cavity barrier, piping, and a support tower. The steam generator absorbs the redirected solar energy from the collector subsystem and converts it to superheated steam which drives the turbine. The receiver is adequately shielded to protect personnel and equipment. A cavity barrier is lowered at night to conserve heat and expedite startup the following day. This volume contains the subsystem design and methodology and the correlation with the design and performance characteristics of the SRE steam generator which was fabricated and successfully tested during the program.

THIS PAGE

WAS INTENTIONALLY

LEFT BLANK

VOLUME IV

TABLE OF CONTENTS

	Page
SECTION 2	2 - 1
Requirements	2 - 1
Design Approach	2 - 3
General Description	2 - 4
Steam Generator	2 - 4
Steam Generator Housing	2 - 6
Corbels	2 - 6
Outer Housing	2 - 10
Cavity Barrier	2 - 11
Radiation Shield	2 - 11
Tower	2 - 13
Tower Foundation	2 - 13
Tower Piping	2 - 15
Design Justification	2 - 16
SECTION 3	3 - 1
Steam Generator	3 - 2
Design Approach	3 - 2
Requirements	3 - 3
Functional Requirements	3 - 3
Physical Requirements	3 - 3
Heat Absorption Requirements	3 - 4
Structural Requirements	3 - 4
General Description	3 - 8
Physical Arrangement	3 - 11
Design Justification	3 - 13
Performance Characteristics	3 - 16

Table of Contents (continued)

	Page
Components	3 - 21
Boiler Section	3 - 21
Superheaters	3 - 24
Drum and Internals	3 - 24
Recirculating Pumps	3 - 26
Attemperator	3 - 29
Support Structure	3 - 31
Pressure Part Support	3 - 34
Steam Generator Ceiling	3 - 36
Functional Performance	3 - 36
Heat Flux Data	3 - 39
Boiler/Superheater Interface	3 - 42
Primary/Secondard Superheater Interface	3 - 49
Boiler Circulation	3 - 53
Static Flow Stability	3 - 57
Superheater Tube Size	3 - 61
Superheater Surface Arrangement and Flow Distribution	3 - 64
Metal Temperatures	3 - 65
Heat Loss and Cooldown Rate	3 - 70
Thermal Radiation Characteristics	3 - 74
Upset Conditions	3 - 74
Cloud Shadowing	3 - 77
Feedwater Temperature	3 - 79
Stress Analysis	3 - 83
Boiler Section	3 - 83
Superheater	3 - 88
Permissible Rate of Temperature Change	3 - 97
Structural Analysis	3 - 99
Material Selection	3 - 99
Operation	3 - 105
Preparations for Startup	3 - 105
Startup	3 - 106
Performance Tests	3 - 107
Shutdown	3 - 108
Water Treatment	3 - 108
Maintenance	3 - 110
Steam Generator Instruments and Controls	3 - 111
Controls	3 - 111
Instrumentation	3 - 111
Comparison to SRE	3 - 113

Table of Contents (continued)

	Page
Steam Generator Housing	3 - 115
Corbels	3 - 115
Outer Housing	3 - 118
Cavity Barrier	3 - 120
Radiation Shielding	3 - 125
Tower	3 - 127
Tower Foundation	3 - 127
Tower	3 - 129
Tower Piping	3 - 132
Receiver Subsystem Loads	3 - 138
Static Loads	3 - 138
Wind Loads	3 - 139
Seismic Loads	3 - 140

GLOSSARY

APPENDIX A
List of Data and Information Items

APPENDIX B
Design Requirements (Receiver Red Book)

APPENDIX C
Major Generator Parts Data
Steam Generator Drawings (5)

APPENDIX D
Heat Balance

APPENDIX E
Receiver Cavity Closure
Seismic Analysis and Design Considerations

APPENDIX F
Drawings S1001 through S1004
Drawings A1001 through A1006

LIST OF FIGURES

Figure	Title	Page
2 - 1.	Receiver - Cavity Configuration	2 - 2
2 - 2.	Receiver Steam Generator Flow Circuit	2 - 5
2 - 3.	Steam Generator Housing & Support Structure	2 - 9
2 - 4.	Typical Consel Thermal Shield Details	2 - 12
2 - 5.	Tower Support Structure & Piping	2 - 14
3 - 1.	Receiver-Cavity Configuration	3 - 5
3 - 2.	Absorption Rate vs. Angle, Elevation - 4.57m (15 ft)	3 - 6
3 - 3.	Average Circumferential Absorption Rate vs. Height	3 - 7
3 - 4.	Steam Generator Flow Circuit	3 - 9
3 - 5.	Pilot Plant Steam Generator Arrangement	3 - 12
3 - 6.	Absorbed Power Distribution versus Time	3 - 17
3 - 7.	Flow versus Total Absorbed Power	3 - 19
3 - 8.	Steam Temperature versus Absorbed Power	3 - 19
3 - 9.	Boiler Section Flow Circuits	3 - 22
3 - 10.	Boiler Section	3 - 23
3 - 11.	Superheater Module	3 - 25
3 - 12.	Recirculating Pump	3 - 27
3 - 13.	Attemperator	3 - 30
3 - 14.	Support Structure	3 - 32
3 - 15.	Typical Horizontal Truss	3 - 33
3 - 16.	Boiler Wall Lateral Support	3 - 35
3 - 17.	Superheater Hangar	3 - 37
3 - 18.	Superheater Lateral Ties	3 - 38
3 - 19.	Cavity Wall Incident Flux Map, 3/21/12PM	3 - 40
3 - 20.	Circumferential Average A/I versus Cavity Position, 3/21/12PM	3 - 41
3 - 21.	Absorption Rate versus Angle at Peak Flux Point	3 - 443
3 - 22.	Absorption Rate versus Angle at Boiler/Superheater Interface	3 - 44
3 - 23.	Absorption Rate versus Angle at Primary/Secondary Superheater Interface	3 - 45
3 - 24.	Absorption Rate versus Angle at Top of Cavity	3 - 46
3 - 25.	Pressure versus Steam Flow	3 - 47
3 - 26.	Turbine Heat Balance Data	3 - 48
3 - 27.	Relative Energy Absorption versus Cavity Height	3 - 50
3 - 28.	Absorbed Power Distribution versus Time	3 - 51
3 - 29.	Flow versus Total Absorbed Power	3 - 52
3 - 30.	Effect of Primary/Secondary Interface on Primary Outlet and Secondary Inlet Enthalpy, 3/21/12PM	3 - 54

List of Figures (continued)

Figure	Title	Page
3 - 31.	Steam Temperature versus Absorbed Power	3 - 55
3 - 32.	Heat Flux versus Boiler Height, 3/21/12PM	3 - 56
3 - 33.	Boiler Circuit	3 - 58
3 - 34.	Pressure Drop versus Recirculation Ratio	3 - 59
3 - 35.	Boiler Tube Circuit	3 - 62
3 - 36.	Static Stability, EN Circuit, 3/21/12PM	3 - 63
3 - 37.	Primary Superheater, Steam Temperature and Heat Flux vs. Azimuth Angle (Before Flow Balancing), 3/21/12PM	3 - 66
3 - 38.	Primary Superheater Circuits	3 - 67
3 - 39.	Secondary Superheater Circuits	3 - 68
3 - 40.	Superheater Flow Schematic	3 - 69
3 - 41.	Pilot Plant Receiver Cavity Convection Losses	3 - 72
3 - 42.	Overnight Cooldown Rate	3 - 73
3 - 43.	Cavity Efficiency vs. Thermal Radiation Coefficient, 3/21/12PM	3 - 75
3 - 44.	Thermal Radiation Properties	3 - 76
3 - 45.	Primary Temperatures vs. Cloud Shadowing (Case 1) 3/21/12PM	3 - 78
3 - 46.	Steam Temperature Variation versus Secondary Superheater Shadowing (Case 2) 3/21/12PM	3 - 80
3 - 47.	Secondary Superheater Temperatures (Case 2) 3/21/12PM	3 - 81
3 - 48.	Peak Metal Temperature versus Absorption, (Case 3) 3/21/12PM	3 - 82
3 - 49.	Temperature Distribution in Boiler Section Membrane Wall, Flat Projected Heat Flux 263 KW/m^2	3 - 85
3 - 50.	Thermal Stresses in Boiler Section Membrane Wall, Heat Flux 263 KW/m^2	3 - 85
3 - 51.	Design-Fatigue Strength for Carbon and Low-Alloy Steels through 5% Cr up to 538°C (1100°F)	3 - 87
3 - 52.	Superheater Tube Geometry	3 - 90
3 - 53.	Superheater Tube Cross Section and Temperature Gradient	3 - 91
3 - 54.	Superheater Tube Displacement, Primary Superheater, Section A_3, 3/21/12PM	3 - 93
3 - 55.	Estimated Elastic Analysis Curves for Croloy 2-1/4, Design Lives not Exceeding 2.5×10^5 Hr	3 - 96

List of Figures (continued)

Figure	Title	Page
3 - 56.	Boiler Circuit Transient Thermal Stresses	3 - 98
3 - 57.	Superheater Transient Thermal Stresses	3 - 100
3 - 58.	Typical Horizontal Truss	3 - 101
3 - 59.	Typical Vertical Truss	3 - 102
3 - 60.	Top Steel	3 - 103
3 - 61.	Steam Generator Housing & Support Structure	3 - 116
3 - 62.	Cavity Closure Approaches	3 - 122
3 - 63.	Cavity Barrier in Closed & Stoned (Open) Position	3 - 123
3 - 64.	Tower Foundation	3 - 128
3 - 65.	Tower	3 - 130
3 - 66.	Diameters of Reinforced Concrete Chimneys of Various Heights	3 - 133
3 - 67.	Main Steam Tower Piping	3 - 135
3 - 68.	Hanger Types	3 - 137

LIST OF TABLES

TABLE		PAGE
2-1	Receiver Steam Generator Nominal Steam Conditions Based on Estimated Heat Balance Data	2-7
2-2	Receiver Steam Generator Physical Characteristics	2-8
3-1	Nominal Steam Conditions	3-10
3-2	Physical Characteristics	3-11
3-3	Range of Operation with Cloud Shadowing	3-14
3-4	Effect of Feedwater Temperature Deviations on Spray Flow Requirements	
3-5	Action Initiated by High and Low Water Level Signals	3-28
3-6	Boiler Flow Circuit Performance Characteristics 3/21/12PM	3-60
3-7	Flow and Enthalpy Variation, Circuit EN, 3/21/12PM	
3-8	Superheater Performance, 3/21/12PM	3-65
3-9	Superheater Metal Temperatures	3-71
3-10	Conduction Losses	3-74
3-11	Attemperator Spray Flow Required to Control Steam Temperature	3-83
3-12	Superheater Tube Thermal Stress Primary Superheater Section A3, 3/21/12PM	3-94
3-13	Typical Croloy 2-1/4 Tube Applications	3-104
3-14	Recommend Limits of Solids in Feedwater for Solar Steam Generator	3-109
3-15	Maintenance Items	3-110
3-16	Pilot Plant Steam Generator Measurements	3-112
3-17	Tower Piping Specifications	3-134

SECTION 1
INTRODUCTION

BACKGROUND

Supplies of most conventional fuels are being depleted rapidly. Consequently, it is necessary to identify alternate sources of energy and to develop the most promising to ensure availability when needed.

An alternative with great potential is the conversion of sunlight to energy. One aspect of this usage is generating electricity through solar energy. A goal of the national energy program is to demonstrate the technical and economic feasibility of a central receiver solar power plant for generating electricity. Pursuant to that goal, the Energy Research and Development Administration (ERDA), on 1 July 1975, awarded Honeywell Inc. a two-year contract for Phase I of such a program.

The initial program phase, which is the subject of this report, consisted of developing a preliminary design for a 10 MW(e) proof-of-concept solar pilot plant. The second phase will consist of building and operating the pilot plant and projecting the information gained to larger-scale plants. This phase is scheduled to be completed in the early 1980's. The third phase will consist of designing, building, and operating two 50-100 MW(e) demonstration plants. The final phase will consist of building and operating plants in the 100-300 MW(e) range.

PHASE I PROGRAM SCOPE

The Phase I program consisted of developing a pilot plant preliminary design by first developing a preliminary baseline design to meet specified

and assumed performance requirements. The baseline was then refined through analysis and experimentation, and evaluated by testing key subsystems, i.e., collector, steam generator, and thermal energy storage.

The complexity of the undertaking dictated a team approach to provide the technical and managerial skills required. The Honeywell team is identified in Figure 1-1.

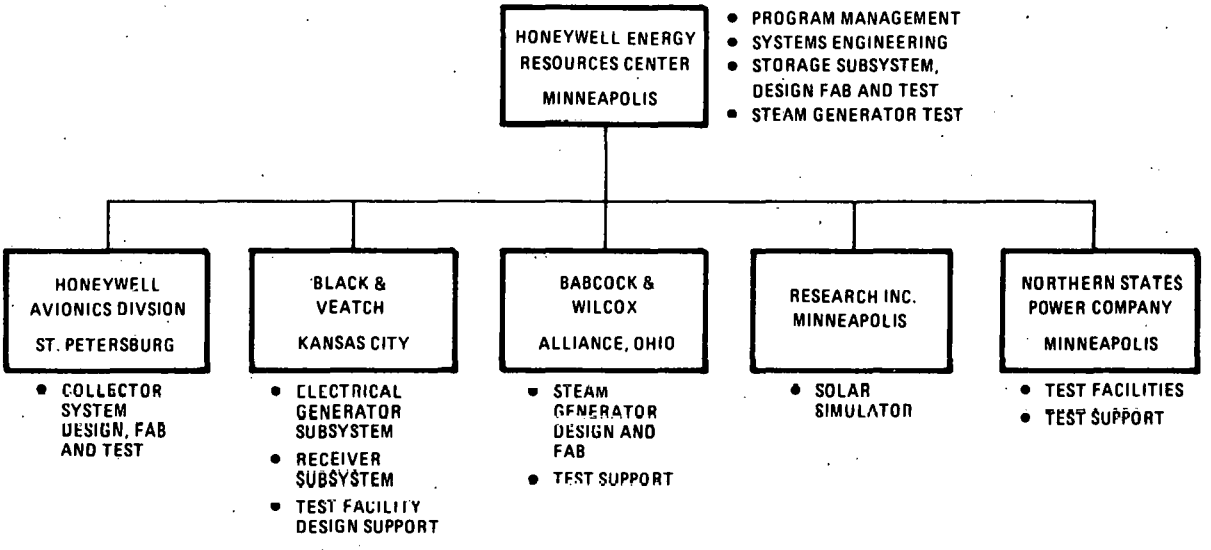

Figure 1-1. Honeywell Team for Phase I Solar Pilot Plant Program.

A unique feature of the test plan was the use of selected facilities of an operating power plant, Northern States Power's Riverside Plant in Minneapolis, Minnesota, to test the steam generator and thermal energy storage subsystems. An ERDA-directed change from latent heat (phase change) storage to sensible heat storage cancelled the storage portion of the test

plan. The steam generator was tested using a solar array to simulate the insolation required to generate steam. The collector subsystem hardware, one mobile and three stationary, full-scale, four-mirror units, was field tested for performance and reaction to operating environments at Honeywell's Avionics Division facility in St. Petersburg, Florida.

The information obtained from the subsystems tests was used to complete the pilot plant preliminary design, and to project performance and cost of a 100 MW(e) plant to facilitate long-range planning.

The chronology of the work done in Phase I is summarized in Figure 1-2.

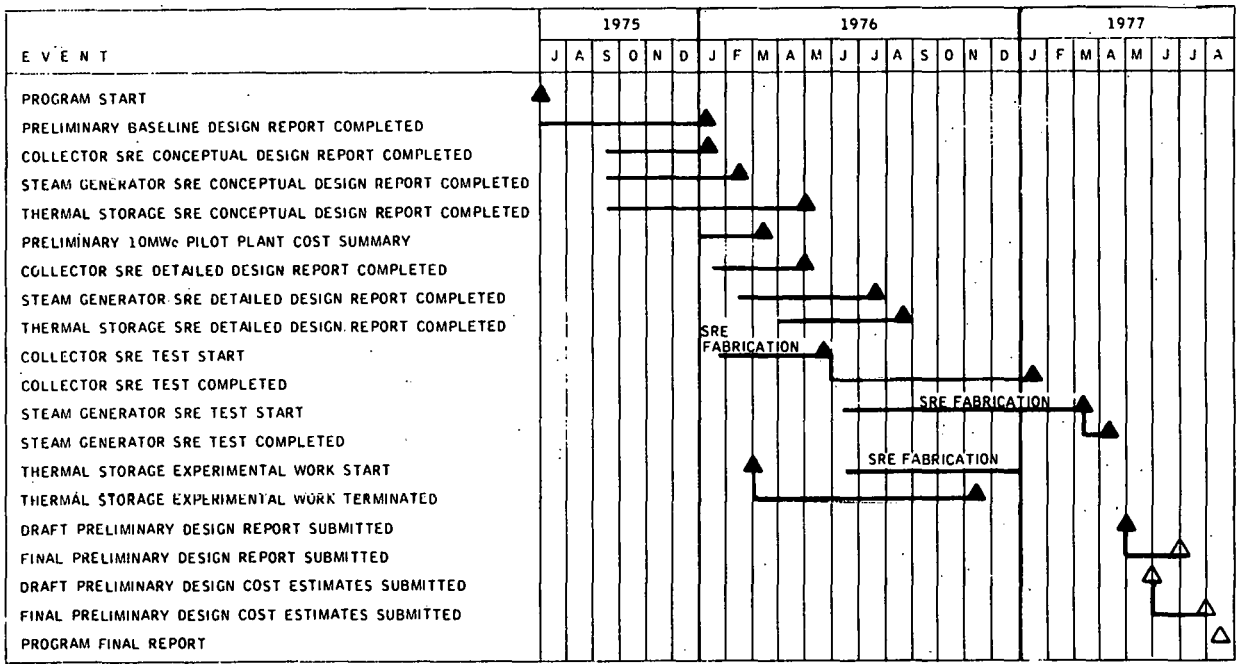

Figure 1-2. Chronology of Phase I Solar Pilot Plant Program

ORGANIZATION OF THE PRELIMINARY DESIGN REPORT

The preliminary design and supportive data resulting from the Phase I work are presented in seven volumes:

I - Executive Overview
II - System Description and System Analysis (3 books)*
III - Collector Subsystem
IV - Receiver Subsystem
V - Thermal Storage Subsystem
VI - Electrical Power Generation/Master Control Subsystems and Balance of Plant
VII - Pilot Plant Cost/Commercial Plant Cost and Performance

Abstracts of volumes other than the one in hand and Volumes I and VII are on the following pages.

*Book 2 is Central Receiver Optical Model Users Manual
Book 3 is Dynamic Simulation Model and Computer Program Descriptions

ABSTRACTS

Vol. II - SYSTEM ANALYSIS AND SYSTEM DESCRIPTION

Honeywell conducted a parametric analysis of the 10 MW(e) solar pilot plant requirements and expected performance and established an optimum system design. The main analytical simulation tools were the optical (ray trace) and the dynamic simulation models. These are described in detail in Books 2 and 3 of this volume under separate cover. In making design decisions, available performance and cost data were used in provide a design reflecting the overall requirements and economics of a commercial-scale plant. This volume contains a description of this analysis/design process and resultant system/subsystem design and performance.

Vol. III - COLLECTOR SUBSYSTEM

The Honeywell collector subsystem features a low-profile, multifaceted heliostat designed to provide high reflectivity and accurate angular and spatial positioning of the redirected solar energy under all conditions of wind load and mirror attitude within the design operational envelope. The heliostats are arranged in a circular field around a cavity receiver on a tower halfway south of the field center. A calibration array mounted on the receiver tower provides capability to measure individual heliostat beam location and energy periodically. This information and weather data from the collector field are transmitted to a computerized control subsystem that addresses the individual heliostat to correct

pointing errors and determine when the mirrors need cleaning. This volume contains a detailed subsystem design description, a presentation of the design process, and the results of the SRE heliostat test program.

Vol. V - THERMAL STORAGE SUBSYSTEM

The Honeywell thermal storage subsystem design features a sensible heat storage arrangement using proven equipment and materials. The subsystem consists of a main storage containing oil and rock, two buried superheater tanks containing inorganic salts (Hitec), and the necessary piping, instrumentation, controls, and safety devices. The subsystem can provide 7 MW (e) for three hours after twenty hours of hold. It can be charged in approximately four hours. Storage for the commercial-scale plant consists of the same elements appropriately scaled up. This volume contains a description of the subsystem design methodology and evolution and the subsystem operation and performance.

Vol. VI - ELECTRICAL POWER GENERATION SUBSYSTEM, CONTROLS, AND BALANCE-OF-PLANT

The Honeywell electrical power generation subsystem centers on a General Electric dual admission, triple extraction turbine generator sized to the output requirements of the Pilot Plant. The turbine receives steam from the receiver subsystem and/or the thermal storage subsystem and supplies those subsystems with feedwater. The turbine condensor is wet cooled. The plant control system consists of a coordinated

digital master and subsystem digital/analog controls. The remainder of the plant, work spaces, maintenance areas, roads, and reception area are laid out to provide maximum convenience compatible with utility and safety. Most of the activities are housed in a complex around the base of the receiver tower. This volume contains a description of the relationship of the electrical power generation subsystem to the rest of the plant, the design methodology and evolution, the interface integration and control, and the operation and maintenance procedures.

Section 2

SUMMARY RECEIVER SUBSYSTEM DESCRIPTION

A brief description of the integral receiver subsystem preliminary design is presented in this section. The design requirements are summarized and the major aspects of the design approach are defined. A general description of the subsystem and its major elements is presented along with a brief discussion of the factors which justify the resulting design.

REQUIREMENTS

The design requirements of the receiver subsystem relate principally to the performance requirements for the solar steam generator which in turn translate to certain design requirements for the receiver tower support structure.

The receiver steam generator is required to efficiently and reliably absorb solar energy and transfer it to the steam-water working fluid. Steam pressure, temperature, and flow at the superheater outlet nozzle are set by the requirements established for supplying steam to the Electrical Power Generation Subsystem. These conditions are summarized for the Pilot Plant as follows.

	Pressure MPa (psia)	Temperature C (F)	Flow kg/s (lbs/hr)
Design (12/21/2 p.m.)	10.6 (1540)	516 (960)	49593 (109,332)
Maximum (3/21/12 p.m.)	11.0 (1600)	516 (960)	61000 (134,429)

The height of the receiver cavity above the ground, its inner diameter, and the configuration of the aperture area between the top of the receiver support tower and the base of the receiver cavity are determined by the power to be generated by the plant, the layout of the heliostat collector field, and minimizing cavity losses due to reflection, reradiation, and convection. The pilot plant receiver subsystem elements, including the steam generator, are therefore required to conform to the basic dimensions shown in Figure 2-1.

The design heat fluxes for the receiver steam generator are established by the geometrical arrangement of the heliostat field, the height and diameter of the aperture aim circle, the cavity dimensions, and the surface absorptance. Peak design heat fluxes are as follows.

	kW/m^2 ($Btu/hr-ft^2$)
Design (12/21/2 p.m.)	258 (81.8×10^3)
Maximum (3/21/12 p.m.)	263 (83.4×10^3)

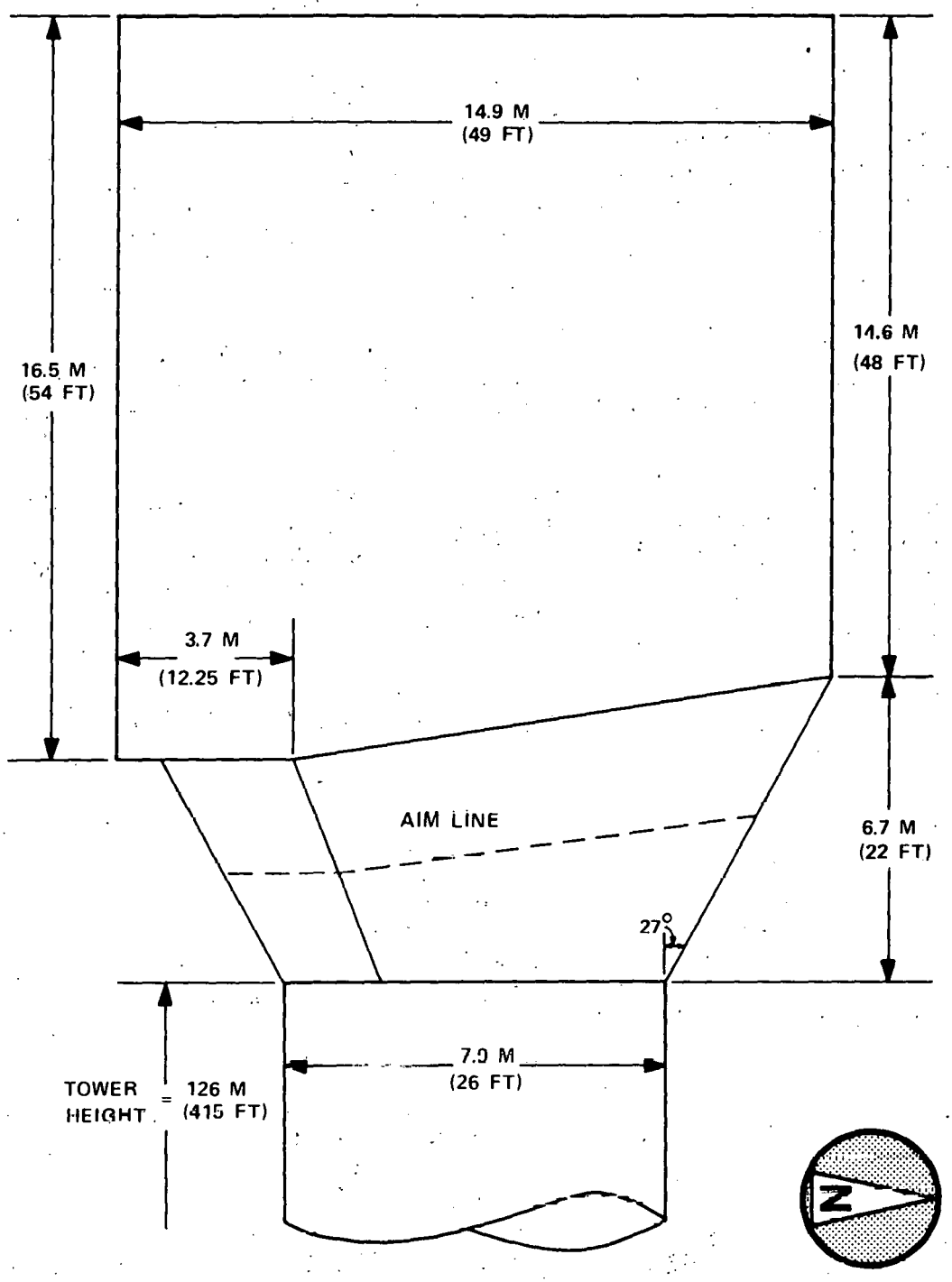

Figure 2-1. Receiver-Cavity Configuration

A unique requirement imposed on solar steam generators is the capability to experience an unusually large number of stress cycles during the 30 year design life. In addition to the diurnal cycle, the performance of the solar steam generator is altered by the passing of clouds and by the requirement to stow the heliostats in such events as high winds, sand storms, etc. Since solar steam generators experience significantly more thermal cycles than fossil or nuclear steam generators, particular care is taken to minimize fatigue, creep, and thermal stresses.

The structural strength requirements for the receiver subsystem elements are determined by:

(1) Live and dead weight loads.
(2) Wind loads.
(3) Seismic loads.

The steam generator support structure and tower are designed for wind and seismic loads that are higher than for an equivalent sized fossil or nuclear steam generator located on the ground. Wind velocity increases with height, and the ground level seismic accelerations may be amplified by the interaction of the steam generator support structure and the receiver tower. This interaction is considered in the report, Seismic Analysis and Design Considerations, presented in Appendix E.

DESIGN APPROACH

In developing the preliminary design of the solar pilot plant receiver subsystem, the primary emphasis has been to achieve a practical, reliable design by using state-of-the-art technology for all elements of the subsystem. Hence, the well established technology of slip form and jump form concrete towers and chimneys is utilized for the design of the receiver tower, erected on a reinforced concrete mat foundation. The existing codes and standards were followed for the design of the receiver housing support legs, or corbels, and for the steam generator support structure and housing.

The receiver steam generator design itself is based on state-of-the-art fossil boiler technology. Design margins consistent with fossil boiler practice are factored into the design. The solar unique effect of cloud cover and motion on the performance of the steam generator was examined by defining several idealized cloud shadowing conditions and analyzing the degree of shadowing that can be tolerated before a steam generator design limit is exceeded. This issue is discussed in depth in Section 3.

It should be noted that the steam generator configuration and the radiation properties of the heat transfer surfaces are selected to maximize effective absorptance so that the efficiency of the receiver cavity is maximized. The steam generator heat transfer surface and ceiling form the inner walls of the receiver cavity. These surfaces are also required to have an absorptance of 0.9 to further increase efficiency.

Steam generator response to changes in solar insolation is designed to be rapid and stable so that the steam generator can be controlled to "follow the sun" while supplying steam at design conditions, thus maximizing the conversion of solar to thermal energy.

GENERAL DESCRIPTION

A general description of the receiver subsystem is presented by considering the receiver steam generator configuration, the steam generator housing, and the receiver tower.

Steam Generator

The steam generator heat transfer surface is an 18-sided polygon which forms the interior walls of the receiver cavity. This geometry traps reflected and reradiated energy to increase cavity effective absorptance. The absorptance of the heat transfer surface is about 0.9 and is achieved by allowing natural oxidation to occur. Reradiation is minimized by locating the cooler heat transfer surfaces near the bottom of the cavity and the higher temperature surfaces at the top.

The steam generator is thoroughly insulated to minimize conduction losses and, in the absence of wind, the bottom opening cavity does not allow the buoyant hot air to escape, minimizing natural convection losses. The approximate cavity efficiencies for zero wind velocity are tabulated below.

	Efficiency
Design (12/21/2 p.m.)	0.914
Maximum (3/21/12 p.m.)	0.916

The steam generator is a pump-assisted recirculating drum boiler with two superheaters and a spray attemperator for controlling steam temperature, as illustrated in Figure 2-2. Feedwater is piped into the steam generator drum. Slightly subcooled water flows from the drum, through a downcomer, and is pumped through the recirculation line to the boiler section.

The water is distributed to the boiler section where steam generation takes place. A saturated steam-water mixture at an average quality of ten per cent exits the boiler section and flows through the risers to the steam drum where the water and steam are separated by cyclone separators and a scrubber.

Moisture free steam from the drum flows through the saturated steam lines to the primary superheater where it is heated to about 475 C (887 F).

The steam exiting the primary superheater passes through the spray attemperator where additional feedwater is injected as required to control

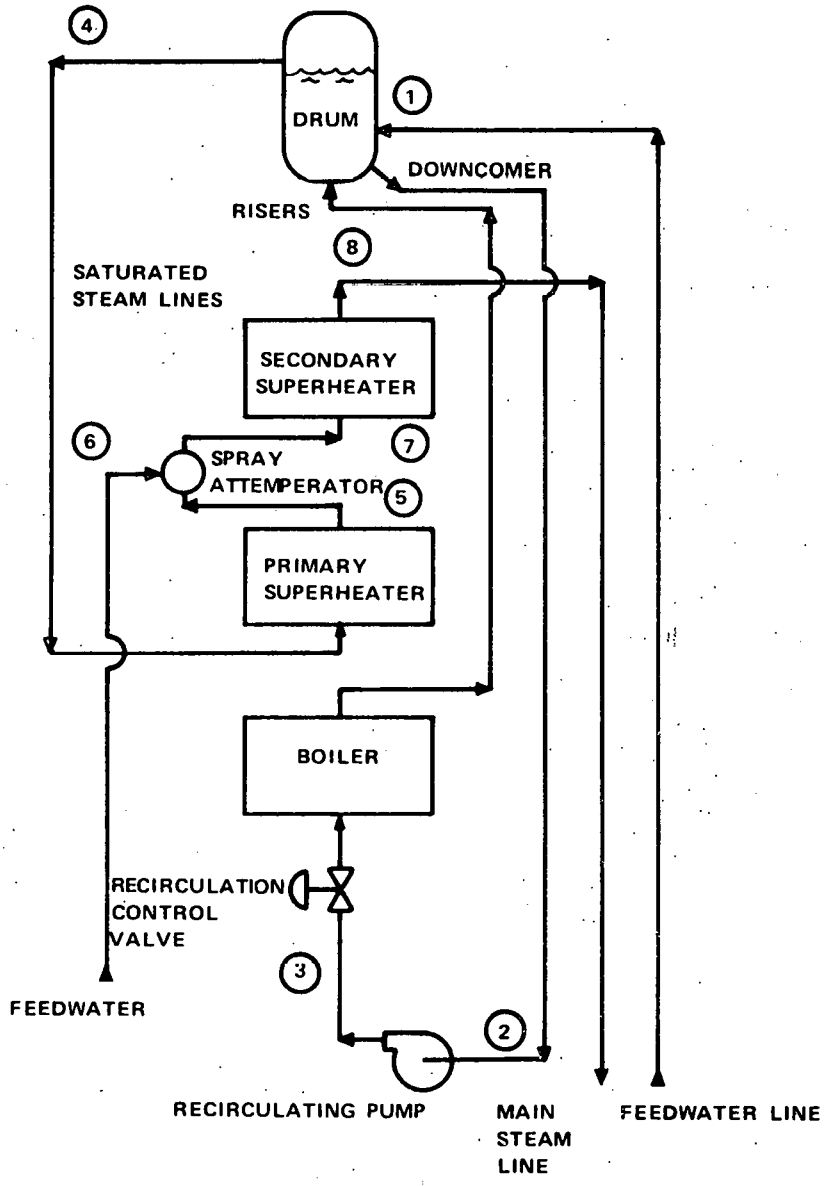

Figure 2-2. Receiver Steam Generator Flow Circuit

exit steam temperature. The attemperated steam enters the secondary superheater at about 375 C where it is heated to 515 C (960 F).

Table 2-1 lists steam pressure, temperature, and flow at various points in the steam generator flow circuit for 3/21/7 a.m., 3/21/12 p.m., and 12/21/2 p.m.

The boiler section heat transfer surface is an 18-sided polygon fabricated from water wall membrane panels. The primary and secondary superheaters consist of three horizontal tangent tube modules. Each module has six flat sides and covers 120° of the cavity circumference. The steam drum is vertical and contains seven cyclone primary separators and secondary scrubber plates to effectively remove moisture from the saturated steam.

The steam generator structure consists of horizontal and vertical trusses which transfer the live and dead weight loads from the steam generator pressure parts and the receiver environmental housing to the three receiver support corbels. The steam generator structure has been designed to withstand a lateral static equivalent seismic load of 3 g. The steam generator is top-supported from the structure by hanger rods which are free to swing outward to accommodate thermal expansion.

The major physical characteristics of the steam generator are listed in Table 2-2.

Steam Generator Housing

The steam generator housing, illustrated in Figure 2-3, provides support, access, protection, servicing, and an acceptable environment for the steam generator, associated equipment, piping, and electrical cables in a configuration which minimizes blockage of redirected solar radiation from the collector field to the receiver cavity and maximizes overall receiver cavity efficiency. The essential elements of the steam generator housing are the receiver support structure legs (corbels), the outer housing structure, the cavity barrier, and the thermal radiation shielding.

Corbels. The receiver support structure legs, or corbels, provide support of, and access to, the receiver steam generator assembly from the tower while blocking the smallest possible amount of solar radiation from the collector field. The corbels provide the only access from the tower to the receiver steam generator and the collector field calibration arrays. Mechanical piping, electrical tray, and a personnel access ladder are contained within the corbels. Because redirected solar radiation from the collector field must pass through the receiver aperture, i.e., the space between the tower and the steam generator, the width of the corbels is maintained at a minimum to ensure the highest possible receiver efficiency.

TABLE 2-1

RECEIVER STEAM GENERATOR NOMINAL STEAM CONDITIONS BASED ON ESTIMATED HEAT BALANCE DATA

Location	Time								
	3/21/7a.m.			3/21/12/p.m.			12/21/2p.m.		
	P	T	W	P	T	W	P	T	W
	MPa (psia)	C (F)	kg/s (lb/hr)	MPa (psia)	C (F)	kg/s (lb/hr)	MPa (psia)	C (F)	kg/s (lb/hr)
Feedwater		116 (241)	228 (B0.1 x 10^3)		179 (353)	928 (122.6 x 10^3)		171 (339)	799 (105.6 x 10^3)
Pump Inlet	10.33 (1499)	310 (590)	10280 (1358 x 10^3)	11.78 (1709)	315 (597)	10280 (1358 x 10^3)	11.36 (1649)	313 (594)	10280 (1358 x 10^3)
Pump Discharge	10.67 (1549)	310 (590)	10280 (1358 x 10^3)	12.12 (1759)	315 (597)	10280 (1358 x 10^3)	11.71 (1699)	313 (594)	10280 (1358 x 10^3)
Drum Discharge	10.20 (1480)	313 (595)	228 (30.1 x 10^3)	11.64 (1690)	322 (613)	928 (122.6 x 10^3)	11.23 (1630)	320 (608)	799 (105.6 x 10^3)
Primary Outlet	10.18 (1478)	480 (897)	228 (30.1 x 10^3)	11.33 (1645)	461 (863)	928 (122.6 x 10^3)	11.00 (1597)	461 (862)	799 (105.6 x 10^3)
Attemperator Spray		116 (241)	9.1 (1.2 x 10^3)		179 (353)	102 (13.5 x 10^3)		171 (339)	74 (9.8 x 10^3)
Secondary Inlet	10.15 (1472)	439 (823)	237 (31.3 x 10^3)	11.10 (1640)	378 (712)	1030 (136.1 x 10^3)	10.97 (1592)	390 (734)	874 (115.4 x 10^3)
Secondary Outlet	10.14 (1471)	515 (960)	237 (31.3 x 10^3)	11.02 (1600)	515 (960)	1030 (136.1 x 10^3)	10.77 (1563)	515 (960)	874 (115.4 x 10^3)

TABLE 2-2

RECEIVER STEAM GENERATOR
PHYSICAL CHARACTERISTICS

Item	Metric Dimensions	English Dimensions
Cavity		
ID	14.9 m	49'
Height	14.6-16.5 m	48'-54'
Header & Diameter	16.9 m	55'-5-5/8"
Drum	8.9 cm Thk. x 1.2 m ID x 4.3 mh	3-1/2" Thk. x 4' ID x 14' h
Boiler Section Height		
South Side	8.0 m	26'-3"
North Side	6.2 m	20'-3"
1st Stage SH Height	3.2 m	10'-5"
2nd Stage SH Height	4.8 m	15'-8"
Weight		
Pressure Parts and Integral Supports	289,198 kg	637,000 lbs
Structure	312,806 kg	689,000 lbs

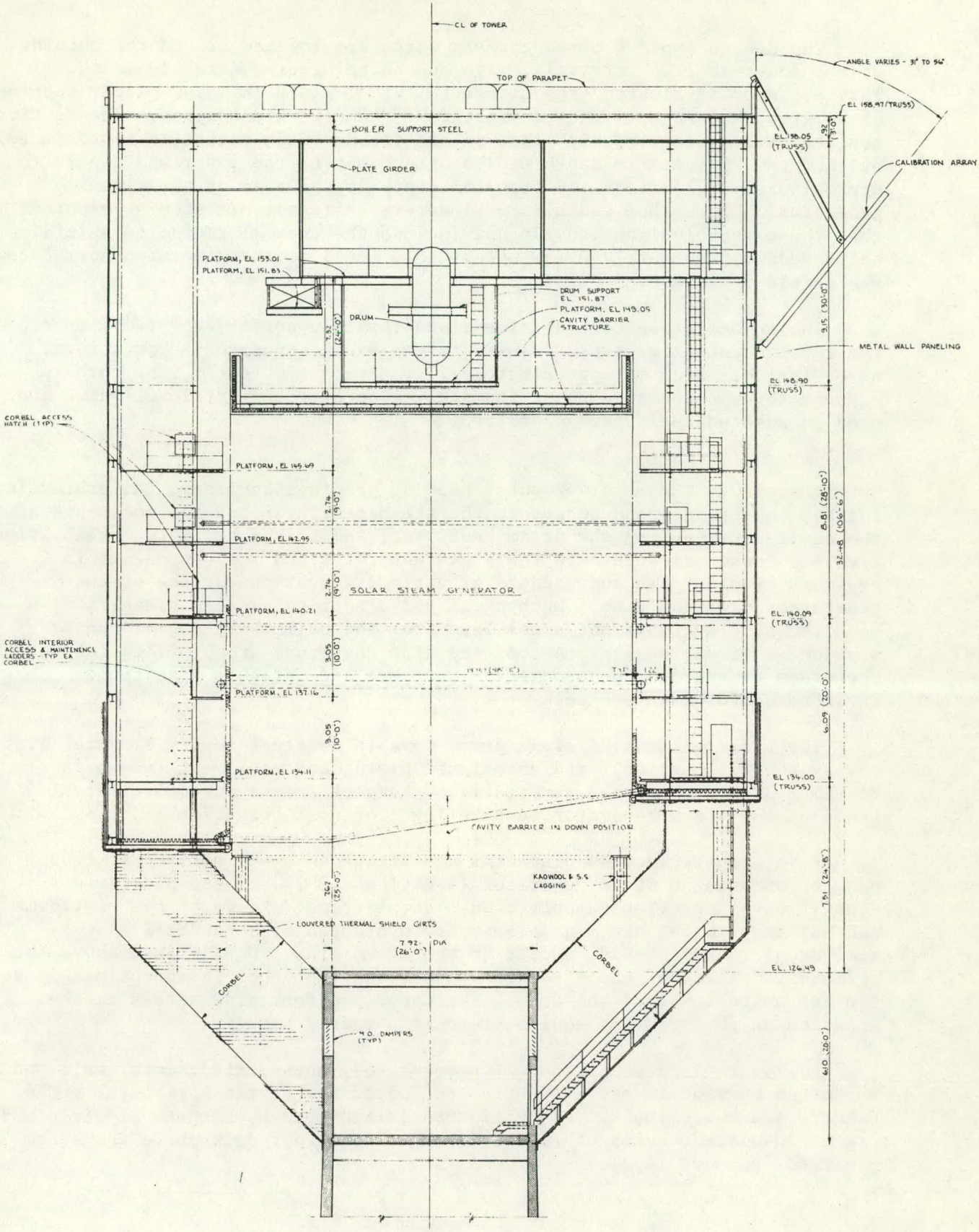

Section-Receiver Housing

Figure 2-3. Steam Generator Housing and Support Structure

The design employs three corbels which are located around the outside of the tower at 120° intervals, with one corbel facing directly south. They are shop fabricated from structural steel plate into box girder sections of as great a length as can be practically handled and shipped. The sections are then welded together in place in the field. Each corbel is approximately 6.1 meters (20 feet) in depth at its attachment to the tower and tapers to approximately 3.1 meters (10 feet) in depth at the base of the steam generator. The corbel width is 0.91 meters (3 feet). It should be noted that these corbel dimensions do not include the thermal radiation shielding which adds approximately 0.152 meters (0.5 feet) to the dimension normal to the shielded surface.

The corbel cross section dimensions remain constant from the base of the receiver steam generator cavity to the steam generator support level, a vertical distance of approximately 27.6 meters (90 feet). The corbels support three plate girders at the steam generator support level which are used to suspend the steam generator.

Outer Housing. The receiver outer housing provides environmental protection, lateral constraint, and access to the steam generator and the enclosure of the cavity surrounding the steam generator, and to the heliostat calibration arrays. Personnel access to the steam generator and its components is provided by platforms and ladders at various elevations at the steam generator and steam drum. Mechanical and electrical access areas, if required at elevations not accessible from the boiler platforms, can be provided in final design. A roof and side enclosure are provided to protect the steam generator and associated equipment and maintain a suitable environment for maintenance.

The steam generator, steam drum, movable receiver cavity closure (i.e., cavity thermal barrier), and associated piping and equipment (shown in Figure 2-3) are supported vertically by hangers from a structural steel frame at the steam generator support level or roof elevation.

Five circular access platforms are attached to the horizontal truss hangers around the steam generator (see Figure 2-3). These platforms consist of bar grating supported on a steel frame. Edges of the platforms not adjacent to the steam generator are protected by a handrail. Two similar platforms provide access to the steam drum. One is just above the permanent ceiling of the steam generator, and the other is approximately at the top third level of the drum. The upper platform also serves as the location of the hoisting equipment for the cavity barrier.

Enclosure is accomplished with segmented, uninsulated, metal wall panels supported by wide flange girts from the outer row of the horizontal truss hangers and the corbels. Top enclosure is achieved by a three ply felt and gravel insulated, built up roof laid on a metal roof deck above the steam generator support level.

Cavity Barrier. The function of the cavity barrier is to insulate the receiver cavity from ambient conditions during the nightly shutdown of the solar plant in order to retain as much energy in the receiver as possible. This energy reduces:

(1) The time required to bring the plant back to rated steam pressure and temperature during start-up the following day.
(2) The cyclic thermal stress imposed on the receiver steam generator.

The advantages of the interior cavity barrier design include a simple configuration requiring a small number of components, rapid closing speeds, low wind loadings, simple linear movement during operation, and a relatively small sealing perimeter. The principle disadvantage of the cavity barrier is that it is exposed to relatively high temperatures and its suspension system and hoisting mechanism are subject to frequent inspection under Federal regulations. Cavity closure is achieved by a single circular disc which moves vertically up and down within the cavity. A hoisting mechanism raises and lowers the barrier from its closed (lower) and stowed (upper) positions. The operating or hoisting mechanism for the cavity barrier uses a single hoist motor, gear, and brake assembly. Sprockets, idler shafts, and other components employed to manipulate the barrier suspension are straightforward in design and simple in arrangement. Roller chain is used for barrier suspension since the roller chain link design, and the use of sprockets to manipulate the chain, offer the capability to accurately establish the barrier position and ensure the cavity barrier is held horizontal when being moved within the receiver cavity. This design minimizes contact between the barrier and the receiver heat transfer surface.

Radiation Shield. The radiation shield, illustrated in Figure 2-4, functions to protect the corbels, tower, and outer housing from solar radiation redirected from the heliostat collector field. Radiation shields are located in areas adjacent to the receiver aperture which are subject to direct, continuous radiation or which may be subject to errant radiation. The shield reflects and diffuses the solar rays so that they are not incident upon the base structural member. Convective cooling of the radiation shield is accomplished by natural convective air flow which develops behind the shield and flows upward through the shield.

The radiation shields extend from the base of the corbels to a point on the outer receiver housing 10 meters (33 feet) above the top of the concrete tower. They cover the faces of the concrete tower, steel corbels, and outer housing metal wall panel.

The shields are also included at the base of the outer housing between the metal wall panel and the receiver aperture. At this location, the shields serve as an enclosure to protect the insulation attached to the outer lower surface of the receiver cavity from wind, rain, and direct solar radiation. The amount of heat entering the outer lower surface of the

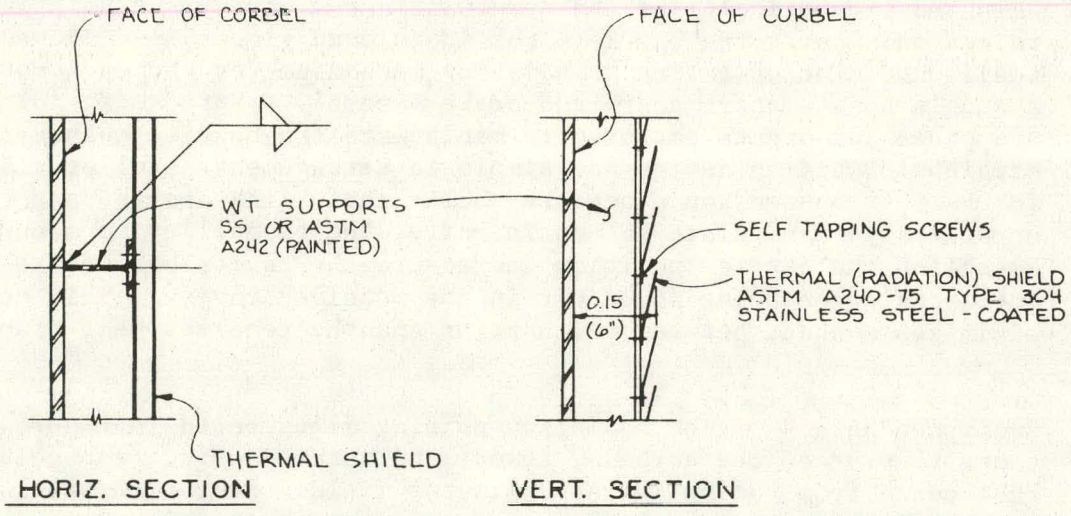

Figure 2-4. Typical Corbel Thermal Shield Details

receiver cavity is minimized by a Kaowool thermal barrier located between the radiation shields and the outer lower surface of the cavity.

The specification of the configuration and design of the shield is similar to that for the ERDA 5 MW Solar Thermal Test Facility. The shields consist of 0.19 centimeter thick (14 gage) stainless steel louvers with a white, modified silicone resin based, high temperature coating. The louvers are approximately 19 centimeters (7.5 in.) in width and inclined at an angle of approximately 15° to their support members.

Tower

The tower, illustrated in Figure 2-5, serves to support the receiver cavity and steam generator at a height above the ground determined by the power to be generated by the plant, the layout of the heliostat collector field, and the design of the receiver cavity. In performing its function of support, the tower provides access, protection, servicing, and an acceptable environment for equipment, piping, and electrical cables associated with the receiver steam generator and the calibration arrays. The major elements of the tower are the tower foundation, the tower structure, and the feed water and steam piping and equipment interfaces between the electrical power generation subsystem located at the ground level and the receiver steam generator at the top of the tower.

Tower Foundation. The tower foundation is the element that transfers the tower structure and receiver steam generator assembly loads to the underlying soil strata. The foundation must be large enough to spread the vertical loads from the tower over adequate soil area to prevent bearing capacity failure or excessive settlements. It also must be sufficiently massive to maintain stability under the effects of wind and earthquake and to resist the internal stresses caused by gravity and lateral loads.

The foundation is a circular concrete mat 39.6 meters (130 feet) in diameter placed on native soil strata. It is 3.05 meters (10 feet) thick across the base of the tower and tapers to 2.13 meters (7 feet) at its edge. The foundation contains 3317 cubic meters (4336 cu yd) of concrete which is to be placed in one continuous pour. Radial and circumferential reinforcing steel are used in the top and bottom faces of the mat. A planar grid of reinforcing steel is used around the center point of the mat to ensure continuity of reinforcing. The top of the mat is located 1.5 meters (5 feet) below grade to allow access for underground utilities.

Tower. The tower function is to provide support and access for the receiver steam generator assembly, including the corbels, and to house certain receiver subsystem equipment, piping, and electrical cables. The tower

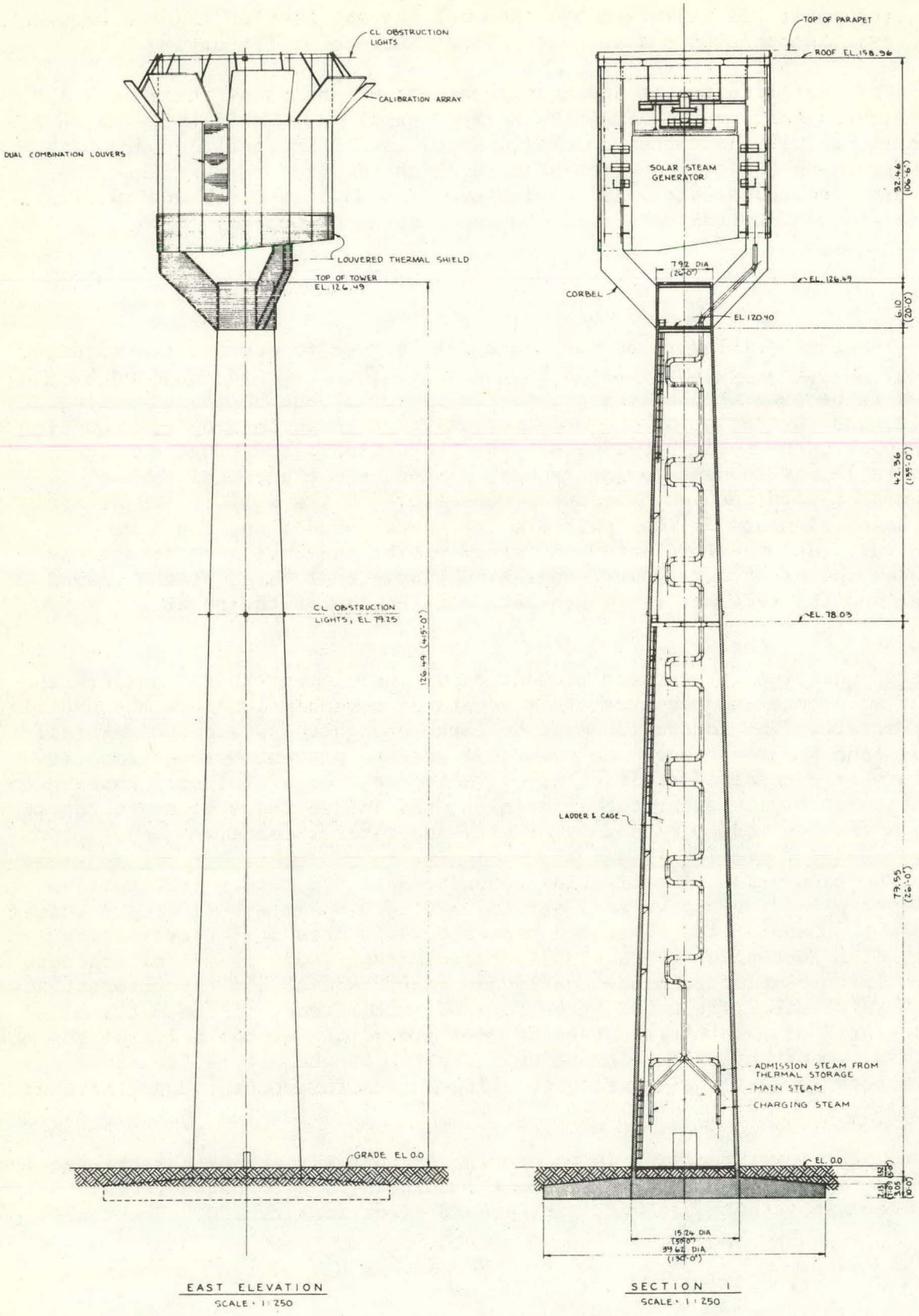

Figure 2-5. Tower Support Structure and Piping

must resist the corbel reactions and its own dead, live, and wind loads as set by the general design criteria of the pilot plant. The tower must also resist seismic forces without loss of stability or structural integrity.

The tower is a hollow, truncated conical structure of reinforced concrete 126.52 meters (415 feet) in height with outside diameters of 15.24 meters (50 feet) at its base and 7.93 meters (26 feet) at its top. The thickness of the tower wall is 0.610 meters (24 in.) at its base and 0.356 meters (14 in.) at its top. The tower wall is reinforced in both faces, and can be erected by either slip form or jump form methods. The top of the tower is a flat reinforced concrete slab approximately 0.305 meters (12 in.) in thickness.

A mechanical equipment room is provided in the tower approximately 6.1 meters (20 feet) below the top surface. This room, which is formed by the wall of the tower and a concrete floor slab on a structural steel frame, houses the receiver circulation pumps, blowdown tank, remote multiplex cabinet for instrumentation signals, and equipment servicing jib crane hoist. It is the highest accessible level within the tower and is the level of access to the corbels.

A service platform is located within the tower at approximately its mid-height. This platform consists of a bar grating floor on a structural steel frame, with a concrete slab provided to support the service water head tank. The platform also serves to access the four obstruction lights located on the outside of the tower.

A concrete grade slab is provided at finish grade for location of the fire water pump, service water pumps, auxiliary cooling water pumps, and demineralizer equipment.

Access to the tower at its base is by a rolling steel door 3.66 meters (12 feet) wide and 4.88 meters (12 feet) high, and by a personnel door 0.91 meters (3 feet) wide and 2.13 meters (7 feet) high. Personnel access up the tower is by ladder and elevator. The ladder is caged structural steel with bar grating landing platforms placed approximately every 9 meters (30 feet). The elevator is enclosed and guided from rails along the tower shell. It has a capacity for approximately twelve people or 1000 kilograms (2200 pounds). Ample space is available within the tower for piping and cable access.

Tower Piping. The two major elements included under the category of tower piping are the feedwater piping and the main or high pressure steam piping. The feedwater piping functions to deliver feedwater from the feedwater pumps of the electrical power generation subsystem to the receiver steam generator. The high pressure steam piping functions to deliver steam generated in the receiver steam generator to the turbine and/or to the

thermal storage subsystem, and to deliver steam generated in the thermal storage subsystem to the turbine. With reference to these principal elements, the tower piping is sized, routed, and supported to provide reasonable fluid velocities and pressure drops and to withstand the stresses which result from internal pressure, thermal expansion, dead loads, and to some extent seismic activity.

The feedwater line and high pressure steam line were sized to contain the maximum rated mass flow at a steam velocity below 34.5 meters per second (6800 feet per minute) and a water velocity below 4.6 meters per second (300 feet per minute). At the maximum rated mass flow, the pressure drop due to friction including a contingency is approximately 655 kPa (95 psi) in the feedwater line and 517 kPa (75 psi) in the main or high pressure steam line.

The requirement for expansion loops results from the long piping runs and the large differential temperatures between the hot and the cold operating conditions experienced by the piping. The expansion loops provide sufficient flexibility to accommodate the thermal expansion and contraction of the lines without causing unacceptable stresses. These expansion loops also provide sufficient flexibility to accommodate the downward thermal expansion of the steam generator. The determination of the number of expansion loops required is the result of employing the commercially available thermal/structural analysis program, ADLPIPE, to an assumed routing of the high pressure steam piping.

The feedwater piping and high pressure steam piping are supported as required by the ANSI power piping code.

DESIGN JUSTIFICATION

The justification for the design of the steam generator housing and support tower is simply that state-of-the-art technology in the construction of concrete towers and chimneys, and existing codes and design practices or standards for the construction of steel structures, were employed in the development of the preliminary design. Prior experience with the design of steel towers and concrete chimneys or towers clearly indicates the economic advantage of the concrete structure.

In considering the design of the receiver steam generator, several types of steam generators, based on fossil boiler technology, can meet the design required to produce superheated steam at subcritical pressure. These are:

(1) The natural circulation drum boiler.
(2) The pump-assisted circulation drum boiler.
(3) The once-through subcritical boiler.

The choice of the pump-assisted circulation concept for the solar steam generator is based on extensive fossil boiler experience which indicates that:

(1) Drum boilers are easier to start up and control during cyclic operation than once-through boilers. Accordingly, fossil boilers designed for daily cycling are drum boilers.
(2) Pump-assisted circulation boilers permit the use of flow resistors to assure adequate flow to each boiler tube even when cloud shadowing reduces heat absorption to zero at some locations while maintaining the maximum absorption at other locations. Pump-assisted circulation fossil boilers are used when the characteristics of the fuel being burned result in the possibility of large local reductions in absorption.

The choice of the physical arrangement of the heat transfer surfaces could only be partially based on fossil technology. The furnace section of all modern fossil boilers, including those used for cycling service, is fabricated from membrane panel walls cooled by a steam-water mixture. The furnace section operates at pressures, temperatures, and absorption rates that equal or exceed the design requirements for the solar boiler. This experience is the basis for selecting membrane panel construction for the boiler section of the solar steam generator.

Fossil boiler superheaters are generally either horizontal or vertical tube banks in the combustion gas path. The superheater tubes are primarily heated by convection with a relatively uniform heat flux around the circumference. For the solar steam generator, however, heat transfer to the superheater tubes is by radiation alone, ruling out the use of tube banks.

The major factors influencing the choice of the superheater configuration are as follows.

(1) The flow circuit arrangement should reduce the effect of heat absorption differences on steam temperature.
(2) The physical arrangement should allow the superheater tubes to expand freely during changes in tube average temperature.
(3) The superheater tube, header, and support geometry should allow the superheater tube to deflect when it is subjected to the temperature gradients caused by one-sided radiant heating.
(4) The superheater should be modular so that it can be shop fabricated to reduce erection costs.

A modular superheater with horizontal tangent tubes and vertical headers has been selected to meet these objectives. There are three flow circuits arranged in a "checkerboard" pattern so that the flow path approximates a one turn helix. Each of the three circuits passes through both low and high heat absorption zones, balancing the total heat absorption and exit steam temperatures in each circuit. The tube support concept permits

relatively free thermal expansion while maintaining the alignment of the superheater tubes. The module size was selected to allow truck shipment.

Fossil boiler superheaters use the lowest cost tube material that meets the design requirements. More than one material is commonly used since metal temperatures vary considerably. The location of the solar steam generator superheater surfaces in the upper half of the cavity and the steam temperature balancing effect of the "checkerboard" flow circuitry results in metal temperatures well within the range of standard fossil boiler tube materials. Croloy 2-1/4, a low alloy steel, has been selected for the superheater tube material rather than the much more expensive stainless steel or nickel alloy high temperature materials. Cost and reliability of both shop and field fabrication is further improved by using Croloy 2-1/4 because heat treatment is not required as it would be for stainless and nickel alloy tubes. An additional advantage is that the thermal expansion of Croloy 2-1/4 closely matches the expansion of the low alloy steels used for the remainder of the pressure parts and for the support devices. If stainless tubes were required, thermal expansion mismatches would result unless stainless steel were used for headers and support attachments where it might not otherwise be required. Further, the vast majority of fossil boiler superheater tubes, including those used in cycling boilers, are fabricated from low alloy steels such as Croloy 2-1/4.

Perhaps the most important consideration to be made in justifying the steam generator design is that the design which is presented fully satisfies the design requirement to produce steam at the required pressure and temperature while absorbing all the available energy from the heliostat field. The details of the performance of the receiver subsystem, and specifically the steam generator, are presented in the following sections.

Section 3

DETAILED RECEIVER SUBSYSTEM DESCRIPTION

This section presents a detailed description of the preliminary design of the major elements which constitute the integral receiver subsystem. The design requirements, or function, of each element are considered, alternative design considerations are summarized, and a description of the element is developed. The performance, operation and control of the elements are discussed when appropriate and other data supporting the preliminary design of the elements are provided.

The major elements of the receiver subsystem are the receiver steam generator, the steam generator housing and support structure, and the receiver support tower. These are discussed in the following subsections.

STEAM GENERATOR

This section of the report describes the Pilot Plant Solar Steam Generator. An overall viewpoint is presented in the first six subsections which discuss the design approach, requirements, general description and physical arrangement, design justification, and performance characteristics. The remaining subsections provide detail on the individual components, functional performance, upset conditions, stress analysis, material selection, operation, instruments and controls, and concludes with a comparison to the SRE steam generator. The preliminary design presented here indicates that steam generators can be designed to meet the technical requirements of the 10 MWe Solar Pilot Plant.

Design Approach

To meet the schedule established by ERDA for Phase I of the Central Receiver Program, the steam generator was designed using existing technology. The schedule did not permit design optimization; instead, the primary emphasis has been to achieve a reliable design, on schedule, by using state-of-the-art fossil boiler technology.

The Pilot Plant steam generator for the most part is scaled up from the Subsystem Research Experiment (SRE) steam generator. The overall arrangement, flow circuit, boiler and superheater tubes, drum and the attemperator are directly related to the SRE. The major refinement in the design is the substitution of a modular, horizontal tangent tube superheater in place of the SRE helical superheater. This change was made to allow shop fabrications of large sections of the superheater. Thermal stresses are also reduced because of the greater flexibility of the modular superheater.

A detailed analysis of the space and time characteristics of partial cloud shadowing of the heliostat field is not available. Therefore, the steam generator design is based on incident energy calculated with clear air models. Design margins consistent with fossil boiler practice have been factored into the design. Several idealized cloud shadows were defined and used to estimate the magnitude of cloud shadowing that can be tolerated before the steam generator design limits are exceeded.

The steam generator pressure parts are designed to meet the requirements of the ASME Code, Section I, Power Boilers. Since Section I does not specifically address cyclic operation at elevated temperatures, the elastic analysis methods of ASME Code Case 1592 were applied to the superheater. This analysis identified the need for inelastic analysis to assess creep-fatigue damage for areas of the superheater operating above 526°C (950°F). However, the required inelastic analysis was considered to be beyond the scope of this preliminary design.

The structure was analyzed for static equivalent seismic loads of 3g's. As shown in the subsection discussing the dynamic analyses of the receiver tower, steam generator component responses can be limited to this level if their natural frequency is high enough. The dynamic analysis required to assure sufficiently high natural frequencies was also considered to be beyond the scope of this preliminary design.

The steam generator design and performance characteristics are based on preliminary heat flux and turbine heat balance data. The difference between the preliminary data and the final data is small and is not expected to significantly alter performance.

Requirements

Solar steam generators must be designed with consideration given to two unique operating conditions:

- The steam generator will be subjected to an unusually large number of stress cycles during the 30-year design life. In addition to the diurnal cycle, the solar energy will be interrupted by clouds and by the requirement to stow the heliostats in high winds.

- The steam generator is located on top of a tower where wind and seismic loads can be more severe than at ground level.

Since solar steam generators must be designed for significantly more thermal cycles than fossil or nuclear steam generators, particular care must be taken to minimize fatigue, creep and thermal stress.

The steam generator configuration and the radiation properties of the heat transfer surfaces must be selected to maximize effective absorptance so that the cost of heliostats can be kept to a minimum.

Response to changes in solar insolation must be rapid and stable so that the steam generator can be controlled to "follow the sun" while supplying steam at design conditions, thus maximizing the conversion of solar to thermal energy.

The steam generator structure must be designed for wind and seismic loads that are higher than for an equivalent sized fossil or nuclear steam generator located on the ground. Wind velocity increases with height, and the ground level seismic accelerations are amplified by the receiver tower.

Functional Requirements - The steam generator is required to efficiently and reliably absorb solar energy and transfer it to the steam-water working fluid. Steam pressure, temperature, and flow at the superheater outlet nozzle must meet the requirements established for supplying steam to the Electrical Generation Subsystem. These conditions are summarized for the Pilot Plant as follows:

	Pressure MPa (psia)	Temperature °C (°F)	Flow kg/min(lbs/hr)
Design (12/21/2PM)	10.6 (1540)	516 (960)	827 (109,332)
Maximum (3/21/12PM)	11.0 (1600)	516 (960)	1017 (134,429)

The steam generator must supply steam at both the design and maximum conditions while accepting all the incident energy available from the heliostat field. Although no specific requirements have been established for other conditions, the steam generator should be capable of accepting all the available energy over a wide range of solar times. Defocusing of heliostats may be required during the earlier phases of startup, the latter phases of shutdown, or when a significant portion (~23%) of the heliostat field is shadowed by clouds.

The permissible rate of temperature change must be on the order of 389°C (700°F) per hour to allow design steam pressure and temperature to be reached about one hour after hot startup.

Physical Requirements - To enhance effective absorptance, the steam generator heat transfer surface and ceiling are required to form the inner walls of the receiver cavity. These surfaces are also required to have an absorptance of 0.9 to further increase efficiency.

The internal diameter and height of the cavity were established as a function of the heliostat field and tower configuration to obtain the required aperture area and cavity efficiency. The steam generator is required to conform to the dimensions shown in Figure 3-1 and summarized as follows:

Diameter, m (ft)	14.93(49)
South side height, m (ft)	16.46(54)
North side height, m (ft)	14.63(48)

Heat Absorption Requirements - The design heat fluxes for the steam generator are established by the geometrical arrangement of the heliostat field, the height and diameter of the aperture aim circle, the cavity dimensions and the surface absorptance. Peak design heat fluxes are:

	kW/m^2 ($Btu/hr-ft^2$)
Design (12/21/2PM)	258 (81800)
Maximum (3/21/12PM)	263 (83400)

Figure 3-2 shows the variation in heat flux around the cavity circumference at a height of 4.57m (15 ft). The variation from top to bottom of the cavity is shown by Figure 3-3.

Structural Requirements - The requirements for the steam generator structure are determined by:

1. Live and dead weight loads,
2. Wind loads on the receiver housing transferred directly to the steam generator structure*, and

*Wind loading is insignificant compared to the high seismic load.

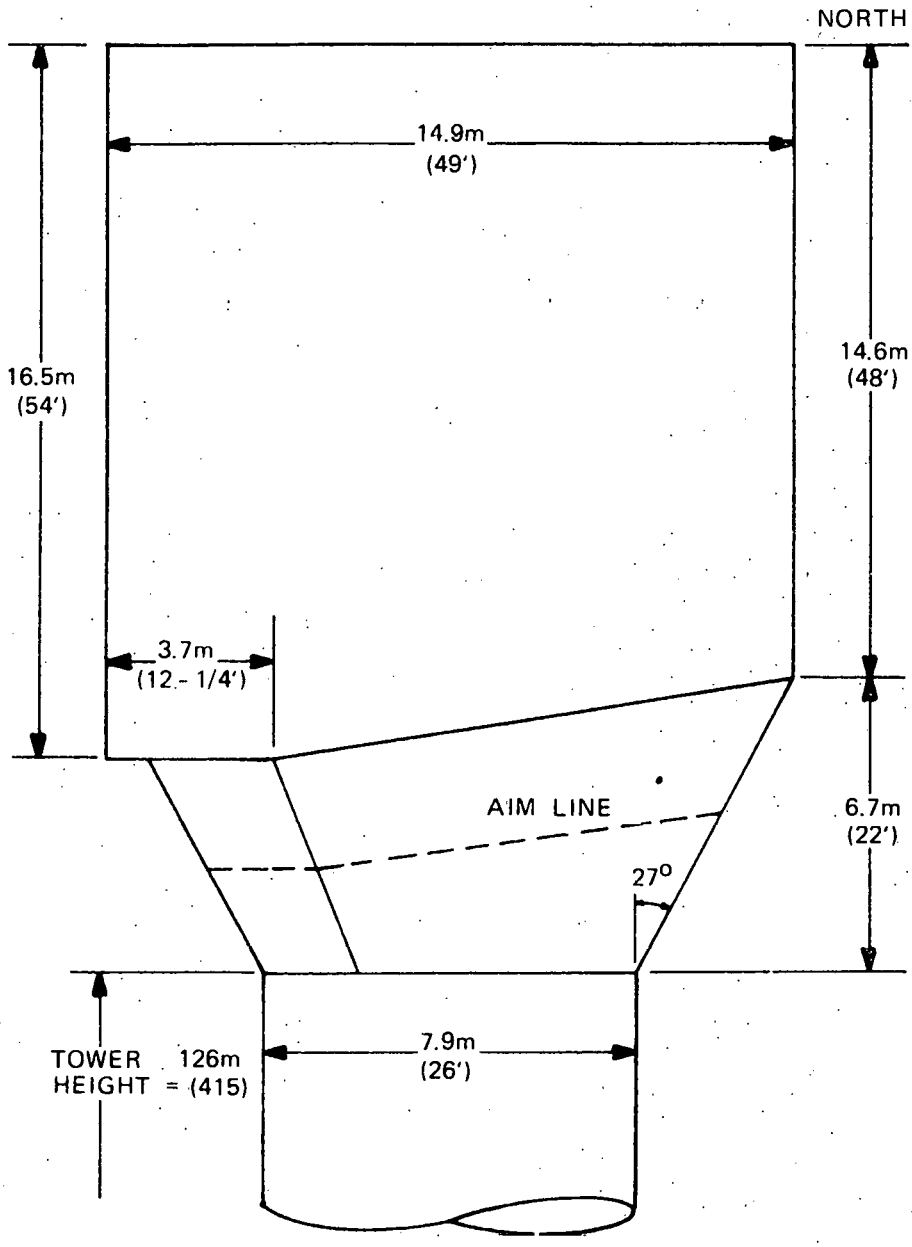

Figure 3-1. Receiver-Cavity Configuration

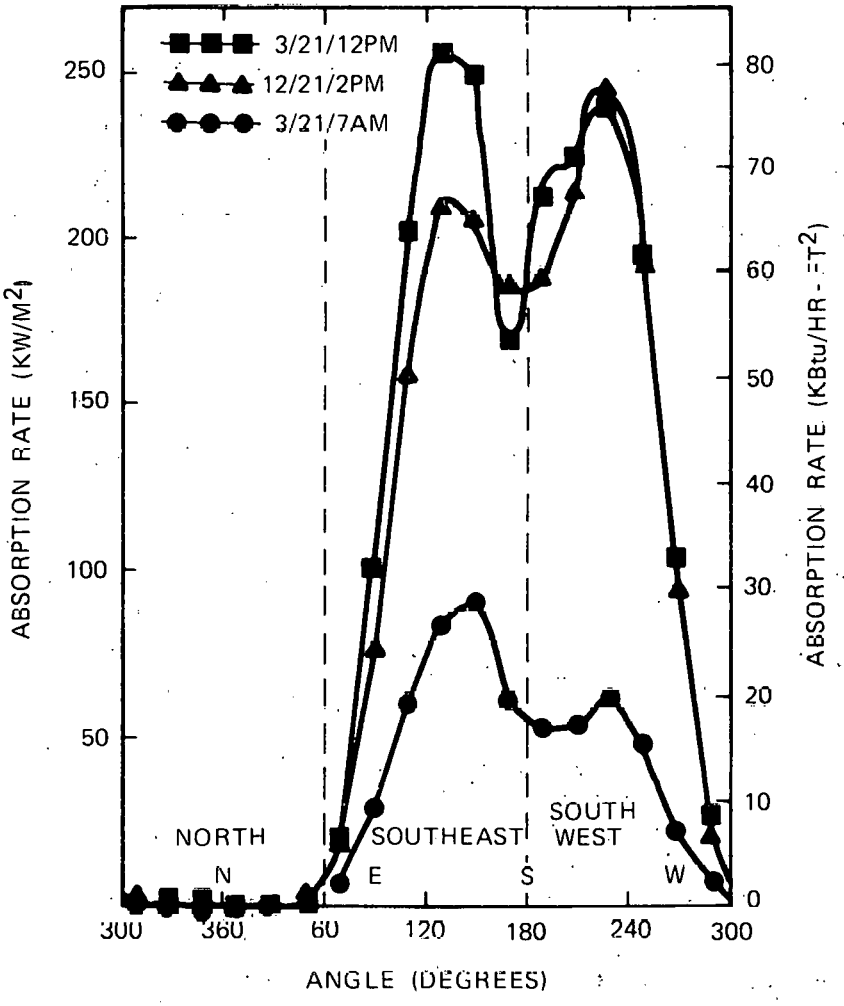

Figure 3-2. Absorption Rate versus Angle, Elevation - 4.57m (15 ft)

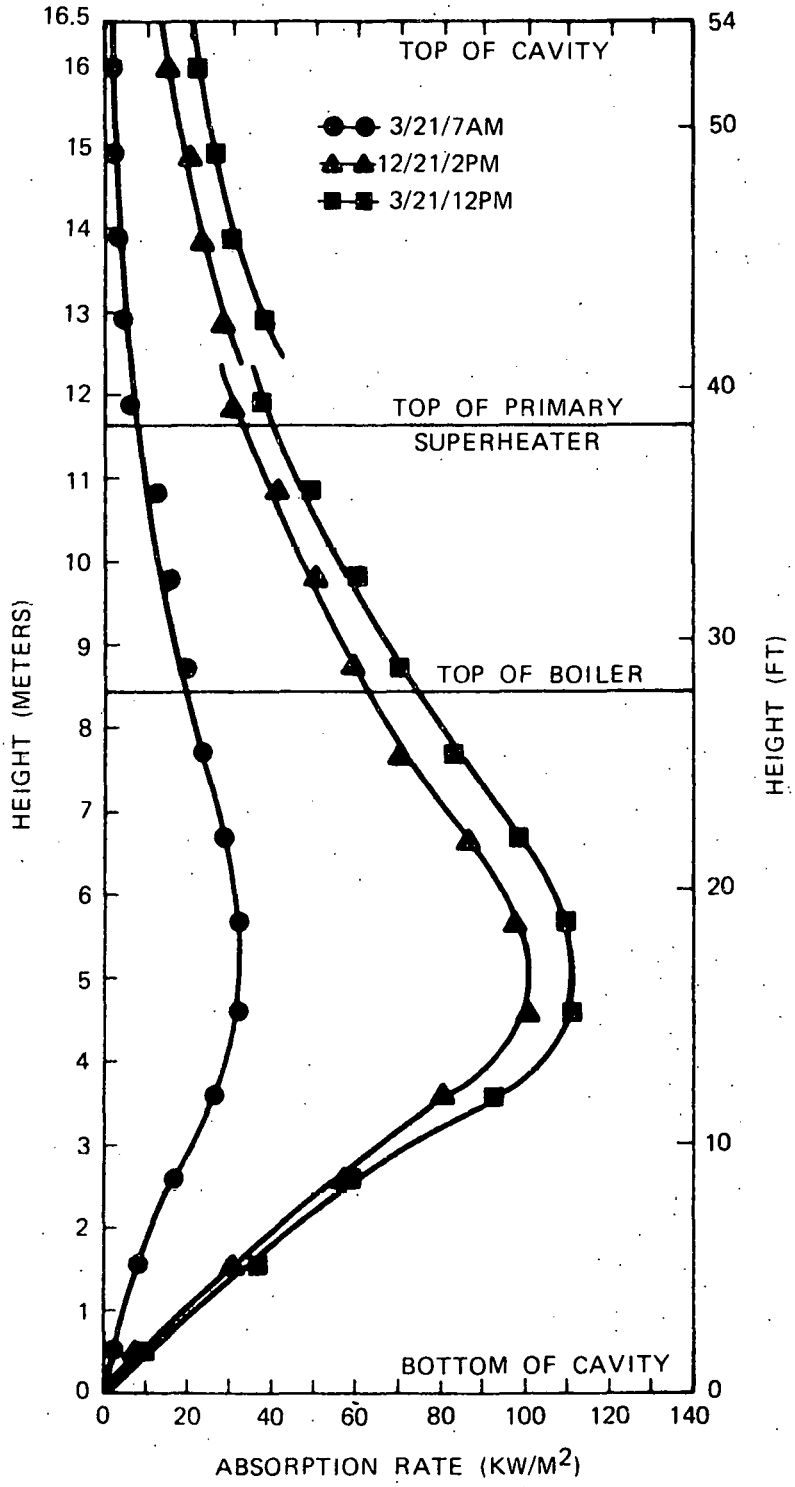

Figure 3-3. Average Circumferential Absorption Rate versus Height

3. Seismic loads transferred from the corbels to the steam generator structure. The structure was designed to withstand a static equivalent load of 3g's.

General Description

The steam generator heat transfer surface is a polygon having eighteen 20-degree segments that form the interior walls of the receiver cavity. This geometry traps reflected and reradiated energy to increase cavity effective absorptance. The absorptance of the heat transfer surface is about 0.9 and is achieved by allowing natural oxidation to occur. Reradiation is minimized by locating the cooler heat transfer surfaces near the bottom of the cavity and the higher temperature surfaces at the top.

The steam generator is thoroughly insulated to minimize conduction losses and, in the absence of wind, the bottom opening cavity does not allow the buoyant hot air to escape, minimizing natural convection losses. The cavity efficiencies for zero wind velocity are tabulated below:

	Efficiency*
Design (12/21/2PM)	0.914
Maximum (3/21/12PM)	0.916

The steam generator is a pump-assisted recirculating drum boiler with two superheaters and a spray attemperator for controlling steam temperature (Figure 3-4). Feedwater is piped into the steam generator drum. Slightly subcooled water flows from the drum, through a downcomer, and is pumped through the boiler supply line to the boiler section.

The water is distributed to the boiler section where steam generation takes place. A saturated steam-water mixture at an average quality of ten percent (at maximum conditions) exits the boiler section and flows through the risers to the steam drum where the water and steam are separated by cyclone separators and scrubbers.

Moisture free steam from the drum flows through the saturated steam lines to the primary superheater where it is heated to about 475°C (887°F).

The steam exiting the primary superheater passes through the spray attemperator where additional feedwater is injected as required to control exit steam temperature.

The attemperated steam enters the secondary superheater at about 375°C (707°F) where it is heated to 515°C (960°F).

Table 3-1 lists steam pressure, temperature, and flow at various points in the steam generator flow circuit for 3/21/7AM, 3/21/12PM, and 12/21/2PM.

*Based on preliminary heat flux and turbine heat balance data.

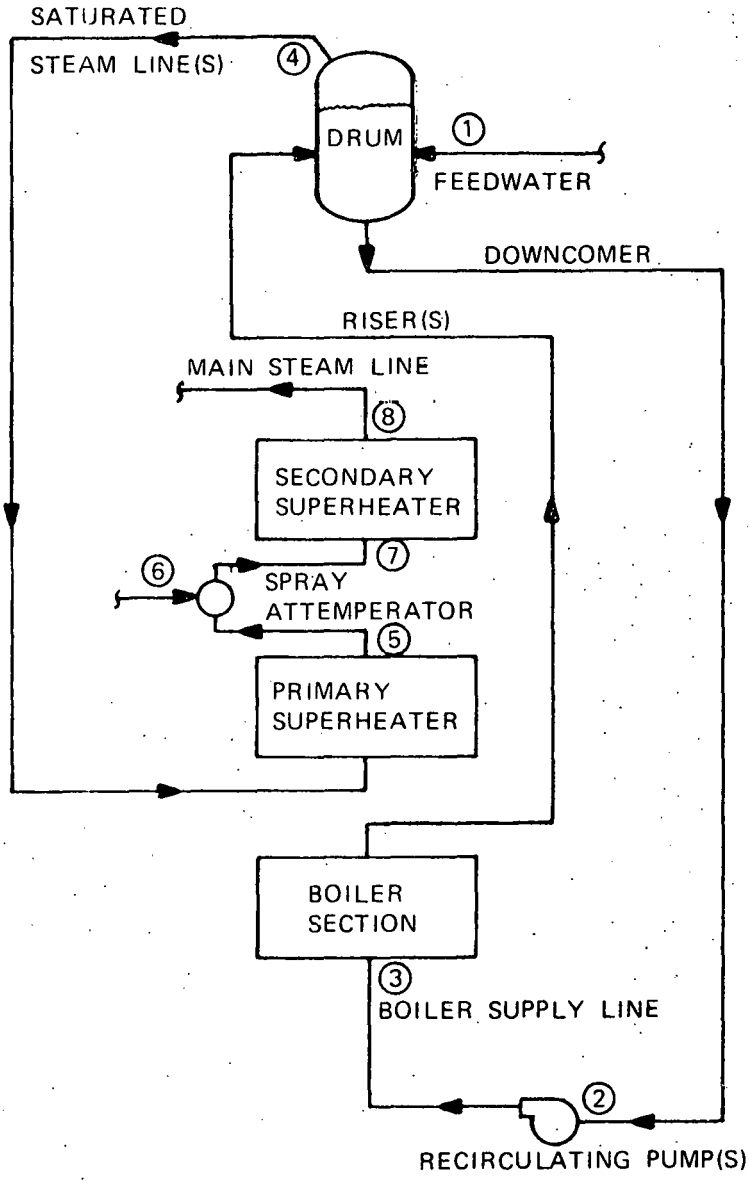

Figure 3-4. Steam Generator Flow Circuit

Table 3-1. Nominal Steam Conditions*

Time	3/21/7AM			3/21/12PM			12/21/2PM		
Location	P,MPa (psia)	T,°C (°F)	W,Kg/min (lb/hr)	P,MPa (psia)	T,°C (°F)	W,Kg/min (lb/hr)	P,MPa (psia)	T,°C (°F)	W,Kg/min (lb/hr)
① ** Feedwater		116 (241)	228 ($30.1x10^3$)		179 (353)	928 ($122.6x10^3$)		171 (339)	799 ($105.6x10^3$)
② Pump Inlet	10.33 (1499)	310 (590)	10280 ($1358x10^3$)	11.78 (1709)	315 (597)	10280 ($1358x10^3$)	11.36 (1649)	313 (594)	10280 ($1358x10^3$)
③ Pump Discharge	10.67 (1549)	310 (590)	10280 ($1358x10^3$)	12.12 (1759)	315 (597)	10280 ($1358x10^3$)	11.71 (1699)	313 (594)	10280 ($1358x10^3$)
④ Drum Discharge	10.20 (1480)	313 (595)	228 ($30.1x10^3$)	11.64 (1690)	322 (613)	928 ($122.6x10^3$)	11.23 (1630)	320 (608)	799 ($105.6x10^3$)
⑤ Primary Outlet	10.18 (1478)	480 (897)	228 ($30.1x10^3$)	11.33 (1645)	461 (863)	928 ($122.6x10^3$)	11.00 (1597)	461 (862)	799 ($105.6x10^3$)
⑥ Attemperator Spray		116 (241)	9.1 ($1.2x10^3$)		179 (353)	102 ($13.5x10^3$)		171 (339)	74 ($9.8x10^3$)
⑦ Secondary Inlet	10.15 (1473)	439 (823)	237 ($31.3x10^3$)	11.30 (1640)	378 (712)	1030 ($136.1x10^3$)	10.97 (1592)	390 (733)	874 ($115.4x10^3$)
⑧ Secondary Outlet	10.14 (1471)	515 (960)	237 ($31.3x10^3$)	11.02 (1600)	515 (960)	1030 ($136.1x10^3$)	10.77 (1563)	515 (960)	874 ($115.4x10^3$)

* These conditions are based on preliminary turbine heat balance data.
** Numbers are referenced to Figure 3-4.

Physical Arrangement

Figure 3-5 is a schematic illustration of the arrangement of steam generator and its relationship to the receiver tower.

The placement of the boiler and superheaters in the cavity was selected to match the heat flux patterns within the cavity. The flux patterns are determined primarily by the geometry of the heliostat field, tower height, aperture area and the geometry of the cavity itself. Essentially, energy from the outermost heliostats is incident on the lower part of the cavity while the innermost heliostats provide the energy for the upper part of the cavity. Since there are more heliostats in the outer portion of the field, incident energy peaks in the lower part of the cavity and tapers off towards the top (Figure 3-3).

To take advantage of this characteristic, the boiler section, which can be designed to operate at high heat fluxes because it is effectively cooled by a saturated steam water mixture, is located in the lower half of the cavity. The first stage, or primary superheater, which receives saturated steam from the drum, is located in the middle portion of the cavity where heat flux and steam temperatures are moderate. The second stage or secondary superheater, which receives higher temperature steam from the spray attemperator, is located in the upper portion of the cavity where heat flux is low. As a result of this arrangement of boiler and superheater surfaces, the maximum metal temperatures in the superheater are lowest where thermal stress is high and highest where thermal stress is low.

The cavity ceiling is insulated and most of the incident energy is either reflected or reradiated to the superheater or boiler.

The boiler and superheater heat transfer surface areas are determined by the requirements of the steam cycle and by the absorbed heat flux distribution within the cavity. The ratio of the energy required to produce saturated steam from the feedwater to the energy required to superheat the steam is 72% at design conditions.* Actually, the boiler surface has been sized to absorb only 65% of the total energy. The extra energy absorbed by the superheater is used to vaporize feedwater injected into the superheater circuit at the spray attemperator. At design conditions, the spray attemperator flow is 10% of the design steam flow.

As the sun changes position or as clouds partially shadow the heliostat field, the vertical distribution of energy changes within the cavity. Steam temperature at the exit of the second stage superheater can then be controlled by increasing or decreasing feedwater flow to the spray attemperator.

The boiler section heat transfer surface is an 18-sided polygon fabricated from membrane panels. It is 8.0 m (26'-3") high on the south side of the cavity and 6.17 m (20'-3") high on the north side. The boiler tubes are 2.223 cm (0.875 inch) outside diameter carbon steel with a minimum wall thickness of 0.376 cm (0.148 inch). Carbon steel membrane bars 0.635 cm (0.25 inch)

*Based on preliminary turbine heat balance data.

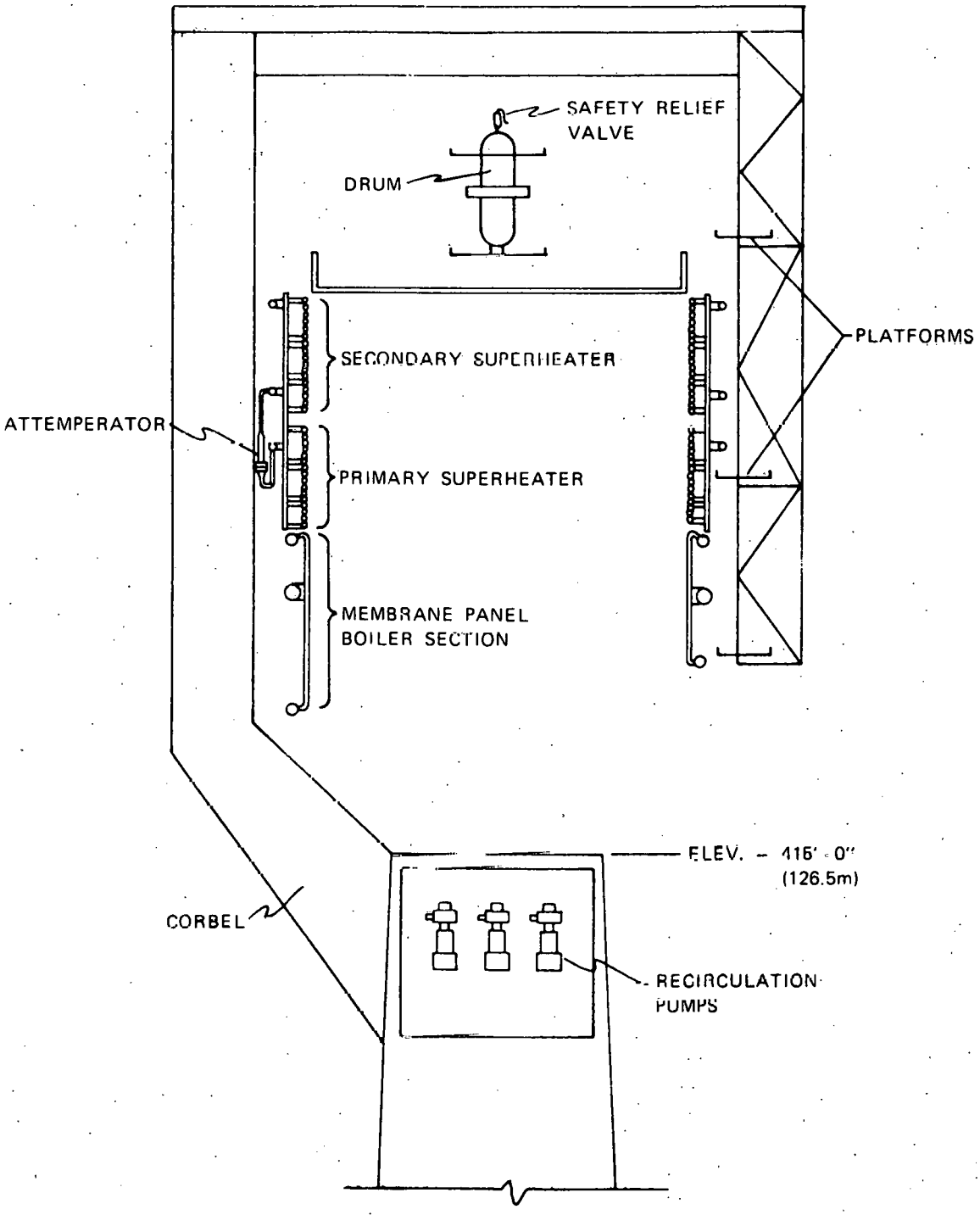

Figure 3-5. Pilot Plant Steam Generator Arrangement

thick are machine welded between adjacent tubes. The tube spacing for the five (5) panels on the cold north wall is 7.62 cm (3 inches) and 3.81 cm (1.5 inch) for the remaining panels.

The primary and secondary superheaters consist of three horizontal tangent tube modules. Each module has six (6) flat sides and covers 120° of the cavity circumference. The primary superheater is 3.17 m (10'-5") high and the secondary superheater is 4.775 m (15'-8") high. The superheater tubes are Croloy 2-1/4, 2.54 cm (1 inch) outside diameter with a 0.419 cm (.165 inch) minimum wall thickness.

The steam drum is vertical and contains seven (7) cyclone primary separators and secondary scrubber plates to effectively remove moisture from the saturated steam.

The steam generator structure consists of horizontal and vertical trusses, which transfer the live and dead weight loads from the steam generator pressure parts and the receiver environmental housing to the three receiver corbels. The steam generator structure has been designed to withstand a lateral static equivalent seismic load of three (3) g's. The steam generator is top-supported from the structure by hanger rods which are free to swing outward to accommodate thermal expansion.

The major physical characteristics of the steam generator are listed in Table 3-2.

Design Justification

To meet design requirements, the steam generator must produce superheated steam at subcritical pressure. Several types of steam generators based on fossil boiler technology can meet this requirement:

Natural circulation drum boiler

Pump-assisted circulation drum boiler

Once-through subcritical boiler

The choice of the pump-assisted circulation concept for the solar steam generator is based on extensive fossil boiler experience which indicates that:

- Drum boilers are easier to start up and control during cyclic operation than once-through boilers because a bypass system and the associated heat recovery equipment are not required. Accordingly, fossil boilers currently designed for daily cycling are drum boilers.

- Pump-assisted circulation boilers permit the use of increased pressure drop to assure adequate flow to each boiler tube even when cloud shadowing reduces heat absorption to zero at some locations while maintaining the maximum absorption at other locations. Pump-assisted circulation fossil boilers

Table 3-2. Physical Characteristics

• Cavity		
ID	14.9m	49'
Height	14.6-16.5m	48'-54'
• Superheater Connecting Piping ℄ Diameter	16.9m	55'-5-5/8"
• Drum	8.9cm Thk. x 1.2m ID x 4.3m h	3-1/2" Thk. x 4' ID x 14'h
• Boiler Section Height		
South Side	8.0m	26'-3"
North Side	6.2m	20'-3"
• 1st Stage SH Height	3.2m	10'-5"
• 2nd Stage SH Height	4.8m	15'-8"
• Weight		
Pressure Parts & Integral Supports	289198kg	637000 lbs.
Structure	312806kg	689000 lbs.

are used when the characteristics of the fuel being burned result in the possibility of large local variations in absorption that could result in the loss of natural circulation pumping head.

The choice of the physical arrangement of the heat transfer surfaces could only be partially based on fossil technology. The furnace section of all modern fossil boilers, including those used for cycling service, is fabricated from membrane panel walls cooled by a steam-water mixture. The furnace section operates at pressures, temperatures, and absorption rates that equal or exceed the design requirements for the solar boiler. This experience is the basis for selecting membrane panel construction for the boiler section of the solar steam generator.

However, fossil boiler superheaters are generally either horizontal or vertical multiple tube banks in the combustion gas path. The superheater tubes are primarily heated by convection with a relatively uniform heat flux around the circumference. For the solar steam generator, however, heat transfer to the superheater tubes is by radiation alone, ruling out the use of multiple tube banks.

The major factors influencing the choice of the superheater configuration are:

- The flow circuit arrangement should reduce the effect of heat absorption differences on steam temperature.
- The physical arrangement should allow the superheater tubes to expand freely during changes in tube average temperature.
- The superheater tube, header and support geometry should allow the superheater tube to deflect when it is subjected to the temperature gradients caused by one-sided radiant heating.
- The superheater should be modular so that it can be shop fabricated to reduce erection costs.

A modular superheater with horizontal tangent tubes and vertical headers has been selected to meet these objectives. There are three flow circuits arranged in a "checkerboard" pattern so that the flow path approximates a one turn helix. Each of the three circuits passes through both low and high heat absorption zones, balancing the total heat absorption and exit steam temperatures in each circuit. The tube support concept permits relatively free thermal expansion while maintaining the alignment of the superheater tubes. The module size was selected to allow truck shipment.

Fossil boiler superheaters use the lowest cost tube material that meets the design requirements. A superheater is commonly fabricated from more than one material since metal temperatures vary considerably. The location of the solar steam generator superheater surfaces in the upper half of the cavity and the steam temperature balancing effect of the "checkerboard" flow circuitry results in metal temperatures well within the range of standard fossil boiler tube materials. Croloy 2-1/4, a low alloy steel, has been selected for the superheater tube material rather than the much more expensive stainless steel or nickel alloy high temperature materials. Cost and reliability of both shop and field fabrication is further improved by using Croloy 2-1/4 because stress relief is not required for tube-to-tube welds as it would be for the stainless and nickel alloys. An additional advantage is that the thermal expansion of Croloy 2-1/4 closely matches the expansion of the low alloy steels used for the remainder of the pressure parts and for the support devices. If stainless tubes were required, thermal expansion mismatches would result unless stainless steel were used for headers and support attachments where it might not otherwise be required. The vast majority of fossil boiler superheater tubes, including those used in cycling boilers, are fabricated from low alloy steels such as Croloy 2-1/4.

However, if detailed analysis of cloud shadowing data indicates that the solar steam generator must operate with local heat absorptions reduced to near zero over 20 percent or more of the surface area, it may be necessary to use stainless steel tubes where peak metal temperatures exceed 593°C (1100°F) or to actively control heliostats to maintain metal temperatures within the limits for Croloy 2-1/4.

Performance Characteristics

The solar steam generator meets the design requirement to produce steam at the required pressure and temperature while absorbing all the available energy from the heliostat field. Figure 3-6 shows the percentage of power absorbed by the boiler and superheater sections as a function of solar time. The distribution is nearly constant except at low incident energy levels in the morning and evening when the percentage of energy absorbed by the superheater falls off. This happens because energy losses from the superheater are relatively independent of incident energy.

Figure 3-7 presents steam flow and attemperator flow as a function of absorbed energy. All the data are grouped together indicating that the attemperator provides an effective means of controlling steam temperature. Attemperator spray flow falls off to zero at about 8 MW absorbed energy. Below this absorption level, steam temperature will drop below 515°C (960°F). However, energy inputs this low occur for only a short time in the morning and evening.

Steam temperatures are presented as a function of absorbed power in Figure 3-8. Steam temperature at the attemperator exit increases rapidly at low power levels consistent with the observation noted previously.

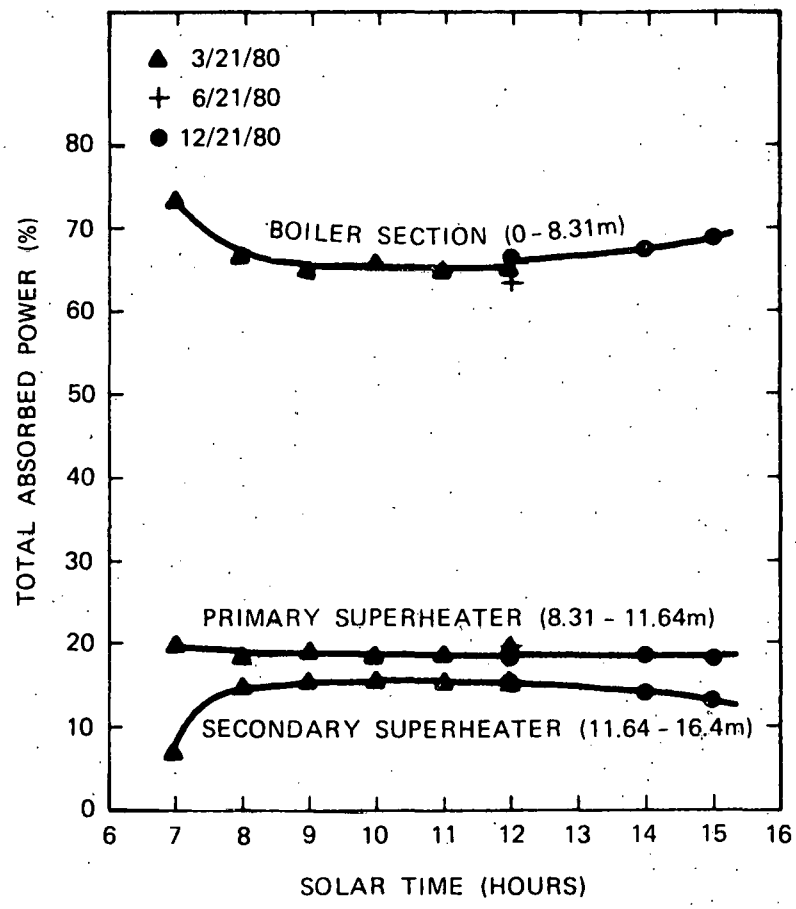

Figure 3-6. Absorbed Power Distribution versus Time

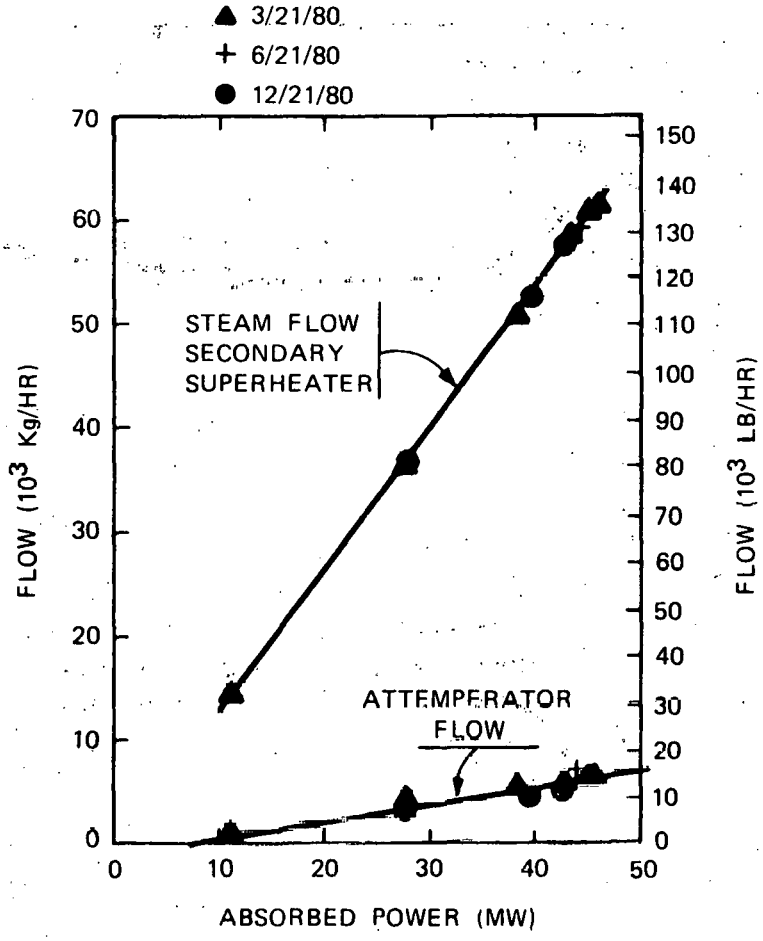

Figure 3-7. Flow versus Total Absorbed Power

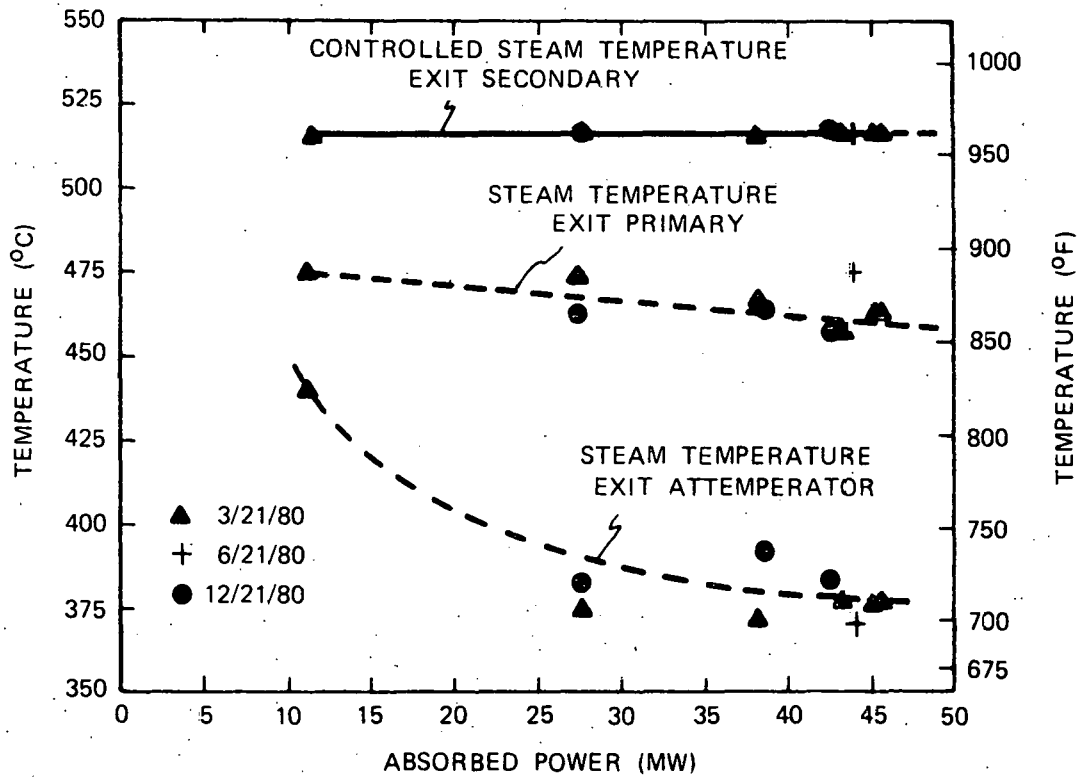

Figure 3-8. Steam Temperature versus Absorbed Power

The performance characteristics shown in Figures 3-6, 3-7 and 3-8 demonstrate that the selected boiler/superheater interface results in good control of steam temperature over a wide range of solar times when the steam generator is supplying steam to the turbine alone.

The steam generator can also produce 515°C (960°F) steam with clouds partially shadowing the heliostat field or with feedwater temperatures which vary from design. Table 3-3 summarizes the range of cloud shadowing that can be tolerated at 3/21/12PM without exceeding design limits on spray attemperator flow or peak superheater metal temperatures.

Table 3-3. Range of Operation with Cloud Shadowing

Case	Description	Reduction in Boiler Absorption	Reduction in Superheater Absorption	Reduction in Total Absorption	Limit
1	Cloud shadows boiler section	20%	0	13%	Metal Temperature
2	Cloud shadows top of superheater	0%	25%	8.75%	Metal Temperature
3	Cloud shadows part of all surfaces	23%	23%	23%	Metal Temperature

Table 3-4 illustrates that steam temperature can be controlled by spray flow without defocusing heliostats over a wide range of feedwater temperatures.

Table 3-4. Attemperator Spray Flow Required to Control Steam Temperature

Case	Description	Feedwater Temperature C, (F)	Spray Flow kg/s (lb/hr)	Steam Flow kg/s (lb/hr)	Absorbed Energy Mw
4	Operation with high pressure feedwater heater out of service	111* (232)	124.6 (16460)	939 (124060)	45.3
5	Feedwater temperature based on revised turbine heat balance data	215 (419)	86.5 (11430)	1098 (145070)	45.3
6a	Steam to thermal storage alone, maximum absorbed energy	140* (285)	8.2 (1085)	966 (127600)	45.3
6b	Steam to thermal storage alone, low absorbed energy	140* (285)	120.7 (15950)	235 (31000)	11.0

*Preliminary turbine heat balance.

These results indicate that steam temperature could be controlled without defocusing heliostats if the high pressure feedwater heater were out of service (Case 4), or if feedwater temperature were increased because of a higher cycle efficiency (Case 5). Steam temperature can also be controlled without defocusing heliostats over a range of absorbed energy when steam is supplied to Thermal Storage alone (Case 6).

Components

The following subsections of the report describe the physical arrangement of the steam generator components. Noteworthy features are illustrated by schematic drawings and tables included in the text. Drawings showing the arrangement of the structure, the steam generator pressure parts, the boiler section, the superheaters and the drum are included in Appendix C, along with tables specifying pressure part size, material and weight.

A brief description of the function of each component is also included. Additional details may be found in the Functional Performance and Stress Analysis subsections.

Boiler Section - There is practically no heat input to the north half of the boiler wall because none of the heliostats in the south field are aimed at the boiler section. However, heat flux on the south half of the boiler wall is quite high. In order to balance flow and heat absorption it was necessary to divide the boiler section into eight (8) flow circuits (Figure 3-9). Each circuit includes a supply tube(s), a hand valve for adjusting flow resistance, a flow orifice meter, an inlet header, membrane panel heat transfer surface, an outlet header, and a riser which returns the steam-water mixture to the drum. The headers and the heat transfer surface form one continuous welded structure to achieve strength and rigidity. Separate circuits are formed by inserting diaphragms in the inlet and outlet headers and providing separate supply tubes and risers for each circuit. The size of each circuit varies and has been selected to achieve a balance between flow and heat input.

The boiler circuits are identified in the following table:

Circuit	N	EN	ES	SE	S	SW	WS	WN
Begins at	310°	50	90	130	170	190	230	270
Ends at	50	90	130	170	190	230	270	310

The boiler section walls (see Figure 3-10) are constructed from flat membrane wall sections composed of panels of a single row of tubes connected by continuously welded membrane bars along the centerline of each tube. This produces a rugged, continuous, pressure-tight wall capable of transferring a large amount of heat. The width and maximum length of the individual panels [2.63m (8'-7½")] and 7.86m (25'-9½")] are suitable for economical manufacture and assembly. The inlet and outlet headers are attached in the shop prior to shipment for field assembly. This type of membrane wall construction is similar to that used in the furnace walls of all modern fossil boilers.

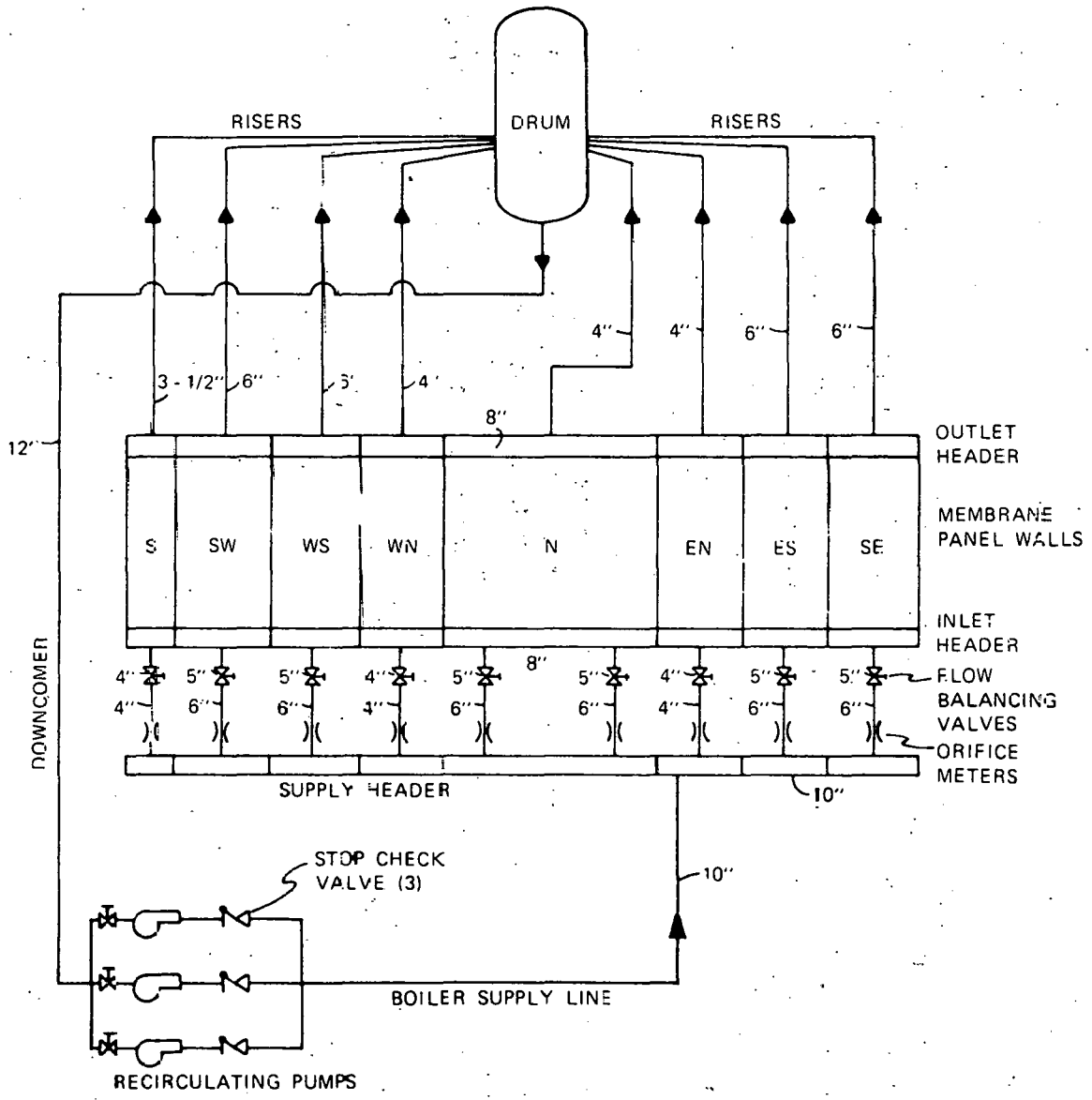

Figure 3-9. Boiler Section Flow Circuits

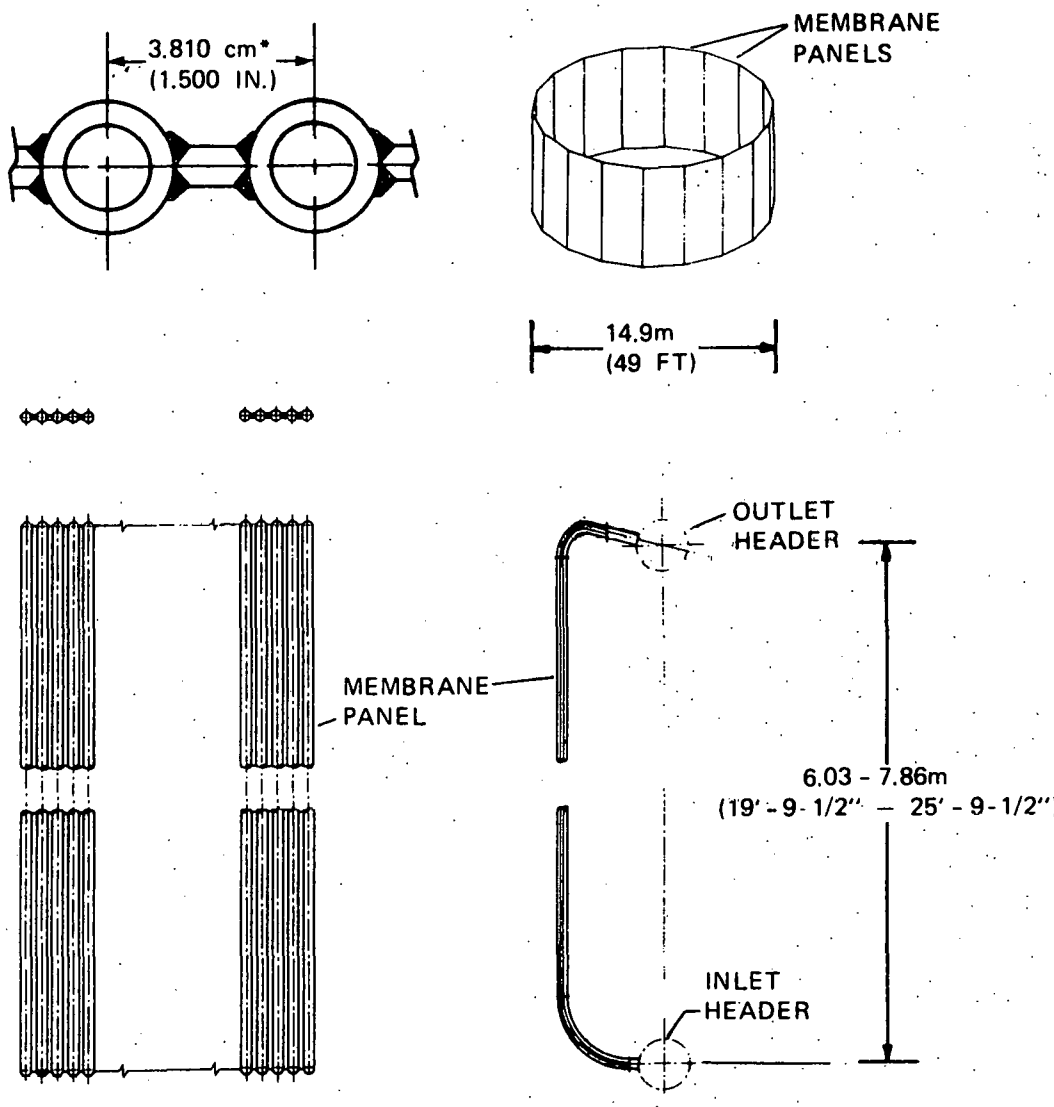

SPECIFICATIONS:

TUBE:

O.D.	2.223 cm (.875 IN.)
MIN. WALL	0.376 cm (0.148 IN.)
MAT'L.	SA 210 GRADE A1CF

WEB:

THICKNESS	.635cm (0.25 IN.)
MAT'L.	CARBON STEEL (C1015 C.F.)

*7.62cm (3.0 INCH) ON NORTH WALL

Figure 3-10. Boiler Section

The boiler tubes have an outside diameter of 2.223 cm (0.875 inches) and a minimum wall thickness of 0.376 cm (0.148 inches). In the north panel with low heat flux, the tubes are spaced on 7.62 cm (3 inch) centers while for the other circuits the centerline spacing is 3.81 cm (1.5 inch). The closer spacing on the hot walls is necessary to maintain maximum wall temperatures below 425°C (797°F). Both the tubes and the web are carbon steel.

The receiver cavity aperture is larger on the north side than on the south. The height of the membrane panels varies accordingly. The five (5) panels in the north circuit are 6.03m (19'9½") high and the remaining panels vary in height up to a maximum of 7.86m (25'9½") in the south circuit.

Superheaters - Both the primary and secondary superheaters consist of three horizontal, tangent tube, shop fabricated modules with vertical inlet and outlet headers (Figure 3-11). Each module covers one-third (120°) of the cavity surface. The vertical headers are divided into three equal length segments by diaphragms so that, in effect, each module has three distinct flow paths. The superheater tubes are Croloy 2-1/4 with an outside diameter of 2.54 cm (1 inch) and a minimum wall thickness of 0.419 cm (0.165 inch).

The superheater supports and lateral restraints are designed to permit the superheater module to freely expand to operating temperatures at which point the vertical headers and the mid-point of the tube span are restrained from further growth.

The shipping envelope for one module is about 3.2m (10'6") high x 4.11m (13'6") wide x 13.7m (45 ft) long which is satisfactory for truck shipment with special handling.

Drum and Internals - A vertical drum with cyclone separators and scrubber plates has been selected for the solar steam generator. Either a vertical or horizontal drum could be designed to meet the steam separation and water storage requirements of the solar steam generator. However, the vertical drum provides a convenient arrangement for collecting the risers which are distributed uniformly around the circumference of the circular steam generator. Furthermore, the flow and steam quality in the risers from the eight boiler circuits vary considerably, and the vertical drum was easily provided with a centrally located plenum to uniformly distribute the steam-water mixture to the seven (7) cyclone separators. The separators are longer than normal to accommodate the wide range of water levels that will occur during sudden cloud shadowing. The drum is fabricated from a 8.9 cm (3.5 inch) thick 122 cm (48 inch) inside diameter SA-299 forging. The pressed hemispherical heads are 7.6 cm (3.0 inches) thick. These wall thicknesses provide reinforcement for the feedwater, downcomer, riser, saturated steam and safety valve connections. The upper and lower heads are provided with manholes for inspection of the internals.

The cyclone separators are 28.6 cm (11-1/4 inches) outside diameter and 118.7 cm (46-3/4 inches) high. The separators are fabricated from carbon steel and are similar to separators used in fossil and nuclear applications. The scrubbers

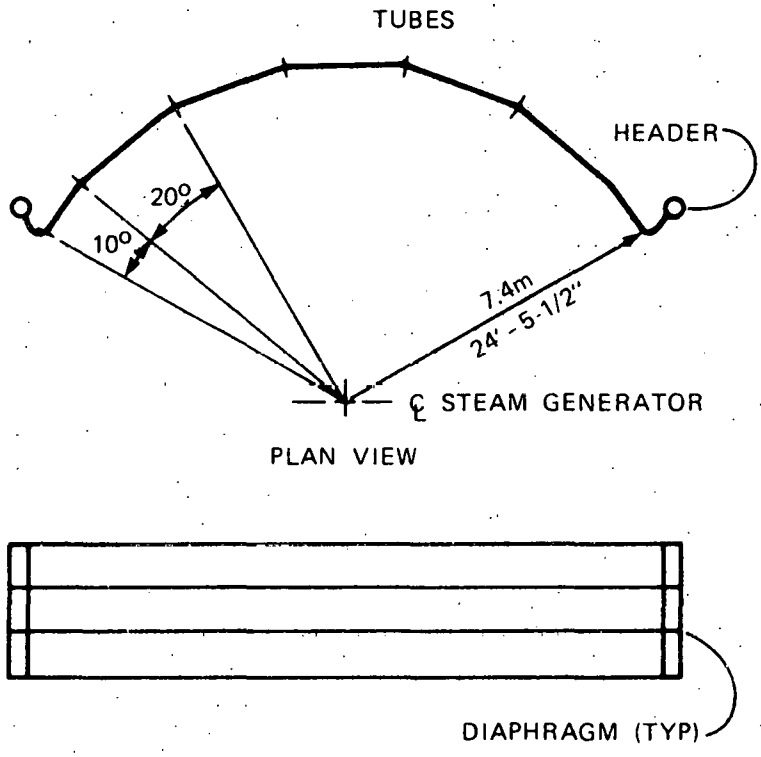

SPECIFICATIONS

TUBES:		HEADERS:	
OD	2.54cm (1.0 IN.)	OD	16.8cm (6.675 IN.)
MIN WALL	0.419cm (0.165 IN.)	MIN WALL	3.27cm (1.286 IN.)
MAT'L	SA 213 T22	MAT'L	SA 335 P22
NO TUBES	126 PRIMARY 189 SECONDARY		

Figure 3-11. Superheater Module

provide 0.746m^2 (8-ft^2) of cross-sectional area for secondary moisture removal. The pressure drop through the cyclone separators is 0.0083 MPa (1.2 psi) as maximum steam flow.

The steam-water mixture from the boiler circuits flows upward through eight (8) risers. The risers penetrate the drum at two levels and discharge to a vertical distribution plenum centered in the drum. The steam-water mixture flows up through the plenum and is admitted tangentially to the cyclone separators developing centrifugal forces many times the force of gravity. The higher density water forms a layer against the cylinder walls, and the lower density steam moves to the center of the separator and flows upward. The water flows downward and is discharged at the bottom of the separator, below the water level, where it mixes with feedwater. The feedwater enters the drum through an 11.4 cm (4.5 inch) nozzle attached to the drum shell by a thermal sleeve.

The water returning from the drum through the downcomer is slightly subcooled and virtually free of steam bubbles assuring that maximum net positive suction head is available for the recirculating pumps.

The steam exiting the top of the separators contains approximately 10% moisture, which is removed by corrugated plate secondary scrubbers installed near the top of the drum. The scrubbers provide a large surface which intercepts water particles as the steam flows between the closely fitted plates. Steam velocity is very low to avoid re-entrainment of water. The collected water is drained from the bottom of the scrubber assembly to the water below.

The combination of cyclone separators and scrubbers provides the means for obtaining steam purity corresponding to less than 1.0 ppm solids content. Steam of this purity is required to avoid deposition in the superheater of solids entrained in the water droplets. If deposition were to occur, superheater tube temperature would increase resulting in distortion and burnout of the tubes. High purity steam is also required to prevent deposits on turbine blades.

Water level indication is used as a control element to increase feedwater flow (low water level) or reduce feedwater flow (high water level). The water level in the drum will vary during changes in pressure and heat input to the boiler section. This change in water level, called "shrink and swell", is proportioned to the steam volume in the boiler section and risers. Table 3-5 lists the actions initiated by high and low water levels [60 cm (23.6 inches)].

Recirculating Pumps - The recirculating pumps are Hayward Tyler glandless boiler circulating pumps (Figure 3-12). These pumps have been used for pump-assisted drum boilers since 1944. Three 8x8x15 pumps are provided, each rated at 7,560 liters/min (2,000 gpm) and 53.3 meters (175 feet) head with an efficiency of about 80% at design conditions. The NPSH required is 9.14m (30 ft) and each pump weighs about 5,902 kg (1300 lbs). Two of the pumps are in operation at all times; the third is a spare.

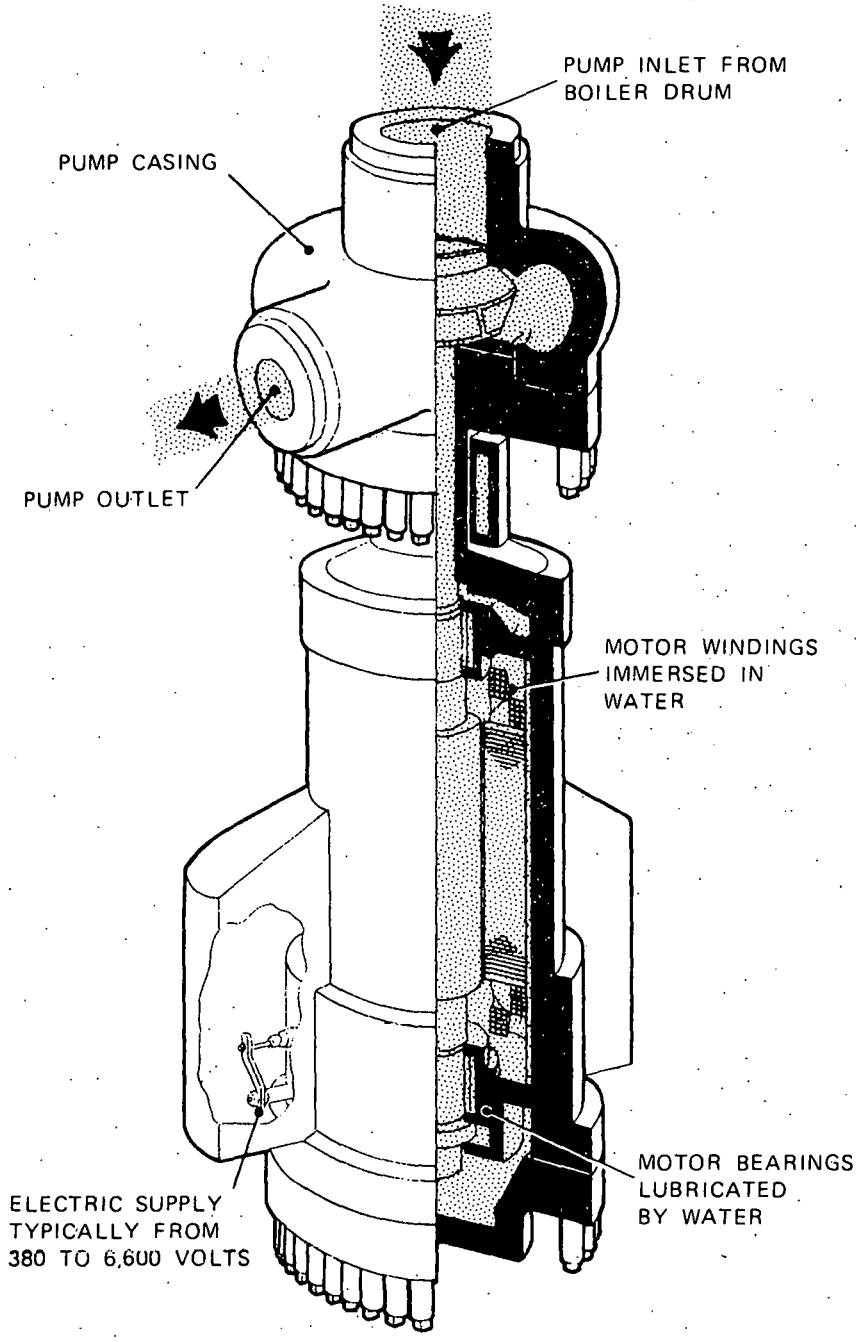

Figure 3-12. Recirculating Pump

Table 3-5. Action Initiated by High and Low Water Level Signals

Condition	Drum Problem	System Problem	Action
High Water Level "Swell"	Water carryover	Water droplets to turbine	1) Blowdown drum
			2) Decrease feedwater flow
		Shock superheater tubes	3) Defocus heliostats
	Loss of control range		1) Switch to manual control
			2) Blowdown drum
			3) Decrease feedwater flow
Low Water Level "Shrink"	Steam carryunder into downcomer	Insufficient NPSH for recirc. pump	1) Increase feedwater flow
			2) Reduce steam flow
		Steam into recirc. pump	3) Defocus heliostats
			4) Trip pump
	Loss of control range		1) Switch to manual control
			2) Increase feedwater flow
			3) Reduce steam flow
			4) Defocus heliostats
			5) Trip pump

The pumps are manifolded to suction and discharge headers. A 10-inch, 1500-pound class carbon steel stop-check valve is provided on the discharge line from each pump along with a 10-inch, 1500-pound class, carbon steel isolation valve in the suction line.

The pumps are glandless. There are no mechanical seals around the pump shaft because the motor is immersed in the water. The stator is wound with water-proof wire insulated with a thick layer of polyvinyl chloride. This is called a wet stator design and the water flows through the windings cooling them. The motor enclosure is a steel forging bolted to the pump case to form an integral shell. The motor is rated at 93.25 kw (125 H.P.), 440 volts, 3 phase 60 Hz.

The pump has one impeller and one discharge nozzle. The impeller has a single wear ring and the hydraulic thrust is applied to a thrust bearing mounted inside the motor case. The first critical speed of the pump shaft is well above the running speed (1740 rpm).

The Kingsbury pivoted shoe bearings are located inside the motor where they are lubricated by cool water. The heat generated by the motor losses is removed in a separate heat exchanger. A built-in auxiliary impeller provides the necessary circulation through the heat exchanger and the motor windings. When the motor is stationary, the cooling circulation is provided by thermosyphon action. The motor is separated from the pump by a neck of reduced diameter, which reduces to a negligible amount the heat conduction from the hot pump case. The motor is placed below the pump and is, therefore, self-venting. This arrangement also avoids thermal convection between the pump and the motor.

Attemperator - The attemperator regulates steam temperature within required limits of control to correct variations in the absorbed energy distribution between the boiler and the superheaters. This control is required to provide secondary superheater and turbine metal temperature protection. The spray attemperator provides a quick acting and sensitive control for regulating steam temperature.

The attemperator (Figure 3-13) is a six-inch, 2500-pound class Copes-Vulcan, variable orifice desuperheater, Model VO-70. A self-regulating flow plug in the attemperator provides thorough mixing and rapid evaporation of the water spray over a wide operating range. This eliminates the need for a thermal sleeve in the downstream piping.

Superheat after attemperation is maintained at all operating conditions by locating the attemperator after the primary superheater. This avoids the possibility of deposition of solids in the superheater in the event of an excursion in feedwater chemistry. This location has additional advantages:

- The average steam temperature in the secondary superheater is reduced, lowering metal temperatures and permitting the use of lower cost tube materials.

- Complete mixing of the steam exiting the primary superheater will occur, providing a uniform steam temperature at the entrance to the secondary superheater.

Feedwater of high purity is introduced into the superheated steam through a spray nozzle at the throat of a venturi section within the attemperator. Because of the spray action at the nozzle and the high velocity of the steam through the venturi throat, the water vaporizes, mixes with, and cools the superheated steam. Any water not instantly evaporated remains in suspension within the mixing chamber or attemperator body. Tests over wide load ranges have shown uniformly dry steam a very short distance down-stream from the desuperheater outlet.

The body of the attemperator is steel. The flanges facilitate installing the body and removing it for internal inspection. The steel mixing chamber is welded into the line to which it delivers the steam.

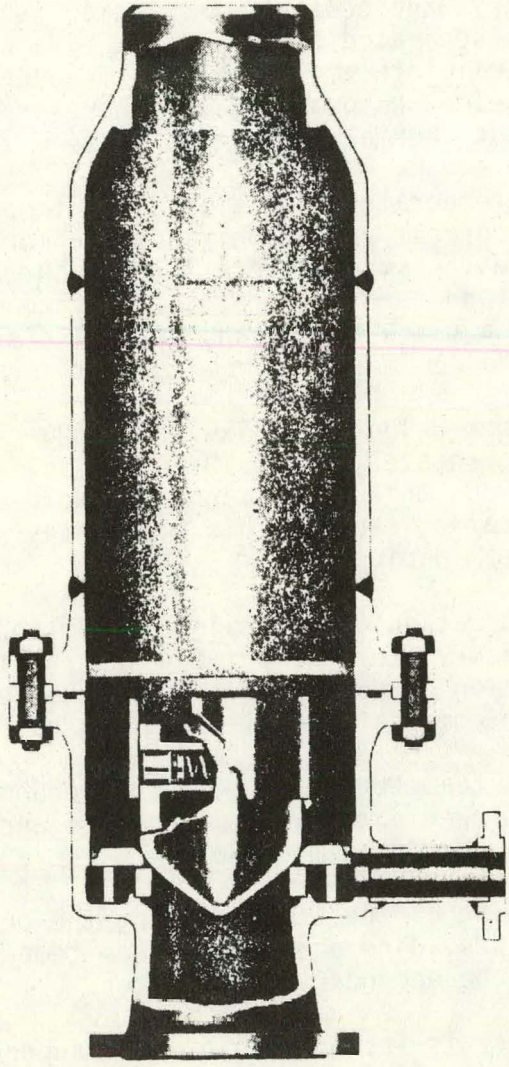

Figure 3-13. Attemperator

Only one outside connection - for spray water - is needed. All adjustments are made at the steam temperature controller. The one moving part is the plug, which is held concentric by the plug guide. A spring inside the plug exerting a force against a wear button acts to stabilize the plug.

Support Structure - The support structure consists of vertical trusses spaced at 20° intervals between the corbels and four levels of horizontal trusses (Figures 3-14 and 3-15).

The horizontal trusses are made up of wide flange sections and are supported by the vertical trusses and the corbels. All four truss levels are identical. The horizontal trusses support the vertical boiler load and also resist the horizontal seismic loads associated with the steam generator components.

The 18 vertical trusses are identical and are also made up of wide flange sections and are supported from a layer of horizontal steel at the top of the unit. These trusses are used for vertical support of the boiler, the horizontal trusses, and the platforms. Outboard hangers are provided to pick up the enclosure.

The horizontal members at the top of the unit form a spoke pattern and are supported by the corbels and the girders which span the corbels. The drum and the steam generator ceiling are supported from the horizontal members by hanger rods.

The support structure must carry the weight of the steam generator and associated equipment and withstand wind and seismic loads. The two latter loads are dynamic forces and it is standard practice to resolve these loads into equivalent static design forces. For the solar steam generator, the governing load is a seismic load of 3 g's on all the components, which is applied as a design load for the analysis of the structure. Wind load is not considered to occur simultaneously with the seismic load. The seismic loads are transferred from the steam generator pressure parts to the structure by earthquake ties. The earthquake loads are distributed and combined with the static forces to size the structural members.

The vertical loads of the various steam generator components are carried by hanger rods either directly to the top steel or indirectly through the vertical trusses. This arrangement for suspending the steam generator allows it to expand freely downward during thermal cycles.

The horizontal trusses were located, not only for structural considerations, but also to provide a convenient means for supporting platforms. The platforms are provided to permit inspection and maintenance of the steam generator.

The sizing of the structural members and the calculation of the end reactions was done by computer analysis. The member sizes calculated by the computer meet the stress requirements based on the AISC Manual of Steel Construction and also meet certain other specified requirements such as maximum and minimum depth specifications.

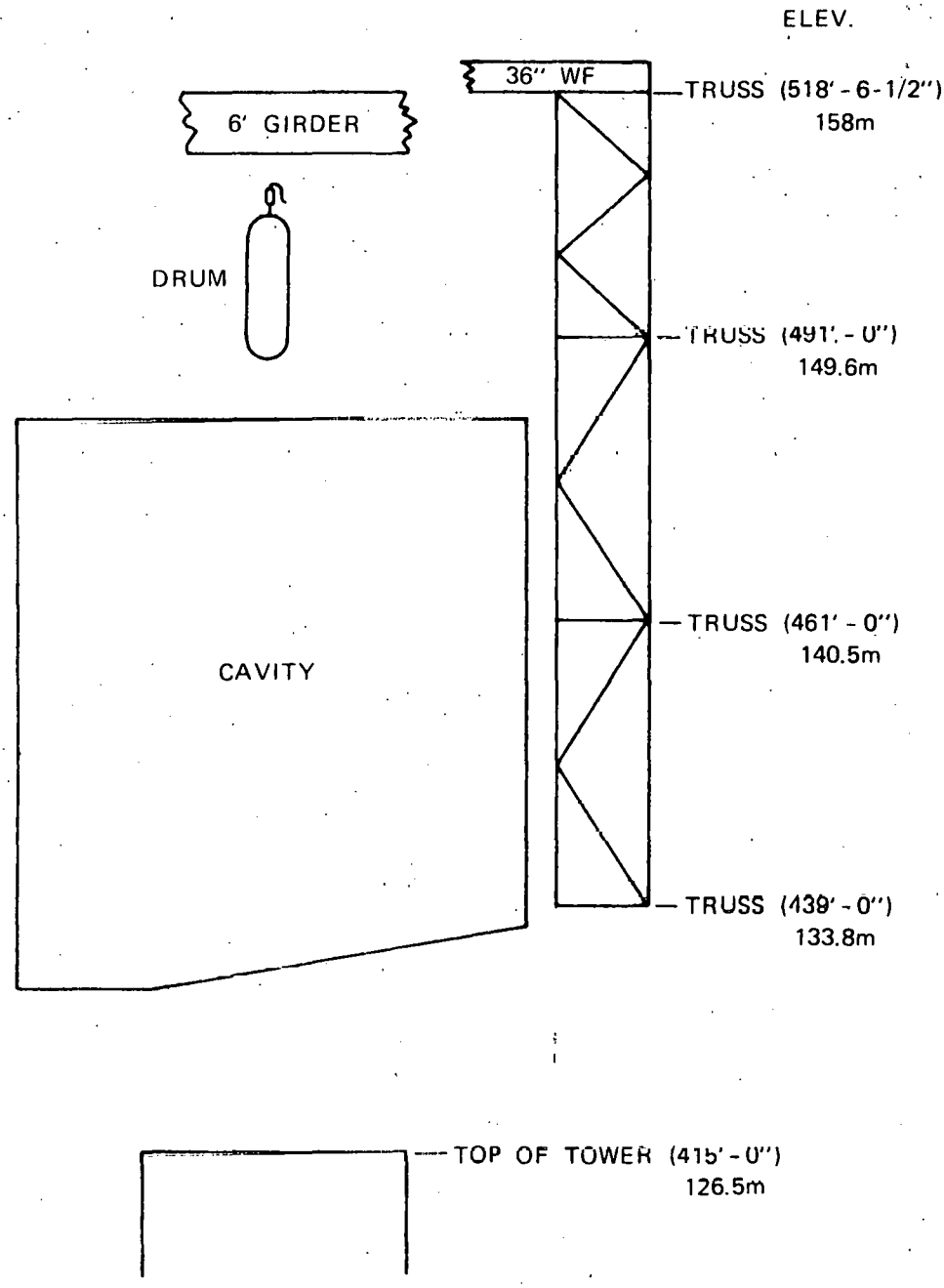

Figure 3-14. Support Structure

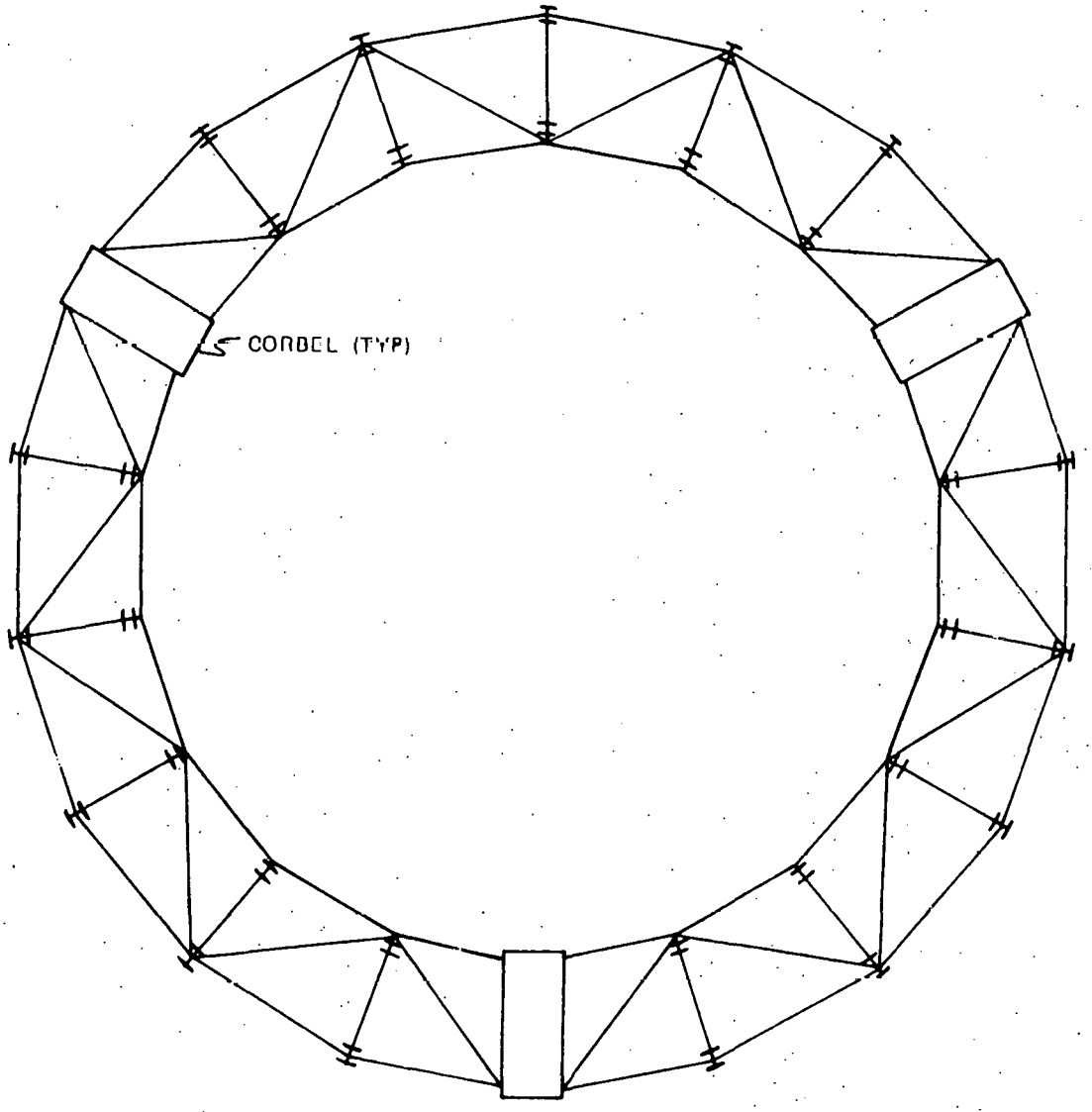

Figure 3-15. Typical Horizontal Truss

Pressure Part Support - The pressure parts are hung from the support structure by rods which are free to swing outward as the steam generator heats up. Lateral motion of the boiler and superheaters during a seismic event is restricted by lateral buckers. The buckers are slotted to allow thermal expansion up to the design temperature, at which point, further lateral motion is restrained.

The boiler section outlet header is supported from the horizontal truss at 140.5m (461') by 18 evenly spaced hanger rods. The boiler supply header is supported from the outlet header at the same circumferential locations by constant load hangers, which allow downward thermal expansion. The rods are attached to the headers by strap hangers minimizing thermal stress in the header during transients. The boiler inlet header is supported by the supply tubes. The boiler membrane walls are self-supporting.

Lateral motion of each header is restricted by nine evenly spaced buckers per header (Figure 3-16). The buckers are slotted to permit thermal expansion up to the design temperature, providing both seismic restraint and a means for keeping the boiler section centered in the cavity. Supports connect the membrane panels and the supply header at 36 evenly spaced locations, increasing the rigidity of the boiler section. The supports are designed to permit thermal expansion.

The secondary superheater connecting piping is supported from the horizontal truss at 149.7m (491 ft) by 9 equally spaced hanger rod assemblies. The inlet piping is similarly supported from brackets attached to the vertical trusses. The primary superheater outlet connecting piping is hung from the secondary inlet piping at the same nine locations. The hanger rods allow free radial expansion of the piping. The rods are pinned to lugs welded to the pipes. The lug thickness is relatively small compared to the pipe thickness, minimizing thermal stress during transients.

The superheater vertical inlet and outlet headers are hung from brackets attached to the vertical trusses. The hanger rods allow free radial expansion of the headers. The rods are pinned to lugs welded to the end of the headers. The lug thickness is relatively small compared to the header thickness, minimizing thermal stress in the headers during transients.

The superheater tubes are hung from the support trusses by adjustable rods and constant load hangers at fifteen locations spaced every 20° except at the inlet and outlet headers, where the tubes are supported by the headers. The upper five sections of the primary and secondary superheaters are hung from the horizontal truss at 149.7m (491 ft.). A linkage mechanism distributes the load in proportion to the number of tubes each rod must support. The bottom section of the primary superheater is supported from the horizontal truss at 140.5m (461 ft.). Both ends of the hanger rods pivot as they swing out to permit radial expansion of the superheater tubes.

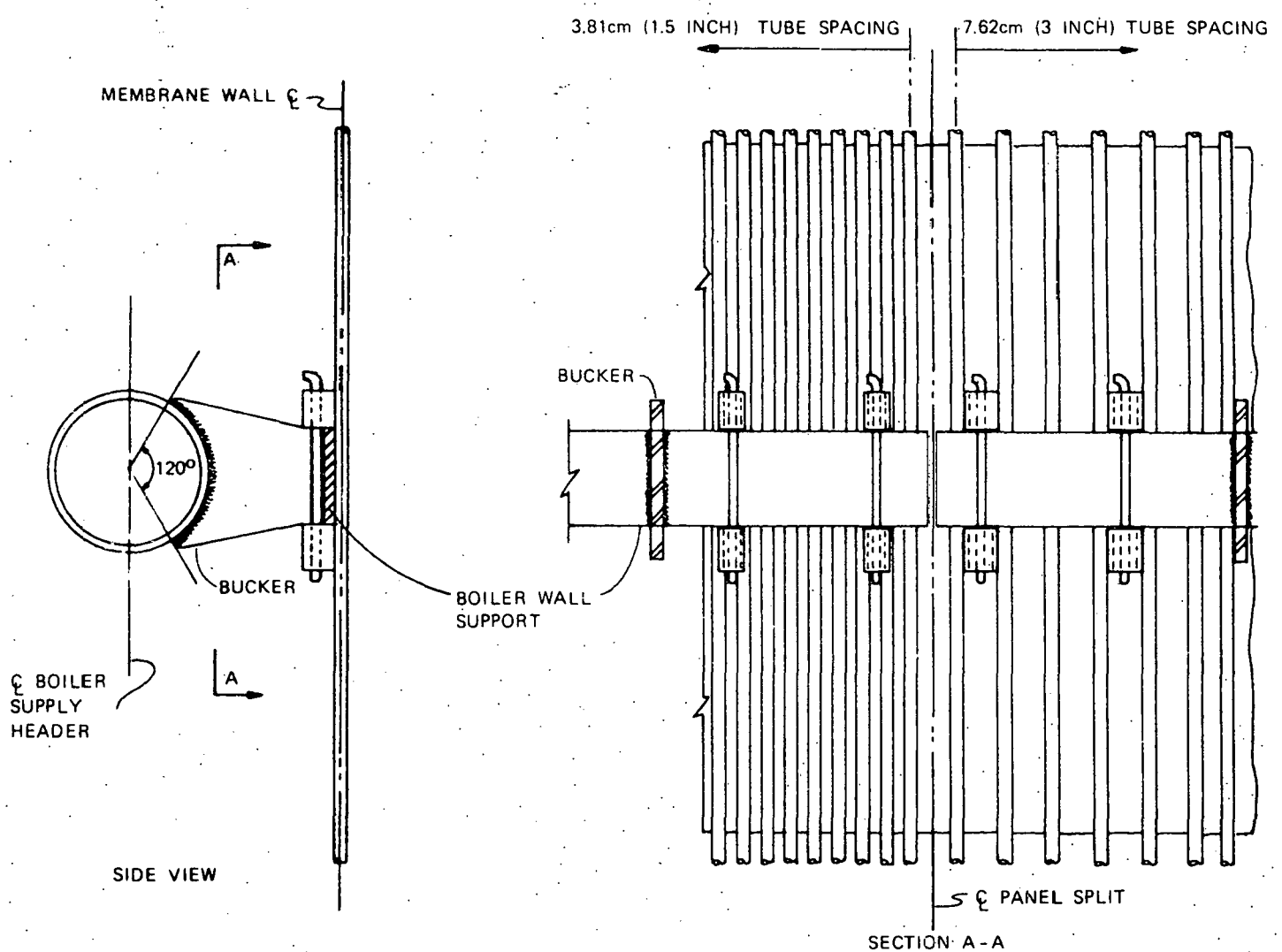

Figure 3-16. Boiler Wall Lateral Support

At the 15 support rod locations each tube is required to support the weight of the tubes above (Figure 3-17). The total deadweight load is transferred from the bottom tube to a bracket which is, in turn, supported by a hanger rod. The twisting moment applied to the bottom tube by the support rod is resisted by the alignment tee. Clips welded to each tube align the tubes with the alignment tee.

Buckers tie each alignment tee back to the vertical support trusses (Figure 3-18). The buckers are pinned at each end to permit vertical expansion of the superheater module and slotted on one end to permit radial expansion up to the design temperature.

Steam Generator Ceiling - The ceiling of the steam generator is insulated and most of the incident solar energy is either reflected or reradiated to the superheater or boiler. During operation, the ceiling is formed by a retractable roof. Overnight, or during prolonged cloud coverage, this roof is lowered to seal the cavity lower boundary against convection heat losses.

Functional Performance

The objective of the functional performance analysis is to size the steam generator so that it will reliably and efficiently produce steam at the specified conditions. The analysis is based on B&W Fossil Power Generation Division design standards.

Before the steam generator functional performance calculations could be initiated, the following data were specified, establishing the design criteria for the steam generator.

- cavity dimensions
- cavity heat flux distribution as a function of solar time
- Steam cycle conditions as a function of steam flow
  - feedwater temperature
  - steam pressure
  - steam temperature
- maximum superheater pressure drop
- required rate of temperature change

After these data were specified, the functional performance was established as follows:

- Three dimensional (3D) incident flux data were converted to 3D absorbed flux data.
- Absorbed energy was calculated as a function of cavity height.
- The boiler/primary/secondary superheater interfaces were determined.

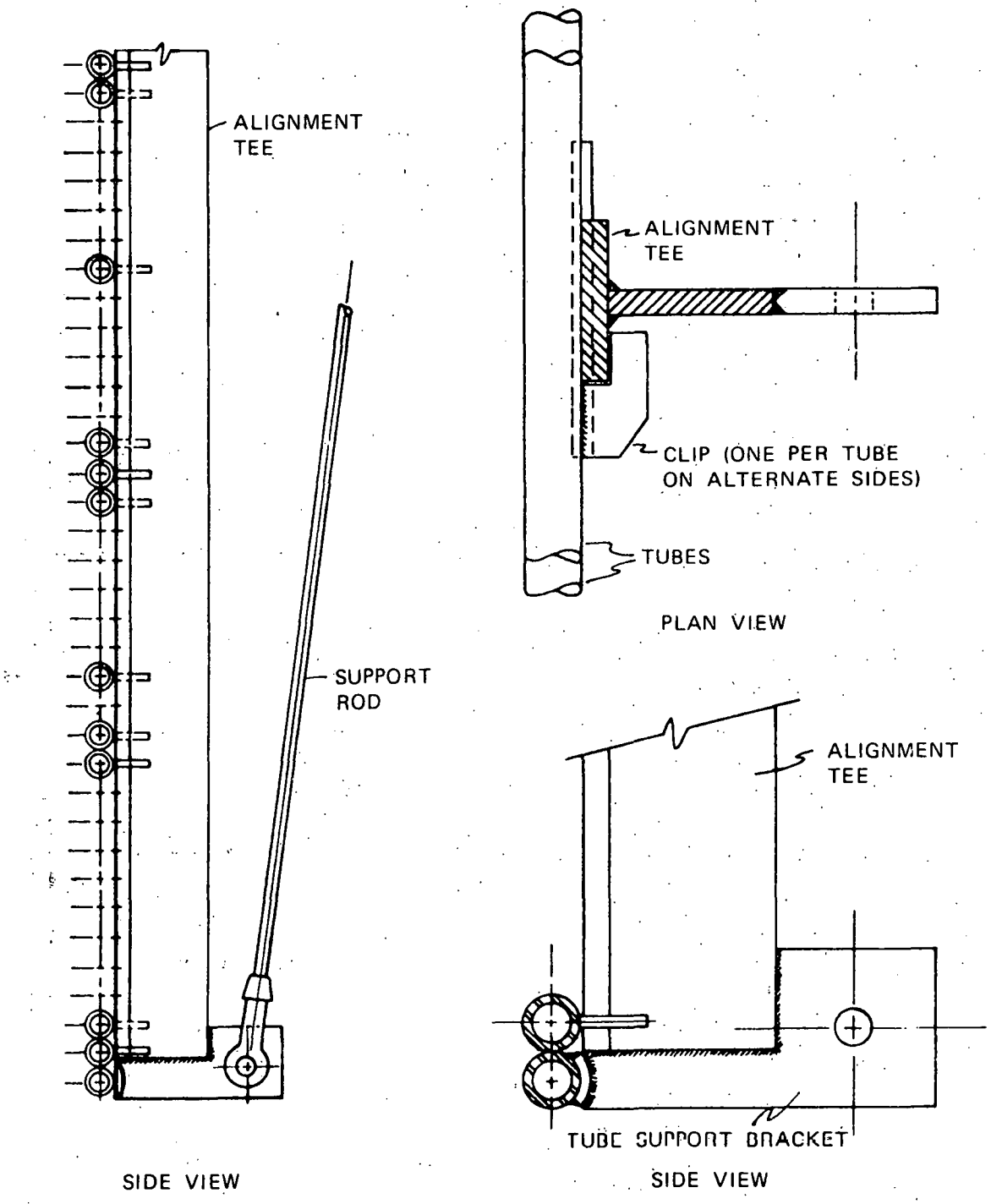

Figure 3-17. Superheater Hanger

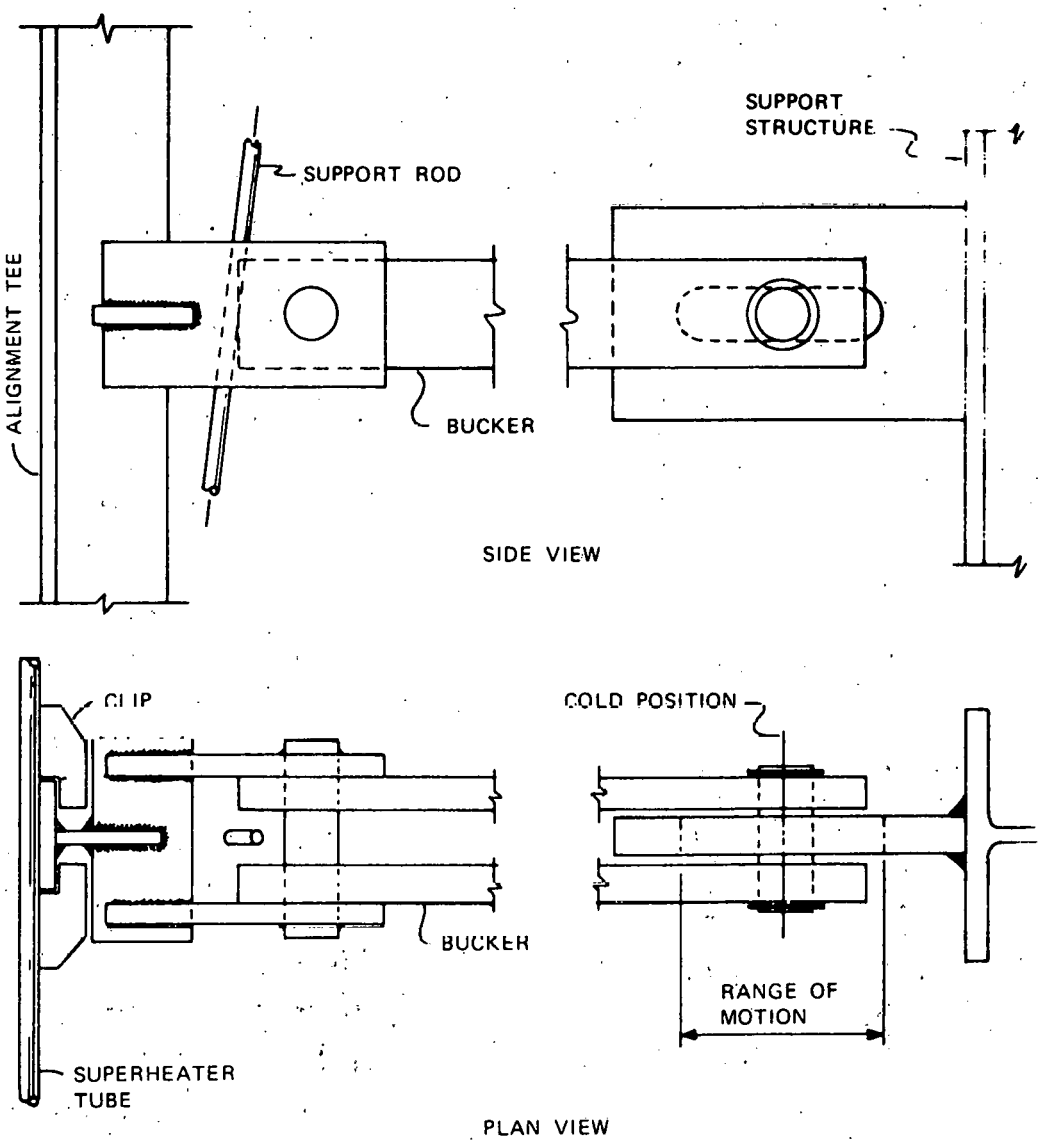

Figure 3-18.. Superheater Lateral Ties

- The number and location of the boiler flow circuits was established.
- The flow to each boiler circuit was matched to heat absorption by individually selecting valve and pipe sizes for each circuit.
- The number and location of the superheater flow paths was established.
- The flow was divided among the superheater flow paths to match the heat absorption by varying the size of the connecting pipes.
- Superheater maximum mean metal temperatures were calculated.
- The acceptable range of cloud shadowing and feedwater temperature variations was determined for 3/21/12PM.

Each of these procedures is outlined in the following paragraphs.

Heat Flux Data - Three-dimensional incident flux data were generated by Honeywell using the Ray Trace Code. Data were provided for the following times:

3/21: 7 AM, 8 AM, 9 AM, 10 AM, 11 AM and 12 Noon

6/21: 12 Noon

12/21: 12 Noon, 2 PM, 3 PM and 4 PM

The data for 3/21/12 PM are plotted in Figure 3-19. Additional data are presented in Volume II, Section 3, Design Specifications.

Honeywell also provided one-dimensional absorbed flux data for the same times. These data were generated with the Rerad Software Model. The Rerad model is essentially a one-dimensional, axisymmetrical, multi-node model of the steam generator which calculates steam flow, attemperator flow, cavity efficiency, water and steam temperatures, and boiler and superheater metal temperatures as a function of input energy, feedwater temperature, steam temperature and steam pressure. These calculations were based on a boiler height of 8.6m (28.2 ft) and a first-to-second stage superheater interface height of 12.56m (41.2 ft). From these calculations, and the circumferential average incident flux data plots of the absorbed to incident flux ratio as a function of cavity height were developed. This ratio is presented in Figure 3-20 for 3/21/12 PM. The increase in absorbed energy at the interface between the primary and secondary superheater occurs because the spray attemperator has cooled the steam, lowering the superheater surface temperature.

The circumferential average incident heat flux data from the Ray Trace output were multiplied by the ratio ϕ_A/ϕ_I to obtain circumferential average absorbed heat flux.

The absorbed heat flux for each circumferential zone was multipled by the area of the zone to obtain the absorbed energy. The absorbed energies were then summed zone by zone to obtain the absorbed energy as a function of cavity height.

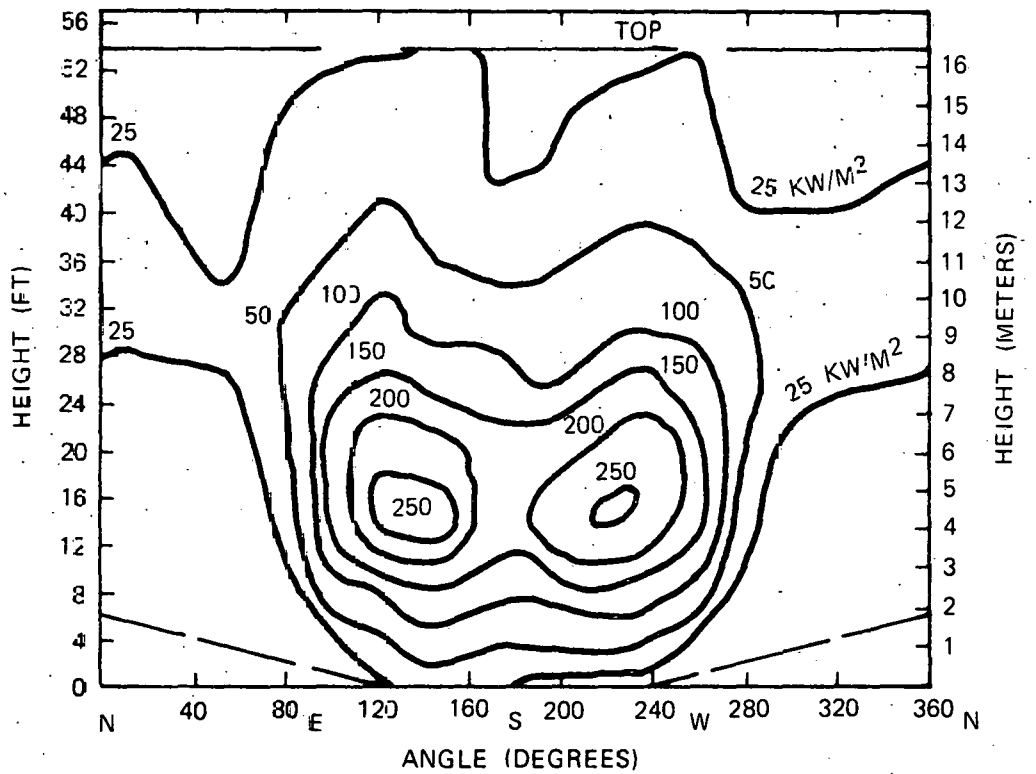

Figure 3-19. Cavity Wall Incident Flux Map, 3/21/12PM

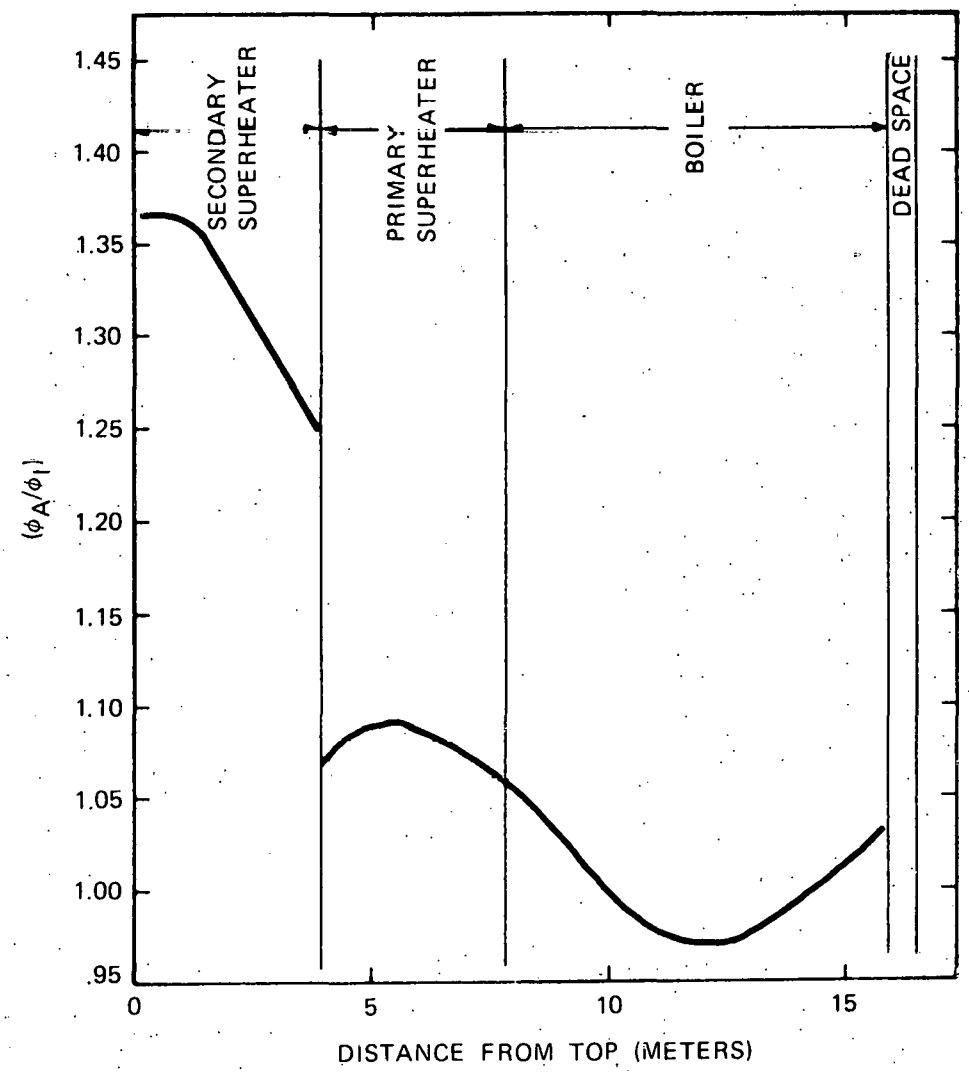

Figure 3-20. Circumferential Average ϕ_A/ϕ_T versus Cavity Position, 3/21/12PM

The three-dimensional incident flux data were also converted to local absorbed fluxes using the ratio ϕ_A/ϕ_I. The circumferential grid spacing for the incident flux data is 22½°. Since the steam generator has eighteen (18), 20° sides, the data at each height was plotted as a function of circumferential angle and the heat flux at each 20° segment was obtained from the graphs. Figures 3-21 to 3-24 are typical examples of the resulting absorption rate plots.

Boiler/Superheater Interface - The boiler/superheater interface was selected so that the steam generator would meet the following performance requirements:

- The steam generator must produce superheated steam at the pressure, temperature and flow required by the turbine at the specified feedwater pressure and temperature.
- On a clear day the steam generator must accept all of the available energy from the heliostats.
- The nominal attemperator flow at maximum heat input conditions and nominal feedwater temperature was set at approximately 10 percent of the total steam flow. This ratio provides a reasonably wide range of steam temperature control with cost effective superheater materials for off design conditions such as feedwater heaters out of service, random cloud shadowing, and misalignment of the heliostats.

The ratio of energy absorbed in the boiler section to the total absorbed energy at maximum heat input with 10% attemperator spray flow can be determined from mass and energy balances on the steam generator (Appendix D).

To determine the relative energy absorbed by the boiler and superheater at maximum conditions and assuming that the attemperator flow is ten (10) percent of the total flow and at the same temperature as the feedwater:

$$\frac{Q_B}{Q_T} = \frac{W_{FW}\,(h_g - h_{FW})}{W_S\,(h_{S2O} - h_{FW})} = \frac{0.9\,(h_g - h_{FW})}{(h_{S2O} - h_{FW})} \qquad (1)$$

Preliminary turbine heat balance data were obtained from the EGS Subsystem specifications. The data consisted of steam flow, pressure and temperature at the secondary superheater outlet for 3/21/12 PM and feedwater temperature as a function of steam flow. By assuming that steam line and total superheater pressure drop are directly proportional to steam flow squared, that the superheater pressure drop is 1.38 MPa (200 psi) at maximum conditions, and that the turbine throttle pressure is 10.1 MPa (1465 psia) at all steam flows, pressures at the drum and the secondary superheater outlet were determined as a function of steam flow. The results are shown in Figure 3-25. These pressures and the preliminary turbine heat balance data were used to determine the enthalpy at the drum feedwater and steam nozzles and at the secondary superheater outlet nozzle as shown on Figure 3-26.

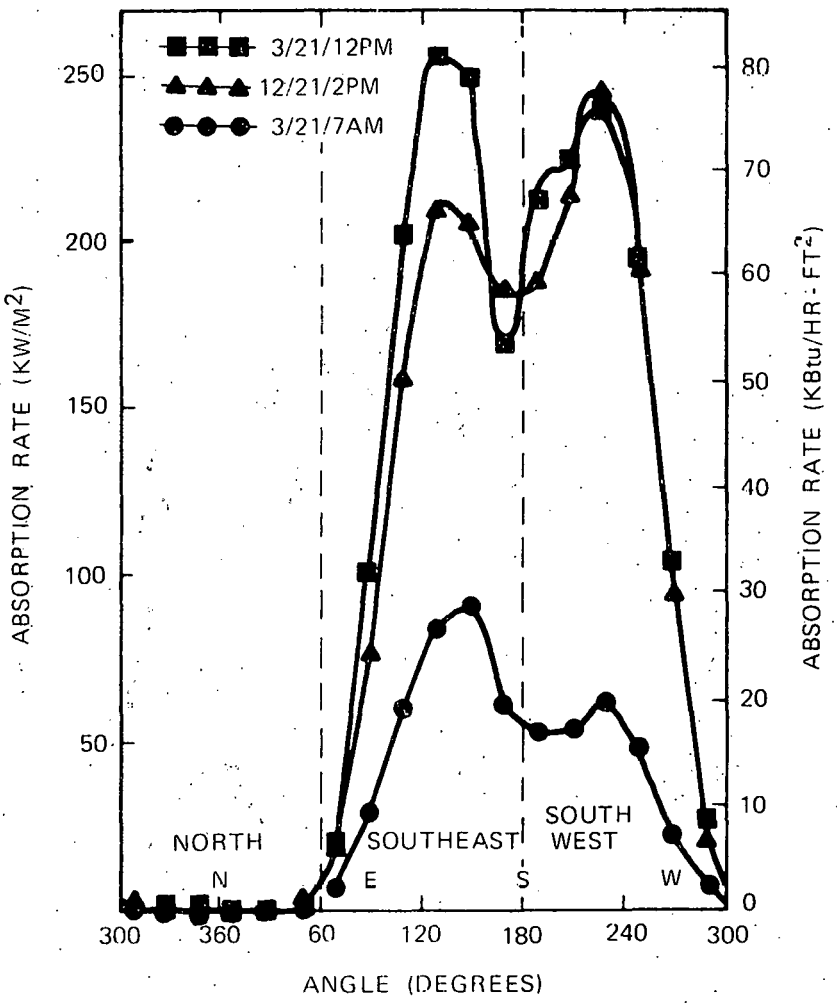

Figure 3-21. Absorption Rate versus Angle at Peak Flux Point

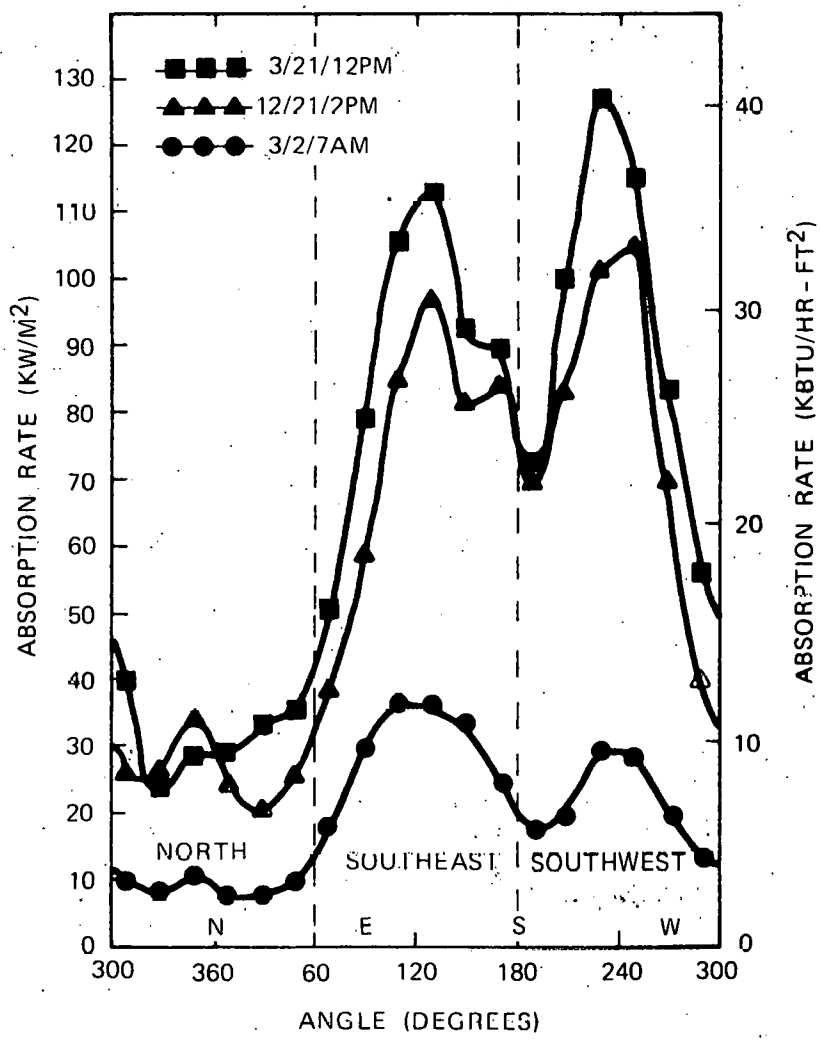

Figure 3-22. Absorption Rate versus Angle at Boiler/Superheater Interface

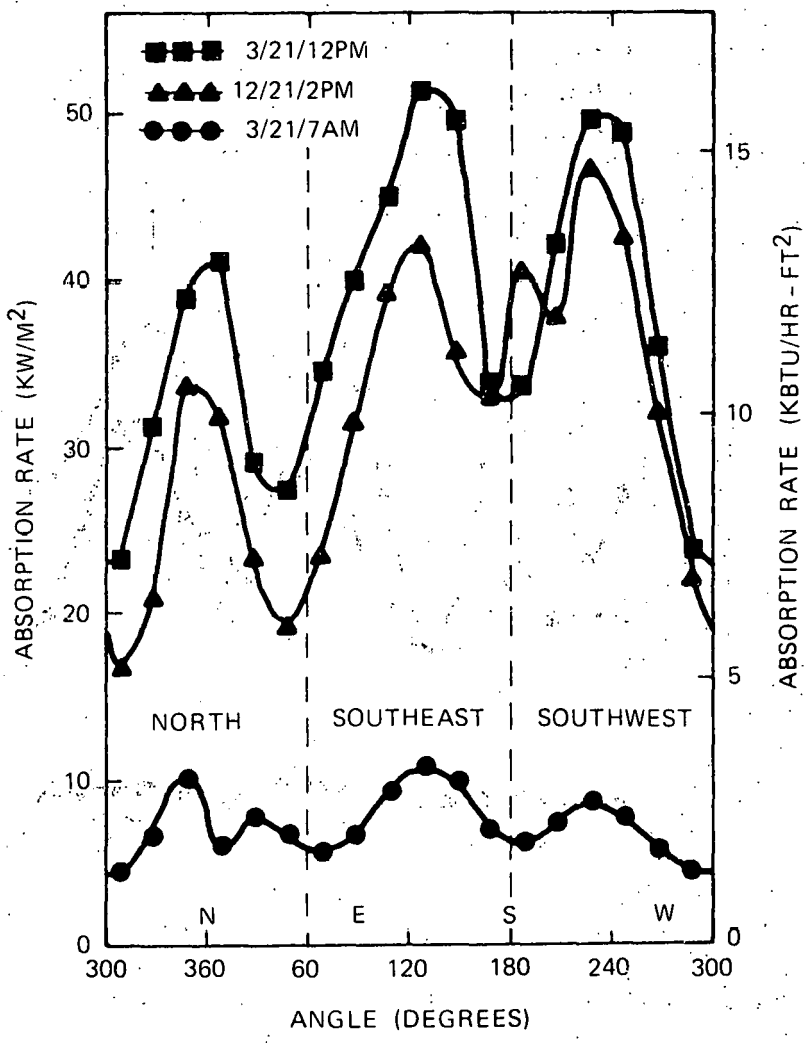

Figure 3-23. Absorption Rate versus Angle at Primary/Secondary Superheater Interface

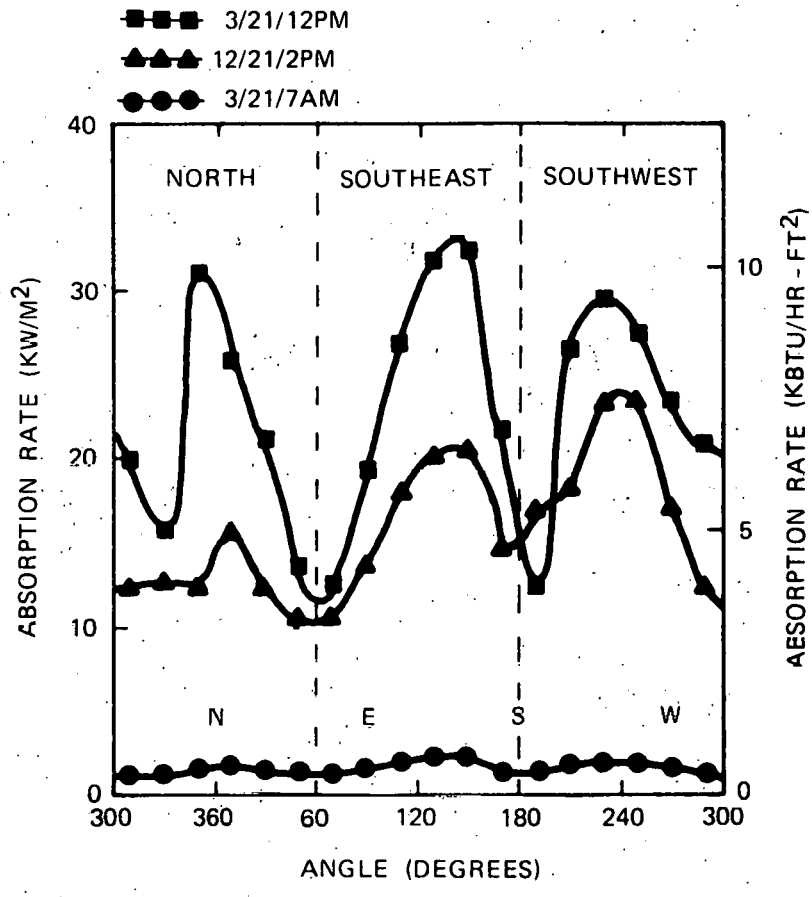

Figure 3-24. Absorption Rate versus Angle at Top of Cavity

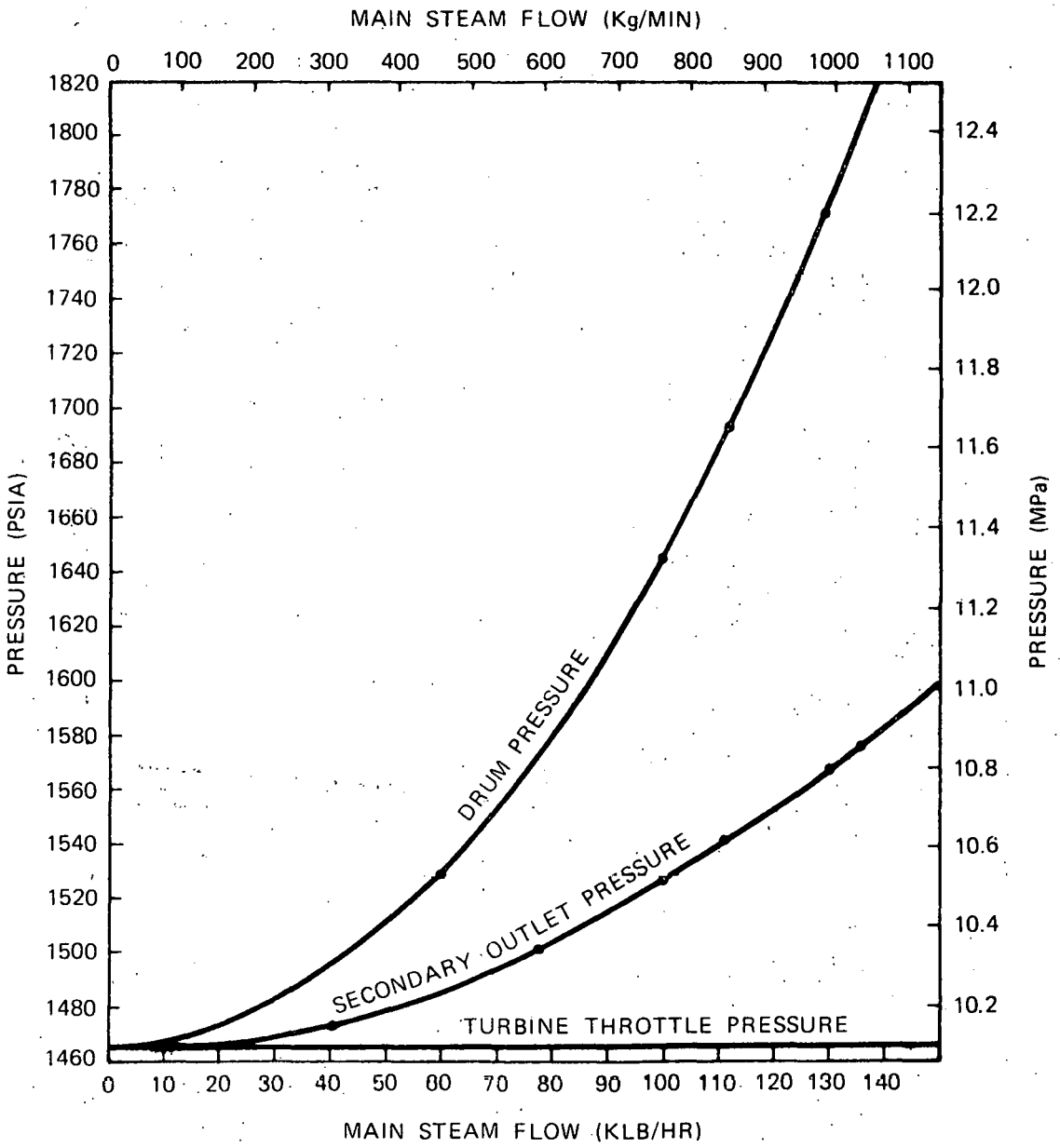

Figure 3-25. Pressure versus Steam Flow

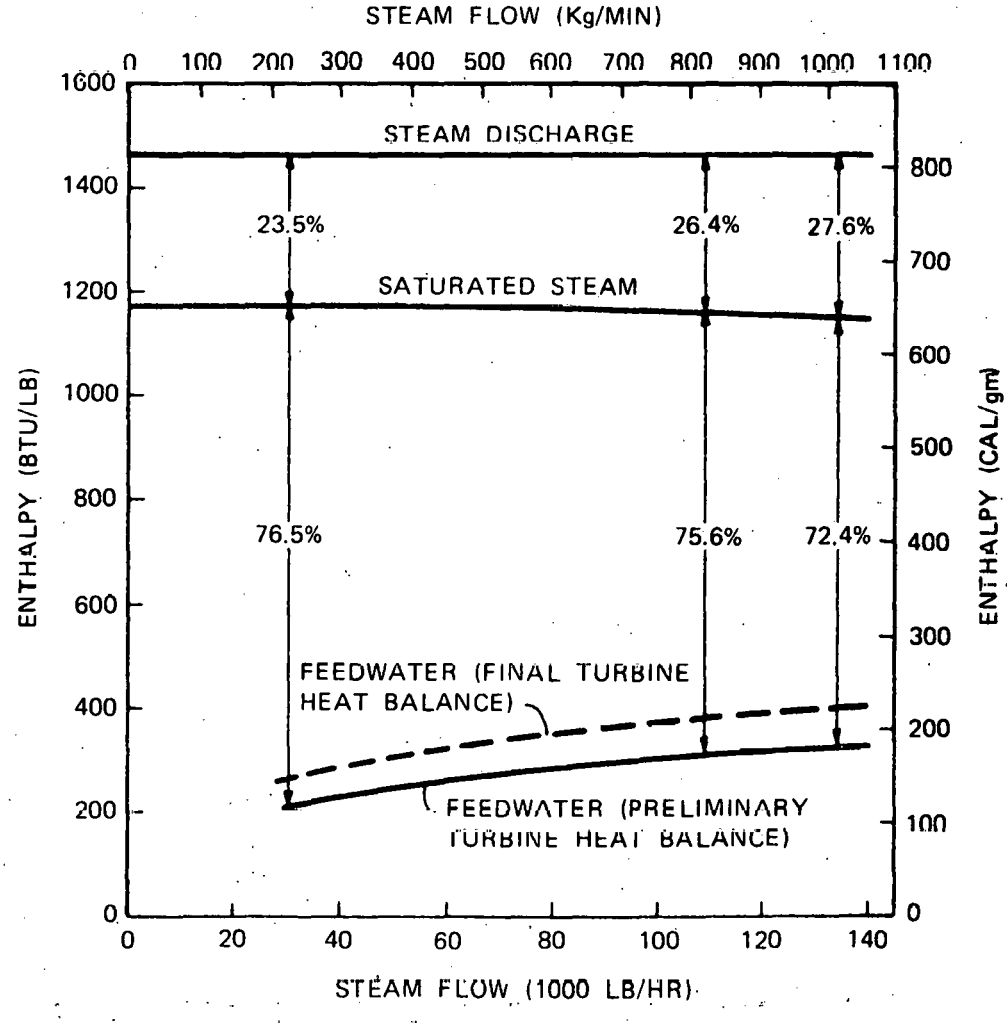

Figure 3-26. Turbine Heat Balance Data

By substituting these enthalpies into equation (1), the ratio of boiler section to total heat input is determined to be 65 percent. Next, the relative heat absorption was plotted as a function of relative cavity height, as measured from the bottom of the south side of the cavity (Figure 3-27). Data for two times are shown, the maximum conditions (3/21/12 PM) and the minimum conditions for which heat flux data are available (3/21/7 AM). The 65 percent boiler heat absorption point at maximum conditions is 8.31m (27 ft 3 in.) from the bottom of the cavity.

The feedwater and attemperator flow can be calculated from equations (2) and (3):

$$\frac{W_{FW}}{W_S} = \frac{Q_B\ (h_{S2O}-h_{FW})}{Q_T\ (h_g-h_{FW})} \qquad (2)$$

$$\frac{W_{ATT}}{W_S} = 1 - \frac{W_{FW}}{W_S} \qquad (3)$$

At 3/21/7AM, Q_B/Q_T is 0.735 (Figure 3-28) and steam temperature control is acheived with 4 percent attemperator flow.

All of the heat flux data were analyzed in the same way. The percentage of total absorbed power for the boiler section is shown on Figure 3-28. The total steam flow and attemperator flow is shown as a function of total absorbed power on Figure 3-29. The data indicate that steam temperature control can be maintained on clear days by the spray attemperator over a 5 to 1 range of absorbed energy without defocusing heliostats. The range of control does not extend to lower power inputs because the relative energy losses from the superheater are inversely proportional to incident energy. Therefore the absorbed energy is not sufficient to superheat the steam at low incident energy levels. The lower feedwater temperature at low steam flow compensates for this trend to some extent.

Primary/Secondary Superheater Interface - The selection of the primary/secondary superheater interface was based on the following considerations:

- The primary superheater local absorbed heat flux is about 50% greater than the secondary superheater local heat flux. Therefore, primary exit steam temperature must be lower than secondary exit steam temperature to keep peak metal temperatures about the same. Actually the primary metal temperatures should be lower than the secondary metal temperatures, if possible, because thermal stresses are higher.

- The steam temperature exiting the spray attemperator should be superheated to avoid the possibility of solids deposition in the second-stage superheater in the event of an excursion in feedwater chemistry. The steam exiting the primary superheater must be at a high enough temperature, so that some superheat remains after the injection of attemperator spray water.

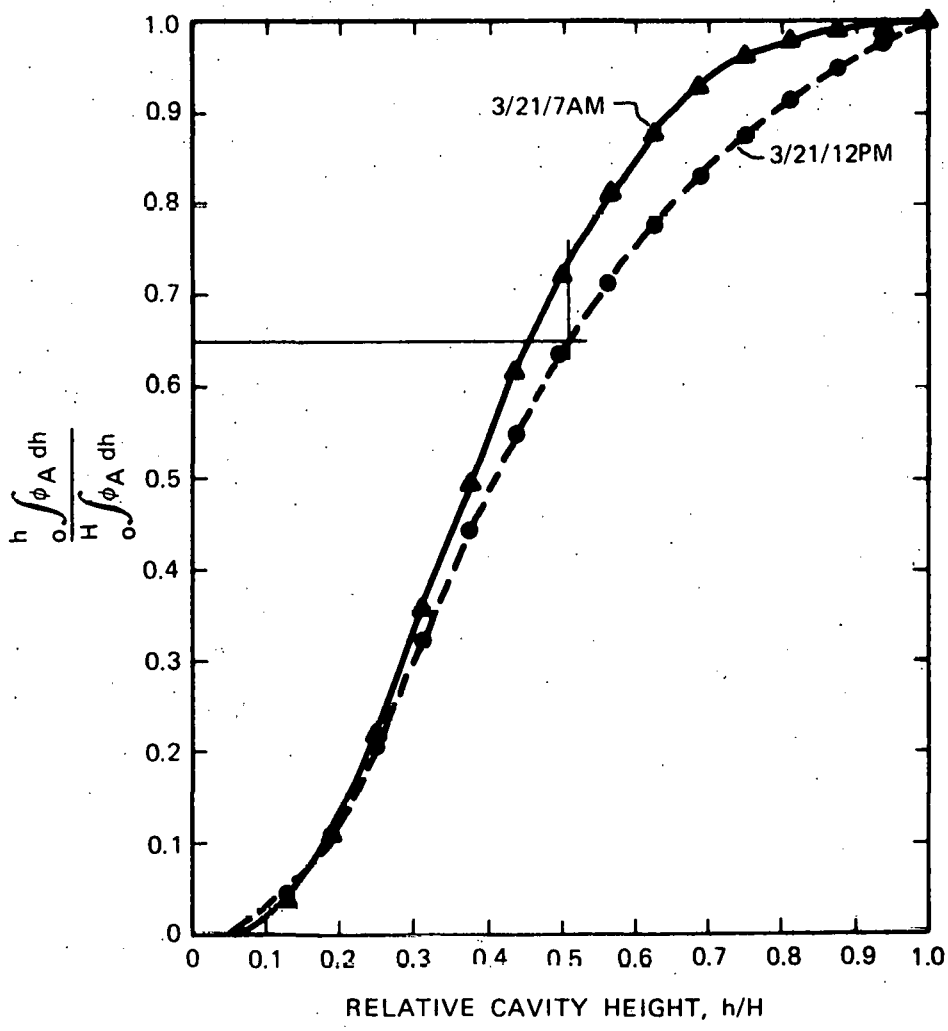

Figure 3-27. Relative Energy Absorption versus Cavity Height

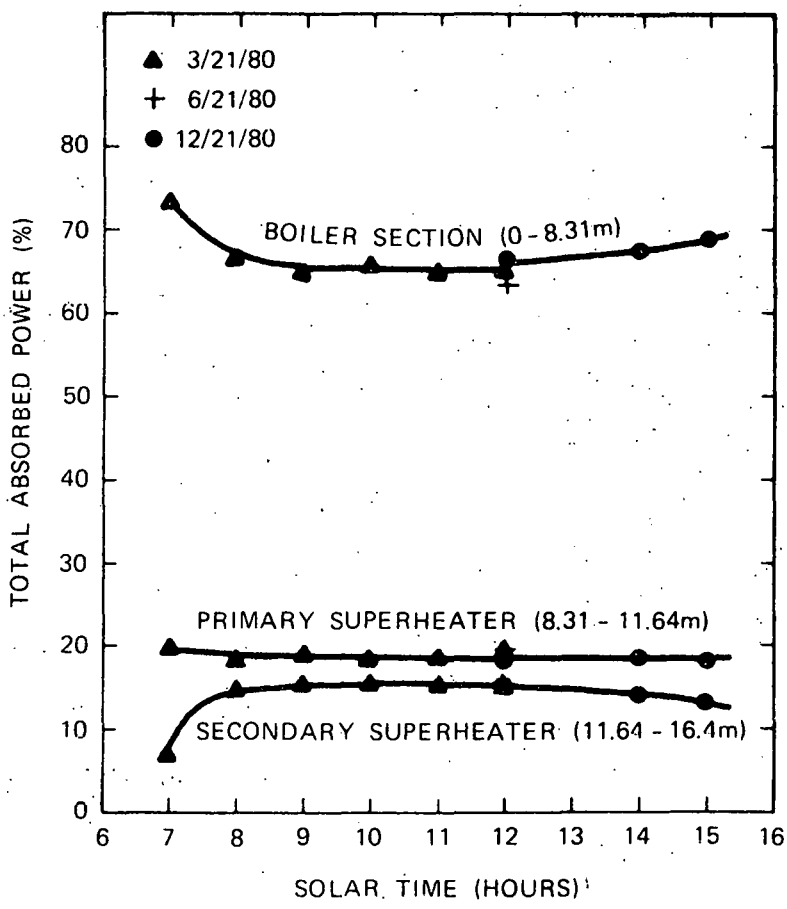

Figure 3-28. Absorbed Power Distribution versus Time

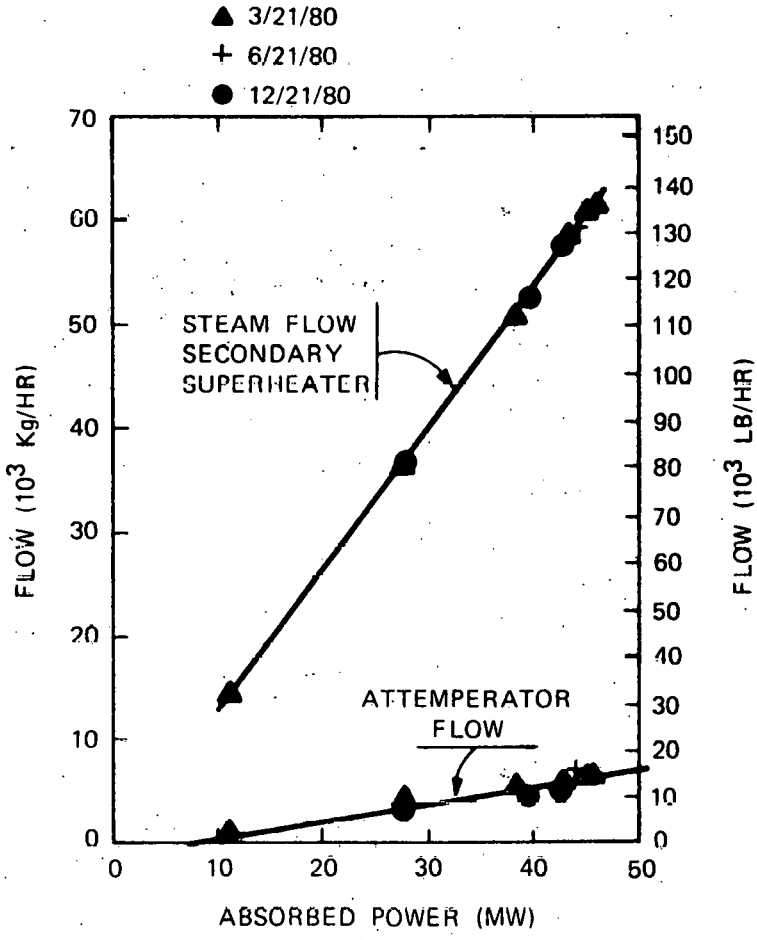

Figure 3-29. Flow versus Total Absorbed Power

The mass and energy balance equations for the steam generator were used to determine the effect of varying the primary/secondary superheater interface:

$$h_{S1O} = h_g + \frac{Q_{S1}}{Q_T} \frac{h_{S2O} - h_{FW}}{\left(\frac{W_{FW}}{W_S}\right)} \quad (4)$$

$$h_{S2O} = h_{S1O} \left(\frac{W_{FW}}{W_S}\right) + \left(1 - \frac{W_{FW}}{W_S}\right) h_{FW} \quad (5)$$

At maximum conditions the nominal feedwater flow is 90 percent of the steam flow and the data from Figures 3-28 and 3-29 can be used to determine primary outlet enthalpy and secondary inlet enthalpy as a function of the primary/secondary interface as shown by Figure 3-30.

The primary/secondary interface was selected to be 70.7 percent from the bottom of the south side of the cavity, making the secondary superheater surface area 50 percent greater than the primary surface area. The steam temperature at the primary outlet, secondary inlet and secondary outlet is shown on Figure 3-31 as a function of absorbed power for the selected primary/secondary superheater interface.

Boiler Circulation - The boiler section absorbed heat flux distribution varies greatly in both the vertical and circumferential directions, even on clear days (Figure 3-32). The heat flux patterns will be further distorted by clouds showdowning the heliostat field, and during startup and shutdown, when it may be necessary to defocus some heliostats to achieve the desired balance between boiler and superheater absorbed energy.

The minimum flow requirements for a boiler tube depend primarily on heat absorption; the higher the heat flux, the more flow is required. The boiler flow circuitry is designed to distribute the total boiler flow to match local flow requirements.

The boiler section was divided into eight flow circuits. On the north wall where heat input is small, one circuit serves a 100° segment. The boiler tubes are also spaced on 7.62 cm (3-inch) centers on this wall because of the low cooling requirements. All the other circuits serve a 40° segment of tubes except for the circuit on the south wall which covers a 20° segment. The tubes in these circuits are spaced on 3.81 cm (1.5-inch).

The minimum required flow per tube was determined for each of the eight flow circuits. The minimum total flow to each circuit was established by considering the following circulation design criteria:

- The boiler tube flow must be sufficient to prevent film boiling anywhere along the length of the tube. Film boiling increases

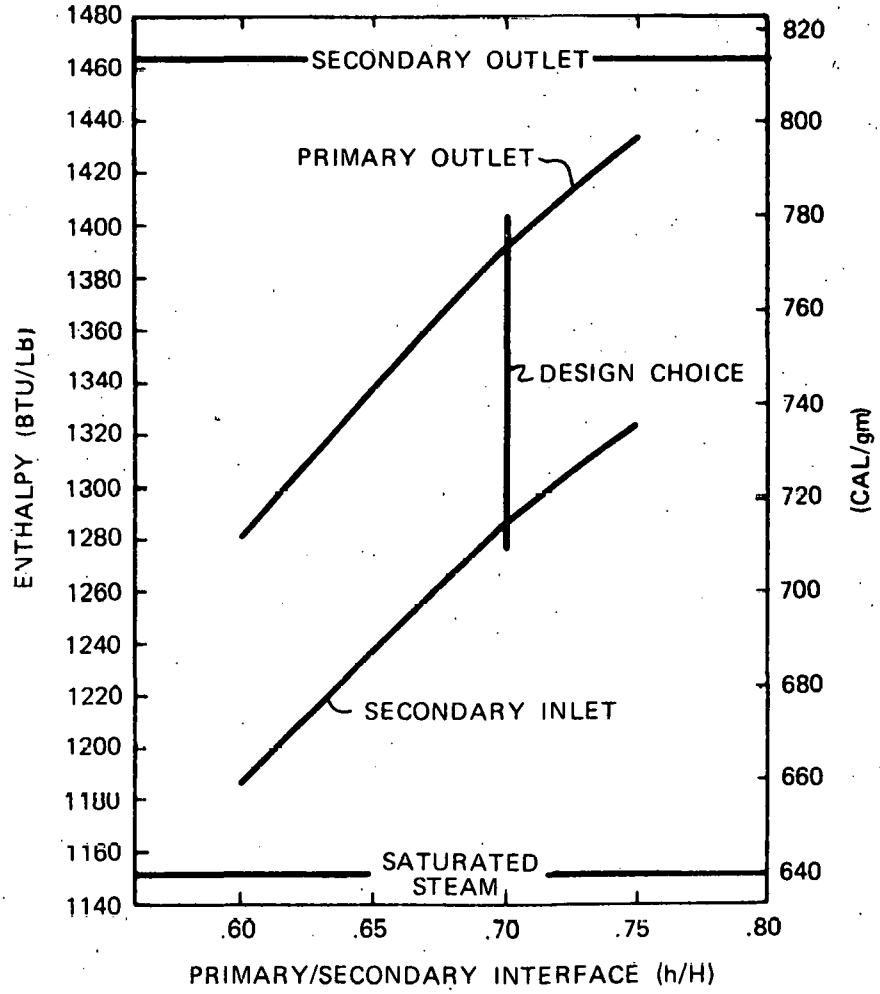

Figure 3-30. Effect of Primary/Secondary Interface on Primary Outlet and Secondary Inlet Enthalpy, 3/21/12PM

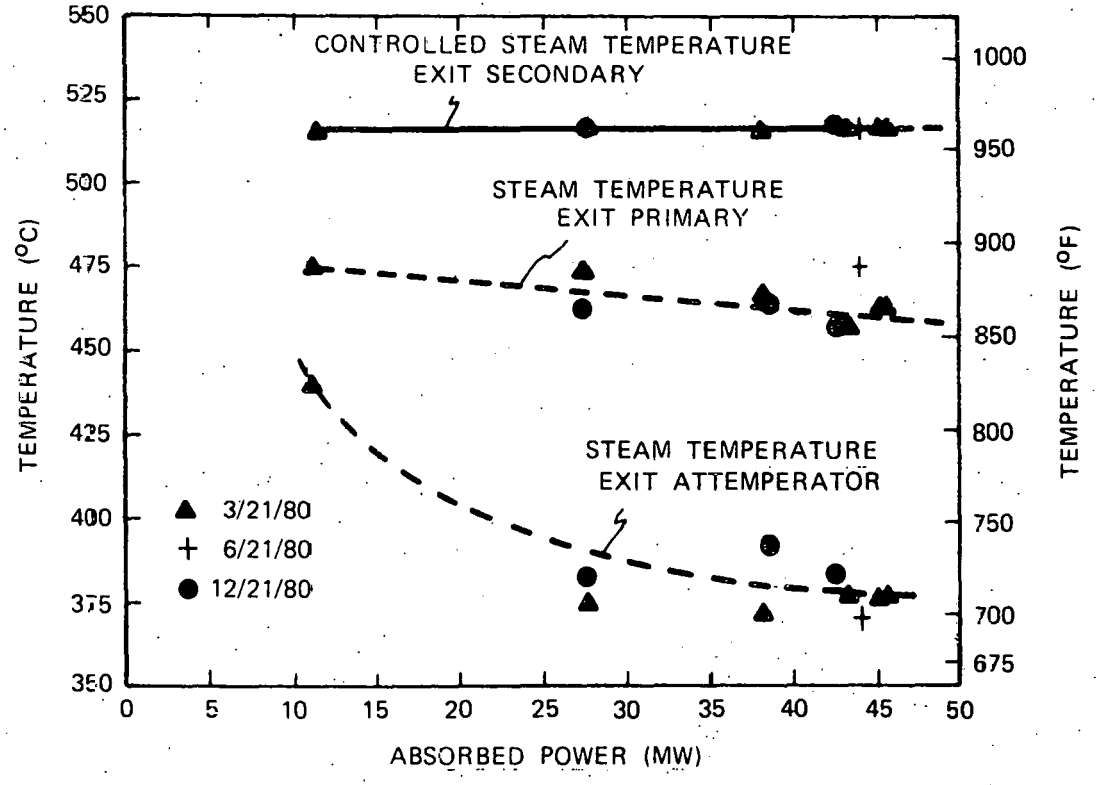

Figure 3-31. Steam Temperature versus Absorbed Power

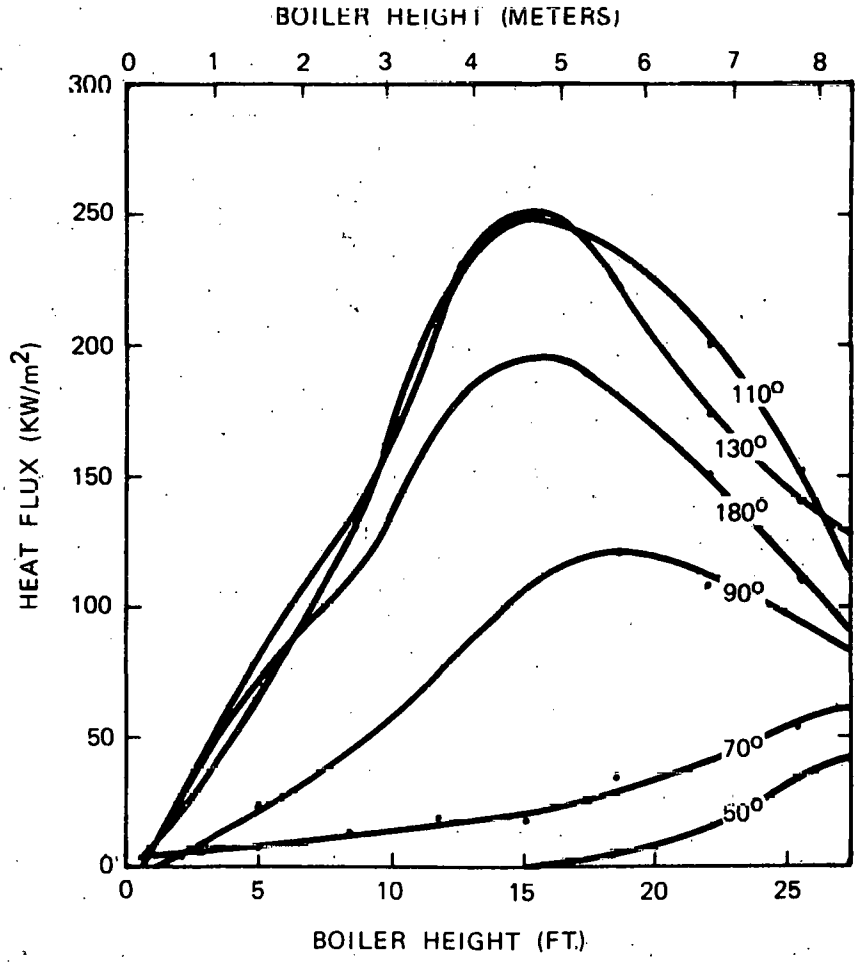

Figure 3-32. Heat Flux versus Boiler Height, 3/21/12PM

tube temperatures and causes failure when material limits are exceeded. This flow requirement increases with increasing heat flux and determines the minimum acceptable flow for all tubes on the south half of the boiler wall.

- The boiler tube flow must be sufficient to prevent downflow from occurring in any of the tubes. This criterion determined the minimum flow for the tubes in the 50 - 90° and 270 - 310° segments of the boiler section.

- The boiler tube inlet velocity must be sufficient to prevent undesirable flow patterns, such as slug flow. This criterion determined the minimum flow for tubes in the north boiler circuit.

The flow to each boiler circuit was balanced to meet the minimum tube flow requirements. Balancing was achieved by varying the size of the supply tubes and riser tubes for each circuit and by providing a hand valve in each supply circuit for final flow adjustment. A typical boiler circuit is shown schematically on Figure 3-33. The pressure drop across each parallel circuit (point A to point B) is identical.

The flow balance calculations indicated that the total boiler section flow rate would be approximately 1638 kg/s (1.3×10^6 lb/hr) in order to meet the minimum circulation requirements for each boiler tube. This corresponds to a recirculation ratio of approximately 10. The recirculation ratio is the ratio of total boiler inlet flow to the total saturated steam flow exiting the boiler. Therefore, 10 was selected as the nominal recirculation ratio.

Figure 3-34 presents the boiler section total pressure drop characteristics as a function of recirculation ratio. Also shown are the recirculating pump head characteristics at the nominal operating conditions.

Table 3-6 summarizes the performance characteristics of each boiler flow circuit.

The flow rates listed in Table 3-7 satisfy the flow per tube requirements of each boiler tube. The pressure drop for the flow balancing valves is for the valve in the wide open position. During cold checkout, each hand valve would be closed slightly to achieve the required flow distribution. As shown by Figure 3-34, ample pressure drop is available for valve adjustment.

The following sections discuss the flow requirements for static flow stability and for preventing film boiling.

Static Flow Stability - The pressure drop versus flow characteristics of the tubes in each boiler circuit were calculated to determine that downflow would not occur in a tube receiving little or no heat input.

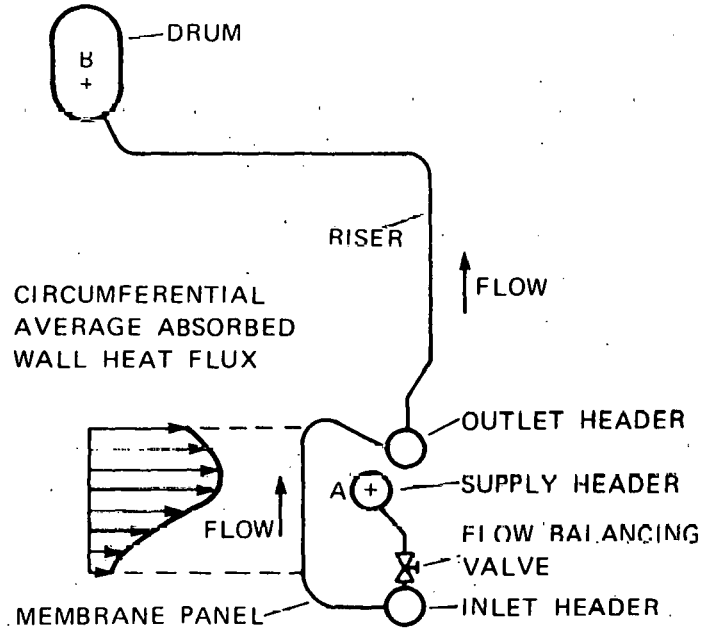

Figure 3-33. Boiler Circuit

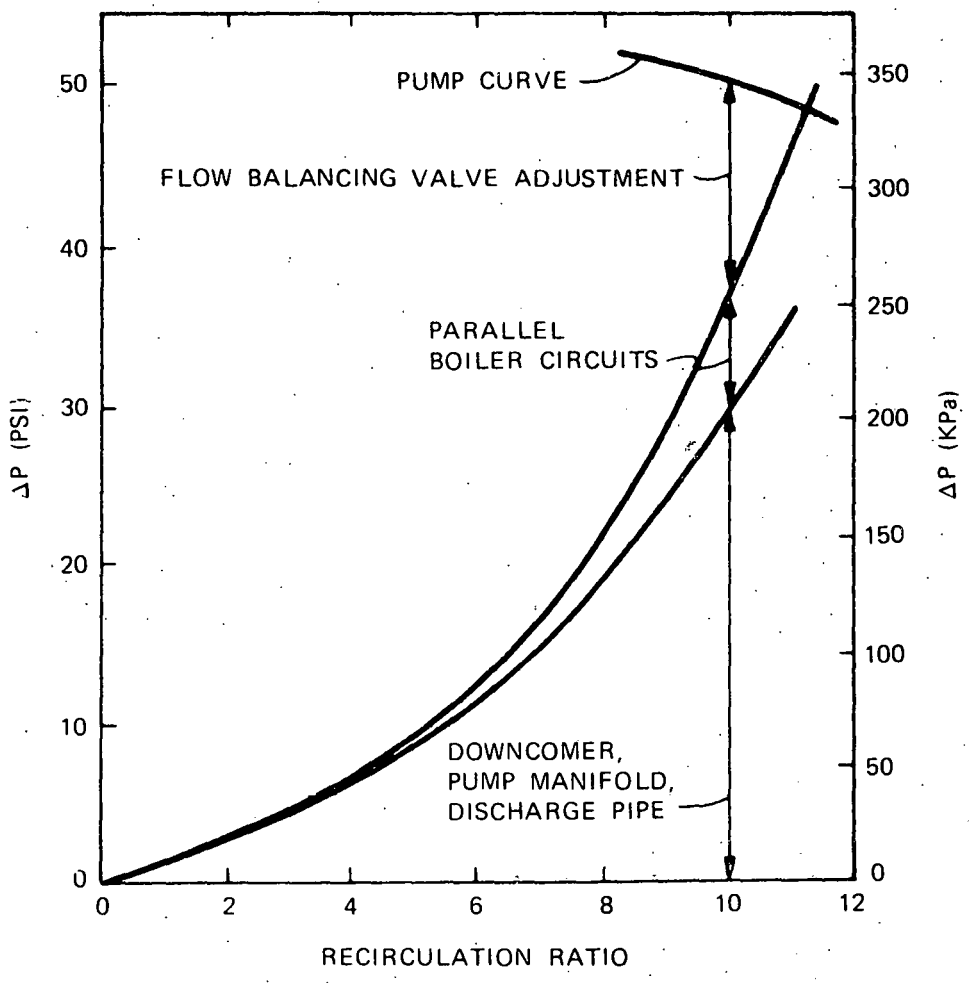

Figure 3-34. Pressure Drop versus Recirculation Ratio

Table 3-6. Boiler Flow Circuit Performance Characteristics, 3/21/12PM

Circuit	Flow Kg/min (lb/hr)	Valve ΔP KPa (psi)	No. Of Tubes	Average Flow Per Tube kg/min (lb/hr)	Average Absorption Per Tube KW (1000 BTU/HR)	Average % SBW @ Outlet
N	1231 (162600)	7.3 (1.06)	173	7.1 (940)	2.6 (8.93)	-2.8
EN	891 (117700)	20.7 (3.0)	138	6.4 (853)	10.1 (34.4)	3.4
ES	1670 (220600)	30.0 (4.35)	138	12.1 (1599)	44.2 (150.9)	14.1
SE	1664 (219800)	30.0 (4.35)	138	12.0 (1593)	48.4 (165.1)	16.0
S	628 (82900)	12.8 (1.86)	69	9.1 (1202)	40.4 (138.0)	18.4
SW	1670 (220600)	30.0 (4.35)	138	12.1 (1598)	47.6 (162.4)	15.6
WS	1660 (219300)	30.0 (4.35)	138	12.0 (1589)	39.9 (136.2)	12.5
WN	866 (114400)	20.3 (2.95)	138	6.3 (829)	10.0 (34.1)	3.53
Total	10280 (1.358×10^6)	-----	1070	9.6 (1269)	28.7 (98.1)	10.7

Figure 3-35 is the schematic of the model used to study the effect of heat input on the total pressure drop between the inlet and outlet headers (A to B) of a membrane wall circuit. Total pressure drop is comprised of losses due to friction, static, acceleration, and form loss. The two-phase pressure drop was calculated by the Martinelli-Nelson correlation. The actual tube geometry was used to include the inlet, outlet, and bend losses.

The results shown in Figure 3-36 are for the boiler circuit located between 50 and 90° from the north. This circuit is critical because it has the largest variation in tube-to-tube heat absorption. Downflow could occur in an unheated tube in this circuit if the total pressure drop between inlet and outlet headers were less than about 53.7 KPa (7.8 psi). This condition is prevented by maintaining sufficient flow through the circuit to keep the total pressure drop above 53.7 KPa (7.8 psi).

Table 3-7. Flow and Enthalpy Variation, Circuit EN, 3/21/12PM

Tube Orientation	Flow Per Tube kg/min (lbs/hr)	Absorption KW (KBTU/HR)	Enthalpy @ Outlet cal/gm (BTU/LB)	% SBW @ Outlet
50°	6.1 (800)	1.96 (6.67)	.352 (633)	-3.0
60°	5.9 (785)	4.98 (17.0)	.359 (646.3)	-0.4
70°	6.2 (825)	7.5 (25.65)	.365 (656.4)	1.6
80°	7.0 (921)	15.2 (51.84)	.379 (681.9)	6.7
90°	7.7 (1015)	28.6 (97.54)	.401 (720.6)	14.43

Table 3-7 indicates the wide variation in flow, heat absorption and exit quality for tubes in this circuit. However, the hottest tube at 90° from the north has sufficient flow to prevent film boiling, while the header-to-header pressure drop is sufficient to prevent downflow in the coldest tube at 50°. Therefore, flow restrictors are not required for individual tubes.

Superheater Tube Size - The superheater tube size is determined primarily by pressure drop and flow distribution requirements. As tube size increases, pressure drop decreases. However, if tube pressure drop is too small, poor tube-to-tube flow distribution will result leading to unnecessarily high metal temperatures.

The specified maximum superheater pressure drop, as measured from the drum to the secondary superheater discharge nozzle, is 1.38 MPa (200 psi). Design calculations for the SRE helical superheater indicated that a tube outside diameter of 2.54 cm (1 inch) would be required to meet this specification. This diameter has been retained for the Pilot Plant superheater even though updated turbine heat balance data have reduced steam flow requirements. A reduction in superheater tube diameter is a possible design refinement.

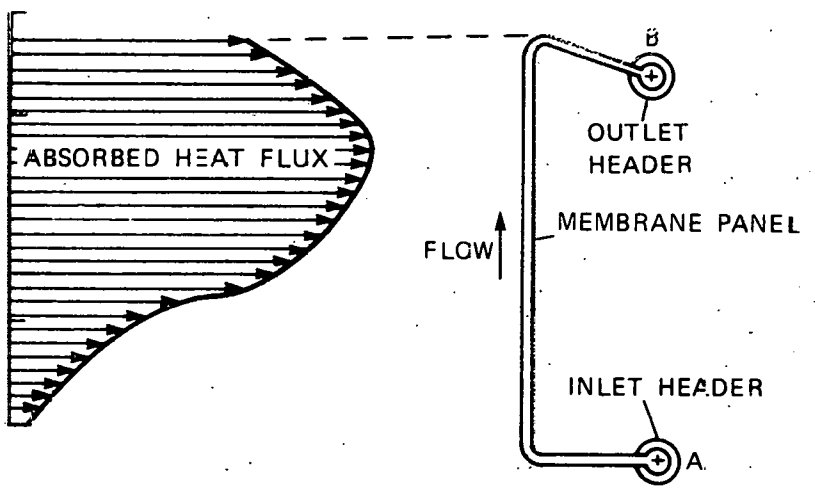

Figure 3-35. Boiler Tube Circuit

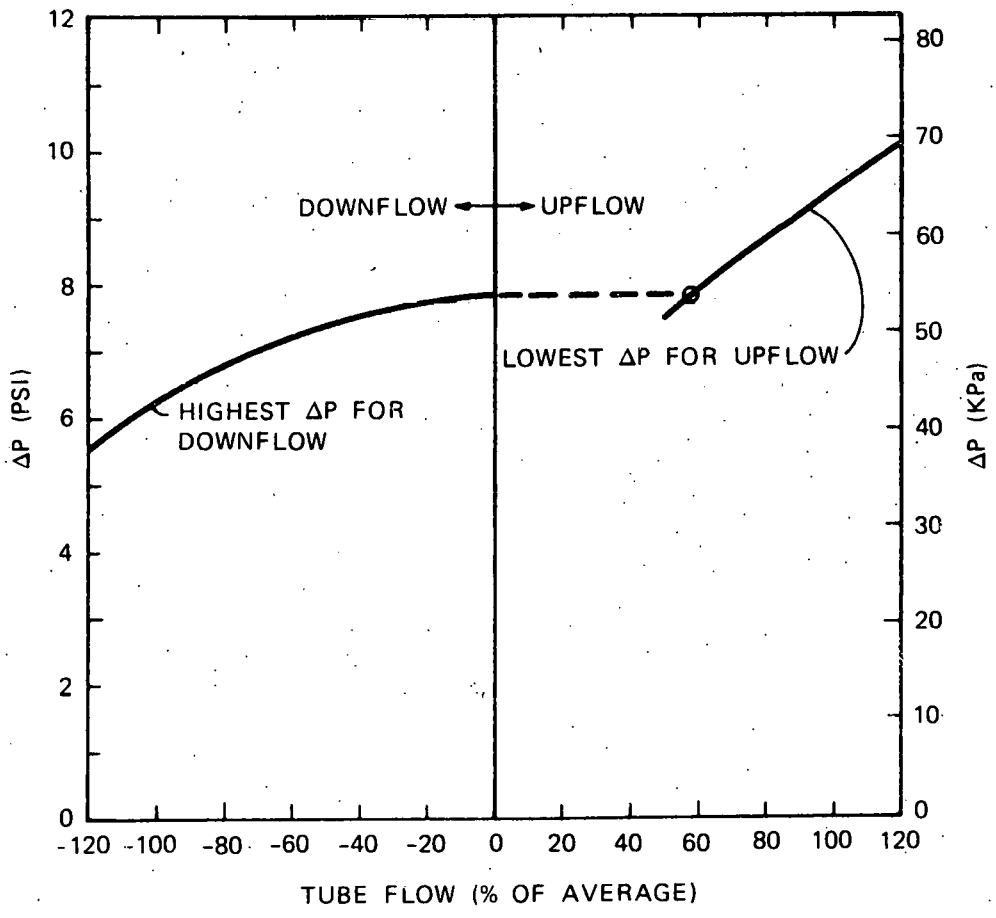

Figure 3-36. Static Stability, EN Circuit, 3/21/12PM

Tube diameter affects not only pressure drop, but to a lesser extent, peak metal temperature, thermal stress, and cost.

A simplified analysis results in the following relationships:

$$\Delta P \propto \frac{1}{d^3}$$

$$T_m - T_s \propto d$$

$$v \propto d$$

$$n \propto \frac{1}{d}$$

$$W_\tau \propto d$$

Tube diameters much less than 2.54 cm (1 inch) would cause the superheater pressure drop to exceed specifications. On the other hand, diameters greater than 2.54 cm would unnecessarily increase peak metal temperature, thermal stress, and the weight of the superheater. The cost tradeoff with tube diameter is not straightforward. Although material weight and cost increase directly with diameter, the number of tubes and fabrication costs are inversely proportional to tube diameter.

Superheater Surface Arrangement and Flow Distribution - There are two reasons why the primary superheater heat flux distribution (Figures 3-23 and 3-24) varies greatly in the circumferential direction:

- There are few south field heliostats aimed at the primary superheater; and
- The heliostats that are aimed at the primary superheater must also be aimed to miss the corbels.

The heat flux in the secondary superheater is more uniform because the heliostats aimed at this superheater surround the tower.

The superheater flow circuitry minimizes the effect of these flux variations on steam temperature. The vertical headers are oriented so that the inlet and outlet headers from one pair of adjacent modules are due south. Thus, the flux peaks at 120 and 220 degrees from north are in different modules rather than the same module. Regardless of the orientation choice, the outlet of at least one module must be somewhere in the high heat flux region between 90° and 270°. The due south orientation minimizes the heat flux at the module outlet where steam temperature is highest. The "checkerboard" flow path balances differences in heat absorption as the steam flows through the superheater. As a result, steam temperature exiting each of the three flow paths is nearly identical.

To illustrate this effect, steam temperatures at the outlet header of each module were estimated for the three flow paths assuming an average specific heat and equal flow per tube. Figure 3-37 indicates how steam temperature and heat flux vary as the steam flows around the circumference of the cavity. Heat flux is generally highest at the inlet where steam temperature is low and lowest at the outlet where steam temperature is high. This characteristic reduces peak metal temperatures.

Even with the checkerboard flow pattern, the total heat absorption differs among the three flowpaths in each superheater. Figures 3-38 and 3-39 shows energy absorption in each of the flow paths for the primary and secondary superheater. Energy absorption varies by ±10% among the primary flowpaths and +5%, -3½% among the secondary flowpaths.

To further balance steam temperatures the flow to each primary superheater flow path was varied to match the heat absorption. Flow balancing was achieved by varying the size of the saturated steam lines and connecting pipe that supply each flow path (Figure 3-40). The heat absorbed, flow, and average outlet temperature are summarized for each flow circuit for both the primary and secondary superheater in Table 3-8.

Table 3-8. Superheater Performance, 3/21/12PM

Flow Path	A	B	C	D	E	F
Absorption, KW (KBTU/hr)	3178 (10837)	2932 (10000)	2582 (8805)	2474 (8435)	2277 (7766)	2330 (7947)
Flow, kg/min (lb/hr)	327 (43200)	315 (41600)	286 (37800)	331 (43690)	353 (46620)	352 (46460)
Average Outlet Temp, °C (°F)	465 (870)	456 (854)	458 (858)	530 (986)	502 (936)	510 (950)

Metal Temperatures - Superheater maximum mean metal temperatures* were calculated for the primary and secondary superheaters according to the following procedure:

- The flow path with the highest exit steam temperature was assumed to have the highest metal temperatures.
- The maximum tube flow reduction due to header geometry effects was calculated and found to be 10 percent. This flow upset was conservatively applied to all tube metal temperature calculations.

*The maximum local mean temperature across the tube wall. The Section 1 maximum allowable stress values are determined at this temperature.

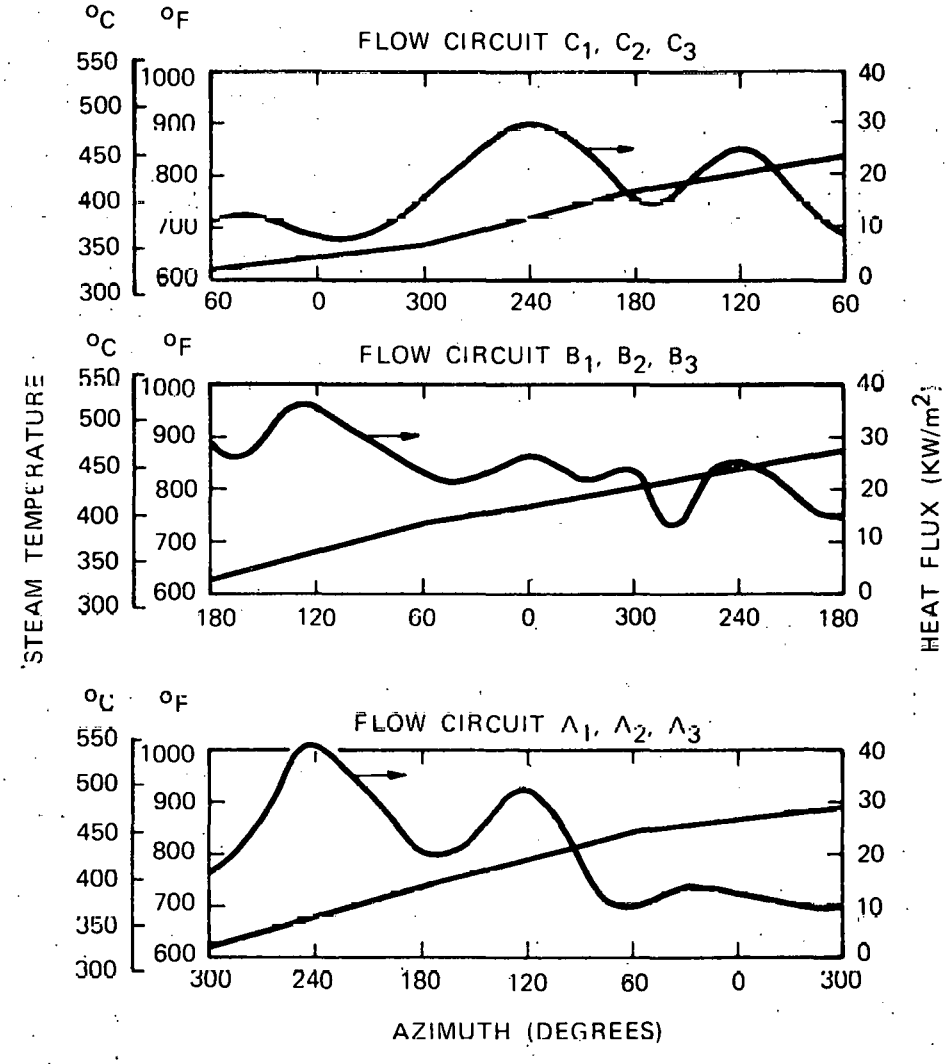

Figure 3-37. Primary Superheater, Steam Temperature and Heat Flux versus Azimuth Angle (Before Flow Balancing), 3/21/12PM

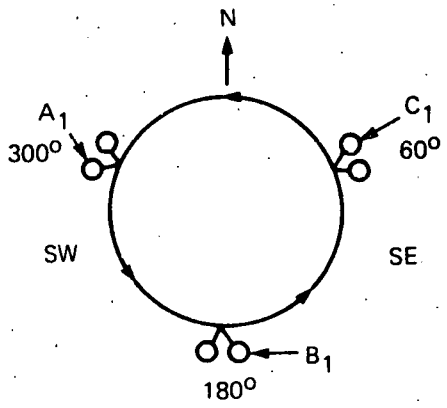

	300°	60°	180°	300°
TOP	A_3	C_3	B_3	
	B_2	A_2	C_2	
BOTTOM	C_1	B_1	A_1	
	N	SE	SW	

FLOW PATHS

$A_1 \rightarrow A_2 \rightarrow A_3$

$B_1 \rightarrow B_2 \rightarrow B_3$

$C_1 \rightarrow C_2 \rightarrow C_3$

HEAT ABSORPTION, 3/21/12PM, MW (KBTU/HR)

A_1	1.470 (5017.1)	B_1	1.410 (4812.3)	C_1	0.567 (1936.0)
A_2	1.129 (3851.6)	B_2	0.652 (2224.6)	C_2	1.158 (3951.7)
A_3	0.577 (1968.3)	B_3	0.868 (2963.6)	C_3	0.855 (2917.4)
ΣA	3.176 (10837.0)	ΣB	2.931 (10000.5)	ΣC	2.580 (8805.1)

Figure 3-38. Primary Superheater Circuits

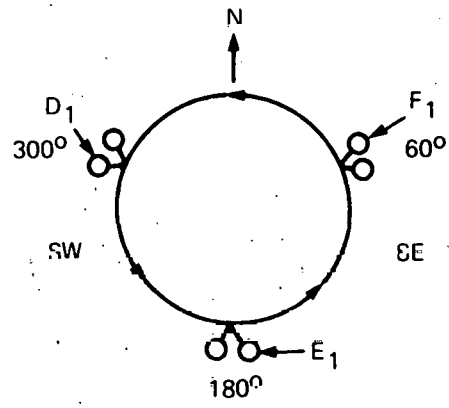

	300°	60°	180°	300°
TOP	D_3	F_3	E_3	
	E_2	D_2	F_2	
BOTTOM	F_1	E_1	D_1	
	N	SE	SW	

FLOW PATHS

$D_1 \rightarrow D_2 \rightarrow D_3$

$E_1 \rightarrow E_2 \rightarrow E_3$

$F_1 \rightarrow F_2 \rightarrow F_3$

HEAT ABSORPTION, 3/21/12PM, MW (KBTU/HR)

D_1	1.04 (3557.2)	E_1	1.034 (3529.7)	F_1	0.801 (2734.5)
D_2	0.869 (2965.9)	E_2	0.606 (2068.0)	F_2	0.874 (2981.8)
D_3	0.560 (1912.1)	E_3	0.635 (2168.6)	F_3	0.653 (2230.9)
ΣD	2.472 (8435.2)	ΣE	2.276 (7766.3)	ΣF	2.329 (7947.2)

Figure 3-39. Secondary Superheater Circuits

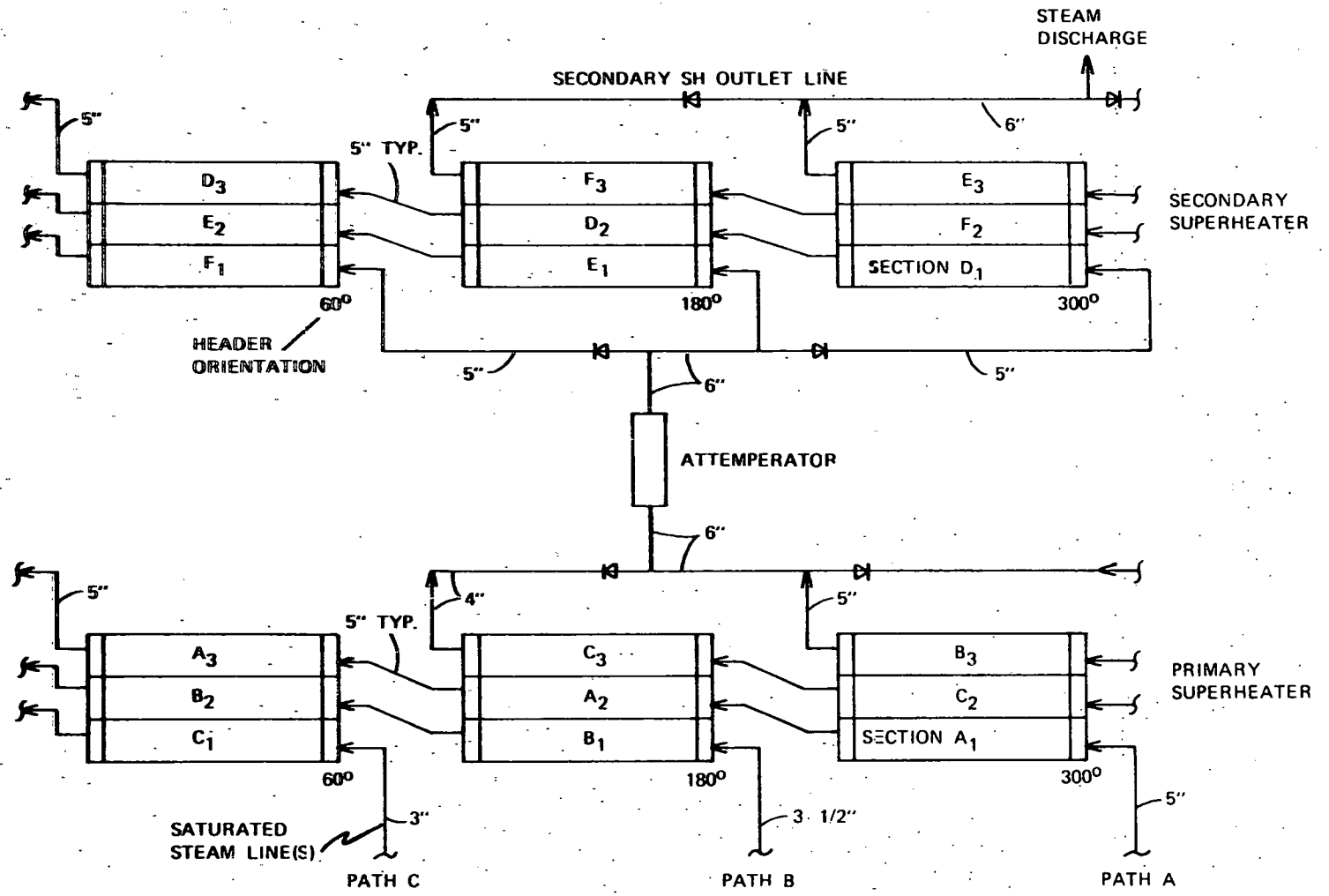

Figure 3-40. Superheater Flow Schematic

- For each of the three superheater sections within the flow path, metal temperatures were calculated at the highest heat flux at that elevation. The highest exit steam temperature was also used to add additional conservatism.

- The maximum flat projected heat flux was increased by a 20 percent uncertainty factor.

The results of these calculations are summarized in Table 3-9. In all cases, the mean metal temperatures are less than the maximum allowable temperature of 582°C (1077°F).

Heat Loss and Cooldown Rate - The major heat losses from the steam generator during operating periods are conduction through the insulation and convection and reradiation from the cavity aperture. Reradiation losses have been estimated using the Rerad Code. Conduction losses through the insulation have been scaled from the SRE steam generator by the ratio of exposed surface areas. The insulation loss (Table 3-10) is based on data for 8.9 cm (3.5 in) Johns-Manville "Thermo-12" insulation. The ambient conditions are 27°C (80°F) still air.

The Pilot Plant Steam Generator conduction losses are about twice the SRE losses because the surface area per unit of absorbed energy has increased by a factor of 1.84.

Convection losses as a function of wind speed at the top of the tower were estimated based on a paper by J. Fox, "Heat Transfer and Air Flow in a Transverse Rectangular Notch", International Journal of Heat and Mass Transfer, Volume 8, pp. 269-279, 1965. The notch studied by Fox was a two-dimensional notch 5.2 cm (2.05 in) long by 5.2 cm deep. Dimensionless parameters for extending the data to larger sizes were recommended by Fox and used to generate the Pilot Plant receiver cavity convective heat loss data presented in Figure 3-41. The wind velocity indicated on the abscissa is the velocity parallel to the mouth of the cavity.

The overnight cooldown rate for the Pilot Plant steam generator with the cavity closure in place was estimated based on the conduction losses presented in Table 3-10 plus an estimated loss through the cavity closure of 57.4 KW at operating temperature. The heat loss was assumed to be a linear function of the difference between the component temperature and an ambient temperature of 27°C (80°F). The metal and water specific heat as a function of temperature was taken from Appendix A of the SRE Detailed Design Report (DDR). The metal and water weights are listed in Appendix C of this report. The heat capacity of the steam, the insulation, the ceiling, and the cavity closure was neglected.

The superheater was assumed to cooldown from an initial temperature of 420°C (787°F) and the boiler circuit from 327°C (620°F). A transient energy balance was performed following the procedure described in Appendix A of the SRE DDR. The results are presented in Figure 3-42. After an average downtime of 12 hours, the temperature drops to 165°C (330°F) and the pressure to 0.86 MPa (125 psia).

Table 3-9. Superheater Metal Temperatures

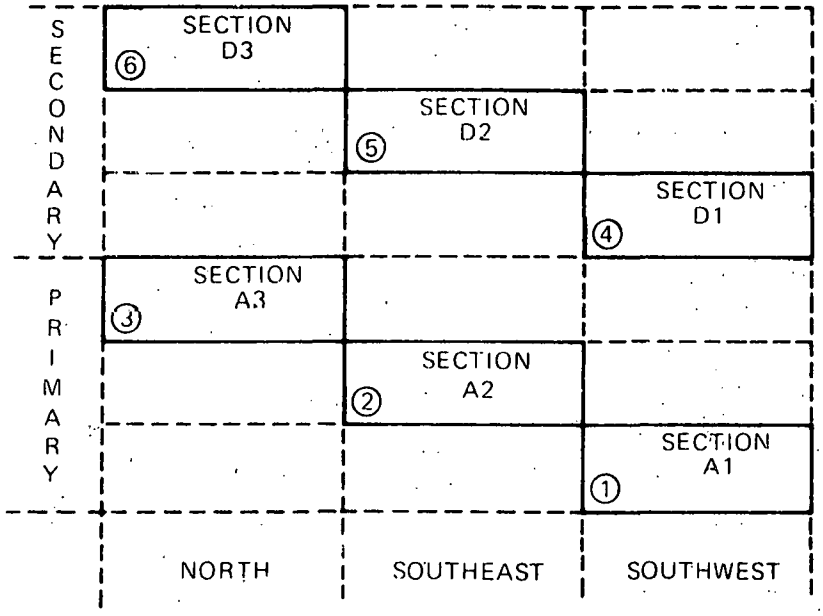

TIME	LOCATION	UPSET STEAM TEMP. °C	(°F)	UPSET ABSORPTION RATE KW/M²	(BTU/HR-FT²)	DESIGN METAL TEMPERATURE °C	(°F)
3/21/12PM	1	386	(726)	154	(49×10^3)	438	(820)
3/21/12PM	2	444	(832)	114	(36×10^3)	488	(910)
3/21/12PM	3	474	(885)	91	(29×10^3)	510	(950)
3/21/12PM	4	443	(829)	66	(21×10^3)	474	(885)
3/21/12PM	5	499	(930)	66	(21×10^3)	531	(988)
3/21/12PM	6	535	(995)	46	(14.5×10^3)	559	(1039)
12/21/2PM	3	468	(875)	74	(23.5×10^3)	500	(932)
12/21/2PM	6	538	(1000)	38	(12×10^3)	563	(1045)
3/21/7AM	3	510	(950)	22	(7×10^3)	529	(985)
3/21/7AM	6	518	(965)	2.3	(0.8×10^3)	521	(970)
6/21/12PM	3	490	(915)	86	(27.4×10^3)	524	(975)
6/21/12PM	6	528	(982)	53	(16.8×10^3)	554	(1030)

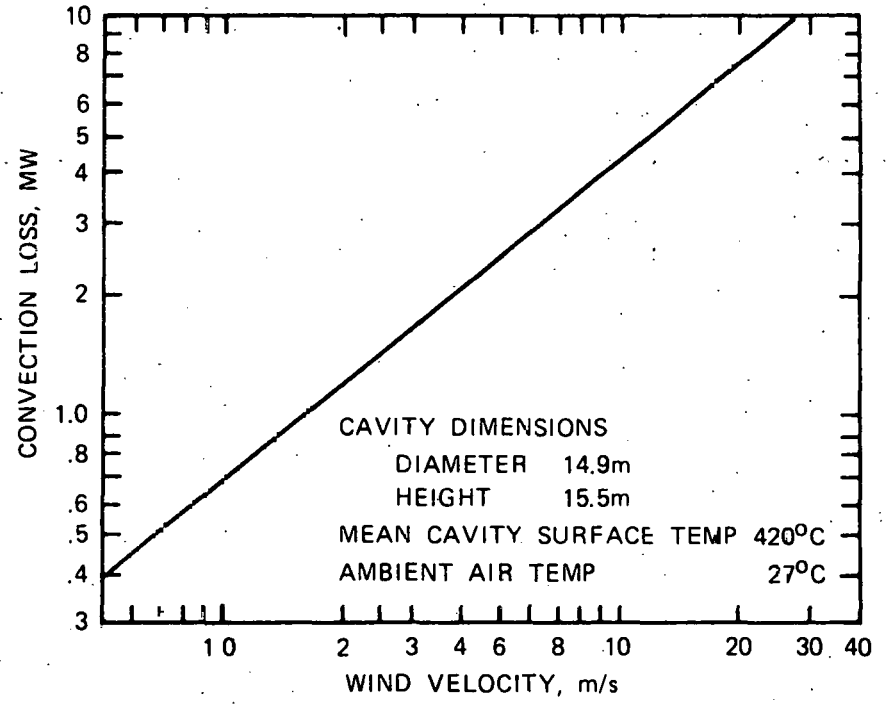

Figure 3-41. Pilot Plant Receiver Cavity Convection Losses

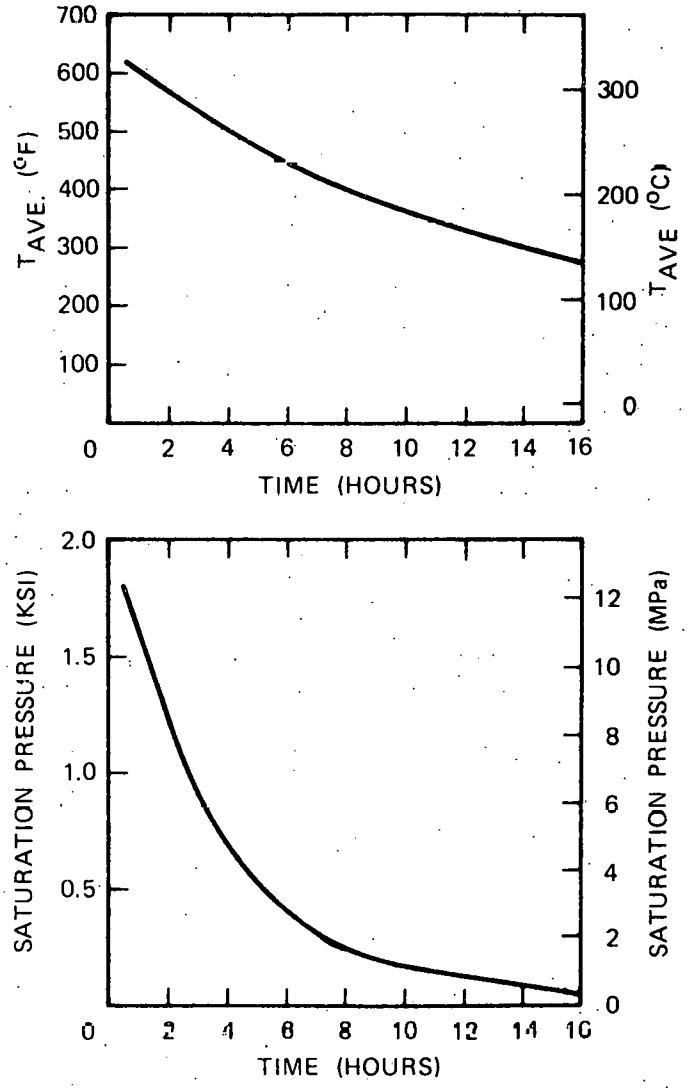

Figure 3-42. Overnight Cooldown Rate

Table 3-10. Conduction Losses

Component	Conduction Loss, KW (KBTU/HR)	
	SRE	Pilot Plant
Boiler Section	17.9 (61.0)	283 (966)
Superheater	23.6 (80.4)	394 (1343)
Ceiling	5.7 (19.3)	104 (356)
Total	47.1 (160.7)	781 (2666)
% of Maximum Absorbed Energy	0.94%	1.72%

Thermal Radiation Characteristics - Although the optical or thermal radiation characteristics of the heat transfer surfaces affect cavity efficiency, the relationship is less than linear as indicated by Rerad calculations. Figure 3-43 indicates the effect of changes in either solar absorptivity (α) or IR emissivity (ε) on cavity efficiency with all other parameters held constant. IR emissivity has relatively little effect while solar absorptivity variations of 0.9 ± 0.1 change cavity efficiency $\pm 2.5\%$.

Figure 3-44 presents a sample of reported thermal radiation properties of carbon steel. The data range between 0.75 and 0.95 although, in general, oxidized steel appears to have a higher emissivity and absorptivity than as-received steel.

Based on the data presently available and the relatively small influence of thermal radiation properties on cavity efficiency, the design basis α and ε were both chosen to be 0.9. Natural oxidation of the heat transfer surfaces was assumed to be adequate to achieve this value. The ceiling is covered with Kaowool. The Kaowool surface is composed of many fibers in the diameter range up to 5 microns, approximately the wave length of the incident radiation. Each fiber absorbs, transmits, reflects and emits incident radiation, significantly increasing absorption compared to a solid ceramic surface. Accordingly, α and ε were also assumed to be 0.9 for the ceiling.

The radiation properties for the heat transfer surfaces could change for the detail design as new data become available. However, Figure 3-43 indicates changes in cavity efficiency would be expected to be less than $\pm 2.5\%$ at maximum heat input. Similar calculations at 3/21/7AM indicate cavity efficiency changes would also be less than $\pm 2.5\%$ at low incident energy levels.

Upset Conditions

Upset or abnormal operating conditions are those conditions which change the design basis heat flux and steam pressure, temperature, and flow. Boiler circulation is pump-assisted and upset conditions will have little or no

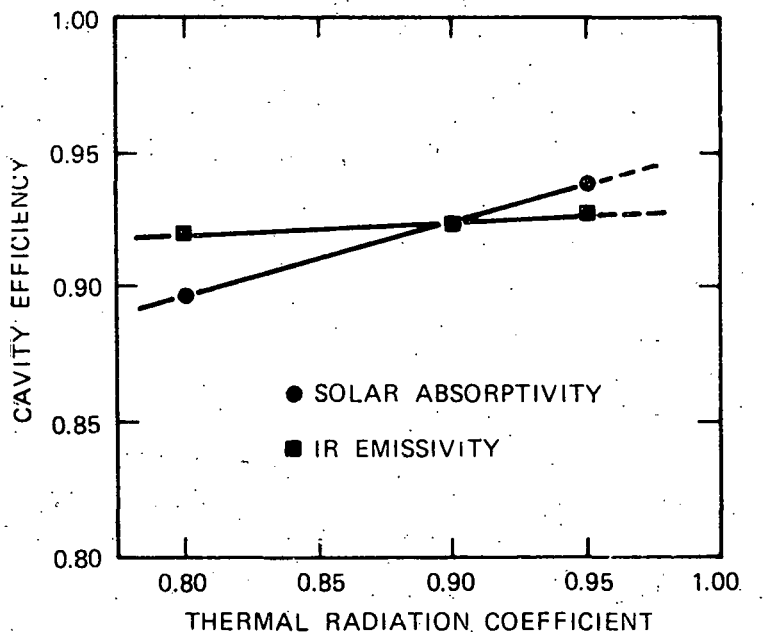

Figure 3-43. Cavity Efficiency versus Thermal Radiation Coefficient, 3/21/12PM

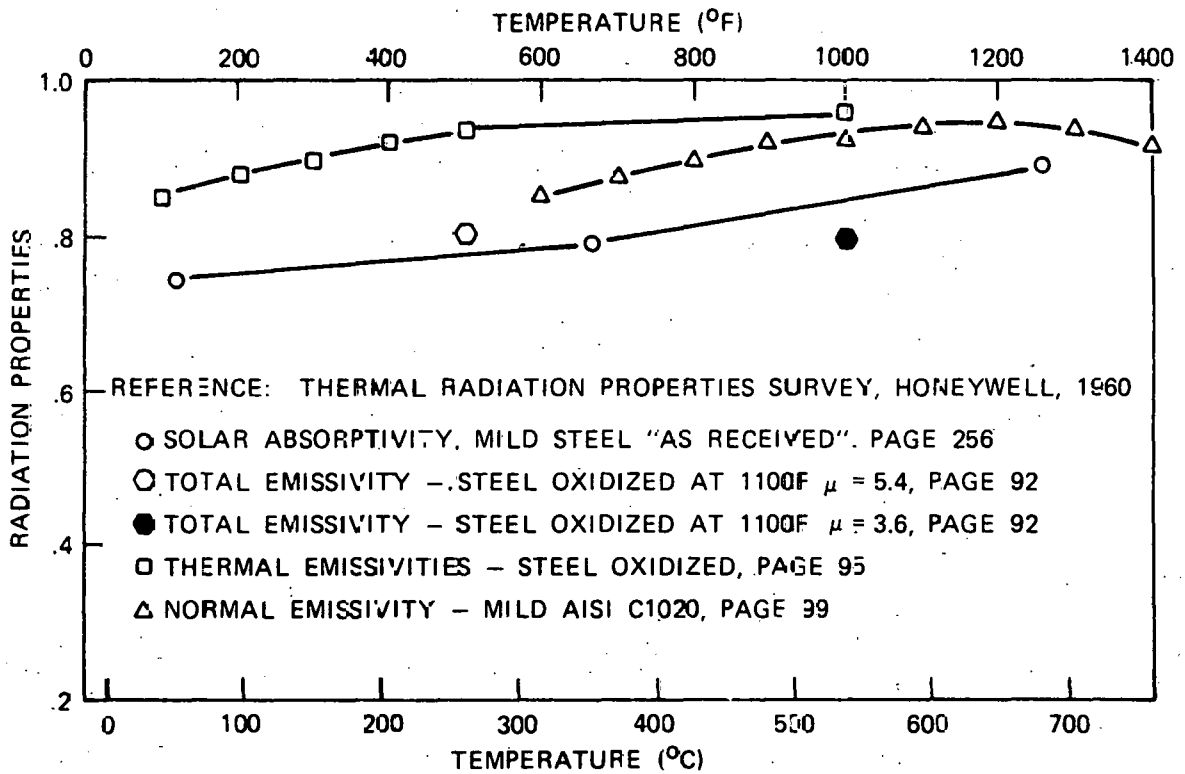

Figure 3-44. Thermal Radiation Properties

effect on the design safety margin. However, superheater metal temperatures are very sensitive to changes in heat flux and steam conditions. Therefore, two upset conditions were investigated, partial cloud shadowing and feedwater temperature excursions.

Cloud Shadowing - Cloud shadowing can cause an infinite variety of effects on the design basis conditions. Sudden interruption of the incident energy by complete shadowing of the heliostat field is not viewed as a design problem because metal temperatures will decline in a relatively uniform fashion. An abrupt application of maximum incident energy could cause operational problems, but these can be avoided by proper control of the heliostats to achieve a gradual startup consistent with steam generator operating constraints.

The major cause for concern is partial shadowing of the heliostat field. Partial shadowing has two significant effects:

- The incident energy distribution changes, which can change the boiler/superheater absorbed energy balance from the design ratio. As a result, steam temperature control requirements may exceed the range of capability of the spray attemperator.

- A reduction in energy absorbed by the boiler section causes a direct reduction in saturated steam flow to the superheaters. If the maximum local heat flux on the superheater is not reduced by cloud shadowing or selective defocusing of the heliostats, superheater metal temperatures will increase.

Three cases, which are representative of a range of cloud shadowing conditions, have been considered.

Case 1 - Cloud shadowing causes a reduction of heat input to the boiler section only.

This would happen if a cloud shadowed the north portion of the heliostat field. Energy absorption in the primary and secondary superheaters would not change significantly. Steam flow to the primary superheater would decrease causing both steam and metal temperatures to increase in the primary superheater. Spray flow would increase reducing inlet temperatures to the secondary superheater. Thus, primary metal temperatures will be limiting.

Figure 3-45 shows how steam and maximum mean metal temperatures increase as heat absorption in the boiler is reduced by cloud shadowing. The design limit of 582°C (1077°F) is reached at a 20% reduction in boiler section absorbed energy. This corresponds to a 13% reduction in total absorbed energy (steam flow).

Case 2 - Cloud shadowing causes a reduction of heat input to the superheater section only.

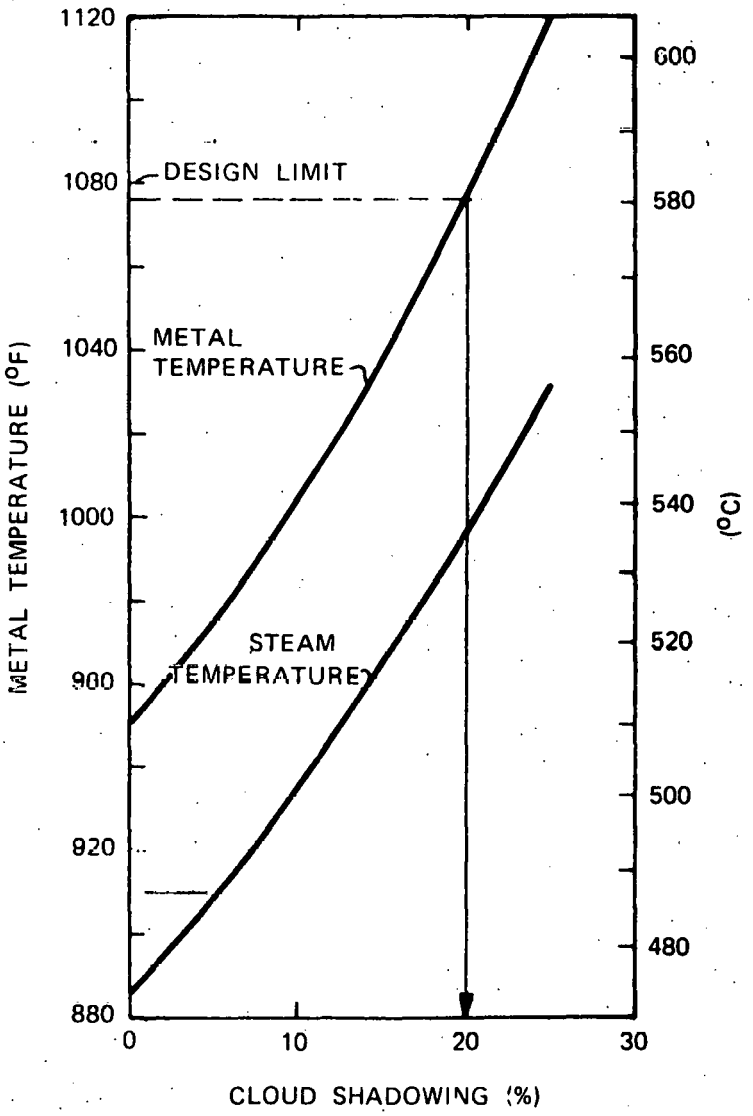

Figure 3-45. Primary Temperatures versus Cloud Shadowing (Case 1) 3/21/12PM

This case would occur if clouds shadowed only the south portion of the heliostat field. Energy absorption in the boiler section would not change significantly, and to maintain steam temperature, spray attemperator flow would decrease. The highest superheater metal temperatures would be reached if it is assumed that the reduction in superheater absorbed energy is caused by progressively blocking out incident energy starting at the top of the cavity. Primary superheater outlet steam temperature would remain high although steam flow to the secondary superheater decreased.

Figures 3-46 and 3-47 show how steam and peak metal temperature vary for the three sections of the secondary superheater as clouds progressively shadow the heliostats aimed at the secondary superheater. Note that absorbed heat for the third, second, and first sections of the secondary superheater is reduced to zero when 11.4, 27.1 and 45.7% of the secondary superheater heliostats are progressively shadowed.

The maximum allowable metal temperature is exceeded only slightly in both Section 1 and Section 2 at about 25% cloud shadowing of the superheater heliostats, which corresponds to a total absorbed energy reduction of 8.75%.

Case 3 - Cloud shadowing causes a uniform reduction of heat input to both the boiler and superheater sections.

This case would occur if a cloud shadowed an equal percentage of heliostats aimed at the boiler section and each of the two superheaters. Feedwater, steam and spray flow would be reduced in direct proportion to the reduction in total absorbed energy. However, peak heat flux would not be reduced in those areas of the superheater not shadowed by clouds.

The highest metal temperatures would be reached if it were assumed that clouds shadowed only one third of the cavity circumference. Consider the superheater flow path for which the first and second sections continue to receive maximum incident flux, with cloud shadowing affecting the third section only. Metal temperatures peak at the exit of the second section.

Figure 3-48 shows that peak metal temperature and unbalanced steam temperature increase as total absorbed energy is decreased. While steam flow is dropping off, the heat absorption on the first and second sections remains constant resulting in higher steam temperatures and lower film coefficients. The maximum allowable metal temperature is exceeded at a 23% reduction in total absorbed energy.

Feedwater Temperature - The selected steam generator boiler/superheater interface allows steam to be produced at rated pressure and temperature over a range of feedwater temperatures. As shown previously in Figure 3-31, steam temperature can be controlled without defocusing heliostats when steam is being supplied to the turbine alone. Several other operating conditions are presented in Table 3-11.

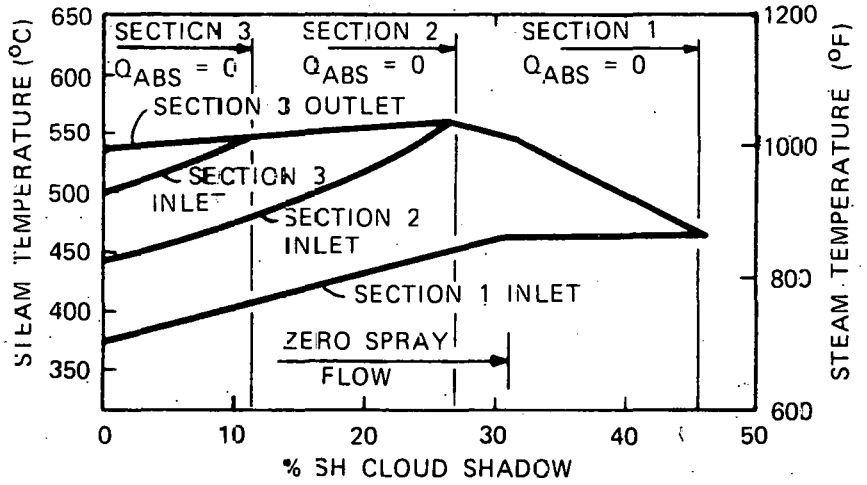

Figure 3-46. Steam Temperature Variation versus Secondary Superheater Shadowing (Case 2) 3/21/12 PM

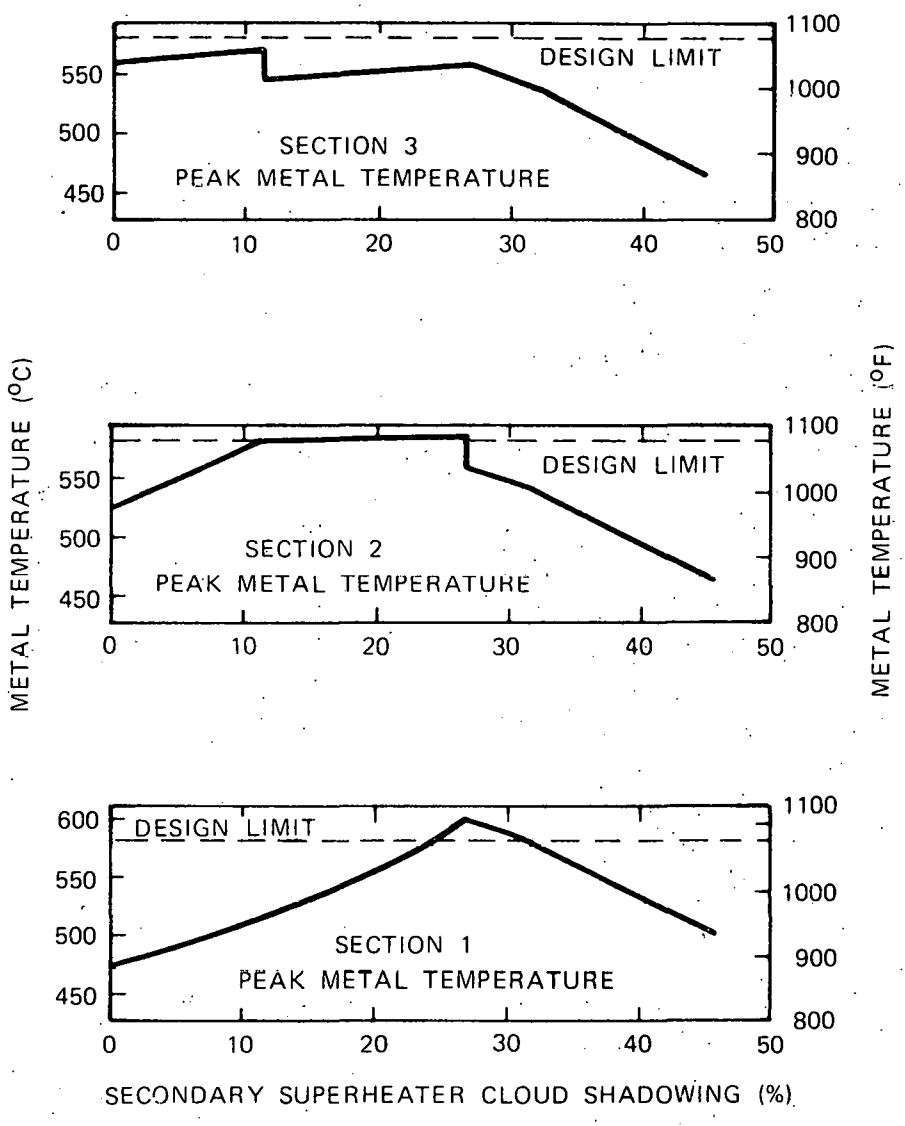

Figure 3-47. Secondary Superheater Temperatures (Case 2) 3/21/12PM

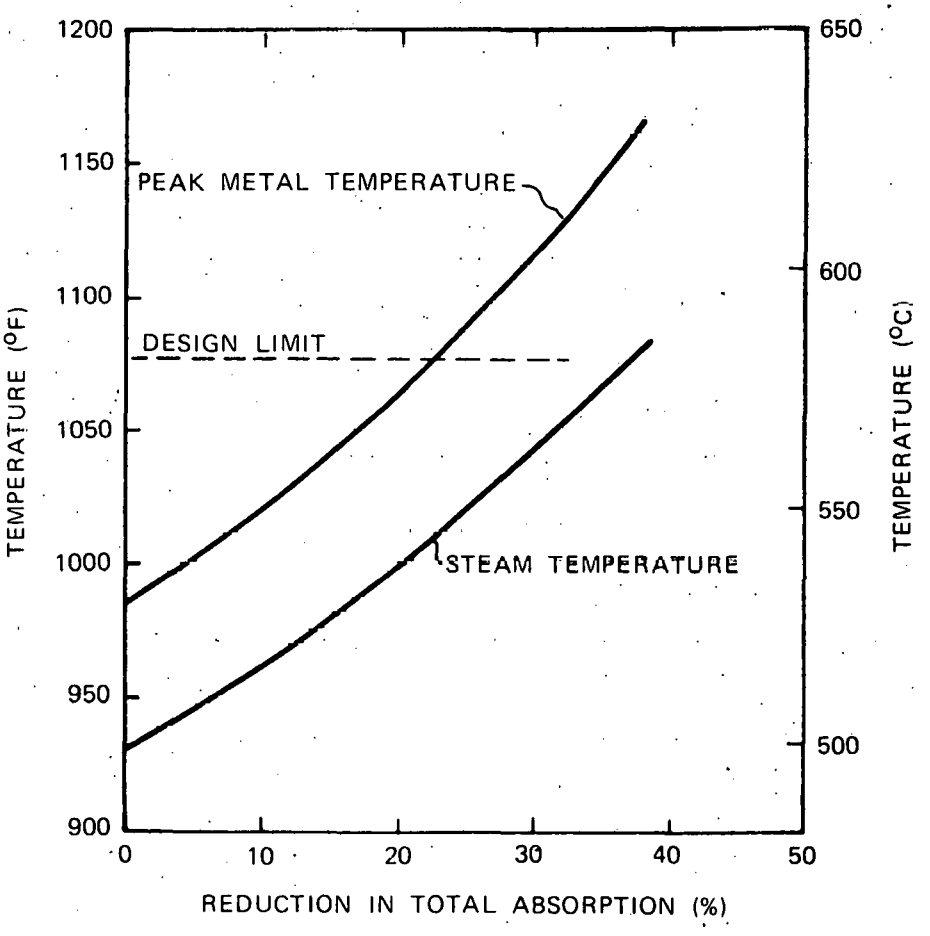

Figure 3-48. Peak Metal Temperature versus Absorption, (Case 3) 3/21/12PM

Table 3-11. Attemperator Spray Flow Required to Control Steam Temperature

Case	Description	Feedwater Temperature C, (F)	Spray Flow kg/s (lb/hr)	Steam Flow kg/s (lb/hr)	Absorbed Energy Mw
4	Operation with high pressure feedwater heater out of service	111* (232)	124.6 (16460)	939 (124060)	45.3
5	Feedwater temperature based on revised turbine heat balance data	215 (419)	86.5 (11430)	1098 (145070)	45.3
6a	Steam to thermal storage alone, maximum absorbed energy	140* (285)	8.2 (1085)	966 (127600)	45.3
6b	Steam to thermal storage alone, low absorbed energy	140* (285)	120.7 (15950)	235 (31000)	11.0

*Preliminary turbine heat balance.

These results indicate that steam temperature could be controlled without defocusing heliostats if the high pressure feedwater heater was out of service (Case 4), or if feedwater temperature was increased because of a higher cycle efficiency (Case 5). Steam temperature can also be controlled without defocusing heliostats over a range of absorbed energy when steam is supplied to Thermal Storage alone (Case 6).

Stress Analysis

The primary objective of the steam generator stress analysis is to verify that the pressure components meet the requirements of Section I of the ASME Boiler and Pressure Vessel Code. Other objectives are to assure that steam generator components are structurally adequate and properly supported to withstand the forces and moments from deadweight, thermal expansion, and external loads.

To achieve the above objectives, Fossil Power Generation Division design procedures, stress analysis techniques, and experience with fossil boilers is used whenever possible. Certain design and analysis aspects of the steam generator are unique. For these areas, state-of-the-art stress analysis procedures, such as finite element, are used to assure structural adequacy of the design.

Boiler Section - The boiler tubes are subjected to two non-self-equilibrating loads; internal pressure and deadweight. Deadweight stresses in the boiler tubes result from the requirement that the boiler tubes carry their own weight, and the weight of the membrane, water and insulation and lagging. The primary membrane stress due to internal pressure and deadweight is limited to the

Section III design stress intensity (S_m). The combination of primary membrane-plus-bending stress is limited to 1.5 S_m. These limitations protect the boiler tubes against ductile rupture.

Secondary thermal stresses in the boiler section result from one-sided heating of the tubes within the boiler cavity. The range of primary-plus-secondary stresses is limited to 3 S_m to insure elastic "shakedown" of the stresses.

Cyclic stresses in the boiler section are limited per the Section III fatigue curves to insure against the fatigue failure mode. Creep of the boiler tubes is not of concern because the maximum anticipated tube temperatures are below the creep regime.

The boiler tubes were initially sized for thickness by the criteria of Section I using a design pressure of 13 MPa (1875 psig) and a design temperature of 371°C (700°F).

The wall thickness required to meet Section I criteria were found to be less than the minimum needed to assure reliable welding of the membrane bar to the tubes [0.368cm, (0.145-inch)]. The stresses induced by the tube deadweight and auxiliary loading on the boiler tubes was analyzed by subjecting a beam element model of a typical tube-web configuration to a gravitational loading as well as the local bending moments at the tube to supply header support locations.

The thermal stresses due to one-sided heating of the boiler panels was analyzed by subjecting one side of a typical tube-web configuration to a uniform heat flux while restraining the configuration in a generalized plane strain condition.

The steady-state temperature distribution in the boiler section resulting from one-sided heating of the panels was found by a finite difference approximation using a half-tube, half-web configuration. The configuration was subjected to a constant heat flux on the heated side, the other side being insulated. Radiant interchange was accounted for between the tube and web surfaces. Figure 3-49 illustrates a typical temperature distribution in the tube-web configuration when subjected to a uniform flat projected heat flux of 263.0 KW/m^2 (83,380 Btu/hr-ft^2), which is the maximum design value for the boiler section. Tube temperatures ranged from near fluid temperature in the rear quadrant of the tube to approximately 362.3°C (684°F) on the heated side of the tube.

To compute the thermal stresses resulting from the asymmetric heating, the tube and web were required to meet a generalized plane strain condition while being subjected to a temperature distribution corresponding to a particular heat flux (Figure 3-49). Figure 3-50 illustrates typical thermal stress states at selected locations on the tube-web configuration resulting from the boiler section being subjected to a flat projected heat flux of 263.0 KW/m^2 (83,380 Btu/hr-ft^2). The maximum stress in the tube occurs at point C and is a longitudinal (axial) stress which results from the asymmetrical temperature distribution.

The fatigue curves shown in Figure 3-51 show the allowable amplitude, S_a, of the alternating stress component (1/2 of the alternating stress range) plotted against the number of cycles. These Section III fatigue curves are obtained from uniaxial strain cycling data.

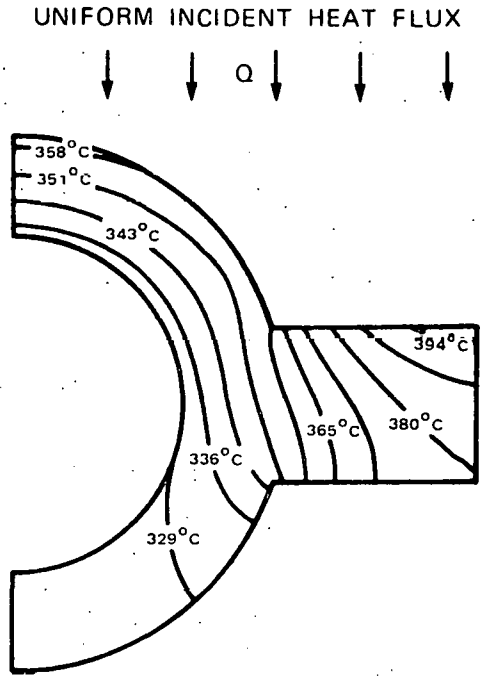

TUBE OD	2.22 cm (0.875 IN.)
TUBE ID	1.47 cm (0.579 IN.) (MINIMUM WALL)
TUBE CENTER-TO-CENTER SPACING	3.81 cm (1.5 IN.)
WEB THICKNESS	0.64 cm (0.25 IN.)
TUBE MATERIAL	CARBON STEEL (SA-210 GRADE A1)
WEB MATERIAL	CARBON STEEL (AISI C1015)
FILM COEFFICIENT	4882 CAL/HR-cm^2-°C (10,000 BTU/HR-SQ FT-DEG F)
FLUID TEMPERATURE	327.8°C (622°F)

Figure 3-49. Temperature Distribution in Boiler Section Membrane Wall, Flat Projected Heat Flux of 263.0 bW/m^2

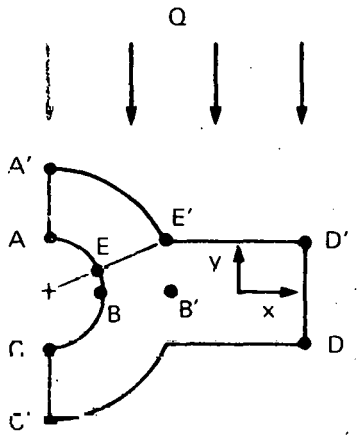

Tube OD	2.22 cm (0.875 in.)
Tube ID	1.47 cm (0.579 in.) (minimum wall)
Tube Center-to-Center Spacing	3.81 cm (1.5 in.)
Web Thickness	0.64 cm (0.25 in.)
Tube Material	Carbon Steel (SA210 Grade A1)
Web Material	Carbon Steel
Film Coefficient	4,882 Cal/hr cm^2 °C (10,000 Btu/hr-sq ft-deg F)
Fluid Temperature	327.8 °C (622°F)

		Thermal Stresses in Tube (MPa)	
Location	Temperature (°C)	Circumferential	Longitudinal
A	334.7 (635°F)	43.1 (6,250 psi)	-54.3 (7,880 psi)
B	333.4 (632°F)	36.1 (5,230 psi)	55.7 (8,080 psi)
C	328.3 (623°F)	29.0 (4,210 psi)	68.1 (9,870 psi)
A'	362.3 (684°F)	-33.3 (-4,830 psi)	-42.8 (-6,200 psi)
B'	359.0 (678°F)	-26.4 (-3,830 psi)	-31.6 (-4,580 psi)
C'	328.7 (624°F)	-19.4 (-2,870 psi)	51.9 (7,520 psi)
E	334.0 (633°F)	67.6 (9,810 psi)	63.6 (9,220 psi)
E'	357.8 (676°F)	-51.7 (-7,500 psi)	-35.9 (-5,210 psi)

		Thermal Stresses in Web (MPa)	
Location	Temperature (°C)	σ_x	Longitudinal
D	381.1 (718°F)	35.0 (5,070 psi)	-53.0 (-7,690 psi)
D'	398.8 (750°F)	-35.0 (-5,070 psi)	-115.2 (-16,710 psi)

Figure 3-50. Thermal Stresses in Boiler Section Membrane Wall, Heat Flux 263 KW/m^2

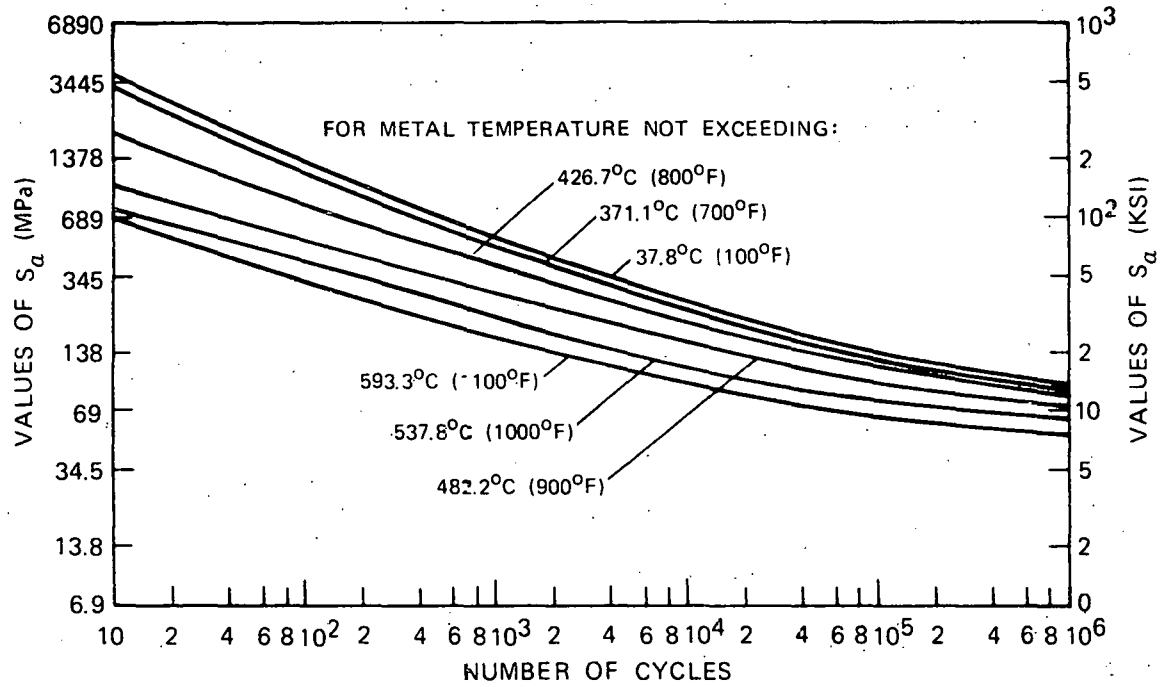

Figure 3-51. Design-Fatigue Strength for Carbon and Low-Alloy Steels through 5% Cr up to 538°C (1100°F)

In the boiler section, it is anticipated that the maximum effective alternating stress range of the boiler tubes will be approximately 103.4 MPa (15,000 psi). From Figure 3-48, this corresponds to a fatigue life in excess of 10^6 cycles. Creep-fatigue interaction need not be considered because the tube temperatures are below the creep regime for carbon steel.

Superheater - Superheater tube metal temperatures are well within the creep regime. Therefore time dependent failure modes must be considered in addition to the time independent modes considered for the boiler section. The design of pressure parts operating at elevated temperatures is covered by both Section I (Power Boilers) and Section VIII, Division I, (Pressure Vessels) of the ASME Code. The stress criteria of these sections consider creep and stress rupture in addition to the short time material strength properties. Detailed stress analysis is not required; rather a wall thickness is established which limits the primary membrane stress below tabulated allowable stresses. When required, specific design rules have been developed by each manufacturer to hold secondary bending stresses and high localized stresses at a safe level consistent with experience. High temperature cyclic operation is not addressed by the Section I rules.

Section III Subsection NB rules consider only time independent failure modes:

- Bursting, gross distortion, and elastic instability (buckling) from a single application of pressure are prevented by the limits placed on primary stresses.
- Progressive distortion is prevented by the limits placed on primary plus secondary stresses. These limits generally assure shakedown to elastic action after a few repetitions of the loading.
- Fatigue failure is prevented by the limit placed on peak stress.

Design rules for elevated temperatures are provided by ASME Code Case 1592. When cyclic load conditions exist, fatigue and incremental cumulative deformation (ratcheting) can be significantly accelerated by elevated temperature effects. Accordingly, Code Case 1592 considers the effect of time and temperature when assessing the damage caused by secondary and peak stresses as well as primary stresses.

Design limits are placed on:

- general primary membrane stress intensity
- local membrane plus bending stress intensity
- maximum accumulated inelastic strain
- accumulated creep and fatigue damage including hold time and strain rate effects.

Code Case 1592 provides for creep-fatigue evaluation based on either elastic or inelastic analysis. The elastic analysis provides a simple, efficient method for identifying potentially critical areas in a design. It is important to note that failure to meet the criteria based on elastic analysis does not necessarily imply that a creep-fatigue failure is to be expected, but rather warns that elastic analysis is not adequate to insure satisfactory service. Inelastic analysis is required when the elastic analysis criteria are exceeded.

The following paragraphs describe a preliminary and simplified elastic analysis of a tube at the outlet of the primary superheater. The resulting creep and fatigue damage is found to meet the criteria set by Code Case 1592. This result is encouraging; however, the scope of the Pilot Plant Preliminary Design study did not permit the superheater to be analyzed in detail. Additional analyses might well reveal areas requiring inelastic analysis.

A finite element model made up of beam elements was used to investigate the thermal stresses and deflections of a superheater tube in Section A_3 of the primary superheater. To reduce complexity, only the outlet half of the tube was modeled (Figure 3-52.). Heat flux and steam pressure, temperature and flow correspond to conditions at 3/21/12PM. Steam temperature was assumed to vary linearly along the length of the tube. The absorbed heat flux was obtained from the 3D absorbed heat flux data discussed previously and was assumed to vary as a sine function around the heated half of the tube circumference. (Nominal absorption rates were used in this analysis rather than the upset absorption rates listed in Table 3-9.) Tube OD temperatures, based on nominal absorption rates, upset tube flow and steam temperature, were calculated using Babcock and Wilcox Fossil Boiler Division design standards.

To simulate one-sided heating of the superheater tube, a thermal moment was applied to each beam element. The thermal moment is based on the temperature profile shown in Figure 3-53. and was calculated as follows:

$$M = \int_A E\alpha\, T(x)\, x\, dA$$

$$T = T_{bulk} \qquad 0 \leq X \leq r_o$$

$$T = 2(T_{OD}-T_{bulk})X + T_{bulk} \qquad -r_o \leq X \leq 0$$

$$M = 2E\alpha\, (T_{OD}-T_{bulk})\, I_{xx}$$

Tube thermal stresses and deflections were determined for the following three cases:

- Case 1 - The superheater tube was allowed to displace when subjected to a temperature change from ambient to the mean metal temperature at operating conditions. The thermal moment was not applied, so the thermal expansion did not cause thermal stresses to develop.

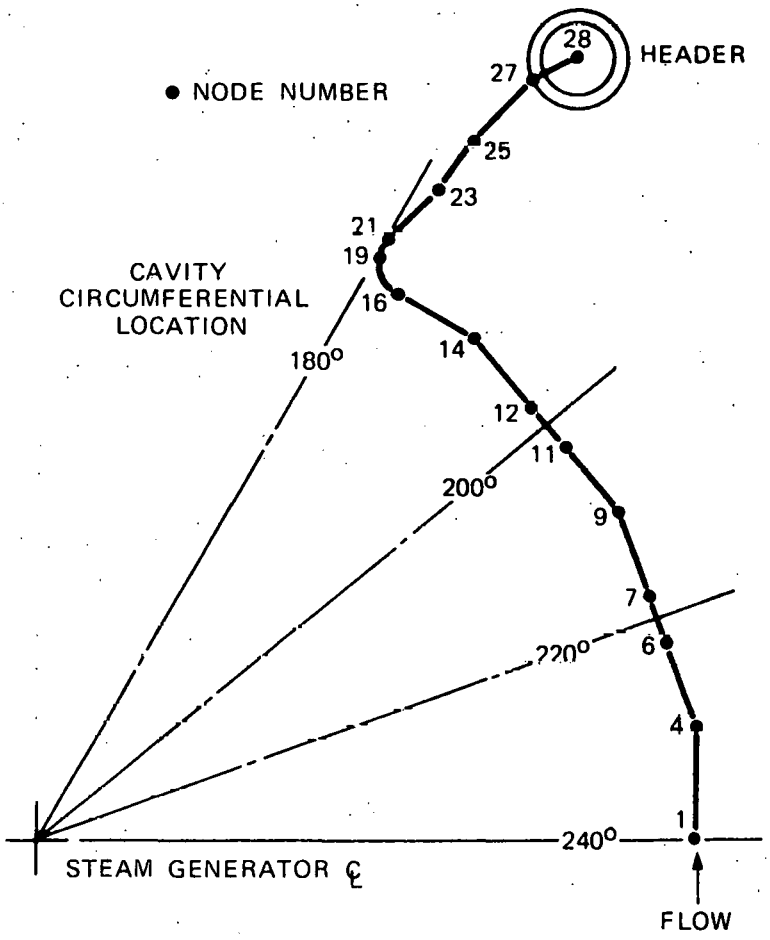

Figure 3-52. Superheater Tube Geometry

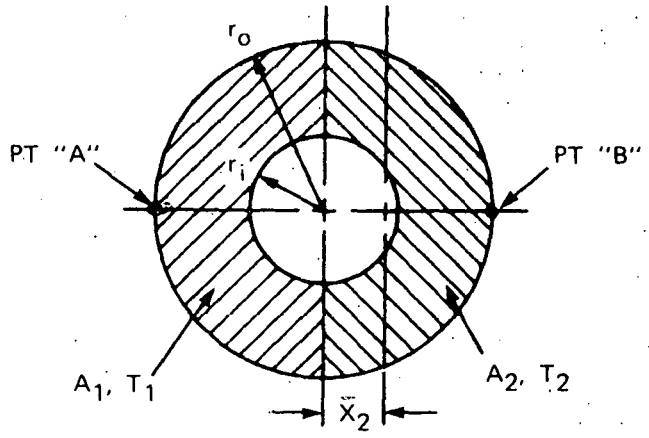

SUPERHEATER TUBE CROSS-SECTION

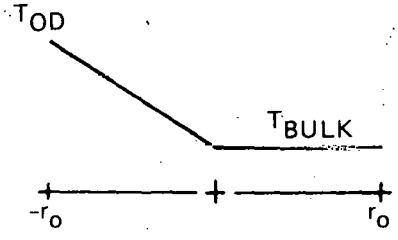

ASSUMED TEMPERATURE GRADIENT

Figure 3-53. Superheater Tube Cross Section and Temperature Gradient

- Case 2 - After the tube displaced radially outward from the center of the cavity in response to the temperature change, the thermal moment was applied to simulate one-sided heating. The tube was restrained from rotation and displacement at the tube mid point (node 1) and was fixed against rotation at the header (node 28).

- Case 3 - The conditions were the same as Case 2 with the addition of radial restraint at the header.

The tube radial displacement for the three cases is shown in Figure 3-54. The absorption rate, steam temperature, mean metal temperature and thermal bending stress are listed in Table 3-12.

The thermal stress for Case 2 reaches a maximum at node 1. The tube is also supported and restrained from radial displacement at this node, so mechanical stresses are at peak values. Therefore, the stresses and strains at this node were compared to the elastic analysis limits set by Code Case 1592.

The stress components at node 1, Point A are:

	σ_ϕ	σ_ℓ	σ_r (ksi)
Pressure	3.1	1.5	0
Mechanical	1.5	0	0
Thermal	0	-7.6	0
	4.6	-6.1	0

(Note that in-plane thermal stresses are not calculated in the simplified beam model analysis presented here. These stresses must be included in the stress analysis for the detail design.)

The stresses, as calculated from elastic analysis, were compared to the limits of Code Case 1592 at the following conditions:

Design conditions

Pressure	13 MPa (1875 psig)
Mean metal temperature	580°C (1077°F)

Normal conditions

Pressure	13 MPa (1875 psig)
Mean metal temperature	493°C (920°F)
Total load duration	10^5 hours
Loading history	11,100 cycles, 9 hours each

All the limits for elastic analysis were satisfied for the assumed conditions. That is,

- Load controlled stresses are acceptable at design conditions

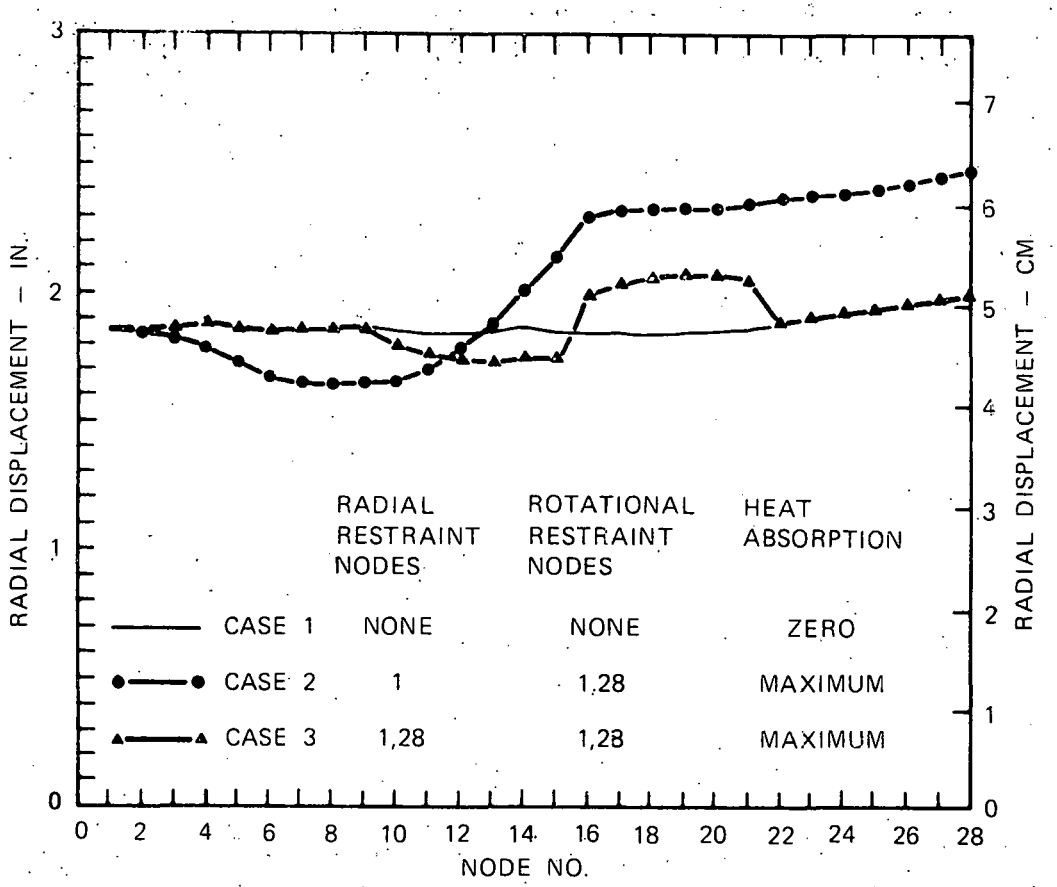

Figure 3-54. Superheater Tube Displacement, Primary Superheater, Section A_3, 3/21/12PM

Table 3-12. Superheater Tube Thermal Stress Primary Superheater, Section A_3, 3/21/12PM

Node	Absorption Rate Kw/m (KBtu/hr-sq.ft.)	Fluid Temperature °C (°F)	Mean Metal Temperature °C (°F)	Thermal Bending Stress, Point A	
				Case 2 MPa	Case 3 (psi)
1	80.8 (25.6)	453.1 (847)	467.6 (873)	-52.7 (-7655)	-43.5 (-6320)
4	80.8 (25.6)	456.8 (853.4)	471.2 (879.4)	-43.8 (-6350)	-44.2 (-6420)
6	80.8 (25.6)	459.5 (858.5)	473.6 (884.5)	-38.5 (-5590)	-41.4 (-6020)
7	64.7 (20.5)	460.9 (861.0)	472.1 (881.8)	-35.9 (-5210)	-40.1 (-5820)
9	64.7 (20.5)	463.8 (866.1)	475.3 (886.9)	-30.7 (-4450)	-37.3 (-5420)
11	64.7 (20.5)	466.2 (871.2)	477.8 (892)	-27.9 (-4055)	-31.6 (-4590)
12	51.4 (16.3)	468 (873.7)	476.8 (890.2)	-26.6 (-3860)	-28.7 (-4175)
14	51.4 (16.3)	470.8 (878.8)	480 (895.3)	-23.9 (-3470)	-23.1 (-3350)
16	51.4 (16.3)	474.1 (884.7)	482.9 (901.2)	24.1 (3500)	13.8 (2000)
19	51.4 (16.3)	474.3 (885.0)	483.4 (901.5)	23.8 (3450)	13.5 (1960)
21	0	474.3 (885.0)	483.4 (901.5)	23.4 (3390)	13.7 (1990)
23	0	474.3 (885.0)	483.4 (901.5)	22.0 (3200)	14.9 (2160)
25	0	474.3 (885.0)	483.4 (901.5)	21.0 (3050)	15.6 (2265)
27	0	474.3 (885.0)	483.4 (901.5)	19.5 (2830)	16.9 (2460)
28	0	474.3 (885.0)	483.4 (901.5)		

- Load controlled stresses are acceptable at normal conditions
- Strain limits to prevent ratcheting and creep enhancement due to thermal cycling are satisfied
- The accumulated creep-fatigue damage is acceptable.

To evaluate fatigue damage, unpublished data from Oak Ridge National Laboratory for Croloy 2-1/4 (Figure 3-55.) were used (M. K. Booker, "An Analysis of the Time-Dependent Fatigue Behavior of 2-1/4 Cr-1 Mo Steel Based on the Concept of Linear Summation of Creep and Fatigue Damage"). The damage evaluation was based on an assumed elastic strain concentration factor of unity. The assumed temperature gradient does not cause a peak thermal strain.

This simplified elastic analysis indicates that the life of the Croloy 2-1/4 primary superheater will meet the requirements of the solar steam generator. A detailed elastic analyses, based on more refined assumptions, would also be expected to show satisfactory life for the primary superheater provided cloud shadowing is not found to cause metal temperatures in excess of 526°C (950°F) for more than a few hours during the life of the unit.

However, a cursory review of the simplified analysis also indicates that the elastic analysis criteria of Code Case 1592 would not be satisfied for mean metal temperatures much in excess of 526°C (950°F). Many sections of the secondary superheater will exceed these temperatures. Fatigue damage is not expected to be a problem even at 580°C (1077°F). The equivalent strain range is small, on the order of 0.05 percent. However, the creep damage, based on elastic analysis, would be excessive resulting in a total creep-fatigue damage greater than the allowable.

Application of the creep damage criteria based on elastic analysis to Croloy 2-1/4 superheater tubes at temperatures greater than 526°C (950°F) indicates that the thermally induced secondary stresses produce significant damage. However, since the secondary stresses are well below the yield point, even at 580°C (1077°F), is is highly probable that they will relax out and not reappear, greatly reducing their damaging effects. Inelastic analysis will be required to verify that these stresses do indeed relax out and do not return on subsequent cycles.

In summary, a simplified elastic analysis indicates that a primary superheater tube meets the cycling requirements for the solar steam generator, provided cloud shadowing does not require operation at temperatures exceeding 526°C (950°F) for long periods. Inelastic analysis will be required to demonstrate that the secondary superheater is satisfactory. Since the thermal stresses are well below the yield strength of Croloy 2-1/4, it is probable that an inelastic analysis would show that many sections of the secondary superheater can meet the cycling requirements of the solar steam generator.

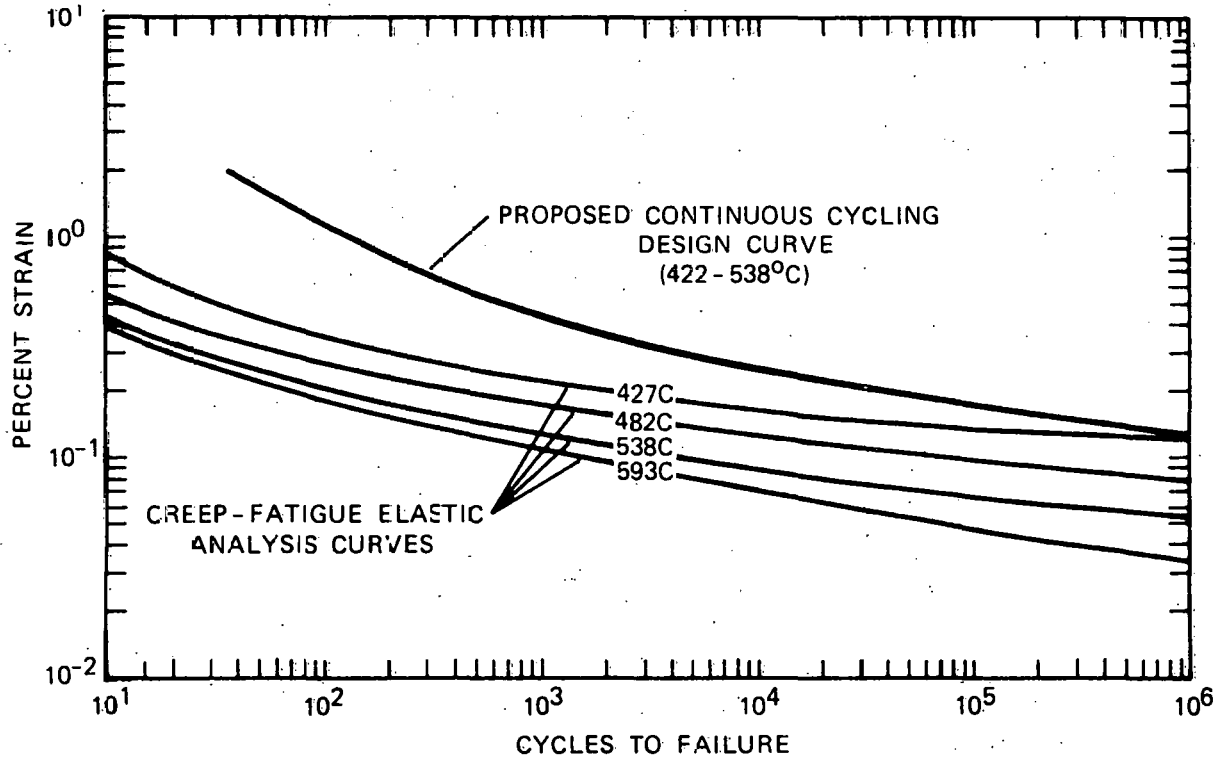

Figure 3-55. Estimated Elastic Analysis Curves for Croloy 2-1/4, Design Lives not Exceeding 2.5×10^5 Hr

Permissible Rate of Temperature Change - The solar steam generator startup rate will be limited by the available solar energy, the maximum permissible rate of temperature change and the requirements on steam pressure and temperature as set by the Electrical Power Generation Subsystem and/or the Thermal Storage Subsystem. A thorough examination of the steam generator during the detailed design phase will be required to establish the permissible rate of temperature change. However, a simplified analysis has been conducted to determine the feasibility of rapid daily startups.

Estimates of the overnight cooldown rate for the steam generator indicate that the pressure parts should remain above 149°C (300°F). If temperature could be increased at the rate of 389°C (700°F) per hour, steam generation at design temperature could be achieved one hour after startup. This would be a significant achievement since conventional steam generators are limited to rates of 111°C (200°F) per hour.

The simplified analysis consisted of calculating the stress in an infinitely long, thick wall cylinder with a fluid flowing inside and the outside surface insulated. The fluid temperature was ramped at 389°C (700°F) per hour. The results of the analysis establish a lower bound on the stresses that would exist in the drum, headers, pipes and tubes of the steam generator.

The maximum thermal stress reached in the carbon steel pressure parts of the boiler section is shown in Figure 3-56 as a function of wall thickness. The stress in the thin wall headers and pipes is negligible compared to the allowable amplitude of the alternating stress intensity for 10,000 hot startup cycles. The maximum thermal stress in the drum, although higher than for the headers, is well below the fatigue limit (Figure 3-51).

However, the drum, headers and pipes have nozzles which cause stress concentrations. Piping loads cause additional stress. During the detail design, care must be taken to minimize stress concentrations by:

- The use of tapers at the juncture of courses of different thickness,
- the use of large fillets at the crotch of the nozzles,
- generous rounding of the inside corners of nozzles,
- Careful profiling and contouring of added reinforcement material, and
- the use of full penetration weldments.

Stress concentrations at support points are avoided by using strap hangers on the headers rather than lugs. The drum is supported by relatively small shear blocks which allow free thermal expansion. The piping must be designed with sufficient flexibility to reduce nozzle stresses to an acceptable level.

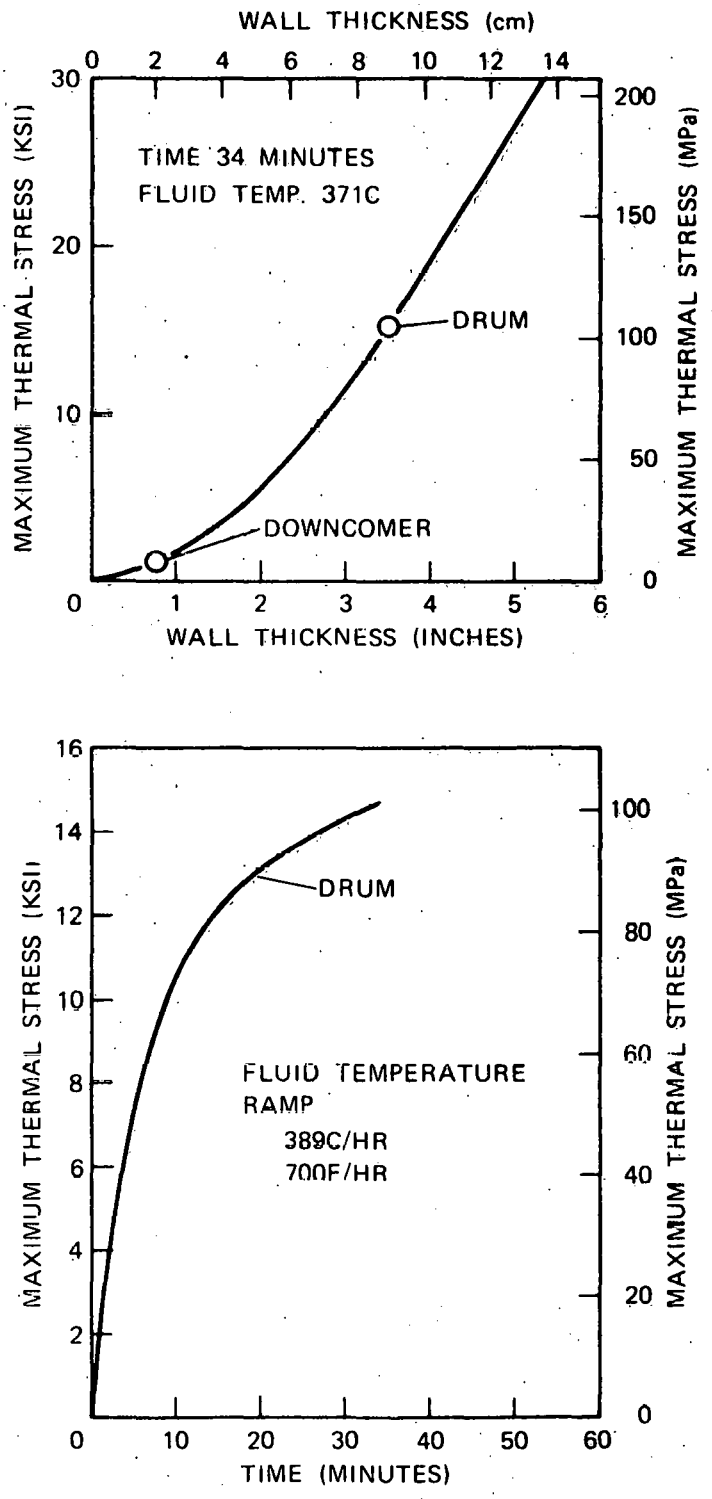

Figure 3-56. Boiler Circuit Transient Thermal Stresses

The maximum thermal stress reached in the Croloy 2-1/4 piping and headers is shown in Figure 3-57 as a function of wall thickness. The superheater headers have the greatest wall thickness and the thermal stress reaches 31.7 MPa (4600 psi), well below the allowable amplitude of the alternating stress intensity for 10,000 hot startup cycles (Figure 3-51). Again, the actual stress could be considerably greater than the stresses presented here, which represent a lower limit. Care must be exercised during detail design to minimize stress concentrations and piping and support loads. In addition, the possibility of creep-fatigue interaction must be investigated.

The preliminary study reported here indicates that startup rates of 389°C (700°F) per hour are feasible considering thermal stress alone.

Structural Analysis - A preliminary design of the steam generator support structure was carried out based on an assumed static equivalent seismic loading of 3g's. The structure is shown schematically in Figures 3-58, 3-59, and 3-60. The member sizes were calculated by computer analysis and met the stress requirements based on the AISC Manual of Steel Construction. The sizes were based on the following preliminary design data:

Supported Weight:

Steam generator, kg (kips)	289,000 (637)
Roof live load, kg (kips)	60,000 (132)
Roof dead load, kg (kips)	40,000 (88)
Siding and girts, kg (kips)	77,000 (170)
Platform live load, kg (kips)	239,000 (527)
Platform dead load, kg (kips)	71,700 (158)

The estimated structural steel weight is:

Top support steel, kg (kips)	56,300 (124)
Hangers, kg (kips)	89,400 (197)
Truss steel, kg (kips)	113,000 (249)
Vertical diagonals, kg (kips)	25,400 (56)
Connections, kg (kips)	28,600 (63)
Total, kg (kips)	312,800 (689)

Material Selection

Carbon steel is a straightforward material choice for the components of the boiler circuit. The maximum fluid temperature in this circuit is 328°C (622°F), the saturation temperature at design pressure. The maximum metal temperature is less than 371°C (700°F) where oxidation rates are low and creep does not occur. Fatigue strength is high because of the ductility of carbon steel.

The material choice for the superheater is not as obvious. Oxidation and corrosion resistance, maximum allowable stress, and high temperature creep and fatigue characteristics are determining factors. Economy dictates the use of the lowest alloy with properties matching the design requirements. In fossil boiler applications, it is common practice to use a range of metals in the superheater,

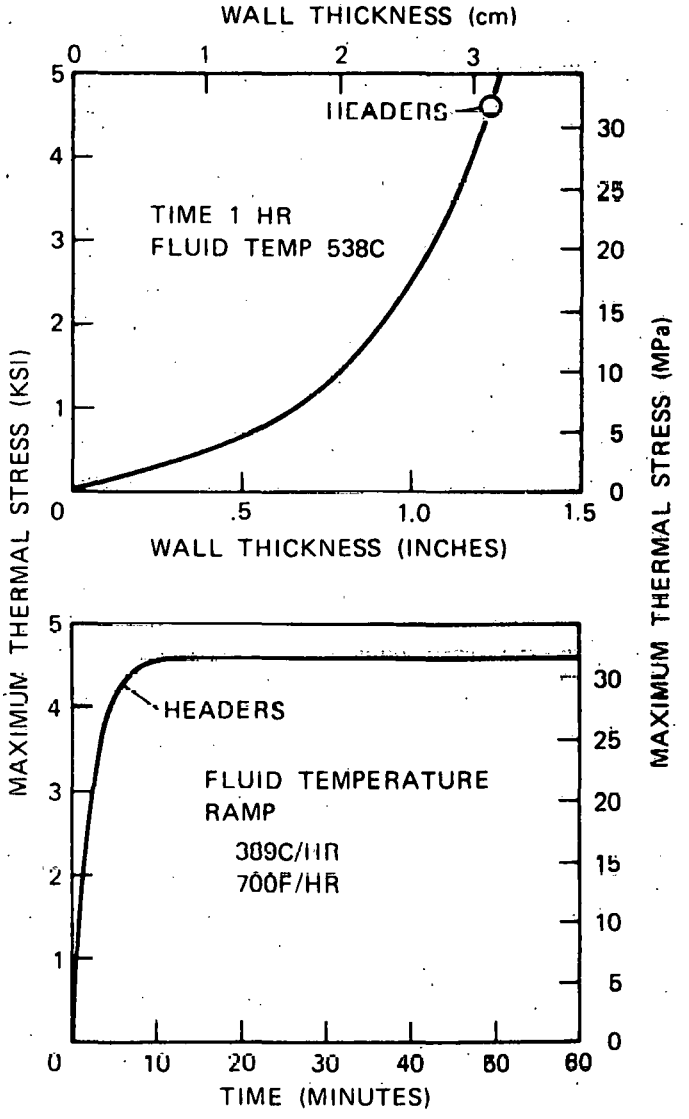

Figure 3-57. Superheater Transient Thermal Stresses

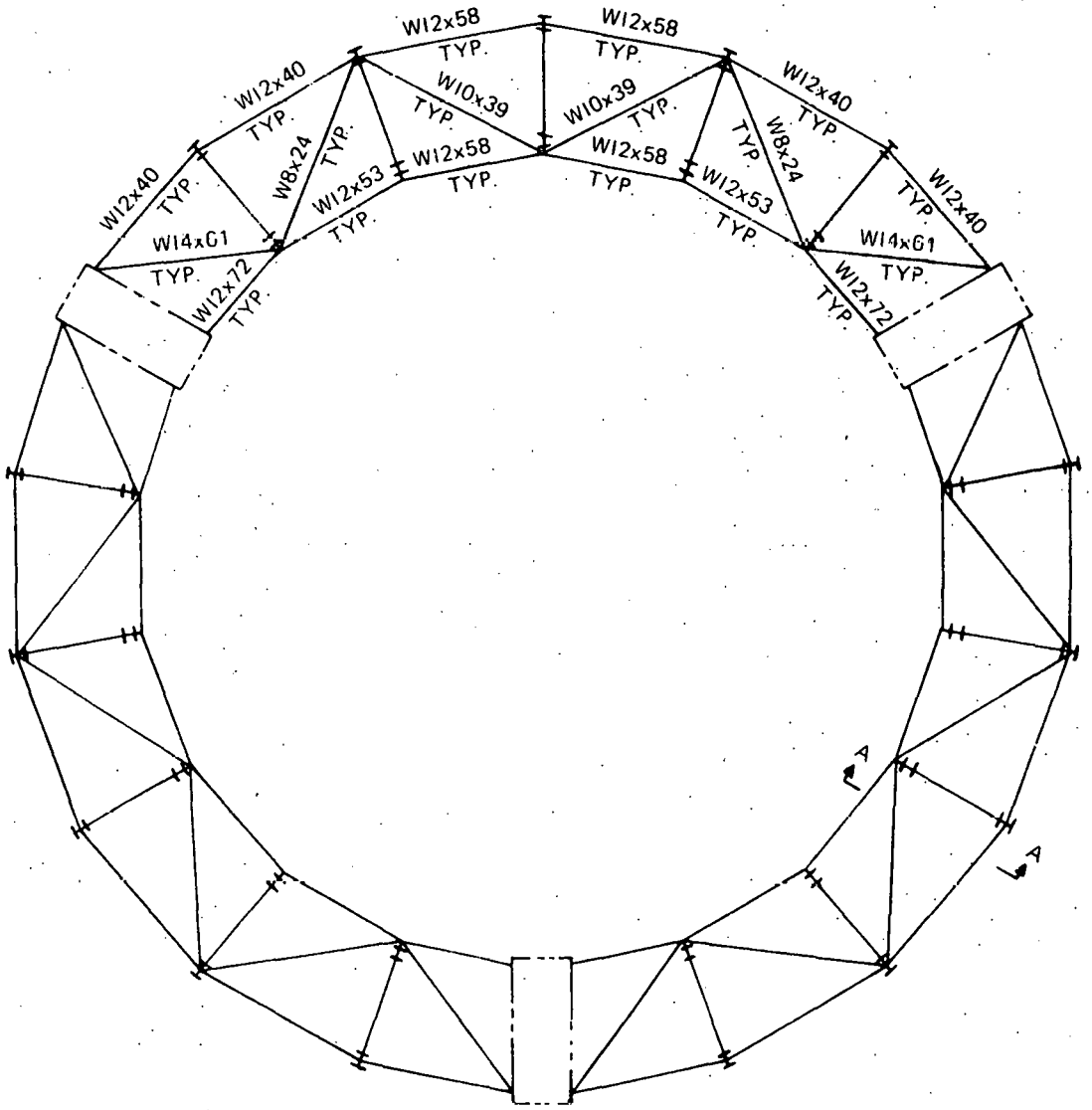

Figure 3-58. Typical Horizontal Truss

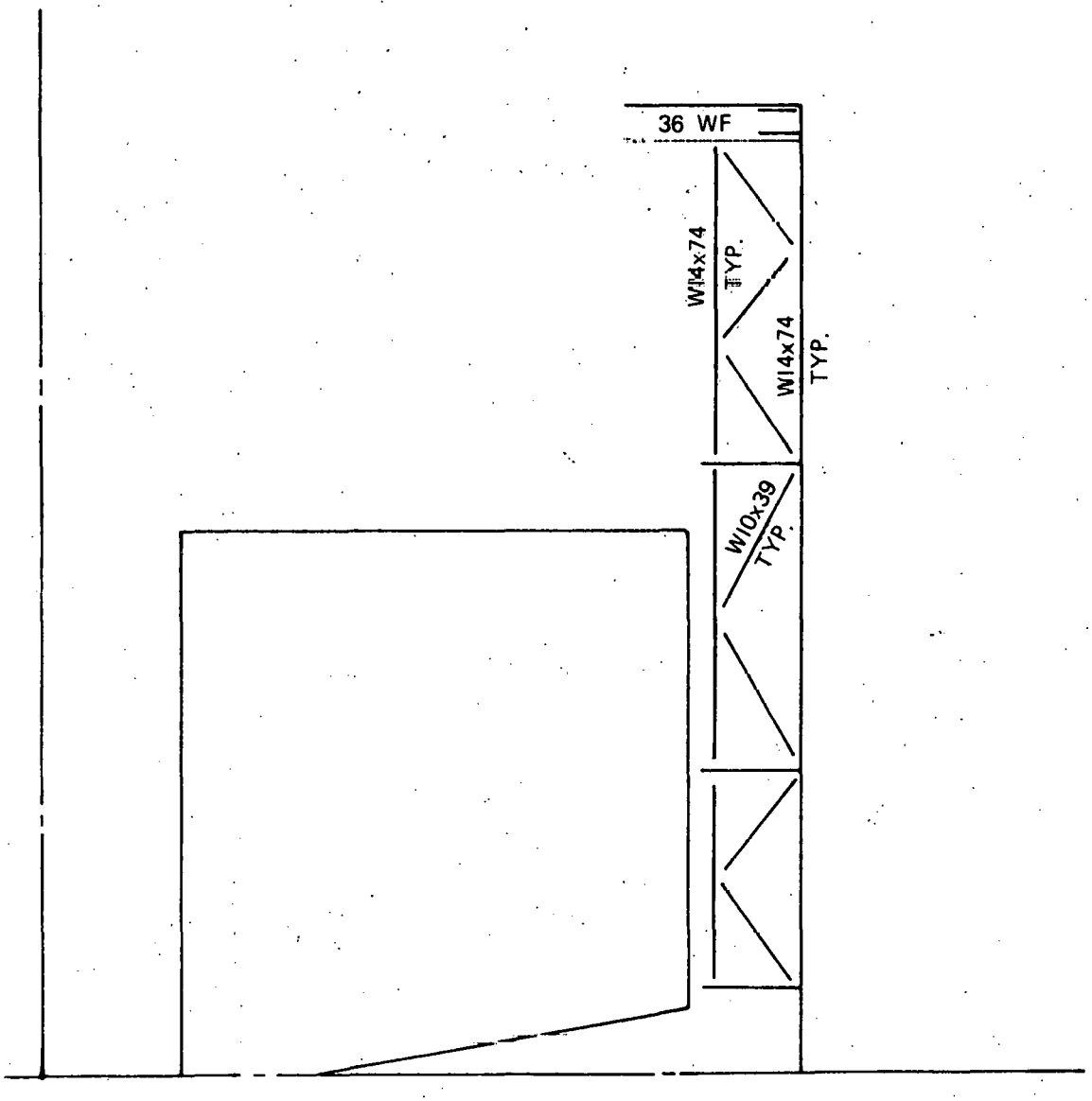

SECTION A-A

Figure 3-59. Typical Vertical Truss

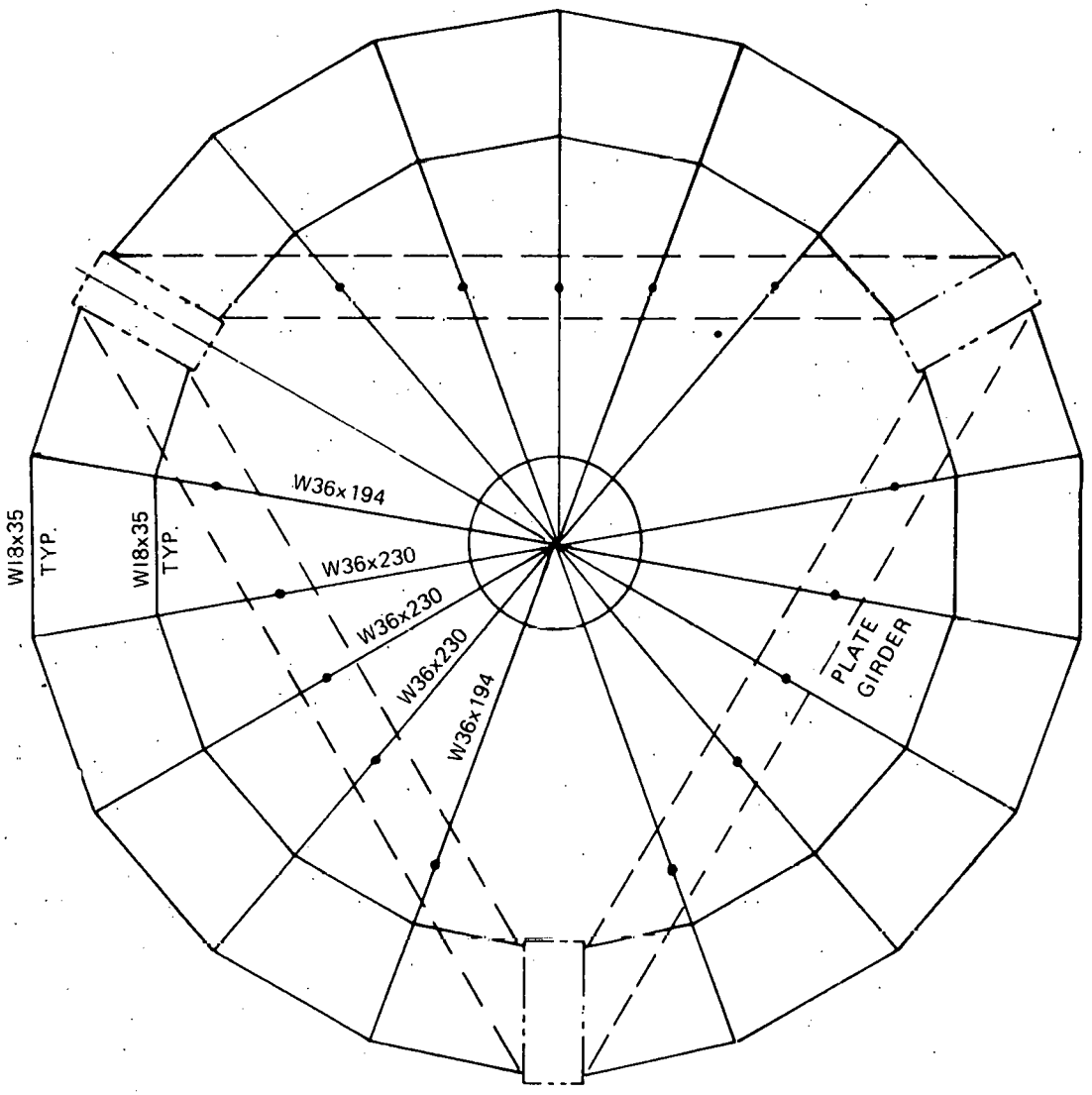

Figure 3-60. Top Steel

stepping up from carbon steel to carbon-molybdenum steel to the lower chromium alloy steels as temperatures increase. For metal temperatures approaching 607°C (1125°F), the lower alloy steels up to and including 2-1/4% chromium are usually adequate. Chromium-molybdenum steel (9% Cr) and the stainless steels are used at higher temperatures where conditions require either an increase in resistance to oxidation or higher load carrying characteristics or both.

Croloy 2-1/4 is the superheater tube material commonly selected for fossil boilers operating at steam pressures and temperatures and metal temperatures equal to or somewhat greater than the solar steam generator. Table 3-13 is a list of design conditions for several oil and gas-fired drum boilers where Croloy 2-1/4 has been successfully used (no reported failures) for superheater and reheater tubes. Therefore, Croloy 2-1/4 was selected for the solar steam generator superheater tubes. At the same time, it is recognized that the cyclic operation and the higher thermal stresses of the solar steam generator could be more damaging to superheater tubes than an otherwise equivalent fossil boiler application. These factors require careful consideration by both the steam generator designer and the customer during the detail design. The choice of higher alloy tubing not only increases cost but also design and fabrication complexity, which could actually decrease reliability.

Table 3-13. Typical Croloy 2-1/4 Tube Applications

Unit	Startup Date	P_{steam} MPa (psig)	T_{steam} °C (°F)	Tube OD cm (in)	Wall Thickness cm (in)	ID Temp. °C (°F)	OD Temp. °C (°F)	Cycles
RB-100	1951	10.2 (1475)	533 (990)	5.1 (2.0)	0.711 (0.280)	562 (1043)	578 (1071)	--
RD-101	1951	10.2 (1475)	533 (990)	5.1 (2.0)	0.711 (0.280)	562 (1043)	578 (1071)	~1000-2000
RB-148	1953	10.2 (1475)	538 (1000)	5.7 (2.25)	0.711 (0.280)	560 (1040)	572 (1060)	--
RB-471 Superheater	1972	15.3 (2225)	526 (979)	5.1 (2.0)	0.889 (0.350)	--	586 (1000)	Daily Cycling
RB-471 Reheater		--	546 (1015)	6.4 (2.5)	0.419 (0.165)	--	587 (1088)	Daily Cycling
RB-472 Superheater	1972	15.3 (2225)	538 (999)	5.1 (2.0)	0.881 (0.347)	--	589 (1091)	--
RB-472 Reheater		--	542 (1007)	5.7 (2.25)	0.376 (0.148)	--	575 (1067)	--

Operation

For the solar steam generator to operate reliably and at peak efficiency, it must be operated safely within the limitations of the equipment, and preventive maintenance must be performed on schedule. Good operation includes operator training as well as equipment preparation. Every operator must be trained to understand and fulfill the responsibility he assumes for the successful performance of the equipment and for the safety of personnel. The operator should be thoroughly familiar with the steam generator and its components, including the purpose, design, limitations, and relationships to other components. This includes inspecting the equipment and studying the drawings and instructions.

Trained operators are particularly valuable during the initial operating period when the controls and interlocks are being adjusted, operating procedure perfected and the preliminary tests are conducted to determine the performance capabilities of the unit.

Preparations for Startup - The systematic preparation for initial startup includes inspection, cleaning, hydrostatic testing, pre-calibration of instruments and controls, auxiliary equipment preparation, steam line cleaning, safety valve testing and setting, and initial adjustments for operations and testing:

- Inspection familiarizes the operator with the equipment and verifies the condition of the equipment. It is particularly important for the solar steam generator to verify that proper provision has been made for thermal expansion. The hanger rods must be free to move as designed and temporary braces, hangers and ties used during construction must be removed.

- Debris and foreign material which accumulates during shipment, storage and erection must be removed.

- After the pressure parts are assembled, but before the insulation and lagging are installed, a hydrostatic test pressure of 1-1/2 times the steam generator design pressure is applied and maintained for a sufficient time for the detection of any leaks. A clean, filtered water is acceptable for hydrotest if the steam generator is completely drained afterwards. The water temperature should be above the dew point temperature to prevent formation of condensate which would obscure and practically prevent the detection of small leaks on the parts being tested.

- The instrumentation and indicators necessary to assure that the steam generator is producing steam at rated conditions while performing within design limitations must be calibrated prior to operation of the unit. The calibrations, such as the water leg corrections for the pressure transmitter, should be included. The automatic controls must be adjusted or provisions made for manual control until the automatic controls can be adjusted during operation.

- The auxiliary equipment must be prepared for operation. This includes the recirculating pumps and the drain system.

- The flushing of all loose debris from the feedwater system and steam generator and the use of high quality water for the hydrotest must be supplemented by proper waterside cleaning before startup. To remove accumulations of oil, grease, and paint prior to initial operation, the steam generator should be given a caustic and phosphate boil-out after the feedwater system has been given a phosphate flush. Acid cleaning for the removal of mill scale and iron oxide may be delayed until operation at fairly high capacities has carried all loose scale and oxides from the feedwater system to the steam generator. This procedure results in a cleaner boiler for subsequent operations.

- High velocity steam can be used to clean the superheater and steam lines of any loose scale or foreign material. The steam is vented through temporary piping to the atmosphere. Steam blowing is preferred to air blowing because the combination of thermal shock and high velocity effectively removes loose scale.

- The set point of each safety valve is normally checked and adjusted, if necessary, immediately after reading full operating pressure for the first time. Safety valve seats are susceptible to damage from wet steam or grit. This is an essential reason for cleaning the boiler and blowing out the superheater and steam line before testing safety valves.

Startup - The following objectives should be included in operating procedures for the solar steam generator: protection of the pressure parts against corrosion, overheating, and thermal stress; protection of the recirculating pumps against cavitation; production of steam at the desired temperature, pressure, flow and purity.

- High purity water should be used in filling the steam generator for startup. The temperature difference between the entering water and the steam generator metal should be limited to 55°C (100°F) or less to minimize thermal stress. Vents should be opened to displace all air with water. Proper drum water level must also be established. Since the water level will rapidly increase once heatup is initiated, an initial gage glass indication of 2.54 cm (1 inch) is acceptable.

- Overheating of boiler tubes is prevented by the flow of fluid through the tubes as provided by the recirculating pump. The superheater tubes must have sufficient steam flow to prevent overheating. During startup, before steam flow is initiated, the incident flux on the superheater must be controlled to limit the superheater tube metal temperature to 510°C (950°F).

- The two pre-requisites for obtaining steam flow through every superheater tube are: removal of all water from each tube; and maintaining a total steam flow equal to or greater than 10% of rated steam flow. Water is removed from the superheaters by opening the header drains and vents. Thermocouples at the outlet of each module section are used to indicate not only steam flow during startup but also to check for excessive temperatures during normal operations. The absorption rate and steam flow must be properly balanced both on an average and local basis. Care must be taken to avoid over attemperation which will maintain correct final steam temperature but possibly allow safe superheater metal temperatures to be exceeded in the primary superheater. The thermocouples located at the exit of each section can also be checked to avoid this situation. During shutdown overnight or longer, condensate will collect in the superheater. The condensate should be drained prior to restarting the unit to avoid flowing slugs of condensate through the attemperator, damaging it.

- The time required to start up the solar steam generator is determined by the permissible rate of temperature change required to limit thermal stresses in the drum, headers and other thick-walled pressure parts. Conventional fossil boiler headers are safe at rates up to 222°C (400°F) per hour. It is anticipated that the Pilot Plant steam generator headers, which have a maximum thickness of 3.3 cm (1.3 in), will be safe at rates up to 389°C (700°F) per hour. Although the drum is thicker than the headers it operates at relatively low temperature where fatigue strength remains high. Preliminary transient stress analysis indicate that a permissible rate of temperature change of 389°C (700°F) per hour is also feasible for the drum. To verify that allowable stress is not exceeded during operating transients, the temperature difference across the drum shell and from top to bottom of the drum must be continuously and accurately determined. Outside thermocouples are required at the top and bottom of the drum and 30.5 cm (one foot) above and 30.5 cm (one foot) below the normal water level on opposite sides of the drum. The inside surface temperatures may be assumed to be the same as the water or steam temperature within the drum.

Performance Tests - Early in the life of the unit when the surfaces are clean and the insulation is new, performance tests should be conducted to determine conduction losses with the cavity enclosure in place. Accurate data should be acquired to serve as a reference for future operations. Procedures for these tests can be adapted from the ASME Performance Test Codes - PTC 4.1, Steam Generating Units.

Shutdown - The steam generator should be taken out of service at regular intervals for internal inspection of the cavity, cleaning and repair. When the heliostats have been defocused, feedwater is no longer required and the main steam stop valve should be closed. Normally the pressure should be allowed to drop naturally without open vents or other intentional means of taking steam from the unit to hasten the lowering of steam pressure. The superheater drains, however, should be opened sufficiently to keep all condensate out of the superheaters. To prevent a vacuum from condensation of steam within the steam generator, the steam drum vent valve should be opened and nitrogen introduced when steam pressure has dropped to about 0.172 MPa (25 psig). Shutting down the steam generator by the foregoing procedure will take a relatively long time. For faster shutdowns, steam may be vented and the thermocouples distributed over the pressure parts can be monitored to establish that the maximum allowable rate of cooling is not exceeded.

Water Treatment - The steam generator will not operate efficiently and might possibly fail if the internal heat transfer surfaces are allowed to foul with scale or if corrosion is permitted to occur.

Steam that is condensed and returned to the boiler system is termed condensate. Steam lost due to blowdown or leakage out of the system has to be replaced by makeup water. The condensate together with the makeup water comprise the feedwater to the steam generator. Feedwater enters the boiler and is evaporated into steam leaving behind solids to concentrate in the boiler water. If the concentration exceeds certain limits, carryover of solids to the superheater could occur. Also, boiler water solids may settle out on the boiler surfaces as sludge. The concentration of solids in the boiler water can be controlled by blowing down a portion of the drum water either continuously or intermittently.

Treatment of the raw water supply varies depending on the water quality and will not be discussed here.

Fossil drum boilers normally do not require condensate polishing systems for satisfactory operation. However, the start-stop operation of a peaking boiler, with its consequent transients and greater off-line periods, can cause higher levels of contamination in the feedwater and greater rates of depositon in the boiler. Therefore, condensate polishing is recommended for fossil peaking boilers and also the solar steam generator.

A condensate polishing system (demineralizer) is also recommended for purifying the condensate for the following reasons:

- Improved turbine capability and efficiency
- Shorter startup time
- Protection from the effects of condenser leakage and longer intervals between acid cleanings

Corrosion protection can be directly related to the ability to prevent oxygen from entering the boiler-turbine system. For overnight or weekend shutdowns, the best method to exclude oxygen from the system is to maintain condenser

vacuum, thus, enabling the steam side of the feedwater heaters, turbine, and reheater to become dry and to stay dry. Maintaining condenser vacuum should also decrease the incidence of condenser leaks by eliminating the transients that occur while making and breaking vacuum. Auxiliary steam is necessary to maintain turbine seals.

During shutdown, the deaerator vents to the atmosphere should be closed when the cycle water temperature falls below the boiling point. Another method of preventing oxygen infiltration is to vent the deaerator to the condenser. In the latter method, a valve in the line from the deaerator to the condenser should automatically open when the deaerator pressure decays to atmospheric pressure. In either case, the deaerator should be designed to withstand full condenser vacuum.

Volatile treatment is recommended for control of pH and oxygen in both the feedwater and the boiler (drum) water. No solid chemicals are added to either the drum or the feedwater cycle. By eliminating solid treatment, the volatile carryover of solids is eliminated and, consequently, turbine deposits are avoided. Cycle pH is controlled at 9.3 to 9.5 with a volatile amine such as ammonia. Hydrazine is added to the feedwater as an oxygen scavenger in quantity sufficient to provide a concentration of 20 to 30 ppb at the inlet to the drum.

Most of the iron entering the steam generator originates in the condensate-feedwater cycle downstream of the condensate polishers. Iron pickup can be minimized by operating with a pH in the range 9.3 to 9.5. Ammonia is injected downstream of the condensate polishers and controlled from a sample taken far enough downstream of the injection point to assure good mixing. Hydrazine is generally fed at the exit of the condensate polishing system and/or at the boiler feed pump suction.

Table 3-14 lists the recommended limits of solids for the solar steam generator drum and attemperator feedwater.

Table 3-14. Recommended Limits of Solids in Feedwater for Solar Steam Generator

	Maximum Limit	Typical Concentrations
Total solids	0.050 ppm	0.020 ppm
Silica as SiO_2	0.020 ppm	0.002 ppm
Iron as Fe	0.010 ppm	0.003 ppm
Copper as Cu	0.002 ppm	0.001 ppm
Oxygen as O_2	0.007 ppm	0.002 ppm
Hardness	0.0 ppm	0.0 ppm
Carbon dioxide	0.0 ppm	not measured
Organic	0.0 ppm	0.002 ppm
pH	9.3-9.5	9.45

Prior to startup, water must be circulated through the condensate-polishing system to reduce dissolved material and suspended particles. The cation conductivity of the cycle water must be reduced to less than 1.0 micromho before heat is added to the unit.

With volatile treatment, the feedwater must not contain hardness or condenser-leak constituents. Since no phosphate is present to remove hardness, any contamination assumes major importance. Failure to take action endangers the future availability of the unit. A condensate-polishing system in the cycle is the best insurance against condenser leakage and hardness constituents.

Maintenance - Steam generator pressure parts require very little maintenance, provided the equipment is operated within specified limits on maximum metal temperature, permissible rate of temperature change and water quality. Table 3-15 is a general listing of scheduled and unscheduled maintenance items.

Table 3-15. Maintenance Items

Component	Scheduled*	Unscheduled
Steam generator pressure parts	Inspection	Chemical cleaning (~5 year interval**)
Recirculating pump and driver	Tear down and inspection (annual)	Bearing replacement Driver repair
Pump cooling water strainers	Clean (as required***)	
Control valves	Observe operating characteristics Inspect for leakage	Actuator diaphragm replacement Packing replacement Trim replacement
Safety valves	Check popping pressure	Correct leakage Correct faulty operation
Drum gage glass	Inspect for leakage	Replace seals Replace lamps
Instrumentation	Recalibrate	

*The interval for scheduled maintenance for many items is established by the standard practice of the operating utility.
**The chemical cleaning interval can be greater or less than listed depending on operating history of the unit.
***Dependent upon cooling water quality.

Steam Generator Instruments and Controls

Instruments and controls are an essential part of all steam generating installations. They assure safe, economic and reliable operation of the equipment. The Master Control Subsystem, Volume VI, controls the complete Solar Pilot Plant with demand requirements applied simultaneously to the heliostat, thermal storage, receiver, and the electrical power generation subsystems. This subsection discusses the general characteristics required of the steam generator instruments and controls. The preliminary design of the instruments and controls system is the responsibility of Black and Veatch.

Controls - The controlled variables for the steam generator subsystem are drum level and superheater outlet temperature control. The drum level control regulates feedwater flow to maintain drum water level between the desired limits. Three-element control is recommended for the solar steam generator. A cascaded-feed-forward control loop maintains water flow input equal to feedwater demand. Drum level measurement keeps the level from drifting due to flow meter errors, blowdown, or other causes.

The drum-level element of the controller applies proportional action to the error between the drum-level signal and its set point. The sum of the drum-level error signal and the steam-flow signal is the feedwater demand signal. This is the "summer" output. The feedwater demand signal is compared with the water-flow input and the difference is the combined output of the controller. Proportional-plus-integral action is incorporated to provide a feedwater correction signal for valve regulation.

Three-element feedwater control systems can be adjusted to restore a predetermined drum level at all loads, or with severely fluctuating loads, such as may occur during cloud shadowing, the system can be adjusted to permit water level in the drum to vary with the boiler loading to compensate for "shrink and swell" effects. If the drum level is allowed to vary in this manner, a nearly constant inventory of water, as opposed to a constant level, is maintained.

Spray flow (attemperation) is the primary means of steam temperature control and will normally be adequate to maintain steam temperature at the desired set point. However, during startup, shutdown, or cloud shadowing, reaiming or defocusing heliostats may be required.

The spray water control should have a feed forward program which is trimmed from the secondary superheater outlet temperature error. The inlet temperature to the secondary superheater is also fed forward to modify the spray flow demand.

Instrumentation - This subsection identifies the instrumentation required for the operation of the steam generator. Also identified is instrumentation that is primarily installed to obtain first-of-a-kind performance data. The estimated instrumentation requirements are summarized in Table 3-16.

The pressure, flow, level and fluid temperature measurements are required for control and/or performance monitoring during startup, shutdown, normal operation, cloud shadowing, turbine trips and other emergency operating conditions.

Table 3-16. Pilot Plant Steam Generator Measurements
(All instruments have an electrical output unless otherwise noted)

Pressure: (4-20 ma)

Feedwater*
Drum
Recirculating pump discharge
Attemperator inlet
Attemperator outlet
2nd stage SH discharge
Turbine inlet*

Flow: (4-20 ma)

Feedwater*
Blowdown*
Recirculation flow
Boiler inlet (9)
Attemperator spray water*
Pump cooling water
Steam flow*

Level: (4-20 ma)

Level (2)
Level gage

Metal Temperatures: (millivolts)

Drum (10)
Boiler (90)
1st stage SH (90)
2nd stage SH (90)
Attemperator (5)
Recirculating pumps (9)
Ceiling (10)
Miscellaneous (30)

Fluid Temperatures: (millivolts)**

Feedwater*
Attemperator spray water*
Blowdown*
Recirculating pump inlet
Recirculating pump outlet
Attemperator inlet
Attemperator outlet
2nd stage SH discharge
Pump cooling outlet

Displacement

Acceleration

Strain

Force

---

*Note - Measurements required by the steam generator subsystem but supplied with the EPGS.
**Fluid temperatures to be measured with dual element thermocouples.

Metal temperatures are monitored to assure that design temperatures and permissible rates of temperature change are not exceeded, and to provide data for determining local heat absorption rates. Local absorption rates are very important indicators of the overall efficiency of the solar energy transfer process.

During the detail design phase, a requirement may be identified for measurements verifying the structural characteristics of the steam generator and its support structure. The potential requirements are:

- Displacement and strain measurement of the pressure parts during transients to verify the design basis loading histograms.
- Reaction force measurements on the pressure part lateral restraints to verify the boundary conditions assumed for stress analysis.
- Acceleration measurements of the pressure parts and structure during expected mild seismic events to verify the seismic analysis.

Comparison to SRE - The Pilot Plant steam generator is based on the design of the SRE steam generator. Many of the SRE design procedures could be applied to the Pilot Plant steam generator because the physical arrangement, the flow circuitry and the boiler and superheater tubes are identical. A discussion of the scaling relationships between the SRE and Pilot Plant Steam Generators is included in the DDR and will not be repeated here.

During the detailed design of the SRE concern developed regarding the difficulty in scaling the helical superheater up to Pilot Plant or commercial scale. Shop fabrication of the helical superheater would not be possible, increasing the cost and complexity of field erection. In addition, thermal stresses would be high because the helical geometry does not allow deflection of the superheater tube to reduce thermal stresses caused by one sided heating.

The modular superheater evolved from the helical design. The "checkerboard" flow circuitry approximates a helical flow path, retaining the steam temperature averaging capability of the helical superheater. Furthermore, the tubes can deflect when subjected to one sided heating, reducing thermal stress and, most importantly, the modular superheater can be shop fabricated.

The SRE test data were not available as this report was written. However, several things were learned during the design and fabrication of the SRE that are applicable to the Pilot Plant steam generator.

- Support lugs and brackets should be replaced by strap hangers and shear blocks when possible, or should be kept small so as not to cause high thermal stress during rapid transients.

- The slots in the seismic snubbers should be field adjustable. The welded attachments to the pressure parts should be no larger than required to minimize thermal stress during transients.

- The superheater tube alignment clips should be machined rather than flame cut to provide a better sliding fit with the alignment tee.

- The design of the insulation of the superheater tube support brackets should assure that the brackets will not be exposed to incident energy.

STEAM GENERATOR HOUSING

The steam generator housing illustrated in Figure 3-61 provides support, access, protection, servicing, and an acceptable environment for the steam generator, associated equipment, piping, and electrical cables in a configuration which minimizes blockage of redirected solar radiation from the collector field to the receiver cavity and maximizes overall receiver cavity efficiency. The essential elements of the steam generator housing are the receiver support structure legs (corbels), the outer housing structure, the cavity barrier, and the thermal radiation shielding. The design of these elements is described in considerable detail in the Preliminary System Design Specifications for the Steam Generator Support System and the Tower Structure System given in Appendix B. The design development of the cavity barrier is presented in the report entitled, "Receiver Cavity Closure," given in Appendix E. Summary descriptions of the elements are provided in the following sections.

Corbels

The receiver support structure legs or corbels provide support of and access to the receiver steam generator assembly from the tower while blocking the smallest possible amount of solar radiation from the collector field. The corbels provide the only access from the tower to the receiver steam generator and the collector field calibration arrays. Mechanical piping, electrical tray, and a personnel access ladder are contained within the corbels. Because redirected solar radiation from the collector field must pass through the receiver aperture, i.e., the space between the tower and the steam generator, the width of the corbels must be maintained at a minimum to ensure the highest possible receiver efficiency. The corbels must be designed to resist dead, live, and wind loads without interruption of normal operation. Design seismic loads must be resisted without loss of stability or structural integrity.

The detail of the corbel design is illustrated in Drawings S1001 through S1004 in Appendix F and described in the Preliminary System Design Specification for the Steam Generator Support System given in Appendix B. The design employs three corbels which are located around the outside of the tower at 120° intervals, with one corbel directly south. They are shop fabricated from structural steel plate into box girder sections of as great a length as can be practically handled and shipped. The sections are then welded together in place in the field. Each corbel is approximately 6.1 meters (20 feet) in depth at its attachment to the tower and tapers to approximately 3.1 meters (10 feet) in depth at the base of the steam generator. The corbel width is 0.91 meters (3 feet). It should be noted that these corbel dimensions do not include the thermal radiation shielding which adds approximately 0.152 meters (0.5 feet) to the dimension normal to the shielded surface.

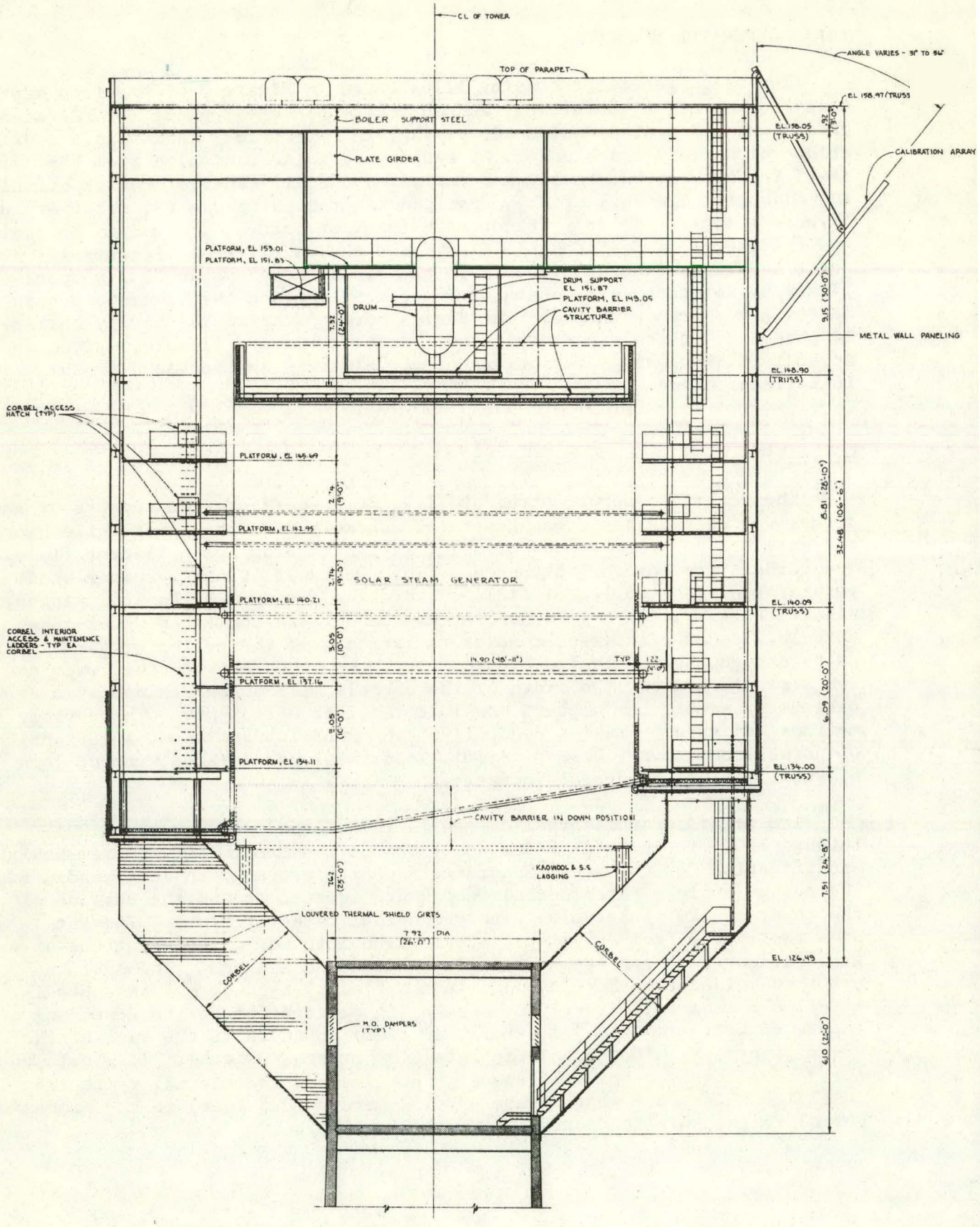

Figure 3-61. Steam Generator Housing and Support Structure

The corbel cross section dimensions remain constant from the base of the receiver steam generator cavity to the steam generator support level, a vertical distance of approximately 27.6 meters (90 feet). The corbels support three plate girders at the steam generator support level which are used to suspend the steam generator.

The south corbel provides access for the recirculation downcomer and riser. The corbel 60° to the west of north provides access for the main steam line, blowdown line, roof drain header line, chemical feed line, service air line, shutdown corrosion protection line, feedwater line, high pressure/low pressure drain line, and the desuperheater spray line. The corbel 60° to the east of north provides access for electrical trays and personnel. In addition, each corbel is provided with access hatches to interior piping or cable for infrequent or emergency maintenance. These are shown in the typical sectional plan through the corbels presented in Drawing S1004 of Appendix F.

The structural steel box girder configuration was selected for the preliminary design of the corbels as the result of a trade-off study with a space truss configuration. A space truss constructed of structural tubes is desirable because of the savings it might offer in weight of steel. Further, its natural openness could enable the thermal radiation shielding, described in a following section, to be attached directly to the truss instead of being supported a distance away from the shielded surface. The elimination of this standoff distance, which is needed for the development of natural convective air flow to cool the radiation shield, would reduce the effective width of the corbels plus the shield. However, preliminary design analysis indicates that the magnitude of the loads on the corbels necessitate the tube sections of the truss be of such size and wall thickness that the space truss was eliminated as a viable alternative, and the box girder system was chosen.

For the box beam girder, the standoff distance required for the cooling of the thermal radiation shield by natural convective air flow is reduced by designing the corbel with vent holes in its shielded surfaces and forcing air to flow within the corbel. This internal air flow cools the corbel structure and supplements the free convective cooling flow of the radiation shielding. The standoff distance needed to establish a free convective air flow that is sufficient to cool the shielding is then reduced, and with that, the total effective width of the corbel is reduced.

In developing the preliminary design of the structural steel box girder corbels, bending moment, shear, and torsion were determined from computer analysis of the dead, live, and earthquake loads on the model of the tower, corbels, and horizontal trusses. Stresses were determined and compared with allowables in accordance with the AISC Manual of Steel Construction, seventh edition. The details of these analyses are summarized

in a later section on receiver subsystem loads, and more thoroughly detailed in the Seismic Analysis and Design Considerations report given in Appendix E.

Several aspects of corbel design require careful review in final design. The restriction of corbel width as discussed earlier creates high stress levels in the minor axis and requires careful analysis of the loading conditions between the corbels and the steam generator supporting structure. The flexibility of the receiver housing and components in comparison with the concrete tower allows the development of a whipping action during an earthquake which can result in high acceleration level being imposed on the equipment within the receiver steam generator assembly. Also, further heat transfer analyses are required to confirm the material selection for the corbels, although it is not anticipated that temperatures which would prohibit the use of ASMT A36 steel, the material selected for the preliminary design, will be encountered. Final design of the corbels requires a complete analysis of all design parameters with particular emphasis on the areas noted.

Outer Housing

The receiver outer housing provides direct support and access to the steam generator and enclosure of the cavity surrounding the steam generator, and to the heliostat calibration arrays. Personnel access to the steam generator and its components is provided by platforms and ladders at various elevations at the steam generator and steam drum. Mechanical and electrical access areas, if required at elevations not accessible from the boiler platforms, can be provided in final design. A roof and side enclosure are provided to protect the steam generator and associated equipment and maintain a suitable environment for maintenance.

The outer housing structural members must resist both the dead and live loads of the steam generator and its structural system, and the wind loads on the cavity enclosure without interruption of normal operation. Design seismic loads must be resisted without loss of structural integrity.

The detail of the outer housing design is illustrated in Drawings S1001 through S1004 of Appendix F and described in the Preliminary System Design Specification for the Steam Generator Support System given in Appendix B. The steam generator, steam drum, movable receiver cavity closure (i.e., cavity thermal barrier), and associated piping and equipment shown in Drawing S1002 are supported vertically by hangers from a structural steel frame at the steam generator support level or roof elevation. This steel frame consists of wide flange sections located on radial lines from the center of the frame. These members are connected at the center of the frame by gusset plates on the top and bottom of the members. Support of the radial members is from three structural steel plate girders which join the three corbels. Lateral support of the steam generator is provided by

four horizontal trusses which circle the unit at various elevations. The trusses are supported vertically by hangers from the radial members attached to the three structural steel plate girders at the steam generator support level. The trusses are connected to each other through vertical bracing. They span laterally between the corbels. The radial member and horizontal and vertical trusses described above are designed and supplied by the steam generator manufacturer.

Five circular access platforms (see Drawing S1003 in Appendix F) are attached to the horizontal truss hangers around the steam generator. These platforms consist of bar grating supported on a steel frame. Edges of the platforms not adjacent to the steam generator are protected by a handrail. Two similar platforms provide access to the steam drum. One is just above the permanent ceiling of the steam generator, and the other is approximately at the top third level of the drum. The upper platform also serves as the location of the hoisting equipment for the cavity barrier.

Access from the tower to the lowest platform on the receiver housing is by the northeast corbel. Access between platforms is by caged ladders attached to the northeast corbel. Roof access is through a trap door hatch. Maintenance and inspection access to mechanical and electrical trays within the corbels is provided by hatch doors, at each platform elevation, and interior hand holds.

Enclosure is accomplished with segmented, uninsulated, metal wall panels supported by wide flange girts from the outer row of the horizontal truss hangers and the corbels. Top enclosure is achieved by a three ply felt and gravel insulated, built up roof laid on a metal roof deck above the steam generator support level. The outer housing wall panel and roof provide protection against rain, snow, and wind.

Cooling of the annular space between the outer housing and the insulated surface of the receiver cavity is provided by air circulating through the corbels and through vertically mounted, motor operated air louvers positioned at three locations on the side enclosure of the outer housing structure. The air flow is driven by powered ventilators mounted on the receiver housing roof.

Other sets of girts, independent of the wall panel girts, are used to support the heliostat calibration arrays as shown in Drawing S1004, Appendix F. The calibration arrays are attached at their base by hinges to wide flange girts and at two thirds of their height by structural WT sections. Each WT is attached to the array in such a manner that the array can be pulled back to the vertical position by a hand winch and adjustment of the structural WT attachment. They can then be accessed for cleaning by either hanging a scaffold from the roof or constructing an access platform below the arrays.

The vertically mounted air louvers are supported by girts from the horizontal truss hangers.

The preliminary layout of the outer housing is based on the support concept, loads, and dimensions provided by the steam generator manufacturer as well as consideration of the protection and access required for mechanical equipment, piping, and electrical cables. Spacing of the girt members and the type of girts selected are common for the metal wall panel and are frequently used for the design wind loads considered.

In the course of developing the design, an alternate concept considered for the outer housing was a continuous steel shell enclosure. It was thought that the shell would provide weather protection for the receiver cavity and, at the same time, provide the stiffness and support required for the steam generator, et al, during an earthquake. The system was rejected, however, in favor of the conventional wall panel system based on the steam generator manufacturer's support system design (horizontal and vertical trusses), receiver fabrication and construction costs, weight limitations, and the need for ventilating the outer cavity.

Several aspects of the outer housing will require closer analysis in the final design. The limited space outside the perimeter of the steam generator will require coordination of the final routing of pipe and electrical raceway with the location and sizing of support trusses and accessways. Design assumptions and loading conditions for the horizontal trusses provided by the steam generator manufacturer must be consistent with the results from a seismic analysis of the structure. Further analysis of the receiver steam generator assembly under wind loads, such as lateral swaying and ovaling due to vortex shedding and nonuniform radial wind pressures, as they pertain to the wall panel and girt system, are to be completed in the final design. A method and procedure for periodic cleaning of the heliostat calibration arrays is also to be finalized. The design resolution of these items is not expected to significantly alter the preliminary design concepts.

Cavity Barrier

The function of the cavity barrier is to insulate the receiver cavity from ambient conditions during the nightly shutdown of the solar plant in order to retain as much energy in the receiver as possible. This energy reduces:

(1) The time required to bring the plant back to rated steam pressure and temperature during startup the following day.
(2) The cyclic thermal stress imposed on the receiver steam generator.

The relative merits of two alternative designs for effecting closure of the cavity are evaluated in the Receiver Cavity Closure report presented in Appendix E. The concepts considered are external aperture doors and an internal cavity barrier. External aperture doors supported from the outer housing of the receiver and doors supported from the receiver support tower were considered. The three configurations for cavity closure are illustrated in Figure 3-62. The advantages of the aperture door concepts include exposure to relatively low temperatures and positive positioning of the doors during their movement to open or close this cavity. Their disadvantages include complex movement of the doors during operation, high wind loading, relatively large sealing perimeters, slower closing speeds, and large number of components required.

The advantages of the interior cavity barrier, illustrated in Figure 3-63, include simple configuration and design requiring a small number of components, rapid closing speeds, low wind loadings, simple linear movement during operation, and a relatively small sealing perimeter. The principle disadvantage of the cavity barrier is that it is exposed to relatively high temperatures and its suspension system and hoisting mechanism are subject to frequent inspection under Federal regulations. The cavity barrier concept was selected for the pilot plant preliminary design development through consideration of these advantages and disadvantages.

Cavity closure is achieved through the simple linear motion of the single circular disc by a hoisting mechanism which raises and lowers the barrier from its closed and stowed positions. The operating or hoisting mechanism for the interior cavity barrier uses a single hoist motor, gear, and brake assembly. Sprockets, idler shafts, and other components employed to manipulate the barrier suspension are straightforward in design and simple in arrangement. Roller chain is used for barrier suspension since the roller chain link design, and the use of sprockets to manipulate the chain, offer the capability to accurately mechanically establish the barrier position and ensure the cavity barrier is held horizontal when being moved within the receiver cavity. This minimizes contact between the barrier and the receiver heat transfer surface.

The roller chain and its associated hoisting mechanism can move the internal cavity barrier at such a rate to achieve aperture closure in between 3-1/2 to 7 minutes of operation. This is equivalent to a hoisting speed of between 2.13 to 4.57 meters per minute (7 to 15 feet per minute).

To protect the receiver heat transfer surfaces and tube segments from damage due the contact with the barrier, and to effect a seal between the barrier and the receiver cavity housing when the barrier is in its closed position, a flexible or soft skid constructed of high temperature resistant fabric material and insulation is provided on the outer edge of the barrier.

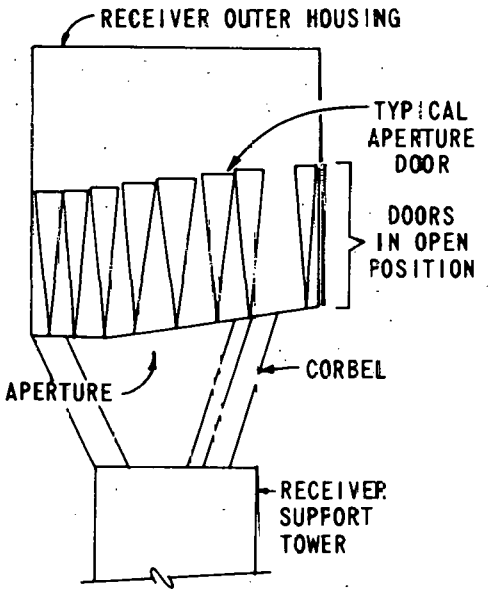

EXTERNAL APERTURE DOORS SUPPORTED FROM RECEIVER OUTER HOUSING

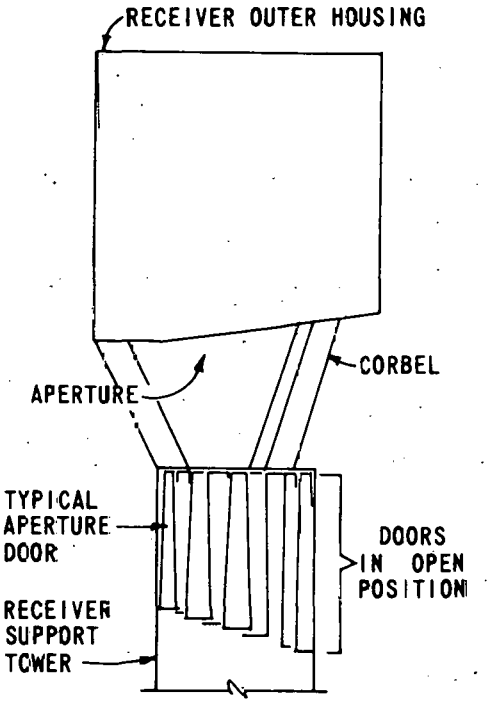

EXTERNAL APERTURE DOORS SUPPORTED FROM RECEIVER SUPPORT TOWER

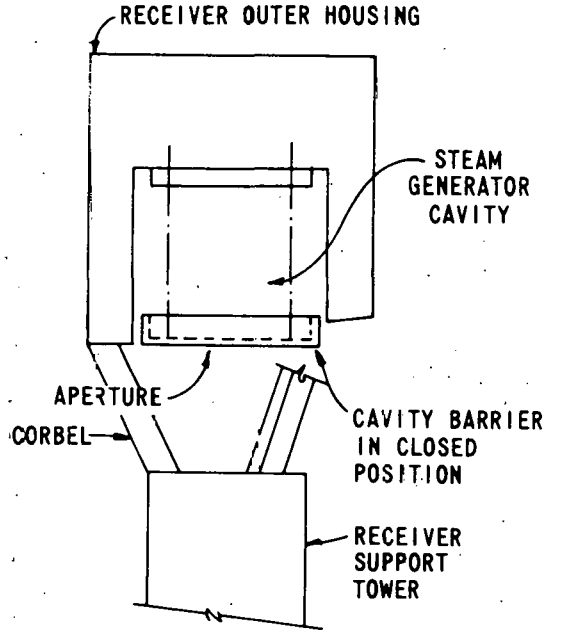

INTERNAL CAVITY BARRIER

Figure 3-62. Cavity Closure Approaches

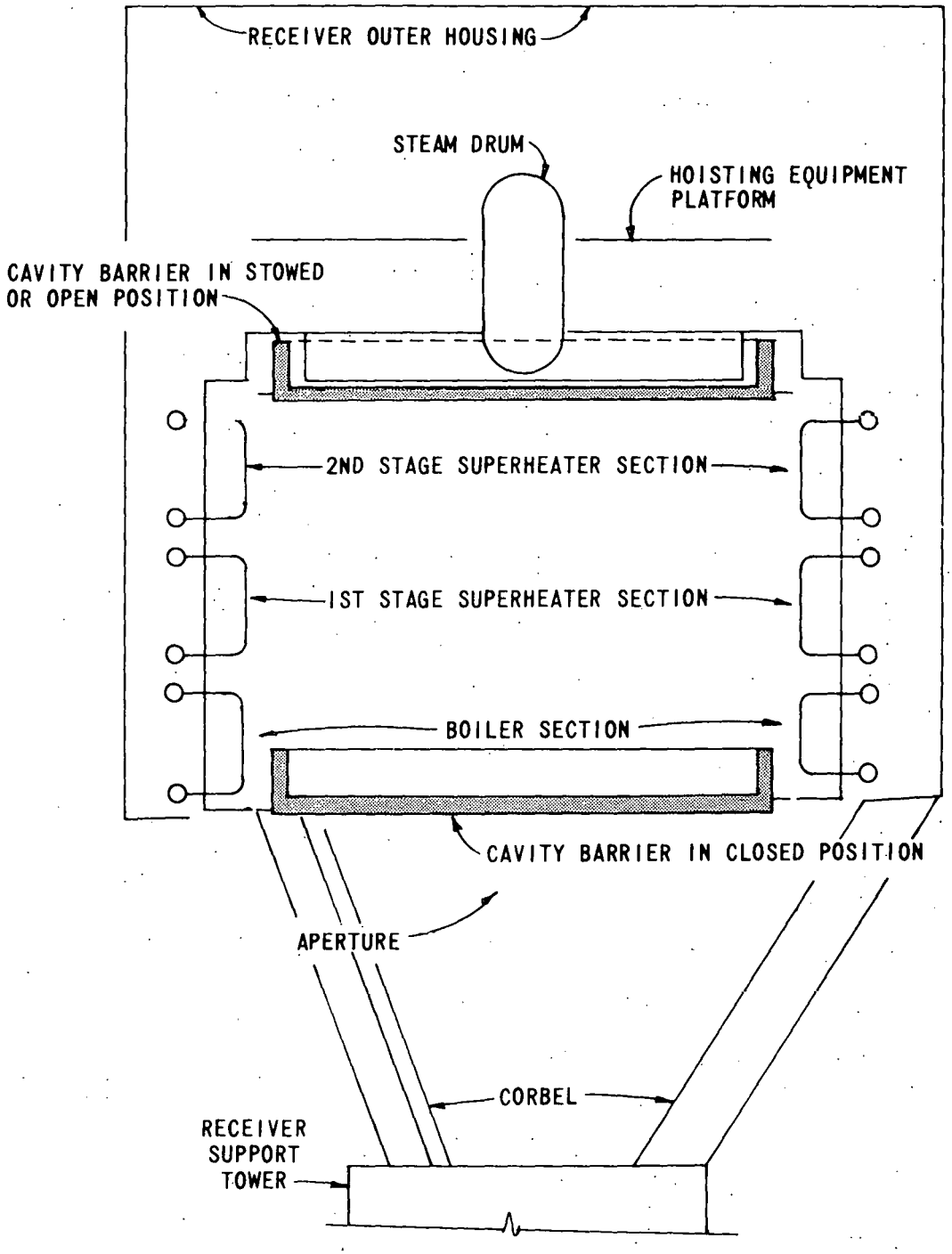

Figure 3-63. Cavity Barrier in Closed and Stowed (Open) Position

The most severe design requirement on the internal cavity barrier is its exposure to the high temperatures of the cavity. During normal operation, the receiver cavity temperatures approach 677 C (1250 F). When solar energy is diverted, cavity temperatures drop quickly to about 327 C (620 F) or the saturation temperature corresponding to the steam drum pressure. Hence, the barrier structure is subject to relatively high temperatures in both the stowed and the closed positions.

Because the barrier structure strength decreases rapidly with temperatures greater than approximately 316 C (600 F), a means to limit the exposure of the barrier structure to that temperature is provided. Since the cavity temperature rapidly decreases to about 327 C (620 F) when the solar energy is diverted, the closed cavity position of the barrier is within the temperature limit criterion. In its stowed position, the barrier structure is protected from the high cavity temperature by insulation on its exposed surface and by a forced air cooling system which maintains the space between the cavity barrier and the permanent ceiling at an acceptable temperature during operation of the plant.

The maximum temperature to which the barrier suspension may be subjected is also limited. Roller chain temperature limits are essentially based on the limitations of their lubricants. Deflocculated colloxial graphite is a suitable roller chain lubricant for temperatures in the 260 to 316 C (500 to 600 F) range.

It should be mentioned that any suspension used for raising and lowering the cavity barrier must be frequently inspected to meet the intent of the Occupational Safety and Health Act. The Federal regulations specifically address wire rope and alloy chain suspensions. The frequency of the required inspections are based on the application of the device. The inspections must include examination for wear, deformation, increase in length, high temperature effects, and so forth. The suspension must be removed from service immediately if defects or deterioration are evident. Roller chain, while apparently not specifically addressed as a suspension in the Federal regulations, should be assumed subject to the same requirements set for alloy chain.

The hoisting mechanism and associated equipment are located above the cavity permanent ceiling and are effectively insulated from the high cavity temperatures.

Since wind speeds at the elevation of the receiver cavity are expected to exceed 201 kilometers per hour (125 miles per hour), the wind loading on the cavity barrier is also an important consideration. Because of the barrier design and location in the receiver cavity, the expected

wind forces should not raise the disc vertically, but will principally induce lateral movement of the barrier. Locking devices are provided to secure the cavity barrier in its stowed and its closed positions and limit its lateral movement due to wind and seismic loads while in those positions.

During the detailed design phase of the pilot plant, a careful analysis should be made of the temperatures which the cavity barrier will assume during normal operation of the plant as well as during the diurnal shutdown periods. If necessary, an alloy with greater strength at elevated temperatures can be employed in the design of the barrier. The operating and maintenance plan developed for the pilot plant should include frequent inspection of the barrier roller chain suspension to meet the intent of the Occupational Safety and Health Act. It is recommended that until plant operating and maintenance experience is gained, the barrier hoisting mechanism and roller chain suspension be inspected after each used cycle.

Radiation Shielding

The radiation shield, illustrated in Drawing S1004 of Appendix F and described in the Preliminary System Design Specification for the Tower Structure System given in Appendix B, functions to protect the corbels, tower and outer housing from solar radiation redirected from the heliostat collector field. Radiation shields are located in areas adjacent to the receiver aperture which are subject to direct, continuous radiation or which may be subject to errant radiation. The shield reflects and diffuses the solar rays so that they are not incident upon the base structural member. Convective cooling of the radiation shield is accomplished by natural convective air flow which develops behind the shield and flows upward through the shield.

The radiation shields extend from the base of the corbels to a point on the outer housing 10 meters (33 feet) above the top of the tower. They cover the faces of the concrete tower, steel corbels, and outer housing metal wall panel.

The shields are also included at the base of the outer housing between the metal wall panel and the receiver aperture. At this location, the shields serve as an enclosure to protect the insulation attached to the outer lower surface of the receiver cavity from wind, rain, and direct solar radiation. The amount of heat entering the outer lower surface of the receiver cavity is minimized by a Kaowool thermal barrier located between the radiation shields and the outer lower surface of the cavity.

The specification of the configuration and design of the shield is similar to that for the ERDA 5 MW Solar Thermal Test Facility. The shields consist of 0.19 centimeter thick (14 gage) stainless steel louvers with

a white, modified silicone resin based, high temperature coating. The louvers are approximately 19 centimeters (7.5 in.) in width and inclined at an angle of approximately 15° to their support members. They are mounted side by side with a small overlap. On the tower and outer housing the shields are supported by a stainless steel tube girt frame. On the tower the girts are attached directly to the concrete shell; while on the outer housing, the girts are attached to wide flange hangers. The shields are supported on the corbels by vertical stainless steel WT sections with the web welded to the corbels and the flange used for attaching the shield.

The tower and receiver outer housing have a 20.3 centimeter (8 in.) air space provided between the shield and its supporting structure to allow convection cooling of the shields. Due to corbel design considerations, only 15 centimeters (6 in.) of air space is available for the convective cooling of the corbel shields. To aid the natural convective cooling, vents are added to the corbels (see Drawing S1004, Appendix F) and cooling air from the tower and mechanical equipment room is forced through the corbels.

To date, no detailed analysis of the actual performance of the radiation shielding has been completed for the operating and design conditions of the 10 MWe Pilot Plant. The results of the work for the ERDA 5 MW Solar Thermal Test Facility indicate the design is adequate for application to the pilot plant. Nevertheless, in developing the final pilot plant design, further consideration should be given to the optimization of the radiation shielding design for the pilot plant to assure its performance at the most reasonable costs.

TOWER

The tower serves to support the receiver cavity and steam generator at a height above the ground determined from the power to be generated by the plant, the layout of the heliostat collector field, and the design of the receiver cavity. In performing its function of support, the tower provides access, protection, servicing, and an acceptable environment for equipment, piping, and electrical cables associated with the receiver steam generator and the calibration arrays. The major elements of the tower are the tower foundation, the tower structure, and the feedwater and steam piping and equipment between the electrical power generation subsystem located at the ground level and the receiver steam generator at the top of the tower. The design of these elements is described in considerable detail in the Preliminary System Design Specifications for the Tower Structure System, the High Pressure Steam System, and the Feedwater System given in Appendix B. Summary descriptions of the elements are provided in the following sections.

Tower Foundation

The tower foundation is the ultimate element that in supporting the tower structure and receiver steam generator assembly transfers the resulting loads to the underlying soil strata. The foundation must be large enough to spread the vertical loads from the tower over adequate soil area to prevent bearing capacity failure or excessive settlements. It also must be sufficiently massive to maintain stability under the effects of wind and earthquake and to resist the internal stresses caused by gravity and lateral loads.

Details of the tower foundation design are illustrated in Drawing S1001 of Appendix F and described in the Preliminary System Design Specification for the Tower Structure given in Appendix B. The foundation in plan and elevation is illustrated in Figure 3-64. The foundation is a circular concrete mat 39.6 meters (130 feet) in diameter placed on native soil strata. It is 3.05 meters (10 feet) thick across the base of the tower and tapers to 2.13 meters (7 feet) at its edge. The foundation contains 3317 cubic meters (4336 cu yd) of concrete which is to be placed in one continuous pour. Radial and circumferential reinforcing steel are used in the top and bottom faces of the mat. A planar grid of reinforcing steel is used around the center point of the mat to ensure continuity of reinforcing. The top of the mat is located 1.5 meters (5 feet) below grade to allow access for underground utilities.

Several design criteria are specified for the preliminary design of the tower foundation. First, the mat is required to have sufficient area to limit soil pressures under maximum loads (gravity loads and overturning moments) to 24,450 kilograms per square meter (5 ksf). This is satisfied

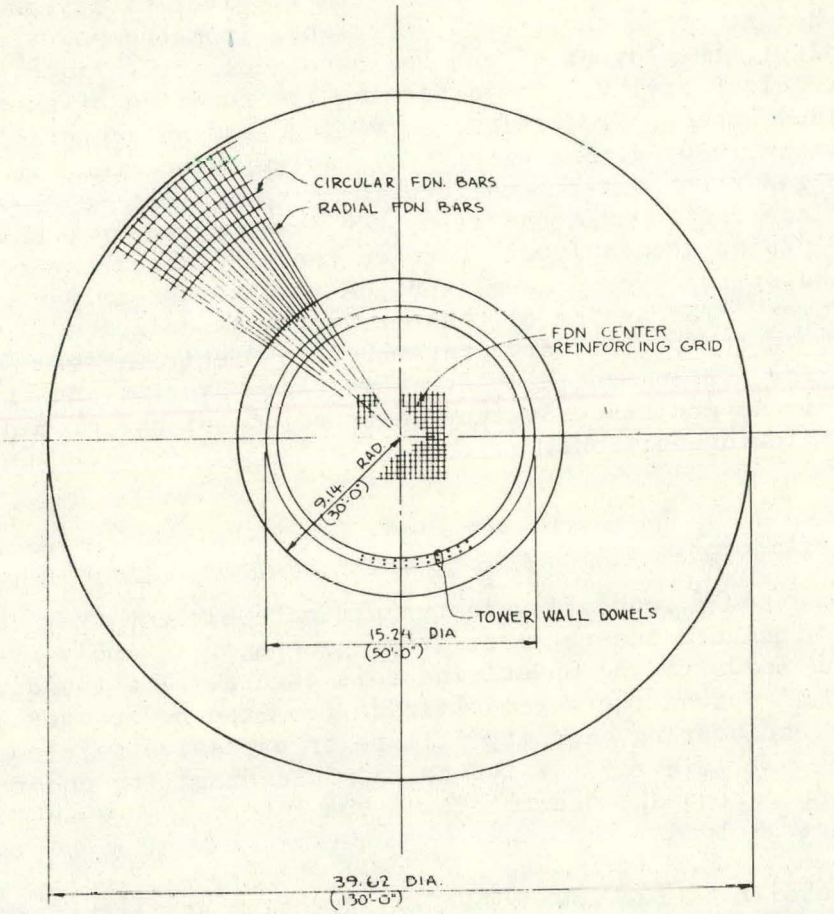

FOUNDATION PLAN
SCALE = 1:200

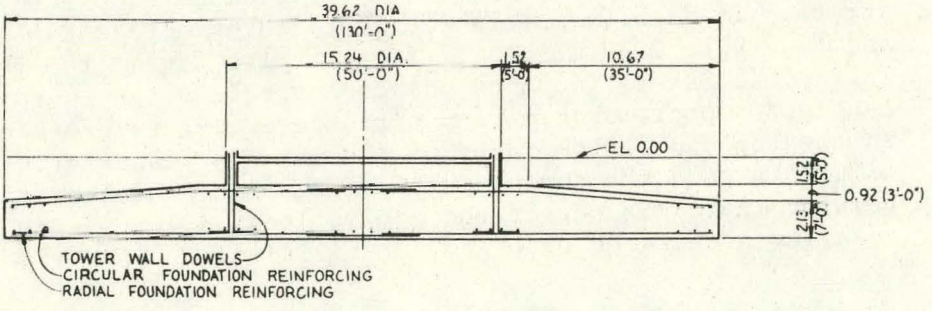

TOWER FOUNDATION SECTION
SCALE = 1:200

Figure 3-64. Tower Foundation

by assuming the gravity loads are distributed uniformly over the entire mat foundation, and the earthquake overturning moment provides a linearly varying load distribution under the mat. The mat is also required to have sufficient area and mass to prevent uplift (separation of mat and soil) at any point on the mat under minimum gravity load (reliable dead load) and maximum lateral load moment. This is satisfied by assuring that the uplift load caused by the earthquake overturning moment when translated into soil pressures is less than the uniform soil pressures caused by reliable dead loads. Third, the mat is required to have sufficient mass to prevent the base shear caused by earthquake loads from creating a sliding stability failure. This was verified for the conservative condition of minimum gravity loads with an assumed soil-concrete friction factor of 0.2. Finally, the mat thickness is sized on beam and punching shear requirements without the use of shear reinforcement. The moments, for which radial and circumferential reinforcing are sized, were found to be acceptable.

As an alternative to a circular foundation with radial and circumferential reinforcing, an octagonal foundation with grids of straight reinforcing was considered. It was found that because of the tight space requirements within the central plant complex, the circular foundation had less interference and isolation problems with the foundations of other plant structures. Further, a savings in reinforcing steel by using the radial and circumferential steel was found. The use of curved reinforcing steel is not considered to cause a fabrication problem because of the large radius involved.

Tower

The detail of tower design is illustrated in Drawing S1001 of Appendix F and described in the Preliminary System Design Specification for the Tower Structure System given in Appendix B. The tower function is to provide support and access for the receiver steam generator assembly, including the corbels, and to house certain receiver subsystem equipment, piping, and electrical cables. The tower must resist the corbel reactions and its own dead, live, and wind loads as set by the general design criteria of the pilot plant. The tower must also resist seismic forces without loss of stability or structural integrity.

The tower, as illustrated in Figure 3-65, is a hollow, truncated conical structure of reinforced concrete 126.52 meters (415 feet) in height with outside diameters of 15.24 meters (50 feet) at its base and 7.93 meters (26 feet) at its top. The height of the tower is fixed by the solar power to be absorbed by the receiver, the layout of the heliostat field, and the design of the receiver cavity aperture. The diameter of the tower at its top is fixed by the surface area and configuration of the receiver aperture, optimized for accepting redirected solar radiation from the collector field while minimizing the reradiated energy losses from the receiver cavity.

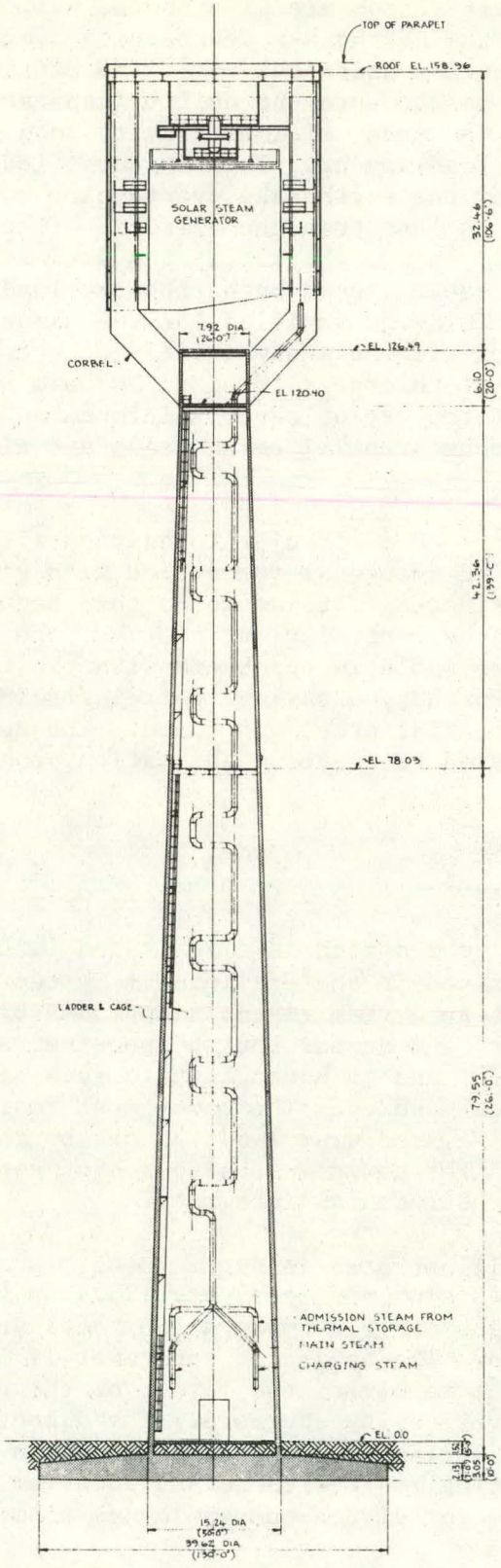

Section - Tower Elevation

Figure 3-65. Tower

The thickness of the tower wall is 0.610 meters (24 in.) at its base and 0.356 meters (14 in.) at its top. The tower wall is reinforced in both faces, and can be erected by either slip form or jump form methods. The top of the tower is a flat reinforced concrete slab approximately 0.305 meters (12 in.) in thickness.

A mechanical equipment room is provided in the tower approximately 6.1 meters (20 feet) below the top surface. This room, which if formed by the wall of the tower and a concrete floor slab on a structural steel frame, houses the receiver circulation pumps, blowdown tank, remote multiplex cabinet for instrumentation signals, and equipment servicing jib crane hoist. It is the highest accessible level within the tower and is the level of access to the corbels.

A service platform is located within the tower at approximately its mid-height. This platform consists of a bar grating floor on a structural steel frame, with a concrete slab provided to support the service water head tank. The platform also serves to access the four obstruction lights located on the outside of the tower.

A concrete grade slab is provided at finish grade for location of the fire water pump, service water pumps, auxiliary cooling water pumps, and demineralizer equipment.

Ventilation of the mechanical equipment room is by motor operated louvers set within the tower wall at the equipment room level. Circulation of air through the enclosed space below the mechanical equipment room is provided by openings in the tower shell immediately below the equipment room level.

Access to the tower at its base is by a rolling steel door 3.66 meters (12 feet) wide and 4.88 meters (12 feet) high, and by a personnel door 0.91 meters (3 feet) wide and 2.13 meters (7 feet) high. Personnel access up the tower is by ladder and elevator. The ladder is caged structural steel with bar grating landing platforms placed approximately every 9 meters (30 feet). The elevator is enclosed and guided from rails along the tower shell. It has a capacity for approximately twelve people or 1000 kilograms (2200 pounds). Ample space is available within the tower for piping and cable access.

The preliminary design of the tower is based on ACI standard 307-69, Specification for the Design and Construction of Reinforced Concrete Chimneys. The tower wall thickness at its top and base, and the tower's base diameter, were estimated from previous experience in designing concrete chimneys. Stresses were calculated from loadings due to gravity, wind, and seismic action. The initial calculation of seismic shears and moments was based on ACI 307 with a base shear of 0.25 g. The accuracy of these stresses was later compared with computer analysis as detailed in the Seismic Analysis and Design Considerations report given in Appendix E and briefly summarized

in a later section of this volume. Local stresses at the top of the tower due to corbel reactions were evaluated and found to be acceptable. Figure 3-66 confirms that the tower design geometry is within the bounds set by experience and good engineering practice.

In developing the final design of the tower further consideration of the radial pressure and dynamic effects of wind loading are to be evaluated. The radial pressure on the side of the tower produces ring moments in the concrete shell. These are resisted by the circumferential reinforcing steel in both faces of the shell. Although experience has shown vortex shedding is not generally an important design factor in tapered concrete chimneys or towers, analytical verification of this expected result is to be developed.

Tower Piping

The two major elements included under the category of tower piping are the feedwater piping and the main or high pressure steam piping. The feedwater piping functions to deliver feedwater from the feedwater pumps of the electrical power generation subsystem to the receiver steam generator. The high pressure steam piping functions to deliver steam generated in the receiver steam generator to the turbine and/or to the thermal storage subsystem, and to deliver steam generated in the thermal storage subsystem to the turbine. With reference to these principal elements, the tower piping is sized, routed, and supported to provide reasonable fluid velocities and pressure drops and to withstand the stresses which result from internal pressure, thermal expansion, dead loads, and to some extent seismic activity.

The feedwater line and high pressure steam line were sized to contain the maximum rated mass flow at a steam velocity below 34.5 meters per second (6800 feet per minute) and a water velocity below 4.6 meters per second (300 feet per minute). At the maximum rated mass flow, the pressure drop due to friction including a contingency is approximately 655 kPa (95 psi) in the feedwater line and 517 kPA (75 psi) in the main or high pressure steam line.

The piping specifications given in Table 3-17 for the feedwater line and the main or pressure steam line are in accordance with the ASME boiler and pressure vessel code for the operating pressures and temperatures of the pilot plant. The routing of a high pressure steam piping within the tower is shown in Figure 3-65 and is basically determined from the site and plant arrangement drawings, A1001 through A1006, which are given in Appendix F. The requirement for the expansion loops shown in Figure 3-65 and detailed in Figure 3-67 results from the long piping runs and the large differential temperatures between the hot and the cold operating conditions experienced by the piping. The expansion loops provide sufficient flexibility to accommodate the thermal expansion and contraction of the lines without causing unacceptable stresses. These expansion loops also provide

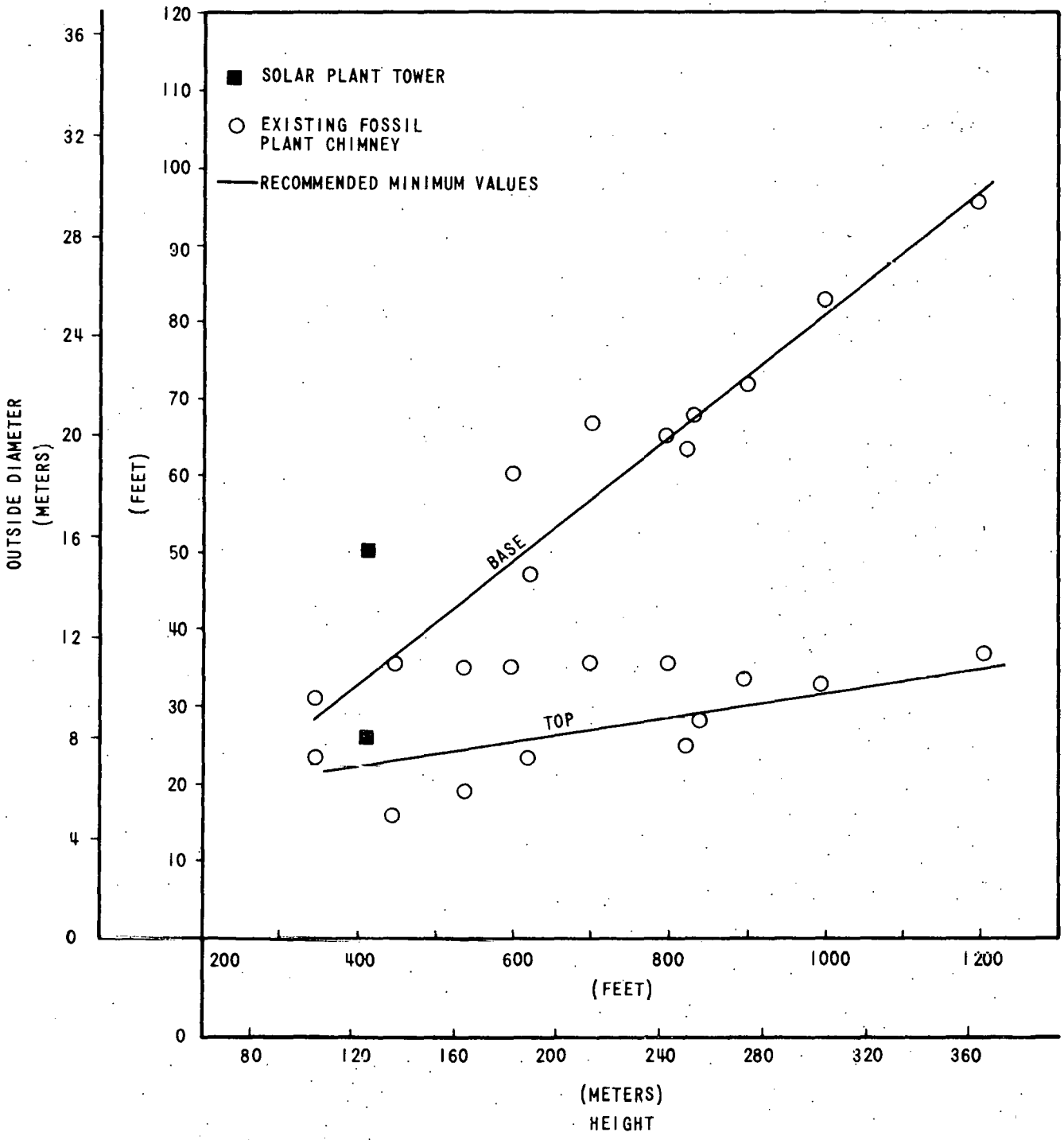

REFERENCE: RUMMAN, WADI S., "REINFORCED CONCRETE CHIMNEYS", HANDBOOK OF CONCRETE ENGINEERING, 1974.

Figure 3-66. Diameters of Reinforced Concrete Chimneys of Various Heights

TABLE 3-17

TOWER PIPING SPECIFICATIONS

	Feedwater Line	Steam Line
Nominal Size	4 in.	8 in.
Schedule	120	160
Material	A106 B carbon steel	P12 alloy steel
Outside Diameter	11.43 cm (4.500 in.)	21.91 cm (8.625 in.)
Inside Diameter	9.20 cm (3.624 in.)	17.31 cm (6.813 in.)

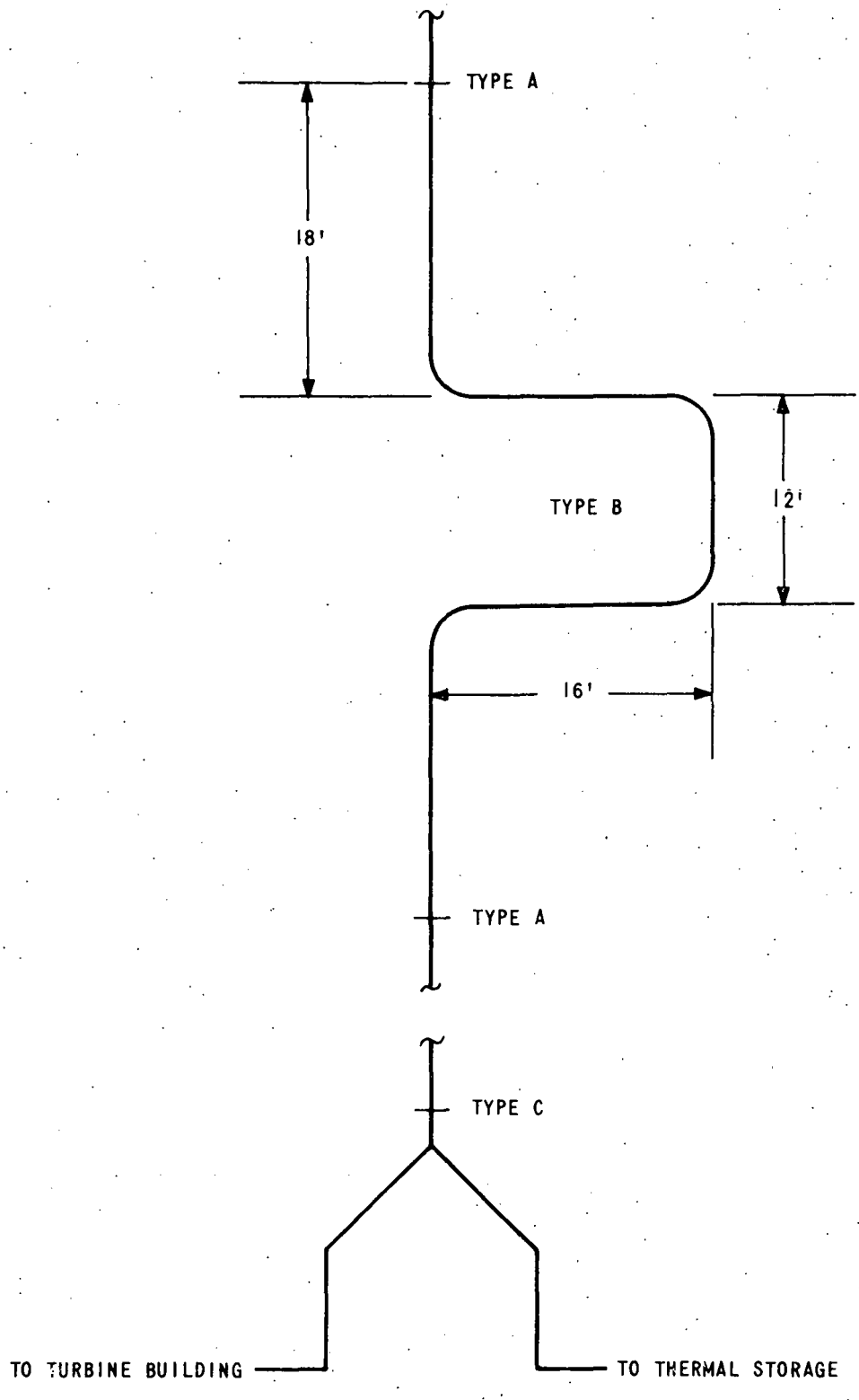

Figure 3-67. Main Steam Tower Piping

sufficient flexibility to accommodate the downward thermal expansion of the steam generator. The determination of the number of expansion loops required is the result of employing the commercially available thermal/structural analysis program, ADLPIPE, to an assumed routing of the high pressure steam piping.

The feedwater piping and high pressure steam piping are supported as required by the ANSI power piping code. The hangers used are shown in Figure 3-68 and are designed to withstand the loads imposed by dead weight, thermal expansion, and seismic activity. The four types of hangers illustrated have the following characteristics.

(1) Hanger Type A is a rigid support and does not allow movement.
(2) Hanger Type B allows movement normal to the pipe axis.
(3) Hanger Type C allows movement along with pipe axis.
(4) Hanger Type D supports the pipe weight and allows movement in any direction.

For the preliminary design of the tower piping, emphasis was placed on the design of the high pressure steam piping since it experiences the most severe thermal expansion and contractions. Detailed seismic analysis of the piping for the design level earthquake was not performed. However, the results of the general seismic analysis of the receiver assembly and tower suggests that the seismic loads which will be experienced by the piping can be resisted without extreme design difficulty. Certainly, the supports illustrated in Figure 3-68 will be sufficient to ensure that the piping remains attached to the walls of the tower even though some failure of the piping as a result of earthquake loading may occur.

In the development of the detailed design of the tower piping, the general analysis of the high pressure steam piping should be updated and extended to cover seismic loads. Further, the specific requirements for the design of the feedwater piping should be addressed. Such analyses are typical detailed design computations and are not expected to present any major difficulties in the finalization of a detailed design for the pilot plant.

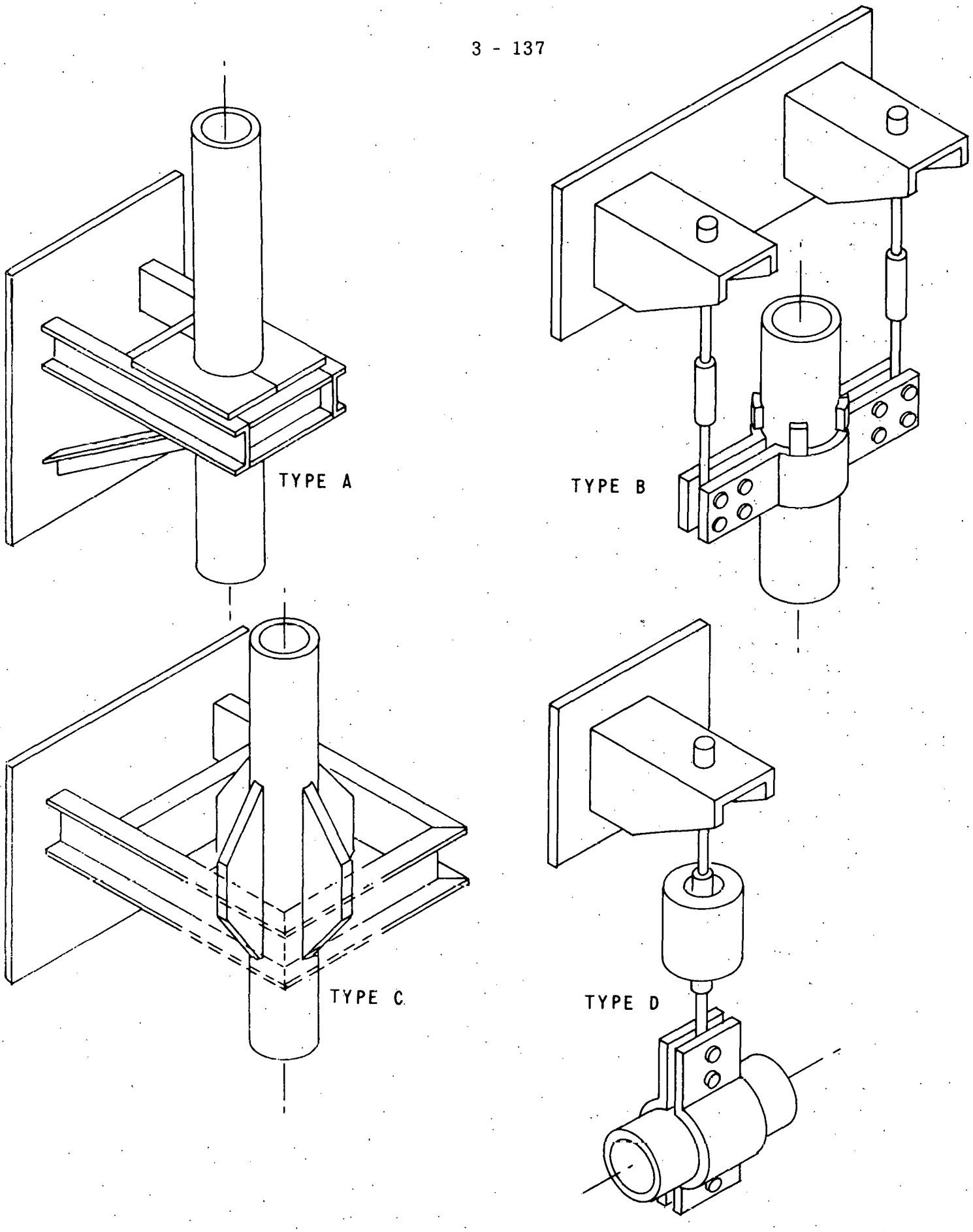

Figure 3-68. Hanger Types

RECEIVER SUBSYSTEM LOADS

The receiver subsystem is designed to resist static loads, wind loads, and seismic loads. These loads are determined from the weight of the supported element, the weight of the support structure itself, the anticipated use of the supported element and support structure, and the location of the integral structure as it relates to ambient conditions and earthquake susceptibility. The design static loads, wind loads, and seismic loads of the receiver subsystem are discussed in the sections which follow.

Static Loads

The static loads of the receiver subsystem include the loads of the supporting structure and equipment, service live loads to account for access and maintenance, roof loads to account for water ponding and snow, and impact loads to account for dynamic effects through the use of equivalent static loads.

Static loads are a major factor in the design of most structural members in the receiver subsystem. Major equipment such as the steam generator, drum, and pumps are the primary contributors to these loads. Access and maintenance floor structural members which do not support equipment generally only have static loads associated with their design. These loads include miscellaneous piping loads, live loads, and dead loads.

The structure and equipment loads are determined individually from the weight of structural members, enclosure material, equipment, piping, and electrical cable. Service live loads are a minimum of 367 kilograms per square meter (75 psf) for grating platforms and 489 kilograms per square meter (100 psf) for concrete platforms. If, however, due to equipment erection, maintenance, or other special situations, the minimum service live loads are not adequate, the actual live load for the area is determined and the structure designed accordingly. Platform live loads at levels below the roof are reduced for column and for corbel design per Black & Veatch Design Guide S-419.00. This is done because all platform levels are not subject to live loads simultaneously.

Roof live loads consist of service and ponding loads. The service load is 122.3 kilograms per square meter (25 psf). It is less than platform service loads because of limited access requirements. The service load is combined with the larger of either the water ponding or snow load to determine the total roof live load. The snow load, which is based on a 100 year recurrence interval per ANSI A58.1, is a basic load of 49 kilograms per square meter (10 psf). This basic value is adjusted by ANSI for roof type, adjacent structures, parapet height, etc. Water ponding can occur on a roof for brief periods during an intense storm when roof drains cannot handle the runoff, or due to minor irregularities in the roof which cause isolated areas to not drain properly. A 97.8 kilogram per square meter

(20 psf) load, which is equivalent to 9.77 centimeters (3.85 inches) of water on the roof, will adequately account for this condition. Consequently, the governing roof live load, which is the combination of service and ponding loads, is 220 kilograms per square meter (45 psf).

Equivalent static loads are used to account for impact caused by moving or rotating equipment and moving material. Impact loads considered are 100 per cent of the lifted load for the elevator, 25 per cent of the lifted load for hoists, 50 per cent of the machine weight for rotating equipment, and 100 per cent of the live load of the steam drum. Pipe impact loads are determined on an individual basis.

The governing design static loading for a structural member is the maximum combination of individual static loads which is likely to occur over the life of the member. Each structural member is also investigated for the combination of design static loading (exclusive of impact load) and the larger of wind or seismic loads which are considered to not act simultaneously. For this design condition, the applicable code permits the allowable stresses of the structural members to be increased by one-third because of the transient nature of wind and seismic loading.

Wind Loads

The receiver subsystem structure is designed for a lateral pressure resulting from wind magnitudes which can be expected at the plant site. The basic design speed is 35.8 meters per second (80 mph) as determined per ANSI AS8.1-1972 for a 100 year recurrence interval at 9.14 meters (30 ft) above the ground. This converts to a basic design pressure of 102.7 kilograms per square meter (21 psf) for flat, open country exposure. The pressure is modified per ANSI for chimney surface type and proportions, and the height above ground of the framing section being considered. The design pressure at the top of the outer housing is 220 kilograms per square meter (45 psf). In addition, the pressure is modified by a pressure coefficient for the design of wall panel and girts to account for windward pressure and leeward suction forces.

An additional wind loading considered is the dynamic effects of vortex shedding. Vortex shedding can result in large deflections and stresses due to lateral swaying and ovaling if the tower and outer housing are not sized and designed to prevent resonance with the shedding of wind vortices.

Wind loads are not generally considered in design as acting alone, but are taken in combination with static loads.

Wind loadings for the overall design of the structure do not govern the design. However, specific components of the receiver subsystem such as the girt for the receiver outer housing is designed specifically for wind. Other areas will require investigation in the final design to ensure

wind is not a major consideration. An example of this is the circumferenti-l reinforcement in the receiver tower which is normally investigated for moments produced by the uneven radial pressures due to wind. Also, lateral swaying and ovaling due to vortex shedding will require further investigation in the final design due to the circular shape of the receiver outer housing. It should be noted that experience has indicated this phenomenon will not be a problem with the concrete receiver tower.

Seismic Loads

The receiver subsystem structure is designed for forces resulting from horizontal and vertical accelerations at the tower foundation caused by an earthquake. The forces are determined from an analysis of the tower and outer housing to the ground response spectrum described in NRC Regulatory Guide 1.60 normalized to 0.25 g maximum acceleration. This value is consistent with accelerations considered appropriate for the plant site. Damping is taken to be two per cent of critical damping.

The structure was dynamically analyzed by the response spectrum method utilizing an idealized "stick" model for the support tower. The receiver housing "stick" model was expanded to a space frame.

A time history analysis was also conducted utilizing a similar model but simplifying the receiver area by use of a plane frame configuration.

The results of these analyses indicate that the tower structure is much stiffer than the structural steel framing for the receiver housing and corbel. This can cause a significant "whipping" action in the upper portion of the structure, magnifying the accelerations.

Seismic forces are a major load consideration in design of the steam generator support trusses, corbels, and receiver tower. In addition the relative stiffeners of the steam generator support frame, its interface with the corbels, and the corbels themselves will require considerable detailed design to reduce or eliminate amplification of these seismic forces.

The use of existing codes for seismic analysis does not appear to be conservative. Hence, an elastic dynamic analysis should be undertaken to establish the equivalent forces or loadings to be considered in detailed design. Once the equivalent loads are established, the existing codes can be utilized to design the receiver structure components.

The report, "Seismic Analysis and Design Considerations" given in Appendix E should be referenced for a more complete description of the seismic study which was performed and the approach which should be followed in detailed design.

APPENDIX A

DATA LIST

LIST OF DATA AND INFORMATION ITEMS

A. DESIGN CHARACTERISTICS

	Pilot Plant	Comm'l Plant	SRE
1. Weight on top of tower[1] (10^3 kg)	602.2	TBD	
2. Weight of housing (10^3 kg)	319.3	TBD	
3. Weight of all pressure parts[2] (10^3 kg)	137.4	427	
4. Height, width, and depth or diameter (m)			
H major/minor	16/14.17	28.5/25.3	3.08
Diameter	14.94	26.1	3.48
5. Area of aperture and/or working surface of boiler and superheater (m^2)			
Aperture	218	651	0.51

Boiler	344.4	1,073	21.72
Primary S.H	150.1	467	11.24
Secondary S.H.	225.3	702	11.24

6. For boiler and superheater, material OD/ID/wall (mm), length (m), number of tubes, and total mass (kg)

Boiler

Material	Carbon Steel SA 210 A1CF	same	same
OD/ID/Min Wall(mm)	22.23/14.71/ 3.76	same	same
Length[3] (m) Maximum/ Minimum	8/6.17	14.2/11.0	1.79
Number[4]	1070	1911	288
Mass-Total (kg)	31977	100×10^3	1893

Superheater

Material	Croloy 2-1/4 SA-213-T22	same	same
OD/ID/Min Wall(mm)	25.4/17.02/ 4.19	31.75/-/ 5.59	same
Length[3] (m)	46.95	16.4/ sect 82/cir- cuit	36.24
Number[4] Primary/ Secondary	378/567	875/325 5 circuits 5 sect.	12/12
Mass Total[5] (kg)	39555	123×10^3	2189

7.	Section of ASME code designed to meet	Section 1	same	same
8.	Composition and optical characteristics including approximate /a, of receiver surface coatings			
	Composition	Oxide	same	same
	a	0.9	same	same
		0.9	same	same
9.	Pressure drop correlations:			
	Single-phase flow	moody	same	same
	Two-phase flow	Martinelli, Nelson	same	same
	Across boiler/super-heater, typical (MPa/MPa)	.277/.46	TBD	.112/.91
10.	Heat Transfer correlations:			
	Water heating	Dittus-Boelter	same	same
	Subcooled nucleate boiling(kW/m^2C)	56.8	same	same
	Nucleate Boiling (kW/m^2C)	56.8	same	same

	Superheater steam	B&W proprietary	Dittus-Boelter	Dittus-Boelter
	Nucleate/film boiling transition	NA	NA	NA
11.	Diameter (m), length (m), and wall thickness (cm), plus material and total mass (kg) of drum			
	Diameter (in)	1.22	215	0.61
	Length (less head)	3.29	3.29	1.88
	Wall Thickness			
	Straight	8.89	15.7	5.08
	Heads	7.62	--	5.08
	Total Mass	12,943	73,100	2,282
	Material	SA 299	Carbon Steel	SA 516-70

B. OPERATING CHARACTERISTICS

	PP[7]		Comm'l		SRE	
	Max	Design	Max	Design	Test	Design
1. Average flow and circulation rates:						
Boiler (kg/s)	171.3	171.3	533	533	17.17	15.92
Superheater (kg/s)	17.17	14.57	53	45	1.74	1.737
Attemperator (kg/s)	1.70	2.85	8.9	5.3	.0212	.145
Feedwater (kg/s)	15.47	13.32	48	41	1.717	1.592
Boiler inlet velocity[8] (m/s)	1.39	1.38	TBD	TBD	0.52	0.48
Boiler outlet quality	.090	.077	.09	.08	.10	.10
Superheater inlet velocity (m/s), avg.	0.03	7.19	TBD	TBD	9.07	8.45
Superheater outlet velocity (m/s), avg.	12.07	10.52	TBD	TBD	19.1	19.1
2. Operating pressure and temperature states:						
Boiler and Drum (MPa/°C)	11.64/ 322	11.23/ 320	TBD	TBD	11.91/ 324	11.87/ 323.8
Superheater (MPa/°C)	11.02/ 515.6	10.77/ 515.6	TBD	TBD	10.95/ 512.8	10.96/ 512.8
Feedwater Inlet (MPa/°C)	12.93/ 215	12.93/ 204	TBD	TBD	13.10/ 226.7	13.10/ 226.7

		Pilot Plant	Comm'l Plant	SRE
3.	Peak Flux:			
	Max. absorbed (kW/m^2)	263	263	NR
	Design absorbed (kW/m^2)	258	258	400
4.	Flux maps	--	--	--
5.	Power onto/into receiver			
	at Max. insolation (MW)	50.25	582.9	--
	at Design insolation (MW)	40.85	582.9	5.14
	at Min. rated steam (MW)	--	--	--
6.	Absorbed power/flow rates:			
	at Max. insolation (MW/kg/s)	17.35	202.8	
	Superheater duty (MW)			
	at Design insolation (MW/kg/s)	13.83	202.8	2.54
	Superheater duty (MW)			
	at Min rated steam (MW/kg/s)	--	--	
	Superheater duty (MW)			
7.	Cavity efficiency			
	at Max insolation (%)	87.2	87.5	
	at Design insolation (%)	85.5	87.5	5.14 (MW)
	at Min rated steam (%)	--	--	
	Annual Average (%)	84.1	84.4	

8. Net annual thermal energy into/onto receiver (MWH)	121,600	--	
9. Net annual into steam (MWH)	102,300	--	
10. Peak metal temperatures on boiler web/boiler tube/ superheater tube			
at Max insolation ($^{o}C/^{o}F$)	399/362/ 559	--	
at Design insolation ($^{o}C/^{o}F$)	386/350/ 563	TBD	436/381/ 588
at Min rated steam ($^{o}C/^{o}F$)	--	--	
11. Typical heat transfer coefficients (design):			
Boiler ($kW/m^{2o}C$)	56.8	same	same
Superheater ($kW/m^{2o}C$)			
Primary superheater			
Inlet	8290	TBD	5826
Outlet	3600	TBD	3390
Secondary superheater			
Inlet	3503	TBD	4281
Outlet	2663	TBD	3765

12. Peak working stresses in boiler:			
From pressure load (MPa)	27.8	TBD	27.8
From temperature (MPa)	68.1	TBD	103.7
Combined stress (MPa)[10]	103.4	TBD	151
Fatigue allowable stress (MPa)[11,12]	137 (10^5H)	TBD	137 (10^5H)
Allowable membrane stress (MPa)[12]	98.6	TBD	98.6
13. Peak working stresses in superheater:			
From pressure load (MPa)	27.8	TBD	27.8
From temperature (MPa)	52.4	TBD	not determined directly
Combined stress (MPa)	73.8	TBD	206.7
Fatigue allowable stress[11,12]	124 (10^5H)	TBD	124 (10^5H)
Allowable membrane stress[12]	29.0	TBD	29.0

C. DESIGN DISCUSSION

The following paragraphs identify the subsections of the report which discuss the 13 topics specified by Sandia Laboratories for the receiver subsystem:

1. Maintenance and repair requirements are discussed in the Maintenance subsection.

2. Heat Losses due to conduction and convection and overnight cooldown rates are discussed in the Heat Loss and Cooldown Rate subsection.

3. Sensitivity of the design to cloud disturbances and other off design conditions is included in the Performance Characteristics and the Conditions subsections.

4. Flow stability is discussed in the Static Flow Stability subsection.

5. The lifetime of the boiler and superheater tubes is discussed in the Design Approach and the Stress Analysis subsections.

6. Seismic design is discussed in the Design Approach, the Components and the Structural Analysis subsections.

7. General startup procedures for the steam generator are discussed in the Operations subsection.

8. Startup limitations are discussed in the Permissible Rate of Temperature subsection.

9. Water quality is discussed in the Water Treatment subsection.

10. The number of thermal cycles is discussed in the Stress Analysis subsection.

11. Emissivity versus wave length is discussed in the Thermal Radiation Characteristics subsection.

12. Future System Optimization is discussed in Appendix D.

13. Safe operation at off design conditions is discussed in the Upset Conditions, the Operational and the Instruments subsection.

NOTES:

1. Pilot Plant - Water and Insulation Masses included
   SRE - Water and Insulation Masses not included

2. Pump(s) not included

3. Heated Lenghts only
   Pilot Plant - one circuit (three circuits with three sections each per superheater)
   SRE - Helix length

4. Pilot Plant - All tubes in each superheater (three circuits with three sections each per superheater)
   SRE - Total number of tubes per superheater

5. Metal Mass of Tubes only

6. Pilot Plant results are based on Preliminary Heat Flux and Turbine Data unless stated otherwise.

7. SRE - Design: 3/21/12 pm Heat Flux Distribution
   - Testing: 70% Absorbed Power into Boiler and 30% Absorbed Power into Superheaters
   Pilot Plant - Design: 12/21/12 pm Heat Flux Distribution
   - Maximum: 3/21/12 pm Heat Flux Distribution

8. Average Mass Velocity at the locations indicated for Respective Tube Cross-sectional Area.

9. Pilot Plant - Refer to Heat Flux Data in Functional Performance Section
   SRE - Refer to Detailed Design Review Report

10. Maximum Effective Stress Range of the Boiler Tubes

11. Continuous Cycling (i.e., No Hold Time); Twice the Alternating Stress.

12. Superheater Allowable Stresses for 538C (1077F)
    Boiler Allowable Stresses for 371C (700F)

APPENDIX B

DESIGN REQUIREMENTS

This Information is Presented in

Volume II Appendix B

APPENDIX C

- MAJOR GENERATOR PARTS DATA

- STEAM GENERATOR DRAWINGS

Table C-1. Major Pressure Parts Summary

Part	OD mm (in)	ID[1] mm (in)	Thickness[2] mm (in)	Schedule Number	Quantity	Material Specification
Drum					1	SA-299
Straight	1397 (55)	1219 (48)	89 (3.5)			
Hemispherical Heads	1384 (54.5)	1219 (48)	83 (3.25)			
Downcomer	324 (12.75)	281 (11.062)	18.8 (0.739)	100	1	SA-106C
Boiler Supply Line	273 (10.75)	236 (9.312)	16.0 (0.629)	100	1	SA-106C
Boiler Supply Header	273 (10.75)	236 (9.312)	16.0 (0.629)	100	1	SA-106C
Boiler Supply Tubes	168 (6.625)	146 (5.761)	9.6 (0.378)	80	8	SA-106C
	89 (3.500)	74 (2.900)	6.7 (0.263)	80	1	SA-106C
Boiler Inlet Header	219 (8.625)	173 (6.813)	20 (0.793)	160	1	SA-106C
Boiler Tubes	22 (0.875)	14.7 (.579)	3.8 (0.148)		1072	SA-210A1
Boiler Outlet Header	219 (8.625)	173 (6.813)	20 (0.793)	160	1	SA-106C
Riser Tubes	168 (6.625)	146 (5.761)	9.6 (0.378)	80	7	SA-106C
	114 (4.500)	97 (3.826)	8.6 (0.337)	80	1	SA-106C
Saturated Superheater Tubes	141 (5.563)	122 (4.813)	8.3 (0.328)	80	1	SA-106C
	102 (4.000)	85 (3.364)	7.1 (0.279)	80	1	SA-106C
	89 (3.500)	74 (2.900)	6.7 (0.263)	80	1	SA-106C
Primary Superheater Inlet Headers	168 (6.625)	103 (4.053)	32.7 (1.286)		3	SA-335-P22
Primary Superheater Tubes	25.4 (1.0)	17.0 (0.670)	4.2 (0.165)		378	SA-213-T22
Primary Superheater Interconnecting Tubes	141 (5.563)	110 (4.313)	13.9 (0.547	160	6	SA-335-P22
Primary Superheater Outlet Headers	168 (6.625)	103 (4.053)	32.7 (1.286)		3	SA-335-P22
Primary Superheater Outlet Line	168 (6.625)	132 (5.187)	16.0 (0.629)	160	1	SA-335-P22
	141 (5.563)	110 (4.313)	13.9 (0.547)	160		
	114 (4.500)	87 (3.438)	11.8 (0.465)	160		
Secondary Superheater Inlet Line	168 (6.625)	132 (5.187)	16.0 (0.629)	160	1	SA-335-P22
	141 (5.563)	110 (4.313)	13.9 (0.547)	160		
Secondary Superheater Inlet Headers	168 (6.625)	103 (4.053)	32.7 (1.286)			SA-335-P22
Secondary Superheater Tubes	25.4 (1.0)	17.0 (0.670)	4.2 (0.165)			SA-213-T22
Secondary Superheater Interconnecting Tubes	141 (5.563)	110 (4.313)	13.9 (0.547)	160	6	SA-335-P22
Secondary Superheater Outlet Headers	168 (6.625)	103 (4.053)	32.7 (1.286)		3	SA-335-P22
Secondary Superheater Outlet Line	168 (6.625)	132 (5.187)	16.0 (0.629)	160	1	SA-335-P22
	141 (5.563)	110 (4.313)	13.9 (0.547)	160		

[1] Based on nominal wall thickness for pipe and minimum wall thickness for tubes.

[2] Minimum wall thickness.

Table C-2. Steam Generator Major Pressure Part Weights

Item	Weight[1] kg	Weight[1] (lbm)	Water Weight[1,2] kg	Water Weight[1,2] (lbm)
Boiler				
Drum	11540	(25410)	4336	(9550)
Internals	1362	(3000)	--	--
Downcomer	7786	(17150)	3024	(6661)
Supply Line	3493	(7693)	1339	(2950)
Supply Header	5625	(12390)	2156	(4749)
Supply Tubes	2710	(5970)	1110	(2444)
Inlet Header	5462	(12030)	1154	(2541)
Heat Transfer Surface	31890	(70230)	1330	(2930)
Outlet Header	5462	(12030)	1154	(2541)
Riser Tubes	6342	(13970)	2480	(5462)
Primary Superheater				
Saturated Superheater Tubes	1568	(3454)	536	(1180)
Inlet & Outlet Headers	2200	(4845)	168	(369)
Interconnecting Tubes	539	(1187)	104	(228)
Tubes	15820	(34840)	1521	(3350)
Outlet Line	1925	(4240)	365	(804)
Attemperator				
Attemperator Line	413	(910)	83	(183)
Attemperator	1192	(2625)	42	(93)
Secondary Superheater				
Inlet Line	2209	(4865)	428	(943)
Inlet & Outlet Headers	3259	(7178)	248	(547)
Interconnecting Tubes	539	(1187)	104	(228)
Tubes	23730	(52260)	2281	(5024)
Outlet Line	2209	(4865)	428	(943)
Pressure Part Insulation	54750	(120600)		

[1]Based on nominal wall thickness for pipe and minimum wall thickness for tubes.

[2]Calculated assuming filled with water having a density of 1000 kg/m^3 (62.4 (lbm/ft.^{3})

Table C-3. Solar Steam Generator - Pilot Plant Valve List

Valve Function	Size Inches	Pressure Class	Type	Body Material	Manufacturer & Figure No.		Number Required
Pump Suction Isolation	10	1500	Gate	C.S.	Powell	11303WE	3
Pump Discharge Isolation	10	1500	Stop-Check	C.S.	Edwards	7506Y	3
Boiler Supply	5	1500	Globe	C.S.	Edwards	7516Y	8
Boiler Supply	3	1500	Globe	C.S.	Edwards	7516Y	1
Drum Vent	1	1500	Globe	C.S.	Rockwell	3624	1
Drum Pressure Gage Isolation	1	1500	Globe	C.S.	Rockwell	3624	1
Total Boiler Flow Meter Isolation	1/2	2500	Globe	C.S.	Rockwell	952	2
Individual Boiler Circuit Flow Meter Isolation	1/2	2500	Globe	C.S.	Rockwell	952	18
Boiler Inlet Header Drains	1/2	1500	Angle	C.S.	Rockwell	1049Y	8
Boiler Outlet Header Drains	1/2	1500	Angle	C.S.	Rockwell	1049Y	8
Boiler Supply Header Vent	1	1500	Globe	C.S.	Rockwell	3624	1
Drum Level Transmitter Isolation	1	1500	Globe	C.S.	Rockwell	3624	4
Boiler Blow Off	1-1/2	1500	Angle	C.S.	Rockwell	3627	1
Boiler Blow Off	1-1/2	1500	Straight	C.S.	Rockwell	3626	1
Primary Superheater Header Drains	1	1500	Globe	F-22	Rockwell	3624	3
Primary Superheater Header Drains (Motor Operated)	1	1500	Globe	F-22	Rockwell	3624	3
Attemperator Drain	1	1500	Globe	F-22	Rockwell	3624	1
Attemperator Drain (Motor Operated)	1	1500	Globe	F-22	Rockwell	3624	1
Secondary Superheater Header Drains	1	1500	Globe	F-22	Rockwell	3624	3
Secondary Superheater Header Drains (Motor Operated)	1	1500	Globe	F-22	Rockwell	3624	3
Primary Superheater Outlet Pressure Transmitter Isolation	1/2	2500	Globe	TP-316	Rockwell	4952Y	1
Primary Superheater Header Vents	1	1500	Globe	F-22	Rockwell	3624	3

Secondary Superheater Header Vents	1	1500	Globe	F-22	Rockwell	3624	3
Primary Superheater Outlet Header Drains	1	1500	Globe	F-22	Rockwell	3624	2
Secondary Superheater Inlet Header Drains	1	1500	Globe	F-22	Rockwell	3624	2
Secondary Superheater Outlet Header Drains	1	1500	Globe	F-22	Rockwell	3624	2
Drum Safety Valve	2" Inlet x 6" Outlet Capacity 111787 #/HR Set Pressure 1875 psig Orifice J Saturated Steam				Crosby	HC-75	1
Superheater Safety Valve	1-1/2" Inlet x 3" Outlet Capacity 30819 #/HR Set Pressure 1675 psig Orifice G 960°F Steam				Crosby	HCA-78	1
Gage Glass Cocks	Integral with Diamond Power Model DP-3000 Duraport gage glass						2

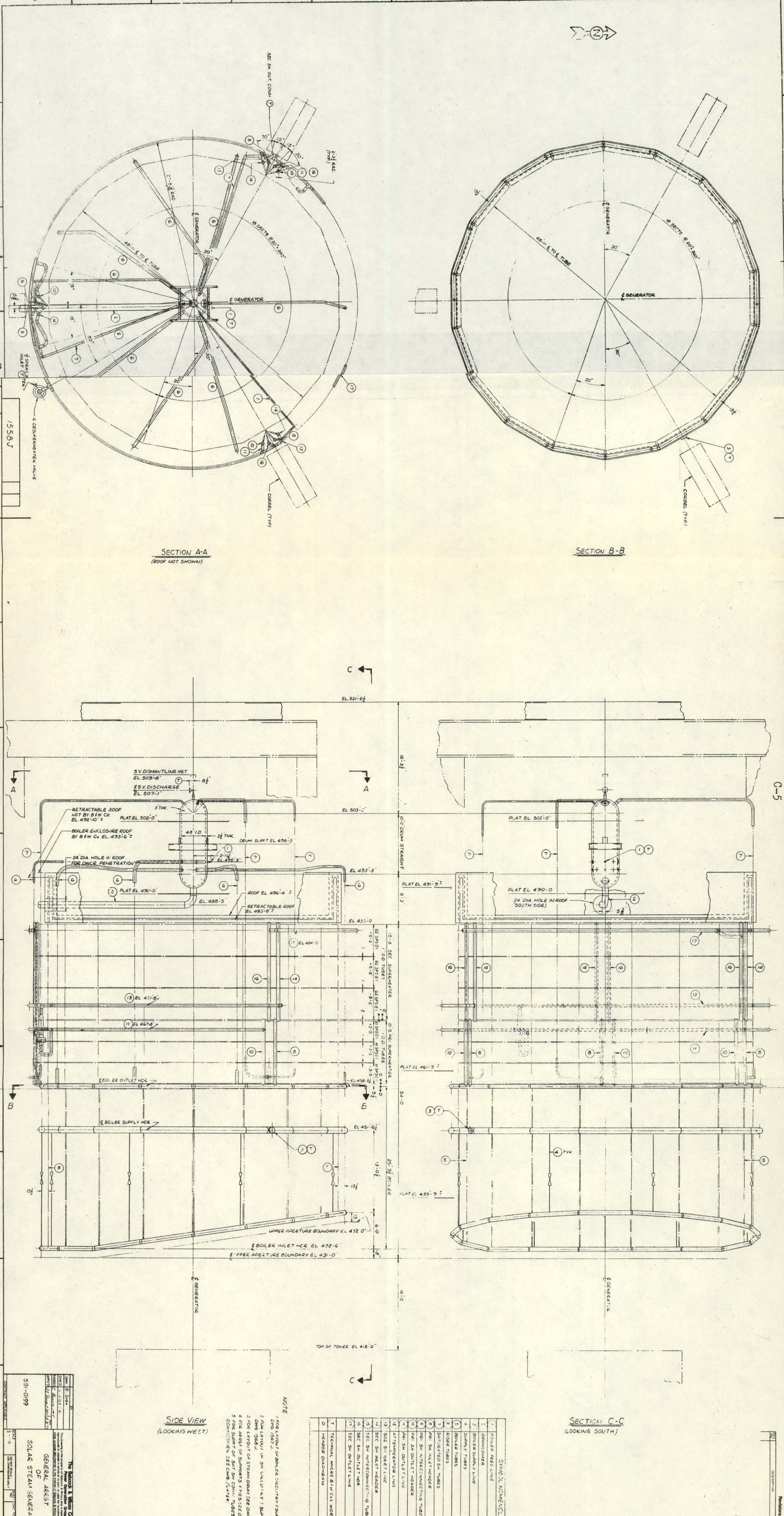

NOTE

1. FOR LAYOUT OF BOILER CIRCUITRY & SUPPORTS SEE DWG. 1567J.
2. FOR LAYOUT OF SH CIRCUITRY & SUPPORTS SEE DWG 1568U
3. FOR LAYOUT OF STEAM DRUM SEE DWG 1569J
4. FOR ARRGT OF SUPPORTS & TIES SEE DWG 247/8E
5. FOR SUPPT OF SAT SH CONN TUBES, RISER TUBES & DOWNCOMER SEE DWGS. (LATER)

SYMBOL NOMENCLATURE

1	BOILER FEED LINE
2	DOWNCOMER
3	BOILER SUPPLY LINE
4	SUPPLY TUBES
5	BOILER TUBES
6	RISER TUBES
7	SATURATED SH TUBES
8	PRI SH INLET HEADER
9	PRI SH INTERCONNECTING TUBES
10	PRI SH OUTLET HEADER
11	PRI SH OUTLET LINE
12	ATTEMPERATOR LINE
13	SEC SH INLET LINE
14	SEC SH INLET HEADER
15	SEC. SH INTERCONNECTING TUBES
16	SEC SH. OUTLET HDR
17	SEC SH OUTLET LINE
T	TERMINAL WHERE B&W Co'S WORK STOPS
D	HEADER DIAGRAM

Revisions

REV NO	DESCRIPTION	DATE	APPROVAL	MF

The Babcock & Wilcox Company
Power Generation Group

GENERAL ARRGT OF SOLAR STEAM GENERATOR

DWN E. SHEA
CHK'D L. NOE

591-0199

CONTRACT APPLICABLE

DO NOT SCALE - USE DIMENSIONS ONLY

DWG NO 1558 J REV 0

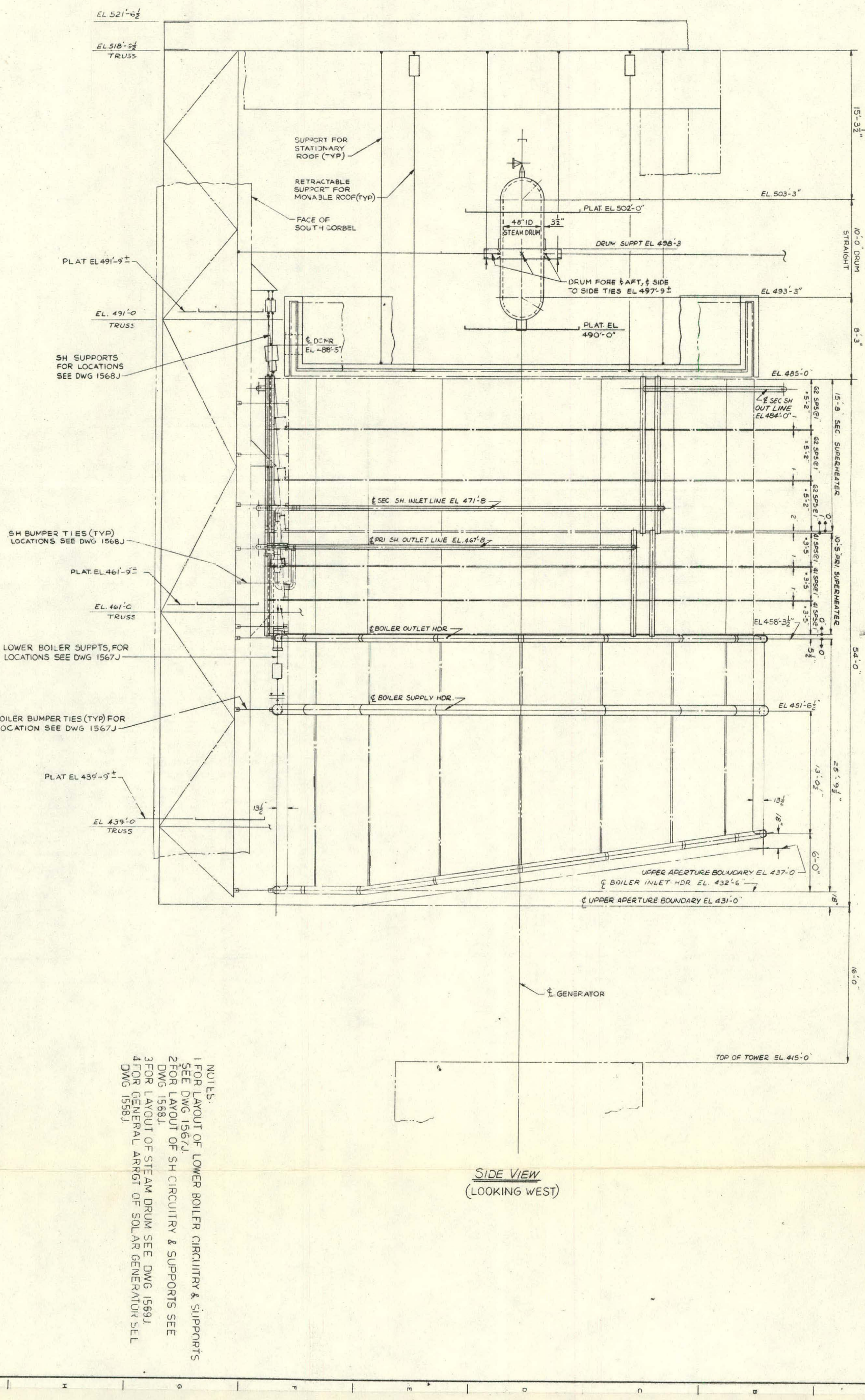

SIDE VIEW
(LOOKING WEST)

NOTES:
1 FOR LAYOUT OF LOWER BOILER CIRCUITRY & SUPPORTS SEE DWG 1567J.
2 FOR LAYOUT OF SH CIRCUITRY & SUPPORTS SEE DWG 1568J.
3 FOR LAYOUT OF STEAM DRUM SEE DWG 1569J.
4 FOR GENERAL ARRGT OF SOLAR GENERATOR SEE DWG 1558J.

REVISIONS			
REVISION NO.	DESCRIPTION	DATE	APPROVAL

DWN. BY R.R. JOHNSON
CHKD. BY L. KOTZEE
PASSED BY
APPVD. BY
STD. | SPL. | DATE 3-31-77

591-0199

DO NOT SCALE USE DIMENSIONS ONLY

SCALE ½" = 1'-0"

GENERAL ARRGT. OF SUPPORTS & TIES FOR SOLAR STEAM GENERATOR

THE BABCOCK & WILCOX CO. POWER GENERATION GROUP

DWG. NO. 247118E REV. 0

C-6

℄ TRUSS EL 461'-0"
℄ OUT HDR EL 458'-3½"
℄ SUPPLY HDR EL 451'-6½"
℄ INLET HDR EL 438'-6"
℄ INLET HDR EL 432'-6"
2'-8½"
6'-9"
13'-0½"
6'-0"
4 TYP
3 T
SECT E-E
(LOOKING SOUTH)
℄ TRUSS EL 461'-0"
2'-8½"
6'-9"
CONSTANT LOAD HGR
BUCKER (TYP)
2 WALL SUPPTS PER PANEL
FACE OF TRUSS VERICAL POST
5'-6"
SECT F-F
4'-9⅛"
4'-3⅛"
12"
18"
13½" (TYP)
BUCKER (TYP AS SHOWN)
VALVE HANDWHEEL (TYP)
3'-9⅛"
20°
10°
30°
℄ GENERATOR
48'-11" ℄ TO ℄ BLR WALLS
4'-6⅛" TO WP OF HDR (TYPICAL)
18 SECTS @ 20° = 360°
3"
PLAN SECT D-D
(SUPPLY HDR & INLET HDR)
10° (TYP EXCEPT AS SHOWN)
VIEW-A
(BOILER INLET, OUTLET HEADER END SLIT DETAIL)
FIELD WELD
D TYP AS SHOWN INLET & OUTLET HDR ONLY
C-7
8'-7¼" BETWEEN W.P'S
34 SPS @ 3" = 8'-6"
35-⅞" OD TUBES
8'-7½" BETWEEN W.P'S
33 SPS @ 3" = 8'-3"
34-⅞" OD TUBES
2¼"
¾"
(1-12) VIEW-A
4'-6⅛" TO WP OF HDR (TYP)
15"
8'-7½" BETWEEN W.P'S SHIPPING PANEL (TYP)
68 SPS @ 1½" = 8'-6 69 ⅞" OD TUBES (TYP EXCEPT AS SHOWN)
2'-10¾" (TYP)
SUPPORT HDR FROM CORBEL (TYP)
BUCKER (TYP AS SHOWN)
PLAN SECT C-C
FACE OF CORBEL
℄ TRUSS EL 439'-0"
℄ TRUSS EL 461'-0
℄ OUT HDR EL 458'-3½"
℄ SUPPLY HDR EL 451'-6½"
℄ INLET HDR EL 438'-6"
℄ INLET HDR EL 432'-6"
25'-9½"
13'-0½"
6'-0"
4 (TYP)
SIDE VIEW
(LOOKING WEST)
NOTE
1. FOR GENERAL ARRG'T OF SOLAR STEAM GENERATOR SEE DWG 1558J
2. FOR SYMBOL NOMENCLATURE CHART SEE DWG 1558J
The Babcock & Wilcox Company
Power Generation Group
DWN J DOWDELL
CHK'D L KOZSZ
591-0199
LAYOUT OF BOILER FOR SOLAR STEAM GENERATOR
SCALE ⅜" = 12"
1567J
0
Revisions
REV NO
DESCRIPTION
DATE
APPROVAL
1567J


VIEW-D
SCALE 3/4"=12"
EL 458'-9"
5 1/4 (TYP)
12 TYP
2 1/4 PRE-SET
TRUSS EL. 461'-0"
15"
3'-11 1/2"
3'-6"
4'-5 1/2"
5'-3"
5'-3"
2'-7"
℄ BUCKERS
EL. 485'-0"
FACE OF TRUSS VERTICAL POST
TRUSS EL. 491'-0"
SECONDARY SUPERHEATER OUT. CONN.
10" (TYP.)
℄ CORBEL
℄ GENERATOR
18-SECTS. @ 20° = 360°
48'-11" ℄ TO ℄ TUBES
30°
20°
FACE OF CORBEL
SUPPORT HDRS FROM CORBEL (TYP)
4'-0" (TYP)
SECTION A-A
VIEW-E (TYP)
SCALE 1/2"=12"
* THESE DIMENSIONS SUBJECT TO CHANGE PENDING FINAL SH FLEXIBILITY ANALYSIS
1568J
TOP
BOTTOM
SUPPORT HDRS FRONT CORBEL (TYP)
SEE VIEW E
VARIABLE SPRING SUPPORT
BUCKER (TYP)
6" DESUPERHEATER VALVE
1 1/2"-2500# FLG CONN FOR SPRAY WATER EL 461'-0 3/16"
SECTION B-B
SEE VIEW D
℄ TRUSS EL. 491'-0"
VARIABLE SPRING SUPPT (TYP)
CONSTANT SPRING SUPPT (TYP)
D FOR HDS MK 8 10
14 16 AT SH SPLITS (TYP)
EL. 485'-0"
15'-8" SECONDARY SUPERHEATER 1" O.D. TUBES
10'-5" PRIMARY SUPERHEATER 1" O.D. TUBES
30'-0"
6'-0"
℄ TRUSS EL. 461'-0"
EL. 458'-9"
(SEE DWG. 1567J)
SIDE VIEW
(LOOKING WEST)
NOTE:
1. FOR GENERAL ARRGT OF SOLAR STEAM GENERATOR SEE DWG 1558J.
2. FOR SYMBOL NOMENCLATURE CHART SEE DWG 1558J.
The Babcock & Wilcox Company
Power Generation Group
LAYOUT SUPERHEATER FOR SOLAR STEAM GENERATOR
591-0199
DRN. B. SHEA
CHK'D L. KOSER
SCALE 3/4"=12"
DWG NO 1568 J
REV NO 0
Revisions
DESCRIPTION
DATE
APPROVAL
C-8

C-9

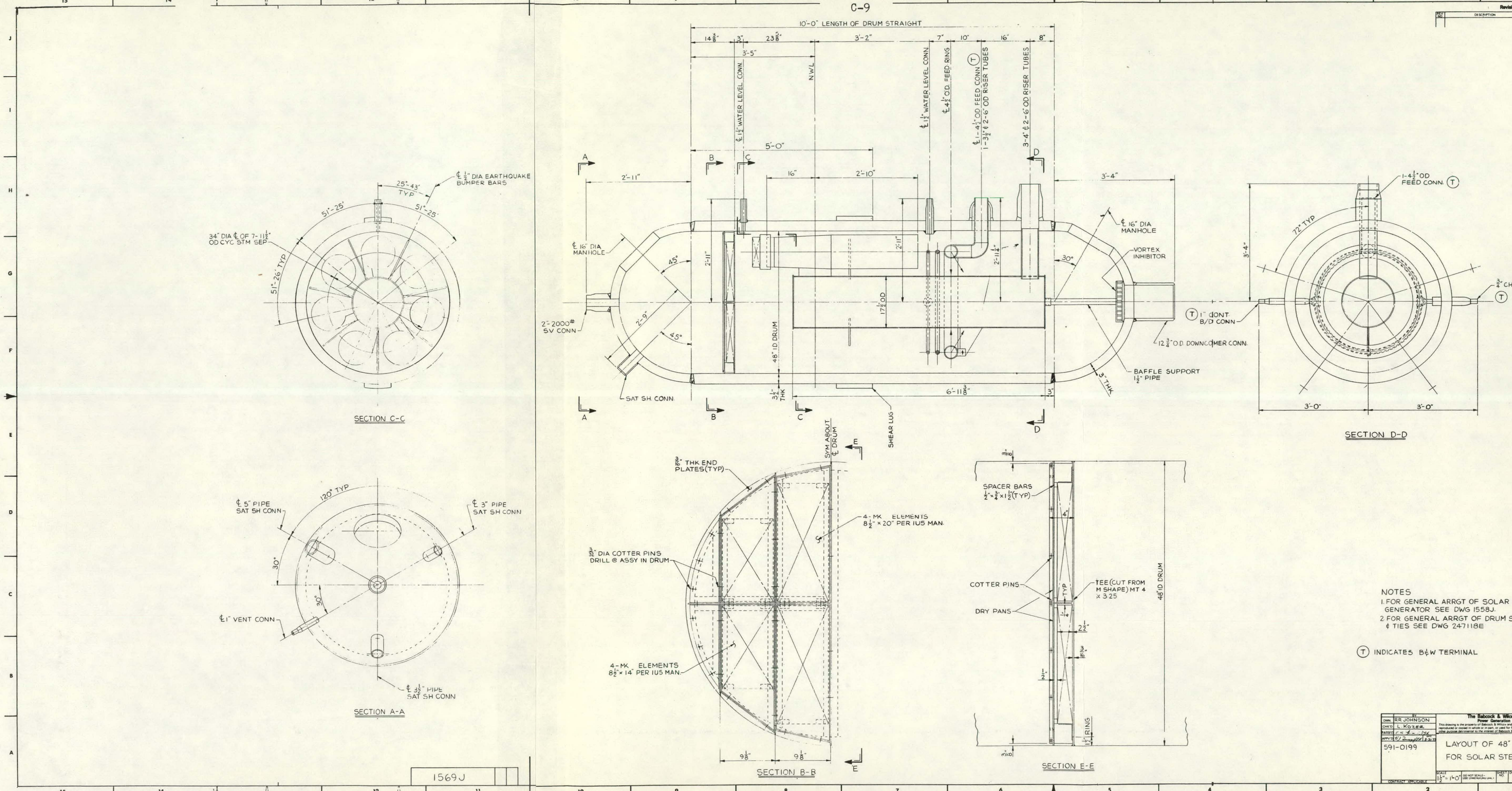

NOTES
1. FOR GENERAL ARRGT OF SOLAR STEAM GENERATOR SEE DWG 1558J.
2. FOR GENERAL ARRGT OF DRUM SUPPORTS & TIES SEE DWG 247118E

(T) INDICATES B&W TERMINAL

The Babcock & Wilcox Company
Power Generation Group

DRN RR JOHNSON
CHK'D L. KOZER

591-0199

LAYOUT OF 48" ID DRUM
FOR SOLAR STEAM GENERATOR

SCALE 1½" = 1'-0"
DWG. NO. 1569J

1569J

APPENDIX D

HEAT BALANCE

Heat Balance

The analysis consists of overall heat and mass balances of the steam generator and the four major components: boiler,* first stage superheater, attemperator, and the second state superheater. Figure D-1 is a flow schematic of the solar steam generator used for the overall heat and mass balance calculations.

The following assumptions are made:

1. The heat input to the steam generator is the energy absorbed by the steam and water. Heat loss corrections are already applied. The energy balance does not include the heat input by the boiler recirculating pump.

2. The blowdown from the drum is zero.

3. The steam-water separation process is 100% effective.

4. The superheated steam and water mixing at the exit of the attemperator is 100% effective.

Flow Balances - Assume steady state conditions.

$$W_S = W_{FW} + W_{ATT}$$

Implied Flow Balances

1. The saturated steam flow out of the drum is equal to the feedwater flow.

2. The superheated steam flow at the exit of the first stage superheater is equal to the saturated steam flow from the drum and, therefore, is equal to the feedwater flow.

Heat Balances - The following heat balance equations are used to calculate flow:

a. The feedwater flow is found by a heat balance on the boiler section.

$$W_{FW} = \frac{Q_B}{h_g - h_{FW}}$$

b. The attemperator flow is found by a heat balance on both the primary and secondary superheater.

*Note that the boiler section as defined in this analysis includes a complete control volume about the heat transfer surface, drum, recirculating pump, etc.

$$W_{ATT} = \frac{(Q_{S1} + Q_{S2}) - W_{FW}\,(h_{S2O} - h_g)}{h_{S2O} - h_{ATT}}$$

If $W_{ATT} < 0.0$, the outlet enthalpy of the second stage superheater is calculated as follows:

If $W_{ATT} < 0.0$; W_{ATT} is set equal to zero

$$h_{S2O} = h_{SS} + \frac{Q_{S1} + Q_{S2}}{W_{FW}}$$

Additional heat balances are made for calculation of enthalpy and temperature at the superheater inlet and outlet stages. These are as follows:

a. Primary superheater outlet temperature

$$h_{S1O} = H_g + Q_{S1}/W_{FW}$$

$$T_{S1O} = f\,(P_{S1O}, h_{S1O})$$

b. Attemperator exit temperature (inlet to the secondary superheater):

$$h_{S2I} = \frac{W_{FW}\,h_{S1O} + W_{ATT}\,h_{ATT}}{W_{FW} + W_{ATT}}$$

$$T_{S2I} = f\,(P_{S2I}, h_{S2I})$$

Future Development

This subsection lists certain areas where future development would increase the performance and/or reliability of the Pilot Plant steam generator:

1. Three dimensional absorption rate data should be generated corresponding to the final turbine heat balance. Final conduction losses, convection losses and reradiation losses should be factored into the incident flux requirements. Absorbed heat flux data corresponding to the early part of hot and cold startup should be generated.

2. The boiler/superheater and primary/secondary superheater interfaces should be refined based on the updated heat flux and turbine heat balance data.

3. The boiler circuit flow balancing calculations should be refined with the objective of reducing total boiler flow requirements. Flow balancing should be checked at additional solar times such as 3/21/7 AM, 6/21/12 PM and 12/21/2 PM.

4. After the flow balancing calculations are refined, the possibility of relocating the recirculating pumps within the steam generator housing next to the boiler supply header should be investigated. This change would significantly reduce pumping power requirements and piping costs. The possibility of eliminating the pumps altogether should also be studied.

5. The superheater circuit flow balancing calculations should also be refined to further reduce temperature differences among the superheater flow paths. In the secondary superheater, for example, steam and metal temperature reductions on the order of 19°C (30°F) are possible. Flow balancing should also be checked at additional solar times.

6. The peak mean metal temperature calculations should be refined by using local absorption rates at each point in the circuit rather than the maximum rate at a given cavity height. This refinement could lower calculated peak metal temperatures on the order of 10 - 15°C (16 - 24°F).

7. The use of thicker insulation to reduce heat loss should be studied.

8. The cooldown rate calculations should be refined by including the heat capacity of the insulation, the ceiling, the cavity closure and a certain fraction of the pressure part support equipment.

9. Thermal radiation data on steam generator materials presently being obtained at the University of Arizona (and elsewhere) should be factored into the design.

10. Additional stress analyses of the superheater should be carried out. Areas requiring inelastic analysis to evaluate creep-fatigue damage should be identified. A simplified inelastic analysis should be carried out to determine if the secondary stresses in the Croloy 2-1/4 relax out and do not reappear during subsequent cycles. If Croloy 2-1/4 is found to be unacceptable for the highest temperature sections of the superheater, alternate materials should be studied.

11. A simplified dynamic analysis of the steam generator should be carried out to identify components where the natural frequency is within the range where significant amplification of ground level accelerations could occur. If any such areas exist, the potential damage should be assessed and means of increasing the natural frequency should be studied if the damage is unacceptable.

12. The transient stress analysis should be refined by considering nozzles and support locations subjected to higher stresses than the areas studied during the preliminary design.

13. The transient model of the steam generator should be refined based on the SRE test results and applied to the prediction of the response of the Pilot Plant steam generator.

4. The SRE boiler and superheater metal temperature measurements should be analysed to determine if local absorption rates can be accurately inferred from the data.

Several other areas are worth investigating on a more general basis:

1. The adaptability of the Pilot Plant steam generator design to other cavity geometries should be studied.

2. Alternate materials for the high temperature regions of the superheater should be studied using inelastic analysis to evaluate creep-fatigue damage.

3. Smaller superheater tube sizes (and additional parallel flow paths if required to maintain superheater pressure drop within acceptable limits) should be investigated as a means of reducing thermal stress.

4. Local radiation heat transfer to individual superheater tubes should be studied analytically and experimentally to verify the circumferential heat flux distribution assumed for the preliminary design.

5. The effect of nonuniform circumferential heat flux on the local steam side heat transfer coefficient should be verified with experimental data.

6. Convection losses from cavities should be measured using scale models.

7. A preliminary design of the steam generator for the commercial plant should be conducted to verify the applicability of the scaling factors used to extrapolate from the Pilot Plant Design.

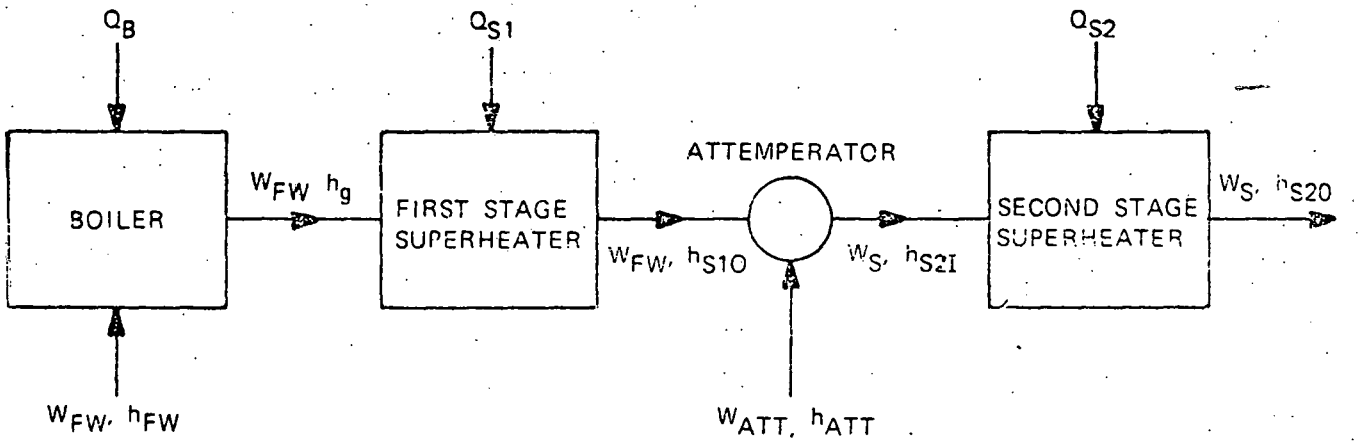

Figure D-1. Solar Steam Generator Flow Diagram for Heat and Mass Balances

ERDA 10 MWe SOLAR PILOT PLANT

RECEIVER CAVITY CLOSURE

SUMMARY

The results of a study to develop a preliminary design for sealing the receiver cavity during the diurnal periods of plant shutdown are reported. The purpose of the cavity closure is to reduce cyclic thermal stressing of the receiver steam generator and to shorten plant startup. The concepts considered include two types of externally mounted aperture doors and an internal cavity barrier. The results indicate that the internal cavity barrier design is the most practical and effective. The details of the preliminary design of the cavity barrier and its auxiliary equipment are presented in the report.

1.0 INTRODUCTION

During normal operation, the metal temperatures in the receiver cavity vary from about 1,250 F at the cavity ceiling to about 600 F at the bottom of the boiler water walls. Without provisions to retain thermal energy in the receiver cavity during the diurnal shutdown periods, the metal temperatures may approach the outside ambient temperature. With provisions to retain energy in the receiver cavity during diurnal shutdown, the metal temperatures can be kept above ∿350 F.

It is therefore desirable to thermally isolate the receiver cavity from ambient conditions during diurnal shutdown. Such isolation will reduce the time required to bring the unit back to rated pressure and temperature, and will minimize the cyclic thermal stresses imposed on the receiver components.

Two approaches are considered for isolating or closing the receiver cavity: external aperture doors and an internal cavity barrier. These approaches are shown in Figure 1. Aperture doors may be supported from either the receiver outer housing or the receiver support tower at a location below the aperture.

This report presents the analysis performed in developing a preliminary design for cavity isolation or closure. The alternative concepts are evaluated against a set of design criteria, the results are presented, and the significant aspects of the selected concept for cavity closure are discussed. Design sketches are also provided.

2.0 EVALUATION OF APPROACHES

The receiver cavity isolation concepts are evaluated against the following three criteria.

(1) Capability to achieve cavity closure.

(2) Environmental considerations.

(3) General design considerations.

2.1 CAPABILITY TO ACHIEVE CAVITY CLOSURE

Both the aperture door and the internal cavity barrier approaches can achieve closure of the receiver cavity. Clearances to accommodate thermal movement and to allow for mechanical misalignment between adjacent parts and the receiver cavity are included in both approaches. Clearances required for proper aperture door operation are smaller than for the cavity barrier approach because the aperture doors are subjected to a lower variation in temperature. However, the total seal length for the aperture door approach is three to four times that for the internal cavity

barrier. The clearance allowed for the barrier can therefore be three to four times greater than for the aperture doors and still achieve the same degree of sealing.

Cavity closure with aperture doors supported from the receiver housing requires opening and closing of wedge shaped door units with hydraulic mechanisms (Figure 1). The different motions required to close these aperture doors include:

(1) Lowering the doors from their stowed (open) position to a "pivot point."

(2) Rotating the doors around their pivot points to their closed position over the cavity aperture.

These linear and rotational motions require at least two hydraulic cylinders per door panel.

The closing of aperture doors mounted on the receiver support tower involves only a rotational motion and requires the doors to rotate approximately 165 degrees around a "pivot point." This rotational motion requires at least one hydraulic cylinder per door panel.

Cavity closure by an internal cavity barrier involves the simple linear motion of a single circular disc by hoisting mechanisms which raise and lower the barrier from its closed and stowed positions. Figure 2 shows the barrier in its stowed and in its closed positions.

Of the two approaches to cavity closure, the internal cavity barrier can achieve aperture closure in the least time. Hoisting speeds normally associated with weights similar to that of the cavity barrier are in the range of 7 to 15 feet per minute. Assuming the distance between the

open and closed positions is about 50 feet, the time required to move the barrier through this distance would be between 3-1/2 to 7 minutes.

The time required to open or close the aperture doors depends on the capacity of the hydraulic oil supply unit. It is estimated that to move all of the aperture doors at the same time, a hydraulic oil unit would have to supply in excess of 300 gallons of oil (low pressure hydraulic system). Considering 20 gpm as a reasonable maximum for a low pressure and a low pump speed hydraulic oil supply unit, about 15 minutes would be required to complete the motion. Three 20 gpm hydraulic oil supply units would be necessary to open or close the doors in approximately the same time as the cavity barrier.

2.2 ENVIRONMENTAL CONSIDERATIONS

Major environmental considerations affecting the aperture door and/or the cavity barrier designs include temperature effects and wind forces.

During normal operation the temperatures in the upper portion of the receiver cavity approach 1,250 F. When solar energy is diverted, the cavity temperatures drop quickly to about 620 F, the saturation temperature corresponding to the steam drum pressure.

These relatively high cavity temperatures have little effect on the external aperture door design. Only when the aperture doors are closed, sealing the cavity, is temperature a consideration. Since the doors are insulated on the side exposed to the high temperature, and the door structure is cooled by ambient air, the effect is minimal. Further, the aperture door opening/closing mechanisms are well insulated from cavity temperature and not affected by it.

Cavity temperature is a major consideration in the internal barrier design. The barrier structure is subjected to relatively high temperatures in both the stowed and the closed positions. Four areas particularly affected by the high temperatures are the barrier structure, barrier suspension, cavity barrier clearance allocation, and barrier guides (if required).

Because the barrier structure (carbon steel) strength decreases rapidly with temperatures greater than approximately 600 F, a means to limit the exposure of the barrier structure to that temperature must be provided. When the solar energy is diverted from the receiver, the cavity temperature rapidly decreases to about 620 F. Hence, in the closed position the barrier temperature limit criterion is satisfied. In the stowed position, the barrier structure is protected from high receiver temperatures by thermal insulation and by a forced air cooling system, illustrated in Figure 3. The forced air cooling system maintains the space between the cavity barrier and the permanent ceiling at an acceptable temperature during normal operation of the plant.

The maximum temperature to which the barrier suspension may be subjected is also limited. Wire rope is normally limited to temperatures less than 300 F, and alloy chain is limited to a practical maximum temperature of 900 F, the approximate temperature at which the chain is tempered.* Roller chain temperature limits are based on the capabilities

---

*Alloy chain must be removed from service (by federal regulation) if it is heated to 1,000 F or above.

of their lubricants. Deflocculated collodial graphite is a suitable roller chain lubricant for temperatures in the 500 F to 600 F range.

Any suspension used for raising and lowering the cavity barrier must be frequently inspected as required by, or to meet the intent of, the Occupational Safety and Health Act. Federal regulation specifically addresses wire rope and alloy chain suspension. The frequency of the inspections are based on the application of the suspension. Inspections must include examination for wear, deformation, increase in length, high temperature effects, and so forth. Where defects or deterioration are evident, the suspension must be removed from service immediately. Roller chain, while apparently not specifically addressed as a suspension in federal regulations, should be assumed subject to the same requirements set forth for alloy chain.

Cavity barrier hoisting equipment, located above the cavity permanent ceiling, can be effectively insulated from the high cavity temperatures and not affected by it.

The wind loading on the aperture doors and the cavity barrier is also an important consideration. Design wind speeds at the elevation of the receiver cavity may exceed 125 miles per hour. Because of the arrangement, configuration, and type of movement required, the wind has a greater loading effect on the aperture doors than on the internal cavity barrier.

Wind on the cavity barrier primarily induces lateral movement. Barrier suspension loads due to the wind forces are therefore relatively small and can be accounted for in suspension design.

The effect of wind on the aperture doors is more significant and affects door design, support, and operating mechanisms. To assure door stability during movement, the door shape must be aerodynamically designed. Further, the aperture door supports and operating mechanisms must be designed to accommodate high wind loads that may be imposed on the doors as they move to open or close the cavity.

2.3 GENERAL DESIGN CONSIDERATIONS

General design considerations include the problems of securing the cavity closure device in its open and closed positions, controlling the position of the device during its motion, and designing a simple, yet dependable, actuation system.

It is desirable that the receiver cavity closure device be secured in both the open and closed position to protect it and the receiver from damage by movement induced by wind and/or seismic forces. The external aperture doors supported from the receiver are difficult to secure because of their arrangement and their motion when either opening or closing. Both the external aperture doors supported from the receiver tower and the internal cavity barrier are more easily secured because of their simpler arrangement and motion.

The vertical motion of the cavity barrier is controlled by a hoisting mechanism designed to maintain the barrier in a level state during its movement. The barrier's lateral movement is limited by the clearance between the heat transfer surface and the barrier. Flexible "guides" mounted on the barrier can be used to reduce the impact of the barrier against the heat transfer surface. In contrast, control during motion

of either cavity door design is more complex and must be capable of withstanding wind forces.

The operating mechanisms for the interior cavity barrier approach are therefore conceptually simpler than those required for external aperture doors. The cavity barrier can be raised and lowered using a single hoist motor, gear, brake assembly. Sprockets, idler shafts, and other components used to manipulate the barrier suspension are straightforward and simple in arrangement.

The external aperture doors require a relatively complex operating mechanism due to the large number of components required and the complex movement of the doors from their stowed to their closed position. Each door requires at least one or two hydraulic cylinders to effect the required motion. Several hydraulic oil supply units are required to supply fluid to the hydraulic cylinders if rapid closure is necessary. Further, equipment maintenance is considerably greater than with the cavity barrier design because of the number of components involved and because of the special attention required for equipment accessibility.

3.0 RESULTS

These considerations indicate that both the aperture door approach and the cavity barrier approach have functional drawbacks. Complex motion and high wind forces are the major design problems for the aperture doors; high temperature is the major consideration for the cavity barrier.

Preliminary design calculations indicate that aperture doors of conventional design and structure would be unstable when subjected to winds in excess of 125 mph because of their shape and movement. Aerodynamic

aperture door design would reduce the effect of high winds, but would likely prejudice "tight" cavity closure. Also, aerodynamic aperture door design would most probably require extensive wind tunnel testing. Accommodating high wind speeds with the external aperture door approach is therefore considered impractical.

The high temperatures which are encountered in the cavity barrier approach can be accommodated in the design of the barrier and its suspension. In the stowed (open) position, the cavity barrier is subjected to temperatures around 1,250 F. To protect the barrier structure (Figure 4) and suspension (Figure 5) from these high temperatures, the barrier is insulated and fitted to the permanent cavity ceiling as shown in Figure 6. When the barrier is in the stowed (open) position, forced cooling of the area above the cavity barrier is provided (Figure 3) to maintain the temperature in the area above the barrier to approximately 600 F. When the barrier is in the closed or lowered position, cavity temperatures are expected to be within acceptable limits for both alloy and roller chain suspensions. The cavity barrier hoisting equipment which is located above the receiver cavity permanent ceiling is effectively isolated from the high cavity temperatures.

To improve cavity closure when the barrier is in the closed position, a perimeter seal is provided as illustrated in Figure 7. The seal consists of a seal ring attached to the receiver outer housing and a seal ring attached to the cavity barrier. The seal ring attached to the receiver outer housing is set to minimize the shadowing of the receiver energy absorbing surfaces. The cavity barrier seal ring follows the

elevation of the boiler section inlet header. Seal ring contact surfaces are an asbestos fabric tube which is filled with bulk high-temperature thermal insulation material. Outside edges of the cavity barrier are covered with suitable guide pads to minimize the effect of contact between the aperture barrier and receiver heat transfer surface.

It is necessary to hold the barrier horizontal when it is moving up and down in the receiver cavity to avoid binding or edge contact between the barrier and the receiver. Roller chain is selected for barrier suspension in order to meet this requirement. The link design of roller chain and the use of sprockets to manipulate the chain offer the capability to mechanically establish the barrier position. With the sprockets properly aligned, a single revolution must raise all suspension members equally. Also, since all moving and contracting parts of the roller chain are lubricated, wear should be relatively small, resulting in a longer service life than alloy chain.

As previously mentioned, hoisting suspensions are subject to inspection through federal regulations. While roller chain is not specifically addressed in the federal regulations for hoisting suspensions, it is assumed to be subject to the same inspections and considerations of alloy chains.

The cavity barrier arrangement and type of suspension requires that the receiver heat transfer surfaces and tube segments be protected from damage due to contact with the barrier. The use of internally mounted guides to prevent the cavity barrier from contacting receiver tube segments presents special problems. Considerable thermal expansion of

the guide tubes must be accommodated by the guide supports and anchors. Conversely, the guide must be sufficiently rigid to protect the receiver tube segments. Also, unless the guide tubes are made an integral part of the receiver steam generator, the cooling they require reduces the receiver efficiency. Since the major concern is local tube damage due to gouging and/or abrasion, a simpler solution is to provide a flexible or soft skid on the outer edge of this barrier. Figure 8 shows the cavity barrier with such skids or guide pads attached for protecting the receiver tubes.

To secure the cavity barrier in its stowed and its closed positions, and hence reduce its motion due to wind and seismic loads, locking devices are provided. These devices are illustrated in Figure 9.

4.0 CONCLUSIONS

It is concluded that the internal cavity barrier with roller chain suspension represents the most satisfactory method of achieving receiver aperture closure. A single motor gear set is used to power the hoisting mechanism, and locking devices are provided to secure the cavity barrier in its open and closed positions.

To meet the intent of the Occupational Safety and Health Act, the roller chain used as the barrier suspension is to be inspected frequently for proper lubrication, chain deterioration, chain damage, and so forth. Further, until service experience is gained, the barrier hoisting mechanisms and suspension are to be inspected after each use cycle. When service experience has been established, inspections and examinations can be set on a less frequent schedule.

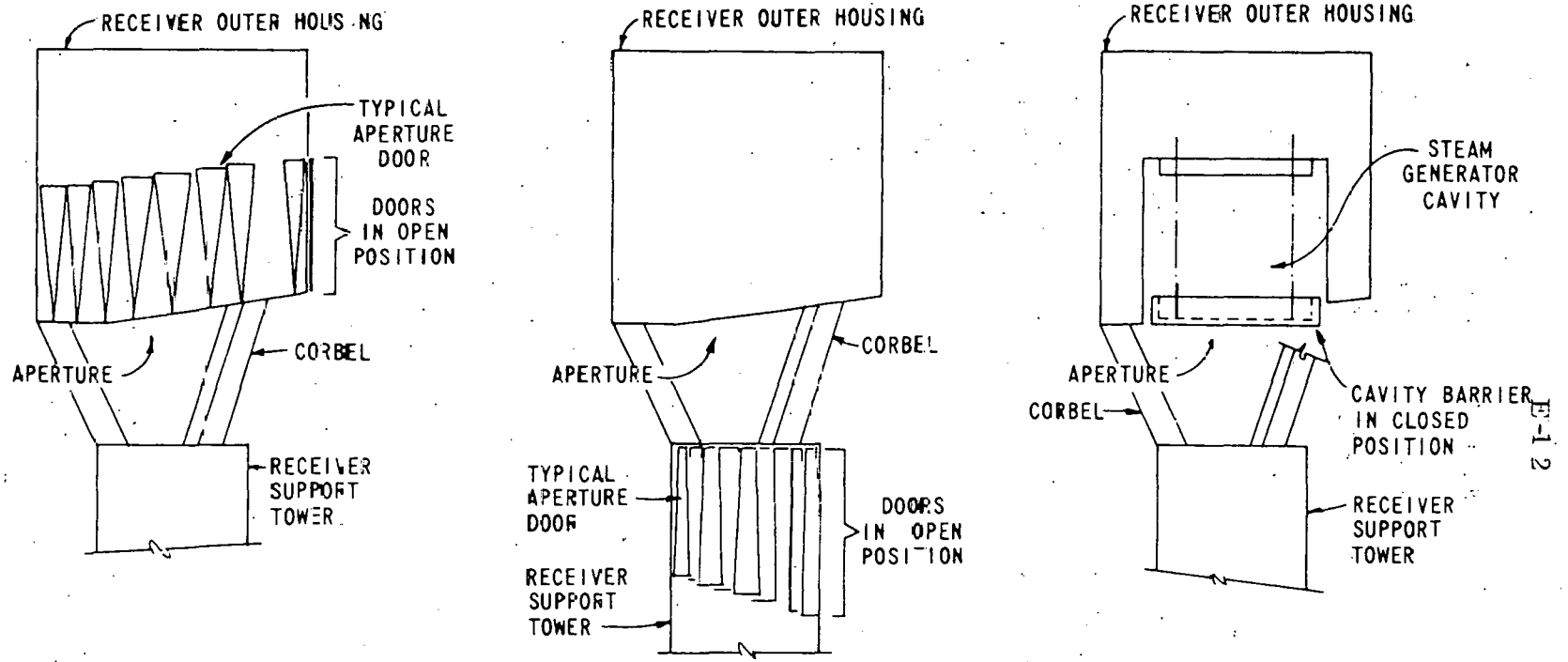

EXTERNAL APERTURE DOORS SUPPORTED FROM RECEIVER OUTER HOUSING

EXTERNAL APERTURE DOORS SUPPORTED FROM RECEIVER SUPPORT TOWER

INTERNAL CAVITY BARRIER

Figure 1. Cavity Closure Approaches

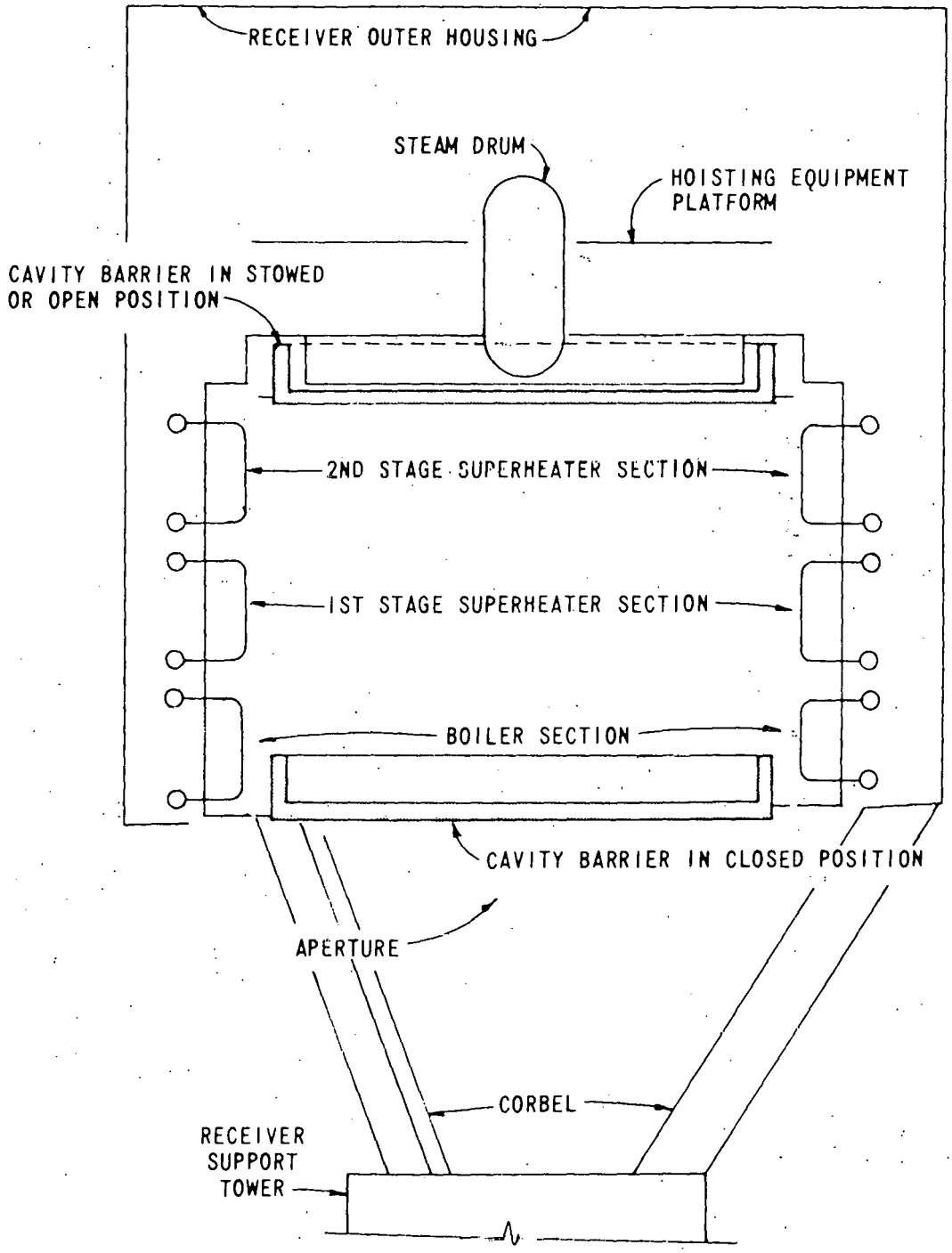

Figure 2. Cavity Barrier in Closed and Stowed (Open) Position

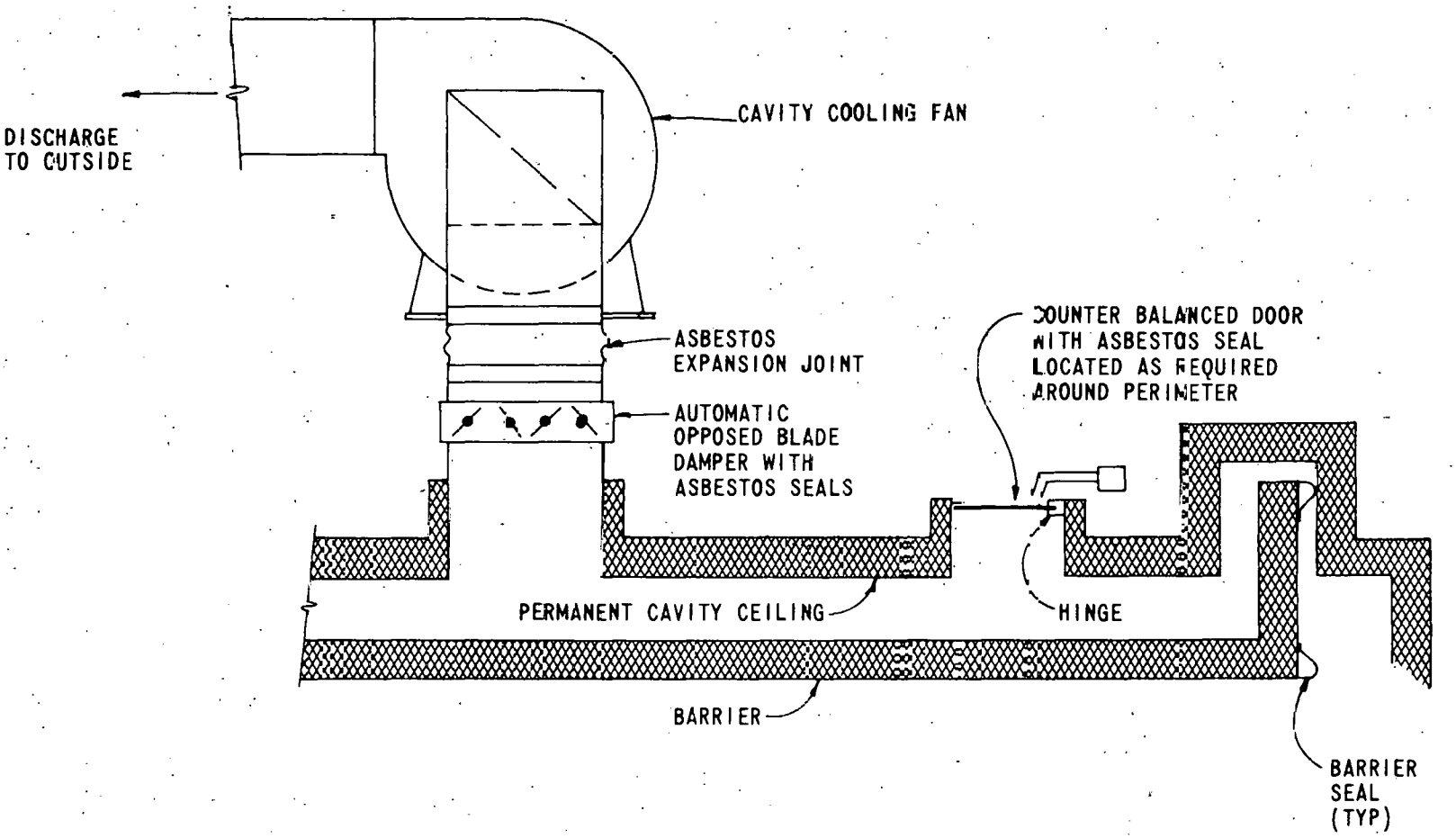

Figure 3. Upper Receiver Cavity Forced Cooling System

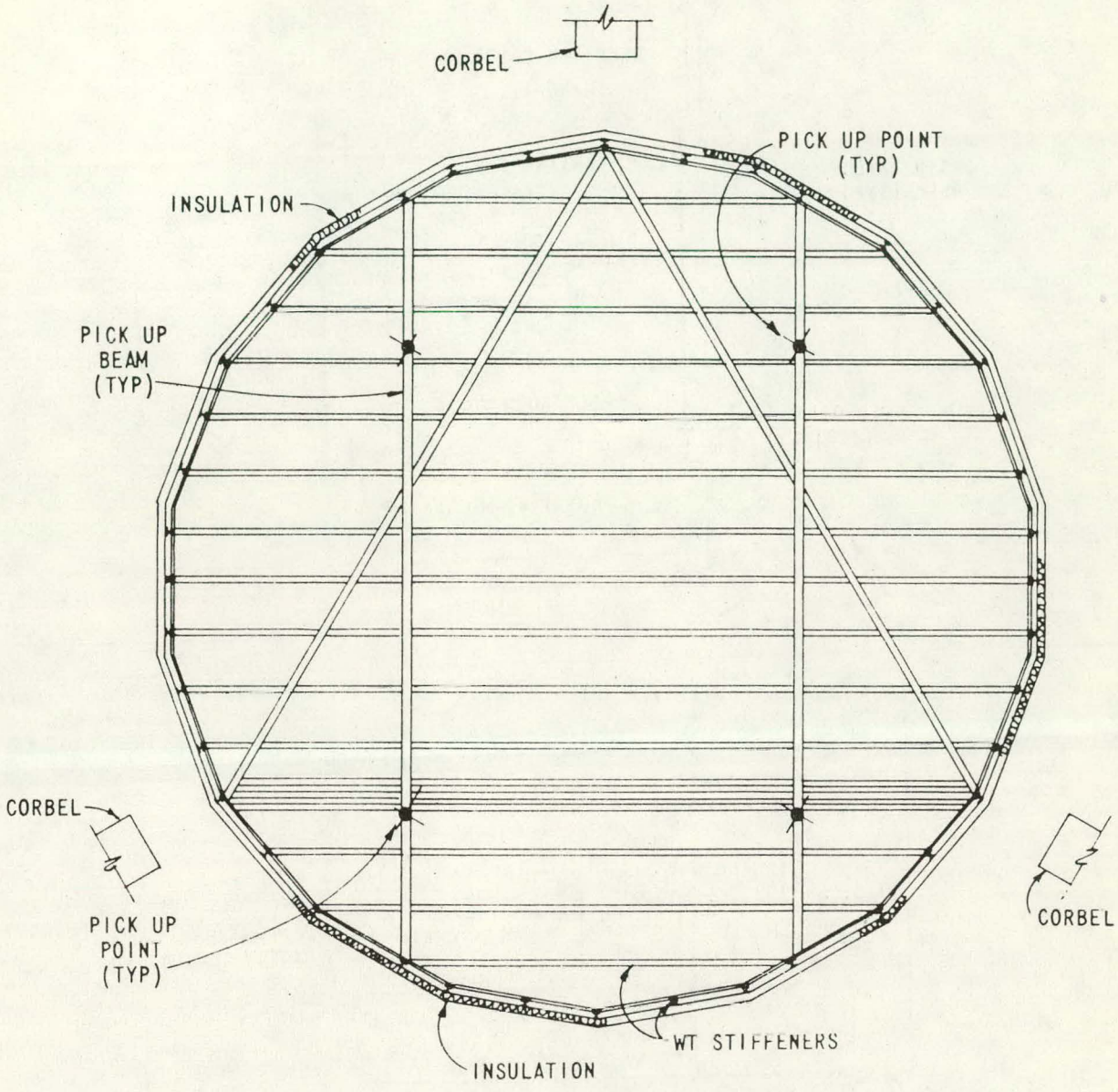

Figure 4. Cavity Barrier Structure

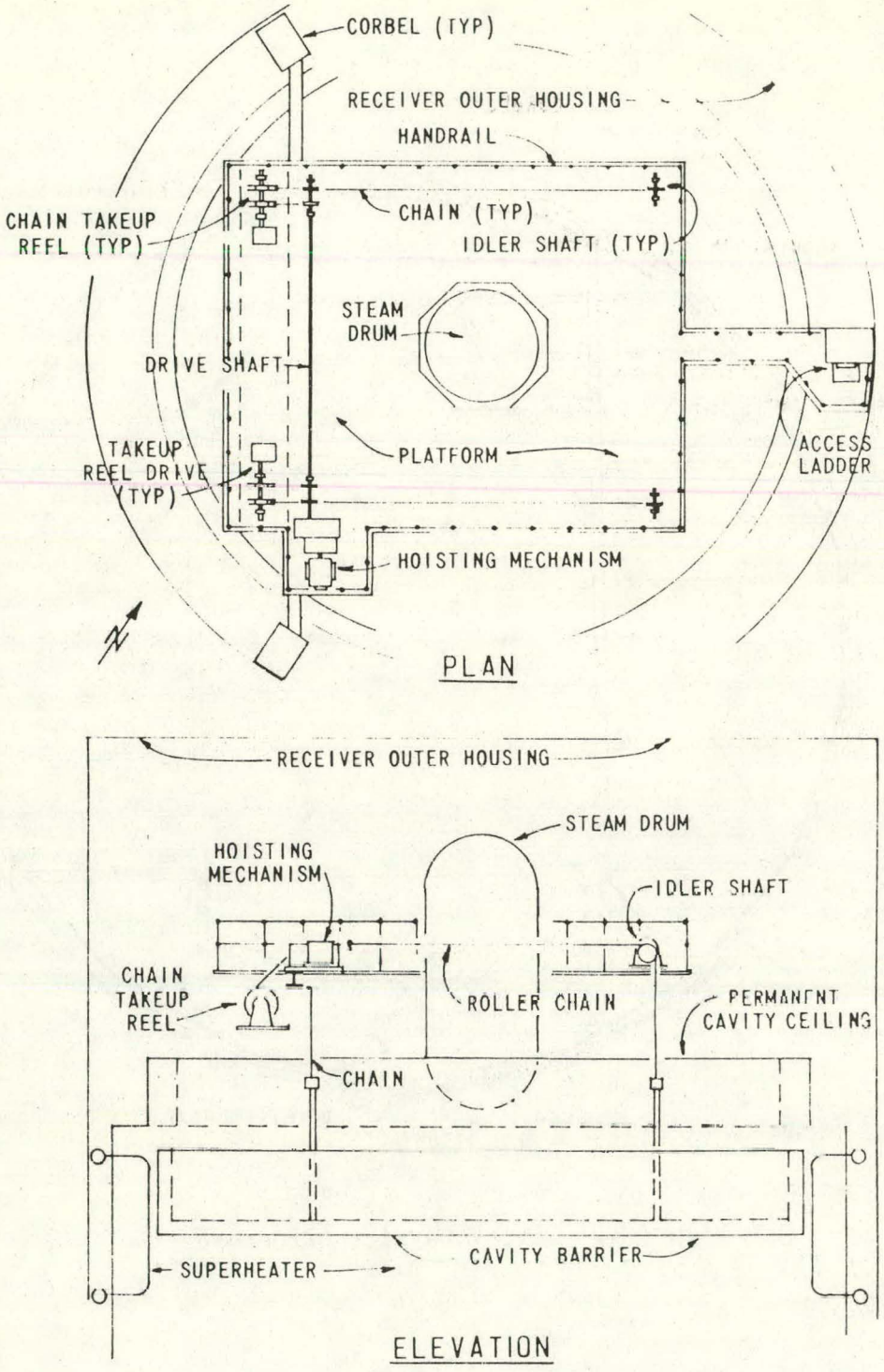

Figure 5. Cavity Barrier Suspension and Hoisting Arrangement

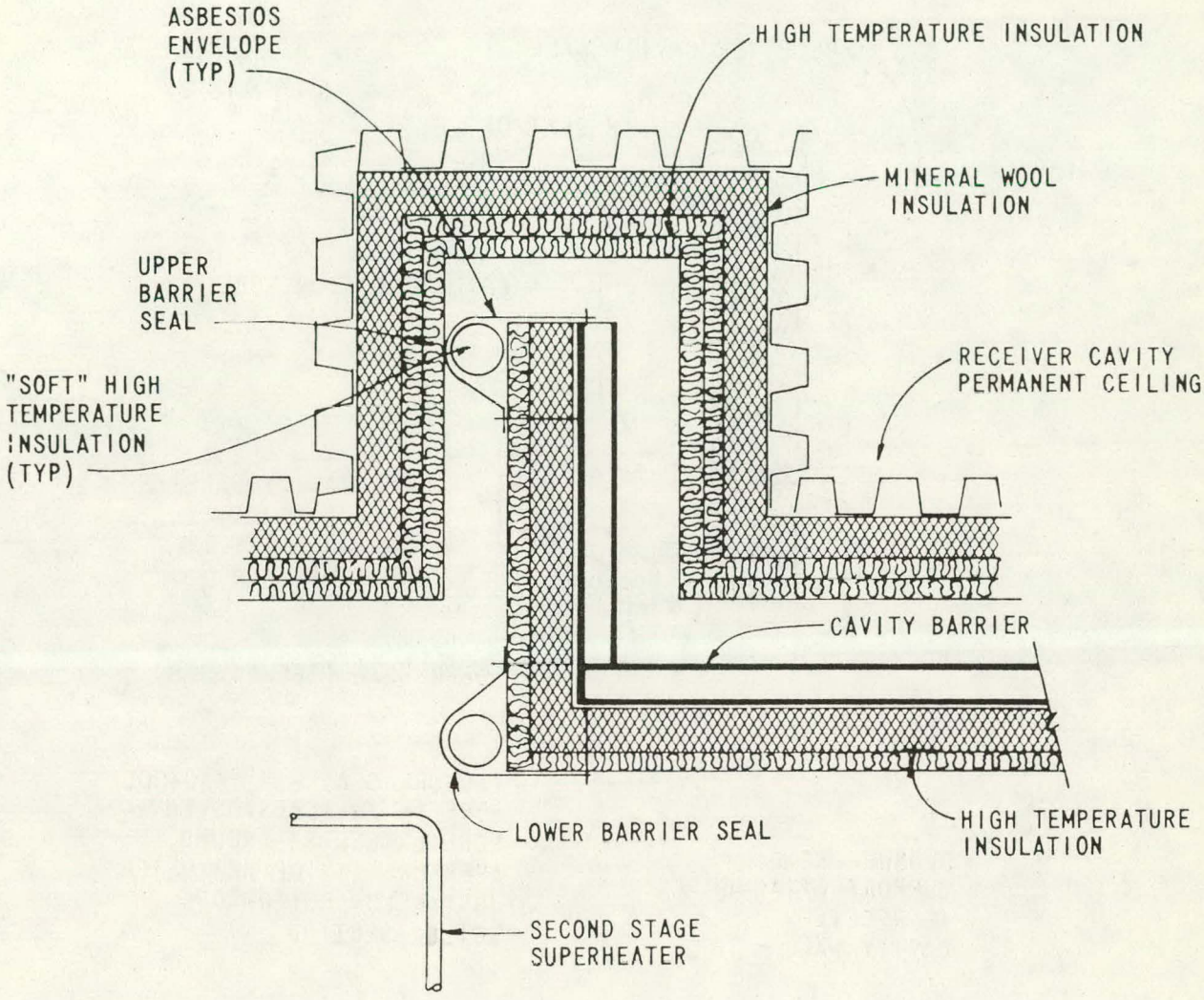

Figure 6. Cavity Barrier Seals

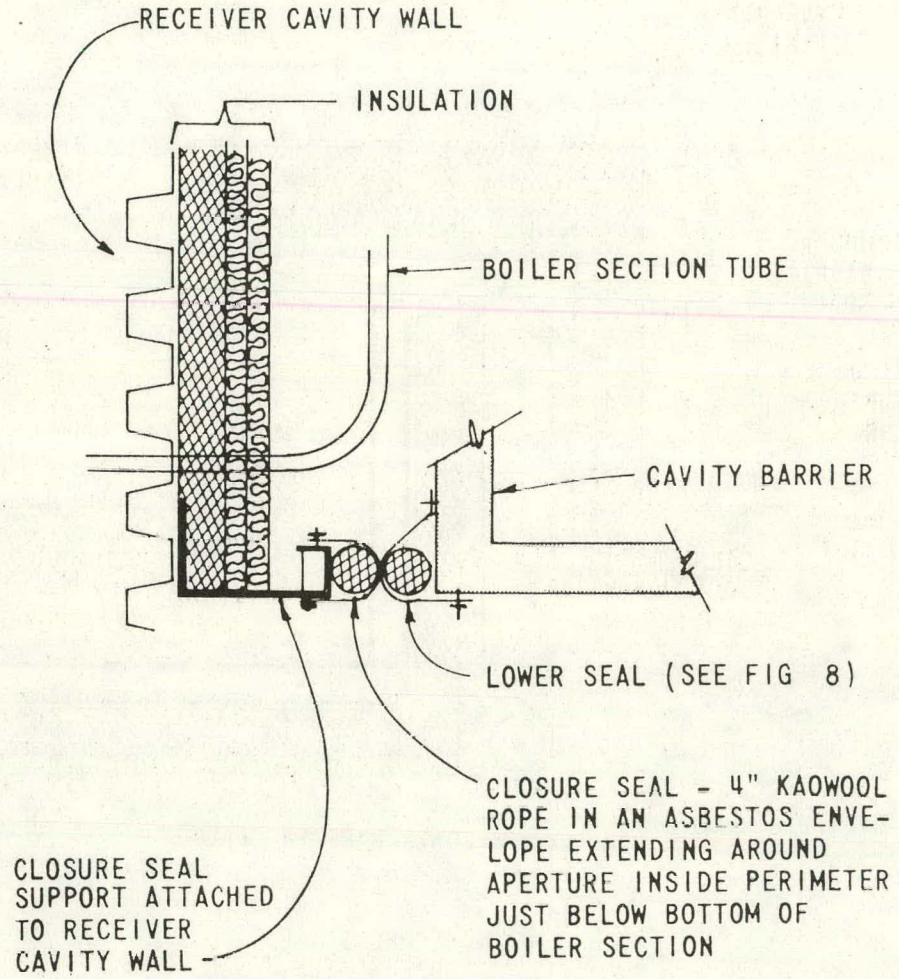

Figure 7. Receiver Cavity Aperature Seal

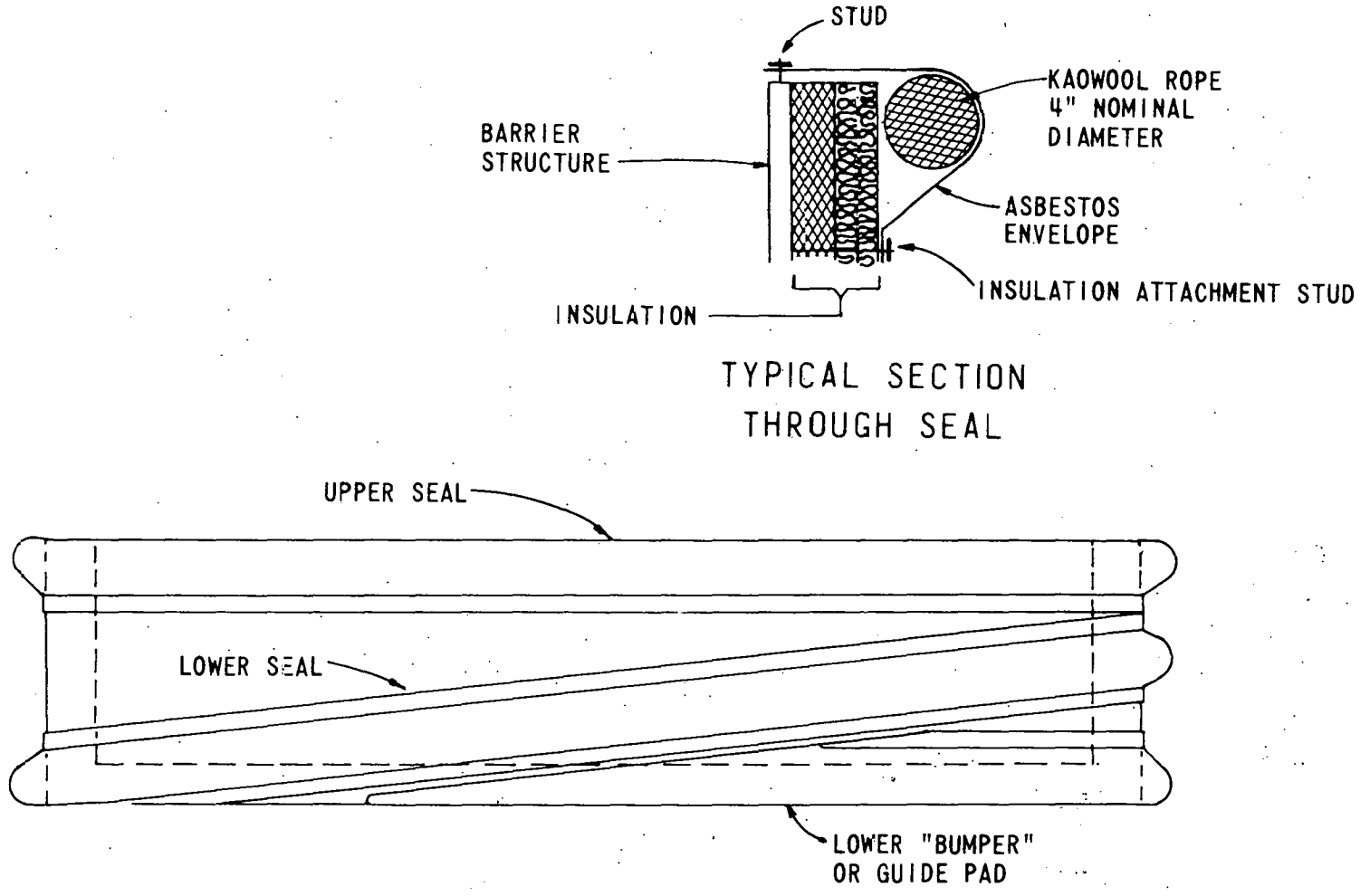

Figure 8. Cavity Barrier Seals and Guide Pad

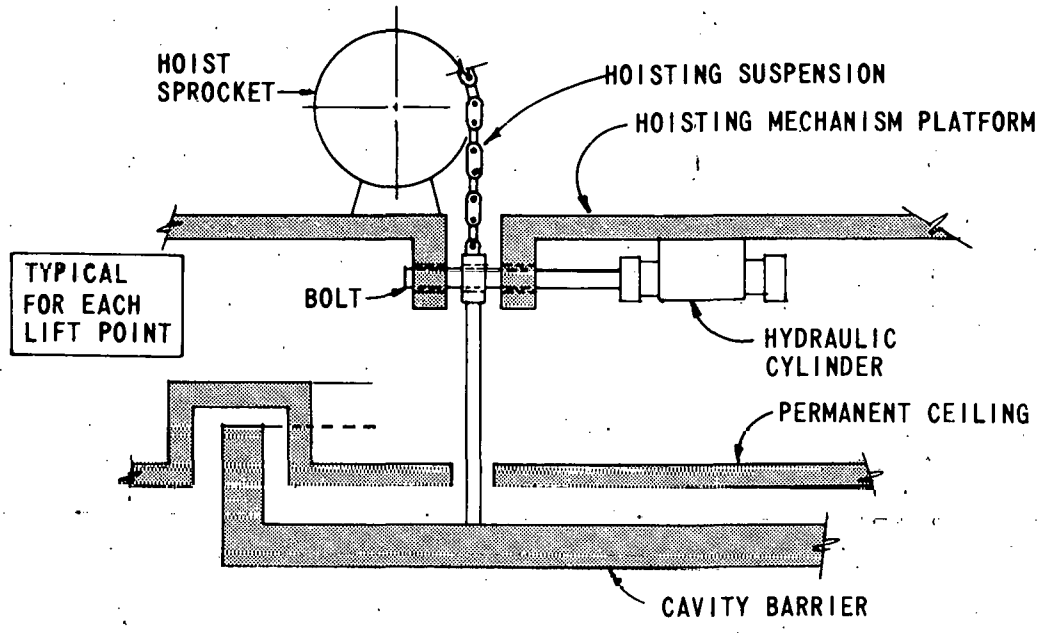

BARRIER LOCK - STOWED POSITION

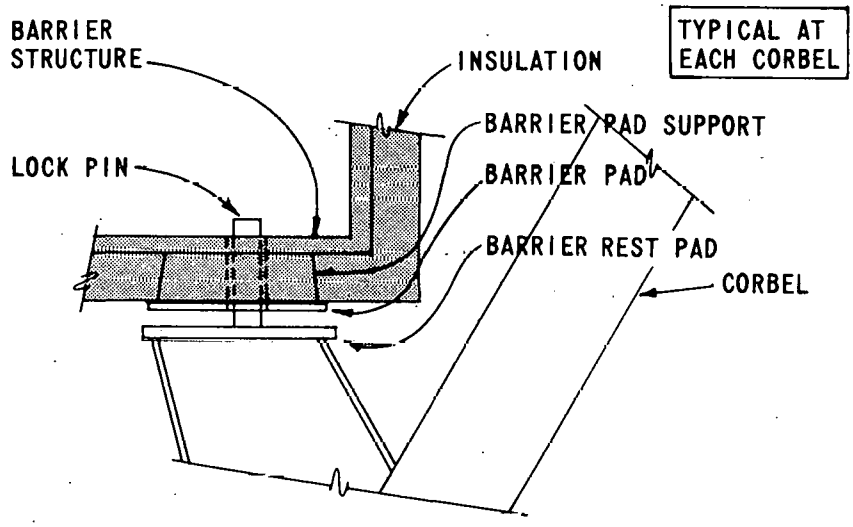

BARRIER LOCK - CLOSED POSITION

Figure 9. Cavity Barrier Locking Devices

ENERGY RESEARCH AND DEVELOPMENT ADMINISTRATION 10 MWe SOLAR PILOT PLANT

PRELIMINARY SYSTEM DESCRIPTION FOR SEISMIC ANALYSIS AND DESIGN CONSIDERATIONS

SUMMARY

For the preliminary design of the 10 MWe solar pilot plant, as well as for conceptual designs of 25 and 60 MWe commercial plants, seismic analyses have been performed to establish seismic forces on the structures, to generate equipment response spectra, and to determine how these design inputs vary with tower height.

In spite of the great height and mass of the support tower and steam generator, the seismic forces, displacements, and accelerations will permit acceptable designs. The structure should survive a major earthquake with minimal damage. No unwarranted construction costs or difficulties are expected. In a major earthquake, some flexible equipment such as piping may be permanently deformed or broken. Although the lines external to the receiver cavity can be seismically restrained, it is probably not economical to design restraints for the boiler and superheater tubes. In brief, the utility should consider damage to certain flexible components to be acceptable, although the unit may be unavailable to the power grid during an extensive repair period.

1.0 INTRODUCTION

1.1 SCOPE

This appendix describes the seismic analysis criteria, procedures, and results. It further compares the results of dynamic analyses with

design code analyses, and discusses the application of equipment response spectra. Finally, conclusions reached as a result of the seismic calculations are presented.

The configuration of the 10 MWe pilot plant is illustrated in drawing S1001. For the 25 MWe and 60 MWe commercial plants the configuration would be similar. The geometry and weights used for the seismic analyses of the three plants are provided in Table 1.

1.2 DESIGN CODES AND REFERENCES

The following design codes and references were used in this study.

(1) ACI 318-71, Building Code Requirements for Reinforced Concrete, American Concrete Institute, 1971.

(2) ACI 307-69, Specifications for the Design and Construction of Reinforced Concrete Chimneys, American Concrete Institute, 1969.

(3) AISC, Steel Construction Manual, American Institute of Steel Construction, 1970.

(4) NRC Regulatory Guide 1.60, Design Response Spectra for Seismic Design of Nuclear Power Plants, U.S. Nuclear Regulatory Commission, November, 1975.

(5) Newmark, N. M., and Hall, W. J., "Procedures and Criteria for Earthquake Resistant Design," Report for Task 3, National Workshop on Building Practices for Disaster Mitigation, U.S. Dept. of Commerce, National Bureau of Standards, September, 1972.

(6) Uniform Building Code, International Conference of Building Officials, Whittier, California, 1976.

(7) SEAOC, Recommended Lateral Force Requirements and Commentary, Seismology Committee, Structural Engineers Association of California, San Francisco, California, 1975.

(8) ASME, Boiler and Pressure Vessel Code, Section 1, Power Boilers, American Society of Mechanical Engineers.

(9) Bathe, K. J., Wilson, E. L., and Peterson, F. E., "SAPIV: A Structural Analysis Program for Static and Dynamic Response of Linear Systems," Report No. EERC 74-4, Earthquake Engineering Research Center, University of California, Berkeley, June, 1973.

(10) Hou, S. N., "Earthquake Simulation Models and Their Application," M. I. T. Department of Civil Engineering, Report R68-17, May, 1968.

(11) Biggs, J. M, Introduction to Structural Dynamics, McGraw-Hill Book Company, New York, 1964.

(12) Wiegel, R. L., editor, Earthquake Engineering, Prentice-Hall, Inc., Englewood Cliffs, N. J., 1970.

(13) ASME, Power Piping, American National Standard Code for Pressure Piping, ANSI B31.1, American Society of Mechanical Engineers.

(14) Rumman, W. S., "Reinforced Concrete Chimneys," Chapter 15 of Concrete Engineering, edited by M. Fintel, Van Nostrand Reinhold Company, 1974.

2.0 ANALYSIS

2.1 SEISMIC DESIGN CRITERIA

According to the Uniform Building Code, (UBC) (Reference (6)), the pilot plant to be built near Barstow, California, will be in seismic zone 3. Ground motion, both horizontally and vertically, may approach

accelerations of 0.25 g. Of paramount importance from both safety and economical viewpoints, is the structural integrity of the support tower and receiver support structure. Important also to personnel safety is prevention of a steam line rupture, at least in those areas where maintenance personnel regularly work. Beyond these basic criteria, the utility and engineer must weigh the capital cost penalty against the consequences of damage (including direct repair costs, and loss of a power generation facility during the repair period, albeit not a major component in the power grid).

No codes are currently applicable for the seismic design of solar power plants. Standards established by the Nuclear Regulatory Commission (NRC) for the design of nuclear-fueled power plants would be too conservative to apply to the design of solar power plants, and no standards exist specifically for fossil-fueled power plants.

The SEAOC recommendations (Reference (7)), which are the basis for the seismic requirements of the Uniform Building Code, in fact explicitly state that: "Many types of structures require seismic design procedures which are beyond the scope of these recommendations. Structures such as power plants, stacks, water towers,... require special design criteria." Nonetheless, the ACI 307 committee (Reference (2)) has adopted the SEAOC approach for the design of reinforced concrete chimneys at power plants. The ACI 307-69 specifications, therefore, provide a reasonable minimum basis for design of the tower, although recent modifications to the SEAOC and UBC recommendations have not yet been incorporated in the subject specifications. Comparisons of the code approaches are made in Section 3.3 of this Appendix.

The design of the steel support structure for the steam generator can justifiably be based on an elastic analysis and the AISC specifications (Reference (3)), but with the energy-absorbing capacity of the multiplicity of components taken into account. A similar approach can be used for the analysis of piping, the steam drum, recirculation pumps, valves, and other mechanical components, except that they must be designed to meet the requirements of the ASME Boiler and Pressure Vessel Code (Reference (8)), and ANSI B31.1 (Reference (13)). Electrical components should simply be adequately anchored to their supports to prevent overturning or shifting. Such a provision is economically justifiable. Equipment response spectra provide the necessary seismic design input for mechanical and electrical components.

2.2 DESIGN EARTHQUAKE MOTION

The horizontal and vertical design earthquakes are expressed in the frequency domain in terms of the design response spectra provided by NRC Regulatory Guide 1.60 (Reference (4)). These elastic ground response spectra are reproduced here as Figures 1 and 2. The curves represent a composite of numerous actual earthquake spectra normalized to a maximum ground acceleration of 1.0 g. For a peak acceleration of 0.25 g, the response at a selected frequency is simply multiplied by 0.25. The several curves shown correspond to different values of critical damping of a simple oscillator in response to the input motion. On this "tripartite" plot the maximum absolute acceleration, the maximum displacement relative to the ground, and the maximum (pseudo) relative velocity of the simple oscillator can be read simultaneously, for a selected frequency and damping.

A complete discussion of the use of this spectrum can be found in many texts and papers, including Reference (5).

The ground response spectrum, normalized to 0.25 g, can be used directly in computer analyses of the structure. Alternatively, a synthetic earthquake for which the response spectrum envelopes the design response spectrum can be used for time history analyses. Such a synthetic earthquake is developed from a random number generator that is constrained by a time function to exhibit the characteristics of an actual earthquake. See, for example, Reference (10). The horizontal acceleration time history used for this study is shown in Figure 3. For this accelerogram the response spectrum given in Figure 4 envelopes the ground response spectrum also shown in the figure. It should be noted that in the low frequency range corresponding to the lowest modes of vibration of the solar plants (see section 3.1) the accelerogram is conservative. That is, responses computed from time history analyses will generally exceed those computed directly from response spectrum analyses. Although the acceleration time history is not required for the design of the structure itself, it must be used to accurately develop equipment response spectra. These latter spectra are described in Section 2.3.

2.3 SEISMIC ANALYSIS PROCEDURE

The structure was dynamically analyzed by the response spectrum method, a procedure described by several authors including Biggs (Reference (11)). First, the structure was idealized as a "stick," wherein nodes are defined at numerous elevations in the support tower, at the ends of all support structure members, and at several other locations required to describe the

geometry of the structure. The upper section of the "stick" model for the pilot plant, as a space frame, is shown in Figure 5. The mass of the structure was judiciously lumped at these nodes. Between the nodes, "finite elements" describe the stiffness of the members.

The design response spectrum was input to the base of the structure. The output consisted of the natural frequencies of the structure, member forces, and node accelerations and displacements. In the response spectrum method, only the mode shapes associated with natural frequencies that participate significantly in the response are considered. The results for individual modes are statistically combined by taking the square root of the sum of the squares to derive the total response. The results will not agree with those from a time history analysis but they are sufficiently close for practical purposes. An enhanced version of the well-known computer program SAP IV (Reference (9)), was used to perform the computations.

Although some response spectrum analyses were performed on space-frame models, succeeding analyses were conducted on simpler plane-frame models once it had been verified that coupling between out-of-plane modes was insignificant. The time history analysis of the pilot plant involved only a plane frame model.

Response spectrum analyses for the horizontal earthquake motion considered five translational modes in the direction of the earthquake for the 10 MWe pilot plant, four for the 25 MWe commercial plant, seven for the 60 MWe commercial plant. Damping was taken to be two per cent of critical damping in all cases, a value judged to be appropriate if the structural concrete is to exhibit only minor cracking during an earthquake. In the bolted steel superstructure the damping would be of the

order of four to five per cent because considerable energy would be absorbed in working of the connections; however, two per cent damping was assumed for all modes.

Equipment response spectra can only be accurately developed from a time history analysis, a more costly procedure than a response spectrum analysis. The base motion, defined by Figure 3, which is input at the base of the structure will cause an output acceleration time history at all other nodes in the structure where such information is desired. These resulting acceleration records will be amplified and altered significantly in frequency content from the base motion by the motions of the structure. When a response spectrum of the tripartite form of Figure 1 is computed for the top of the tower, the spectrum will display large peaks at the natural frequencies of the tower. Because only accelerations are normally useful for the design of the components, the tripartite spectrum is usually waived in favor of an easier-to-read acceleration response spectrum.

3.0 RESULTS

3.1 NATURAL FREQUENCIES AND MODE SHAPES

The pilot plant and the 25 MWe plant designs were first analyzed as space frames. That is, each node could translate in three orthogonal directions and rotate about three orthogonal axes. Vibration modes corresponding to translation in two horizontal directions, one vertical direction, and twist about the vertical axis were therefore detected. The lowest natural frequencies and the corresponding mode types are given in Table 2. Figure 5 shows the relative deformations, or mode shapes, of the upper section of the pilot plant in detail. The mode shapes for the first four translational modes in the X-direction are shown in Figures 6 through 9.

A study of the frequencies and modal participation factors indicated that there is not significant coupling of the modes. The lumped mass model for the 60 MWe plant tower was therefore analyzed as a plane frame. That is, translation in only the X-direction was permitted. The natural frequencies for this tower are also given in Table 2.

A review of the translational mode shapes indicates that the support tower is much stiffer than the steel framing supporting the steam generator. Significant "whipping" action is likely to occur, magnifying the accelerations considerably above those at the top of the reinforced concrete tower. The seismic response is therefore sensitive to the stiffness of the three legs supporting the steam generator and to the mass which they support. Final design of the steam generator and its supports should therefore be followed by a seismic analysis to verify the design loads.

3.2 SHEARS IN THE SUPPORT TOWER

The seismic shears in the support tower were plotted in a nondimensional form for comparison with those given by Rumman (Reference (14)). Figure 10 shows the approximate shear distribution which Rumman found from seismic analyses of many tapered, reinforced concrete chimneys. Results for the three solar plants agreed very well with each other and are in reasonable agreement with Rumman's work, especially when plotted as a function of the overall tower height. For clarity, only "average" curves for the three solar plants are shown in the figure. Once an estimate of the base shear has been determined, the shear at any height can be readily found from this figure.

3.3 COMPARISON OF BASE SHEARS FROM ELASTIC ANALYSES WITH UBC AND ACI 307

The base shear is also of interest in order that comparisons with the Uniform Building Code and the ACI 397-69 specifications can be made. From

such comparisons seismic design criteria can be established. In Table 3 are given the base shears calculated from the elastic response spectrum analysis and from the above specfications. All values are "elastic" values to be used with code allowable stresses. The obvious questions are as follows. Why are the results obtained from the three approaches so different? Which approach should be used for design? The answers: the differences lie in the bases of the codes, and the design value is to be decided by the engineer.

The 1976 edition of the Uniform Building Code (Reference (6)), is based upon the 1975 edition of the SEAOC recommendations (Reference (7)). The base shear, V_{UBC}, is given by:

$$V_{UBC} = ZIKCSW$$

Where

Z = Zone factor (0, 3/16, 3/8, 3/4, 1 corresponding to zones 0, 1, 2, 3, 4, respectively)

I = Importance factor ($1.0 \leq I \leq 1.5$)

K = Force factor based on construction ($0.67 \leq K \leq 2.5$)

C = Base shear coefficient ($C \leq 0.12$)

= Maximum base shear force/structure weight

= $\frac{1}{15\sqrt{T}}$ where T = fundamental elastic period, secs

S = Site factor concerning soil-structure interaction effects ($1.0 \leq S \leq 1.5$)

W = Weight of Structure

For the solar plants the following values were used.

Z = 0.75 (Barstow, California is in zone 3.)

I = 1.25 (Not an essential structure.)

K = 2.0 (Tower has no multiplicity of structural and non-structural components.)

S = 1.0 (Taken as 1.0 to facilitate comparisons.)

Hence

$$V_{UBC} = \frac{0.125\ W}{\sqrt{T}}$$

In developing their recommendations, the SEAOC committee established the base shear coefficient, C, in such a way that, although it reflects the simultaneous influence of all the modes of vibrations, it resembles an acceleration response envelope for a cantilever with a uniform mass and a straight line fundamental mode shape. Using the response spectra for four maximum credible earthquakes for the Los Angeles Basin, the committee performed elastic analyses with ten per cent damping. The resulting base shear coefficients were then reduced for a materials safety factor of 1.33/1.70 in order to arrive at coefficients representing a yield stress state. (The factor of 1.33 arises from the 1/3 allowable overstress permitted by most codes in designing for seismic conditions. The factor of 1.70 approximates the ratio of yield stress to normal allowable stress.) The curves were then further reduced to account for ductility, multi-mode effects, and other judgment factors.

Chimneys at power plants are currently designed to comply with ACI 307-69 (Reference (2)), which is based on the 1967 SEAOC recommendations. In ACI 307-69 the base shear, V_{ACI}, is given by:

$$V_{ACI} = ZUCW$$

Where

Z = Zone factor (0, 0.3, 0.5, 1.0 corresponding to zones 0, 1, 2, 3, respectively)

U = Use factor ($1.3 \leq U \leq 2.0$)

C = Base shear coefficient

$= \frac{0.10}{3\sqrt{T}}$ where T = fundamental elastic period, secs

W = Weight of structure

For the solar plants, the following values were used.

Z = 1.0 (zone 3)

U = 2.0 (Chimney will be relatively damage-free and serviceable after a strong earthquake)

Hence

$$V_{ACI} = \frac{0.20\ W}{3\sqrt{T}}$$

It should be noted that the zone factor in ACI 307-69 is not the same as that in the 1976 edition of UBC. Furthermore, the selection of the use factor in ACI 307-69 greatly impacts the equation.

The UBC code takes advantage of the ductility of the structure. That is, inelastic (or yielding) behavior of components will absorb much of the earthquake energy imparted to the structure. This means that elastic analyses by the response spectrum method give forces much in excess of those computed by design codes, yet structures designed in accordance with these codes have performed acceptably during major earthquakes. The ductility factor, μ, is defined by the ratio:

$$\mu = \frac{\text{ultimate deflection}}{\text{yield deflection}}$$

In the Uniform Building Code μ is of the order of four to six.

The solar plant support towers, like chimneys, depend on the stiffness of one major component for their stability, unlike multi-story frames comprised of many beams and columns. In the frame structure, yielding is

permitted in some beams during strong earthquake motion. However, yielding of the solar plant support tower should not be permitted. The design should be based on an elastic analysis with the critical stress limited to, or below, the yield value. That is, the ductility factor is equal to one.

In order to compare the elastic analysis approach with those of UBC and ACI 307-69, the base shears must have a common datum. The appropriate datum for this study is the shear corresponding to yield of the tower reinforcement. For the UBC this value would be approximately:

$$\frac{1.70}{1.33} \cdot V_{UBC} = \frac{1.70}{1.33} (990) = 1265 \text{ kips}$$

Clearly, since the elastic analysis shear exceeds 1265 kips, as it does even for ten per cent damping, a ductility factor greater than one is required. Therefore, the UBC value is not acceptable for design of the support tower.

The ACI 307-69 code specifies a factor of safety in the reinforcement of approximately 2.2 against yield. The base shear corresponding to yield would therefore be approximately:

$$2.2 \cdot V_{ACI} = 2.2 (1820) = 4000 \text{ kips}$$

This value exceeds the shear from the elastic analysis, therefore no yielding would occur in the reinforcement. Since the ACI 307-69 code has no one-third increase in allowable stresses for load combinations involving earthquakes, it is logical to compare 1.33 (1820), or 2430 kips, with the elastic analysis value of 2740 kips. These results compare favorably.

Therefore, for design it is reasonable to use the elastic analysis results together with ACI 318-71 and AISC codes (which permit a one-third increase in normal allowable stresses for load combinations involving

earthquakes). The ACI 307-69 code forces and allowable stresses would lead to a comparable, but slightly less conservative design.

3.4 BENDING MOMENTS IN THE SUPPORT TOWER

The distribution of bending moments in the three support towers is plotted in a nondimensional form in Figure 11. The curve shown is an "average" of the almost identical distribution in the three towers. The base moments were computed by the response spectrum method as follows:

(1) For the 10 MWe plant the base moment is 484,000 ft kips.

(2) For the 25 MWe plant the base moment is 2,089,000 ft kips.

(3) For the 60 MWe plant the base moment is 7,809,000 ft kips.

3.5 MAXIMUM ACCELERATIONS AND DISPLACEMENTS

The maximum absolute accelerations and displacements relative to the base for the pilot plant tower structure are plotted in Figure 12. Results from both the elastic time history analysis and response spectrum analysis are shown. Values from the time history analysis are highest because the ground design response spectrum generated by the synthetic earthquake exceeds the NRC Regulatory Guide 1.60 spectrum in the low frequency range of the solar towers. Furthermore, the response spectrum analysis method is only an approximate, although acceptable, method. Design accelerations, displacements, equipment response spectra, and forces could be reduced to reflect the conservatism of the time history analysis, but that has not been done here.

For selected nodes, the maximum accelerations and displacements for the three solar plants are given in Table 4 and plotted as a function of height of the tower in Figure 13.

3.6 RESPONSE TO VERTICAL COMPONENT OF EARTHQUAKE

Table 5 indicates the vertical natural frequencies of the 10 MWe pilot plant tower. When this plant was dynamically analyzed by the elastic response spectrum method, using the design spectrum of Figure 2 normalized to 0.25 g and two per cent damping, the peak vertical accelerations were 1.20 g and 1.86 g at elevations 410 and 523, respectively, and the corresponding peak vertical displacements were .022 ft and .031 ft. Although the displacements are small, as anticipated, the vertical accelerations are significant. Equipment response spectra therefore must be generated for the vertical component of the earthquake as well as for the horizontal component. However, these vertical spectra were not computed for this preliminary design. The axial force in the support tower varied almost linearly from 1930 kips at elevation 410 ft to 7080 kips at the base.

The vertical responses of the 25 MWe and 60 MWe solar plants were not computed for this study.

3.7 EQUIPMENT RESPONSE SPECTRA AND THEIR APPLICATION

Acceleration response spectra, which indicate the maximum acceleration of a simple, damped oscillator of a particular frequency when subjected to the acceleration time history experienced at that elevation, are shown for various elevations in the pilot plant in Figures 14 through 19. Two per cent damping has been assumed, an appropriate value for piping. The heavily lined envelopes should be used for design purposes. The computed spectra have been broadened plus and minus fifteen per cent in frequency to account for mass and stiffness uncertainties, then the envelope has been constructed by hand.

It will be noted that not only are accelerations in certain frequency ranges very high, but the spectra differ significantly from one elevation to the next because of the significant "whipping" action near the top of the tower and the presence of vibration nodes near several of the elevations selected for plotting. Clearly, if equipment is not to be significantly damaged in a major earthquake, it should be designed to have its lowest natural frequency greater than about 10 Hz. Seismic accelerations of the order of two or three g's would then be experienced, and these levels can be tolerated in the design of most components and piping.

4.0 CONCLUSIONS AND RECOMMENDATIONS

The solar plants can be seismically analyzed by state-of-the-art dynamic analysis procedures and designed in conformance with current building codes. In this report, seismic analysis criteria, procedures, and results have been presented. Following are the major conclusions and design recommendations.

(1) The solar power pilot plant to be located new Barstow, California, should be designed for ground motion, both horizontally and vertically, of 0.25 g. The ground response spectra for these accelerograms should envelope those of NRC Regulatory Guide 1.60.

(2) Dynamic analyses should be performed by either the response spectrum method or the time-history method. (The latter is required if accurate equipment response spectra are to be developed.)

(3) Elastic behavior with two per cent damping should be assumed. (Higher damping, four or five per cent, is justifiable in the steel superstructure.)

(4) The distribution of seismic shears and bending moments in the support tower is almost independent of the size of the plant.

(5) Although the maximum seismic displacements are almost linearly related to the height of the tower, the maximum accelerations are, for practical purposes, independent of the tower height.

(6) The codirectional responses (displacements, stress resultants) from the horizontal and vertical components of the ground motion should be combined by the square root of the sum of the squares method to determine the design response.

(7) The UBC approach to seismic analysis is unconservative for the design of the support tower. Although the ACI 307-69 chimney design code will provide a satisfactory design for the tower (assuming that a reasonable analysis can be made for the vertical earthquake component), a slightly more conservative approach is recommended wherein the tower is elastically, dynamically analyzed and then designed according to the ACI 318-71 specifications.

(8) Steel components should be designed according to the elastic, dynamic analysis and the AISC Manual.

(9) Mechanical and electrical components must be adequately anchored to their support structure to prevent overturning or shifting.

(10) Steam piping external to the steam generator should be sufficiently restrained that it will not experience the high seismic accelerations evident in the equipment response spectra. If the restraints are located such that the lowest natural frequency of the piping is above 10 Hz, then the piping should retain its integrity.

(11) The steam generator itself should be horizontally restrained by hydraulic or mechanical snubbers that eliminate rattle space between the generator and its supporting structure, yet will accommodate thermal growth. (It was assumed in the analyses for this study that such snubbers would be provided.)

TABLE 1

TOWER GEOMETRY AND WEIGHT

Tower Geometry and Weight							Steam Generator and Framing					
Power MW	Height ft	Base Diameter ft	Top Diameter ft	Base Thick in.	Top Thick in.	Weight kips	Aperture Height ft	Generator Height* ft	Generator Diameter ft	Weight kips	Overall Height ft	Total Weight kips
10	415	50	26	23	14	10,950	16	90	49	1,090	521	12,040
25	650	77	40	36	27	44,100	25	129	78	2,725	804	46,825
60	1,000	124	64	45	36	141,000	39	182	120	6,540	1,221	147,540

*Generator height includes drum height, girder depth, and parapet.

TABLE 2

NATURAL FREQUENCIES (Hz) OF THE THREE SOLAR PLANTS[a]

Mode	10 MWe Plant[b]	25 MWe Plant[c]	60 MWe Plant[d]	Mode Type
1	0.43	0.31	.23	1st X - Translation
2	0.43	0.31		1st Y - Translation
3	0.58	0.52		1st Torsion
4	0.95	0.72	.56	2nd X - Translation
5	0.95	0.72		2nd Y - Translation
6	2.37	2.42		2nd Torsion
7	2.51	1.74	1.23	3rd X - Translation
8	2.51	1.74		3rd Y - Translation
9	4.43	3.42	2.56	4th X - Translation
10	4.43	3.42		4th Y - Translation
11	4.62			3rd Torsion
12	6.30		3.44	5th X - Translation
13	6.30			5th Y - Translation
14	6.44			1st Vertical
15	7.07			4th Torsion

[a] Modes not given were not computed, arranged in ascending order for 10 MWe Pilot Plant.

[b] Space frame analysis, 15 modes computed.

[c] Space frame analysis, 10 modes computed.

[d] Plane frame analysis, 7 modes computed.

TABLE 3

BASE SHEARS FROM ELASTIC ANALYSES AND CODES

Plant	Base Shears				
	W	T	Elastic[a]	UBC-76	ACI 307-69
	kips	sec	kips	kips	kips
10 MWe	12,040	2.30	2,740 1,500[b] 4,400[c]	990	1,820
25 MWe	46,820	3.15	8,200	3,300	6,370
60 MWe	147,540	4.30	24,400	8,890	18,160

[a]Elastic analysis by response spectrum method with two per cent damping, except see notes b and c.

[b]Elastic analysis by response spectrum method with 10 per cent damping.

[c]Elastic analysis by time history method with two per cent damping.

TABLE 4

MAXIMUM ACCELERATIONS AND DISPLACEMENTS

Plant	Elevation ft	Location	Maximum Acceleration g[a]	Maximum Displacement ft[a]
10 MWe	521	Highest point	1.72	2.43
			0.91[b]	1.55[b]
			2.07[c]	2.98[c]
	415	Top of support tower	0.93	0.89
			0.48[b]	0.57[b]
			1.36[c]	1.03[c]
	210	Mid-height of support tower	0.62	0.25
			0.33[b]	0.15[b]
			0.83[c]	0.34[c]
25 MWe	804	Highest point	1.69	3.52
	650	Top of support tower	0.75	1.57
	350	Mid-height of support tower	0.45	0.50
60 MWe	1,221	Highest point	1.80[d]	4.81
	1,000	Top of support tower	0.82	2.48
	480	Mid-height of support tower	0.45	.65

[a]Elastic analysis by response spectrum method with two per cent damping, except see notes b and c.

[b]Elastic analysis by response spectrum method with 10 per cent damping.

[c]Elastic analysis by time history method with two per cent damping.

[d]Maximum acceleration of 1.90 g occurred at elevation 1,126.

TABLE 5

VERTICAL NATURAL FREQUENCIES (Hz)
OF 10 MWe PILOT PLANT*

Mode	Frequency Hz
1	6.66**
2	12.94
3	21.07
4	31.30

*A secondary frequency of 13.01 Hz occurs in the receiver support legs.

**As space frame, frequency computed to be 6.44 Hz, see Table 2.

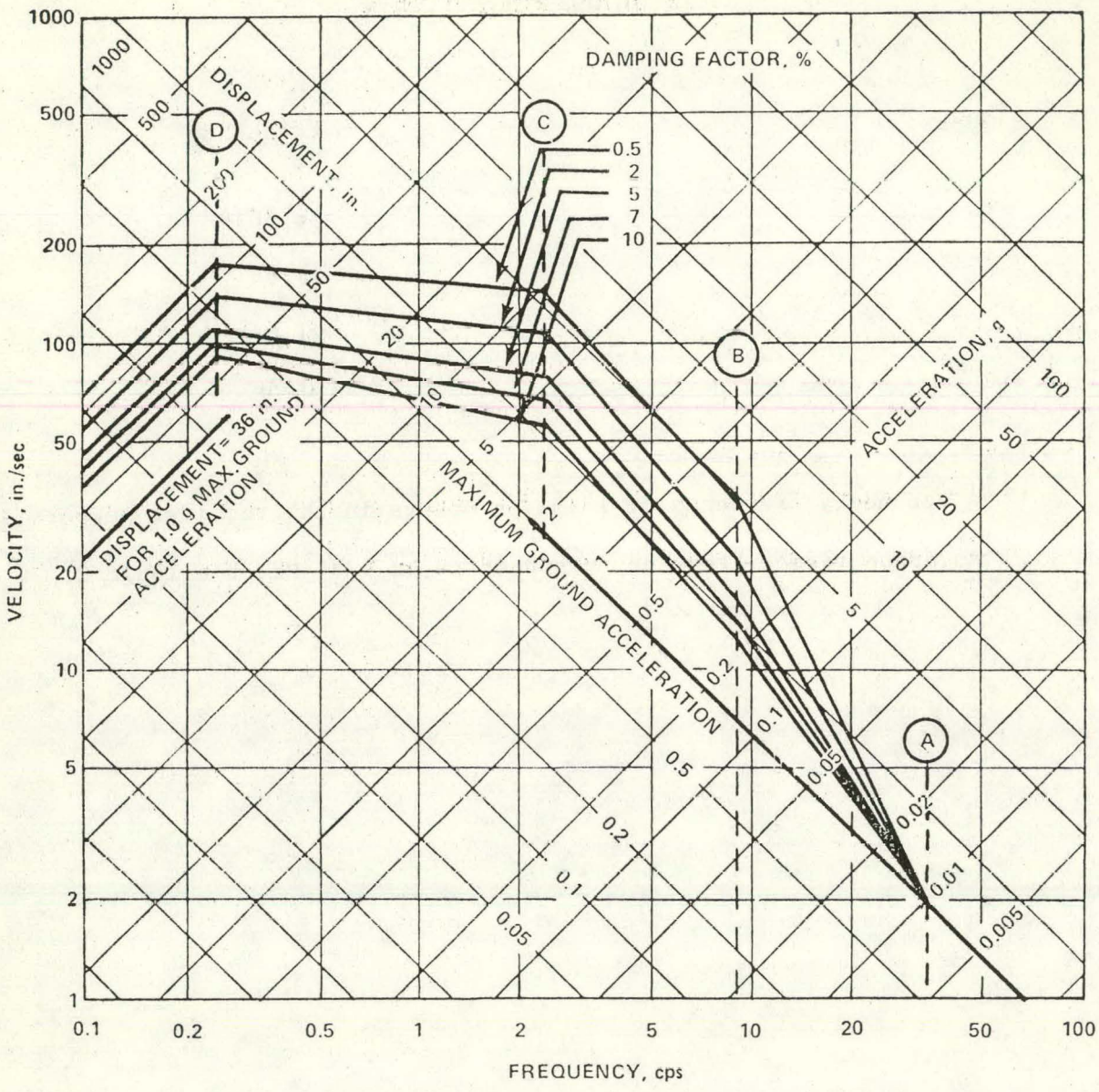

Figure 1. Horizontal Design Response Spectra - Scaled To 1g Horizontal Ground Acceleration

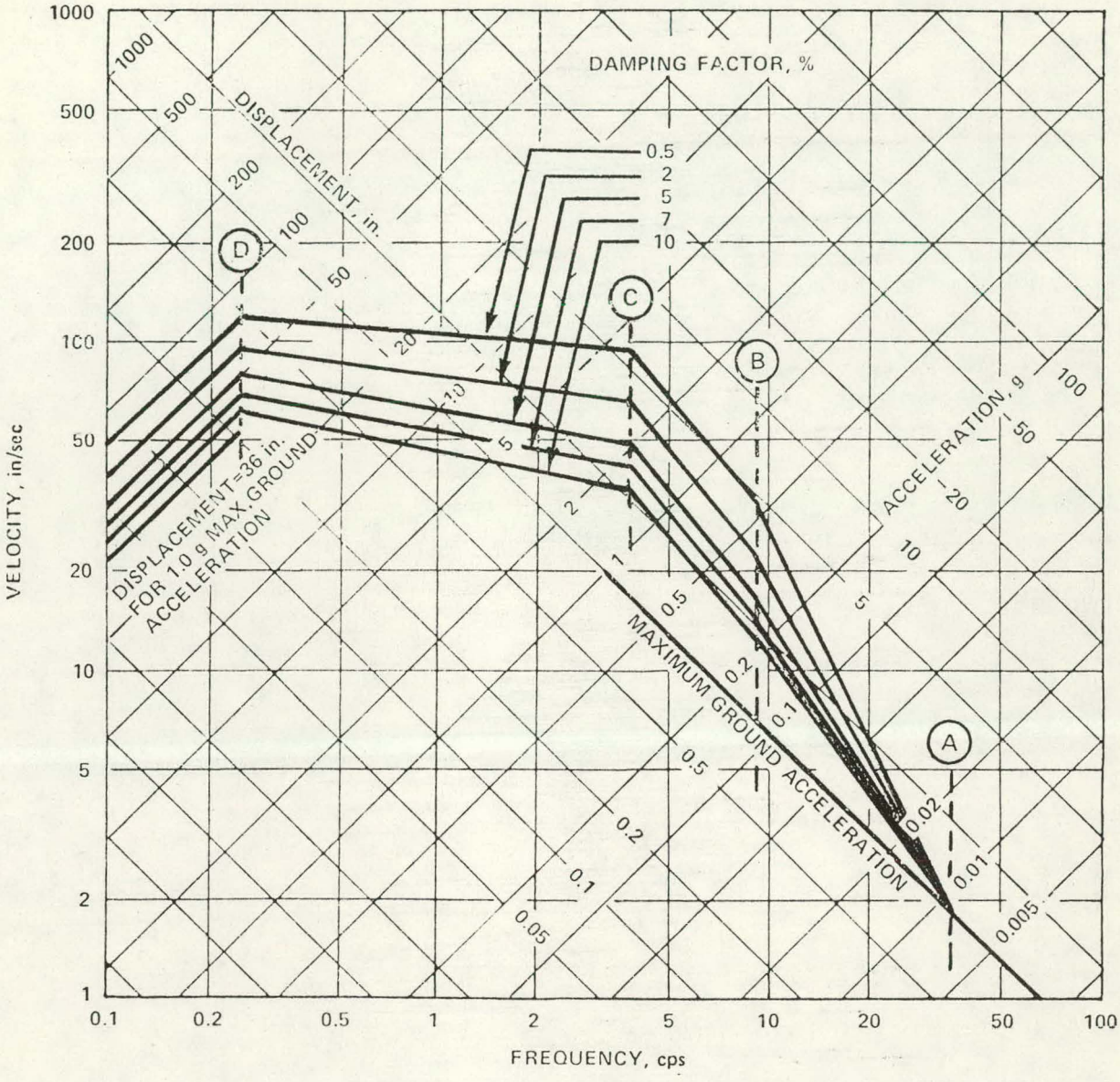

Figure 2. Vertical Design Response Spectra - Scaled To 1g Horizontal Ground Acceleration

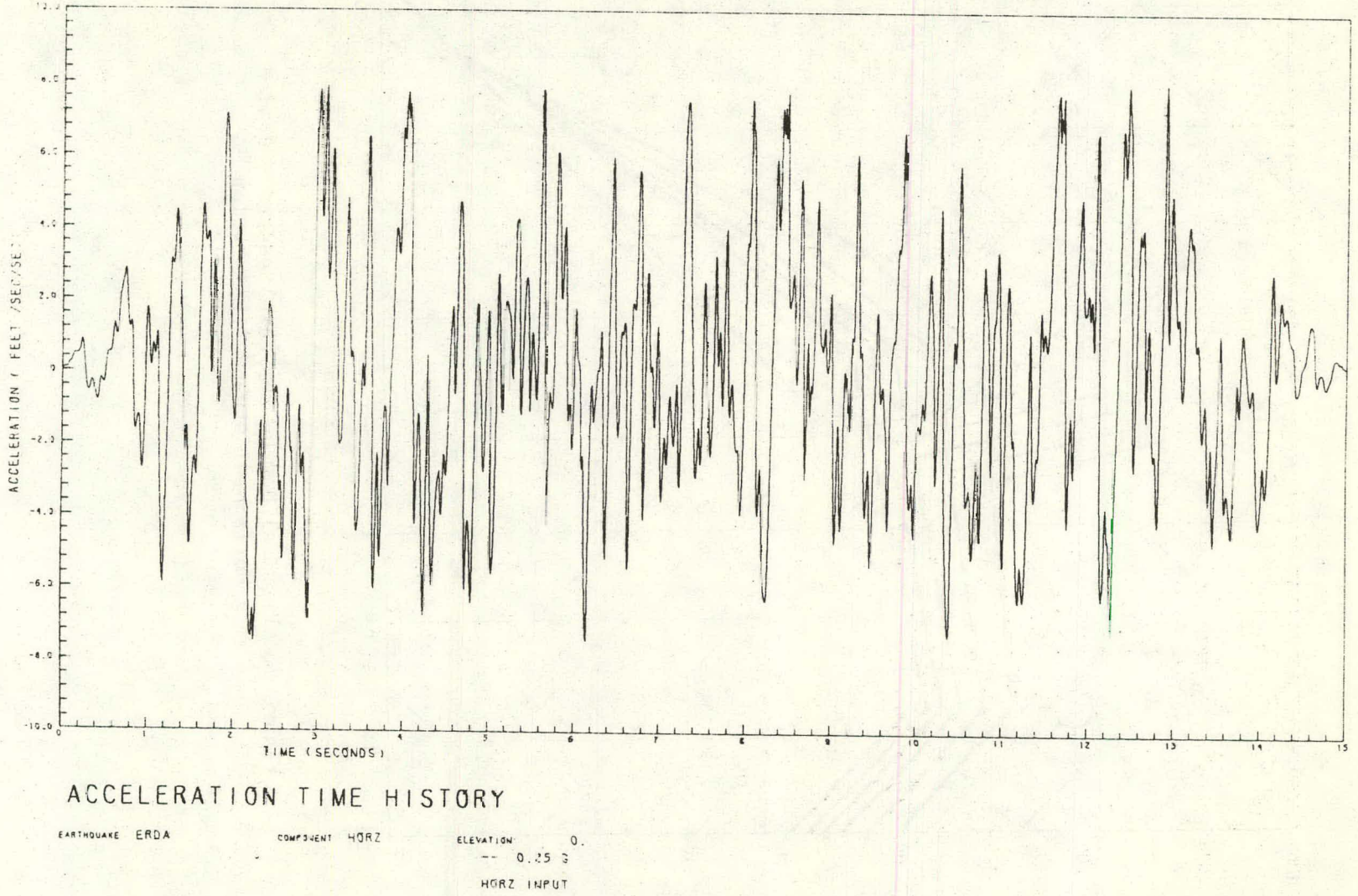

Figure 3. Design Horizontal Acceleration Time History

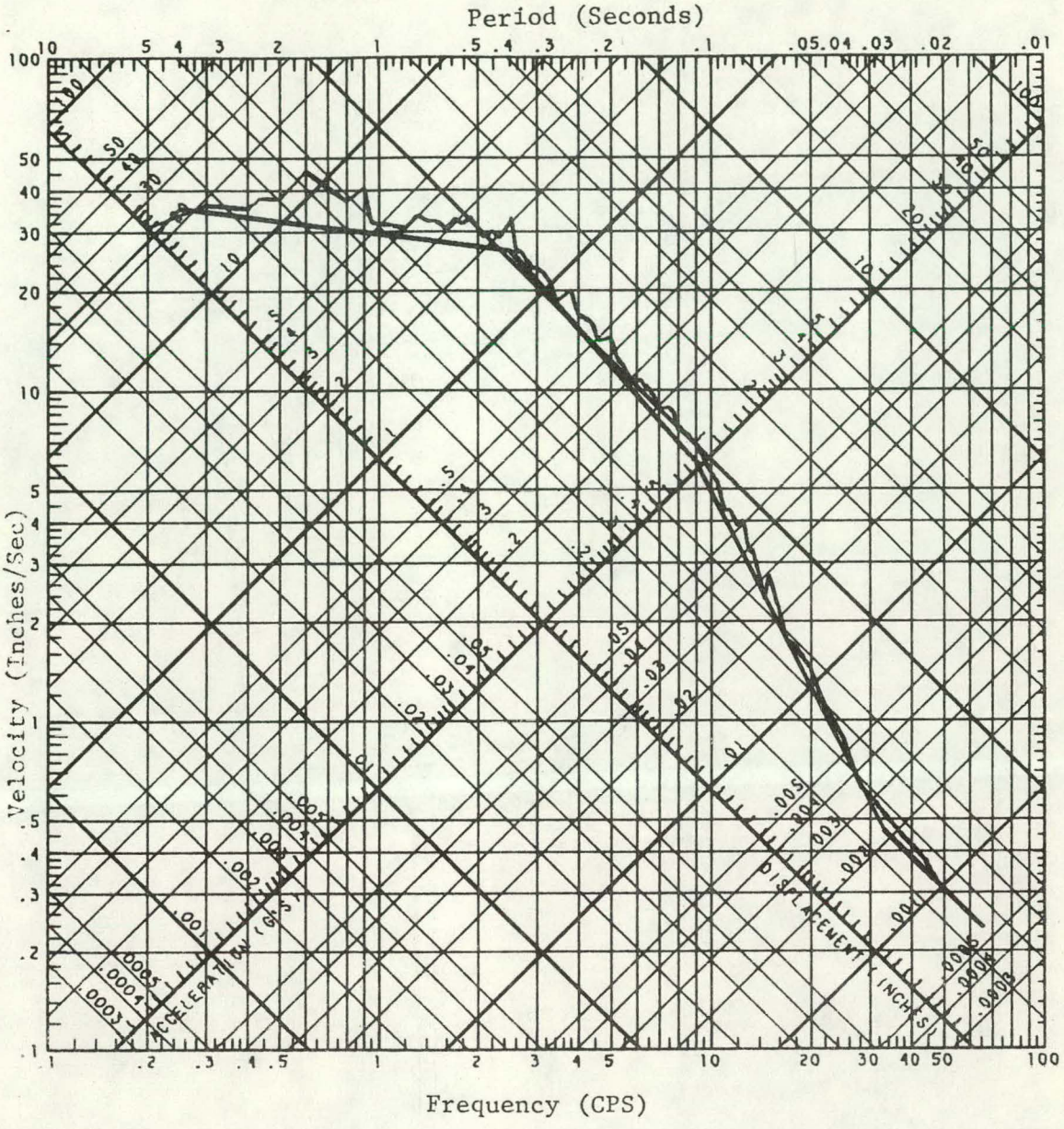

Figure 4. Horizontal Response Spectrum Computed From Design Acceleration Time History

** ERDA ** 10 MW SOLAR PILOT PLANT ** 415 FOOT TOWER **

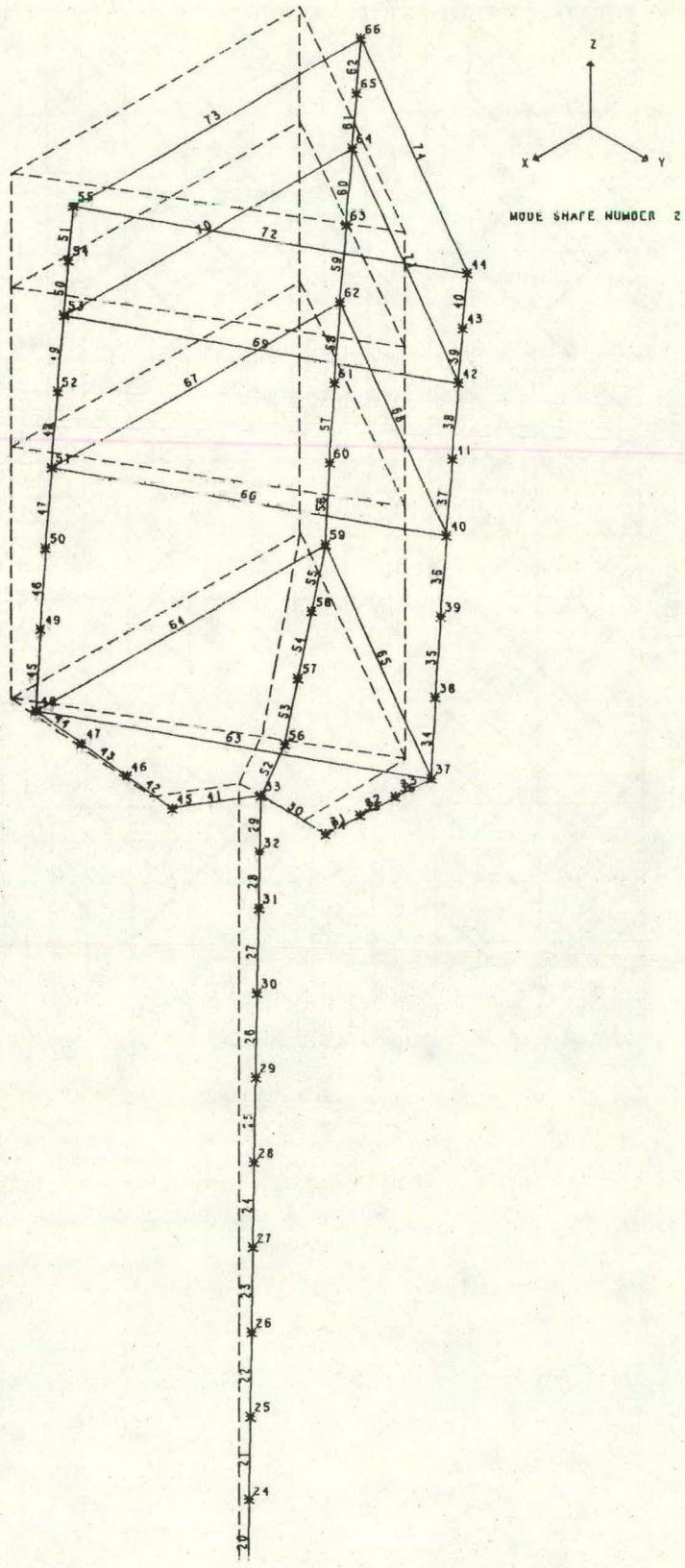

Figure 5. Dynamic Analysis Model of Upper Section of 10 MWe Pilot Plant

ERDA ** 10 MW SOLAR PILOT PLANT ** 415 FOOT TOWER

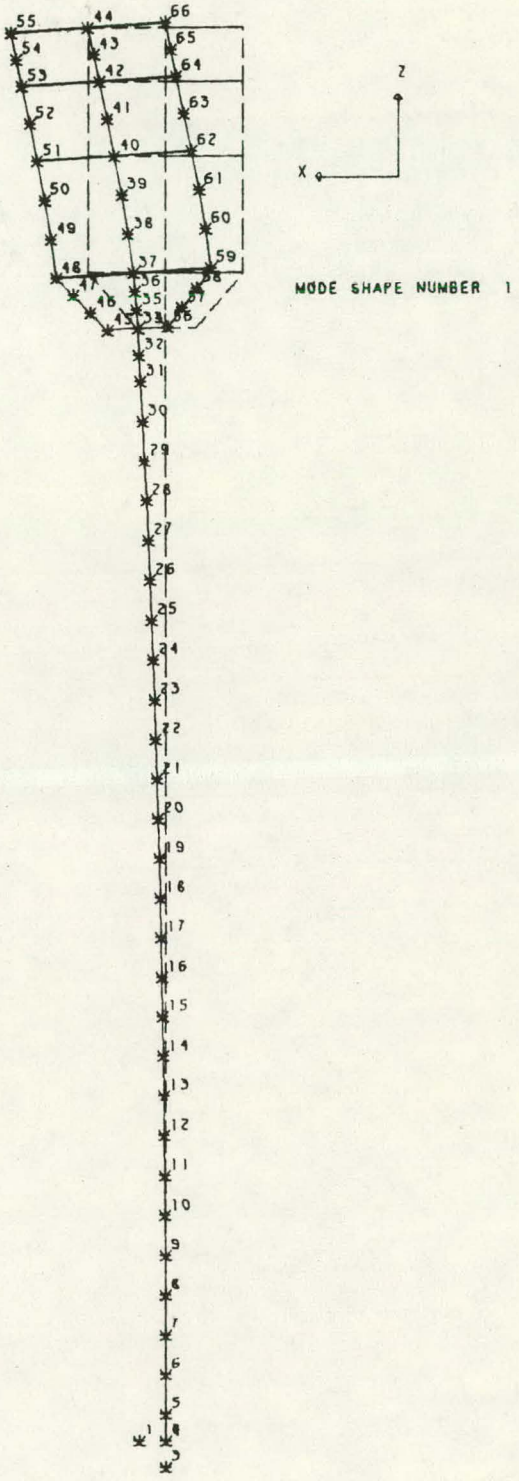

Figure 6. Lateral Vibration Mode 1 For Pilot Plant

ERDA ** 10 MW SOLAR PILOT PLANT ** 415 FOOT TOWER

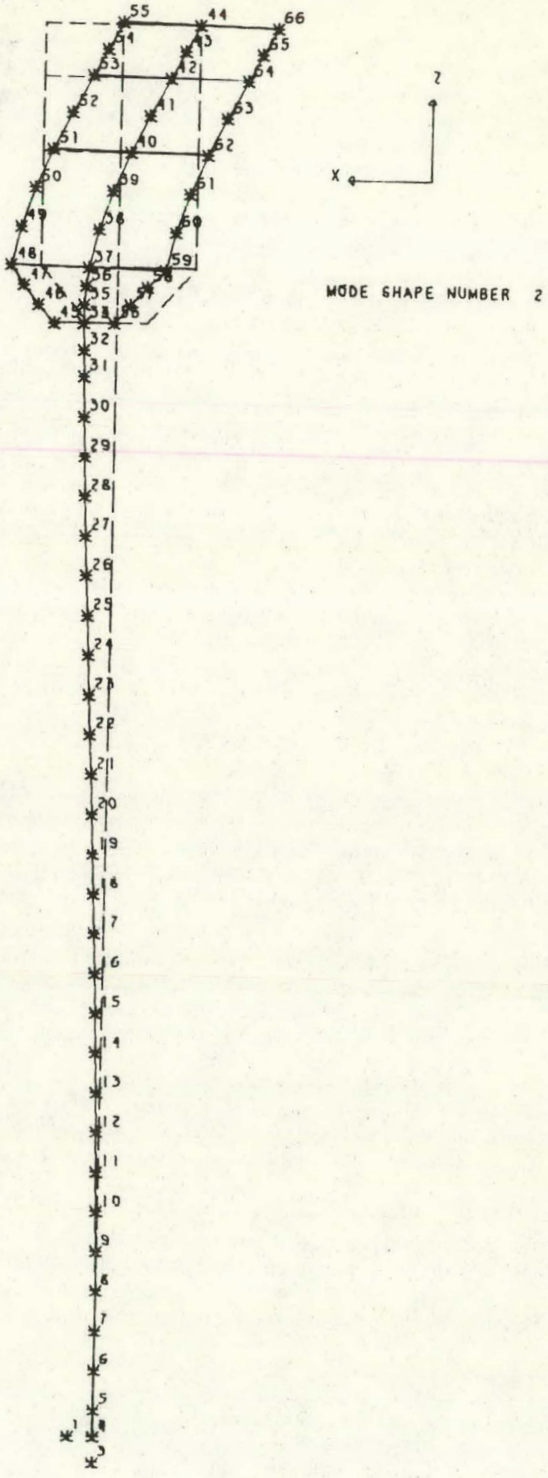

Figure 7. Lateral Vibration Mode 2 For Pilot Plant

ERDA ** 10 MW SOLAR PILOT PLANT ** 415 FOOT TOWER

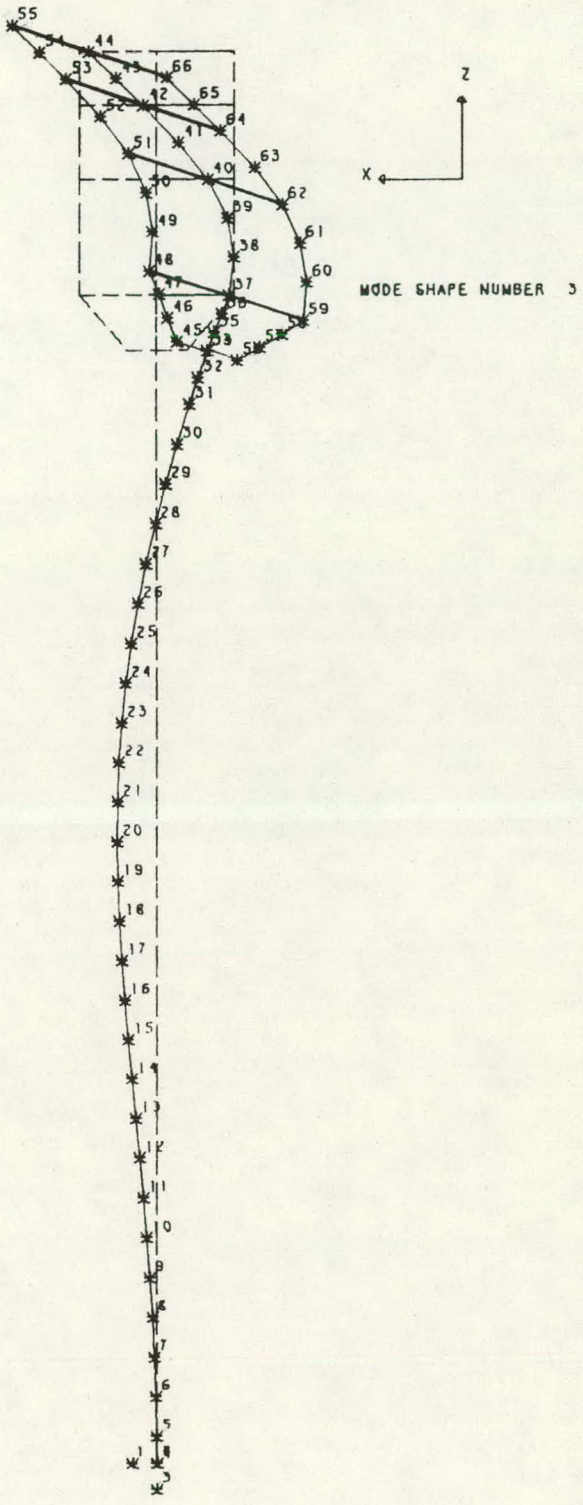

Figure 8. Lateral Vibration Mode 3 For Pilot Plant

ERDA ** 10 MW SOLAR PILOT PLANT ** 415 FOOT TOWER

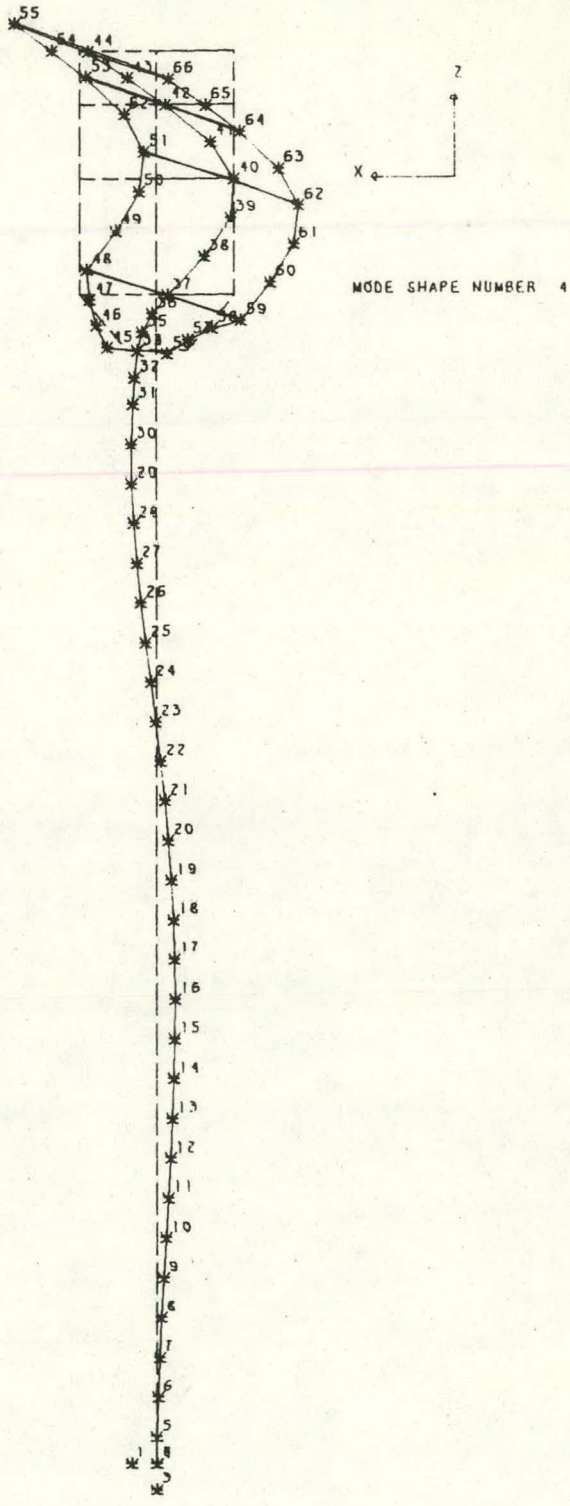

Figure 9. Lateral Vibration Mode 4 For Pilot Plant

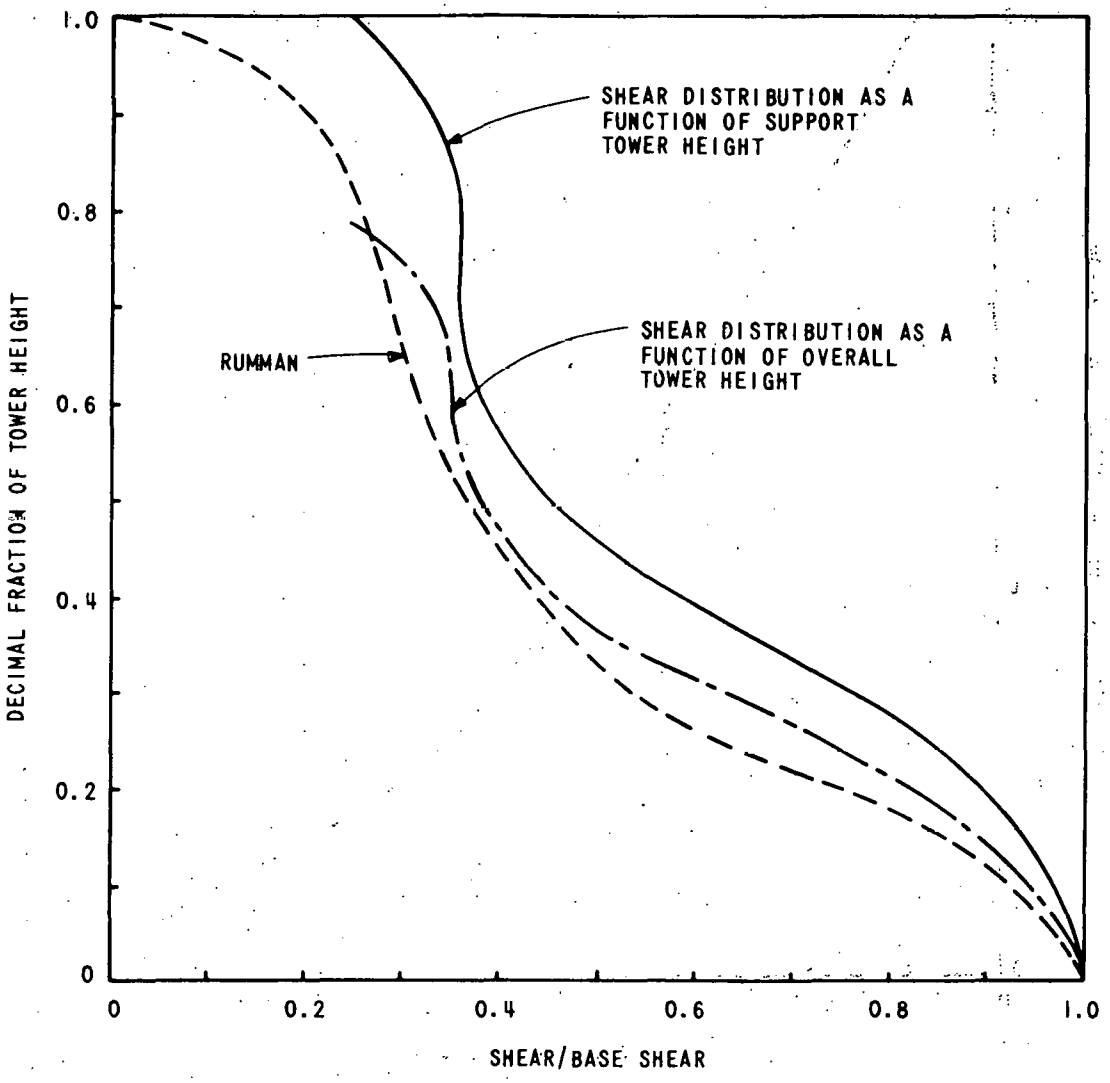

Figure 10. Shear Force Distribution in Support Tower

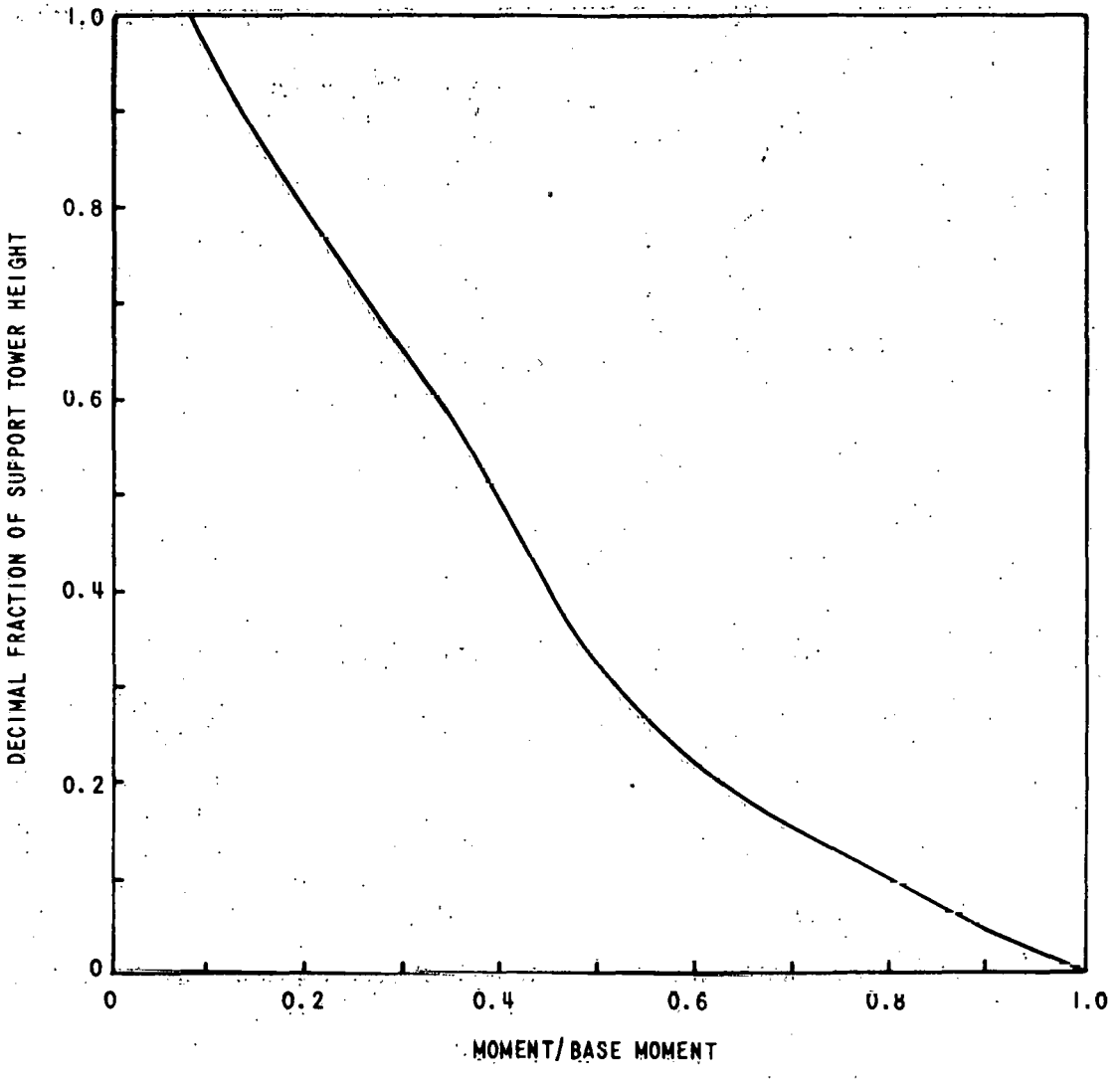

Figure 11. Bending Moment Distribution in Support Tower

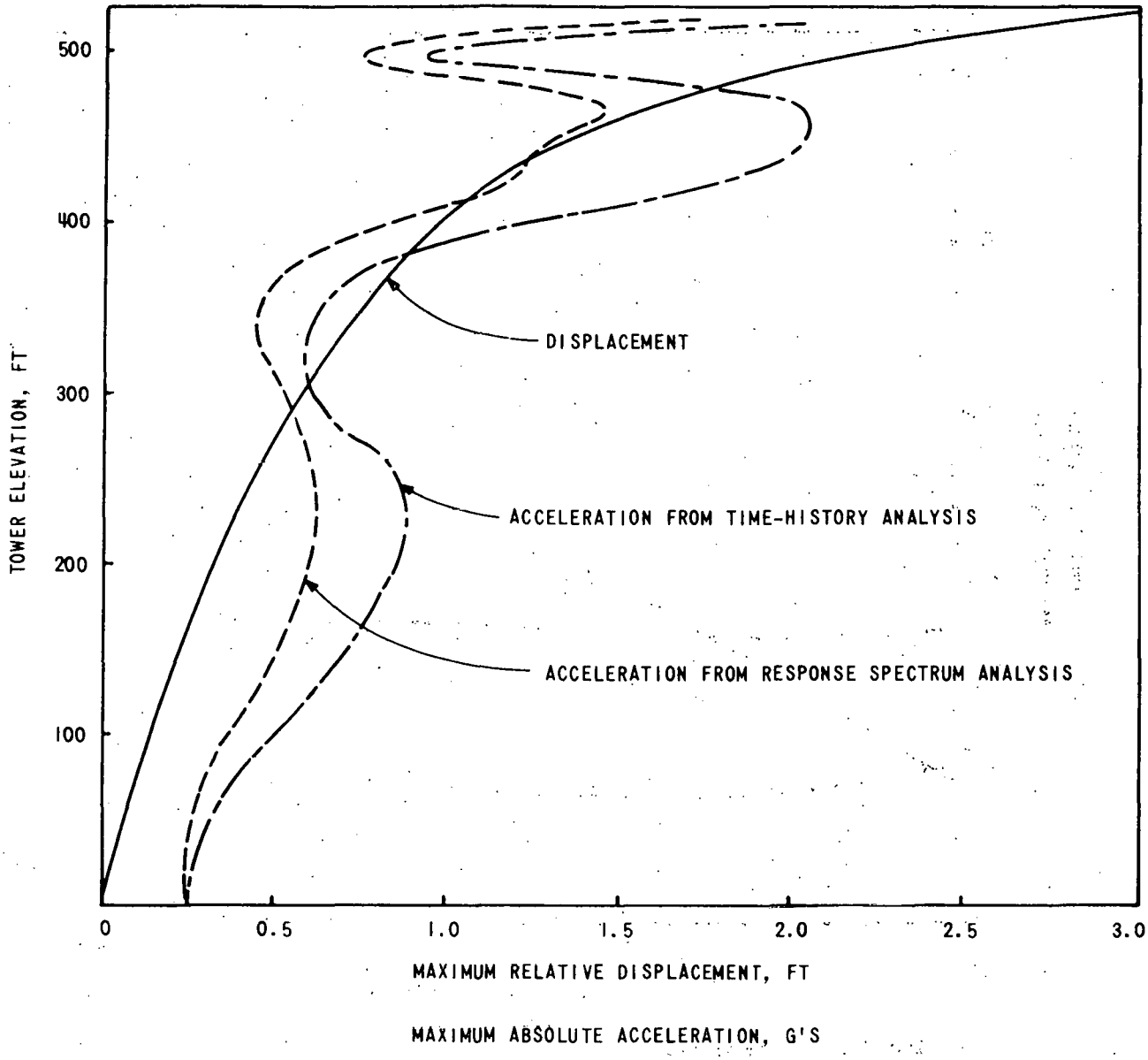

Figure 12. Maximum Accelerations and Displacements in Pilot Plant Tower

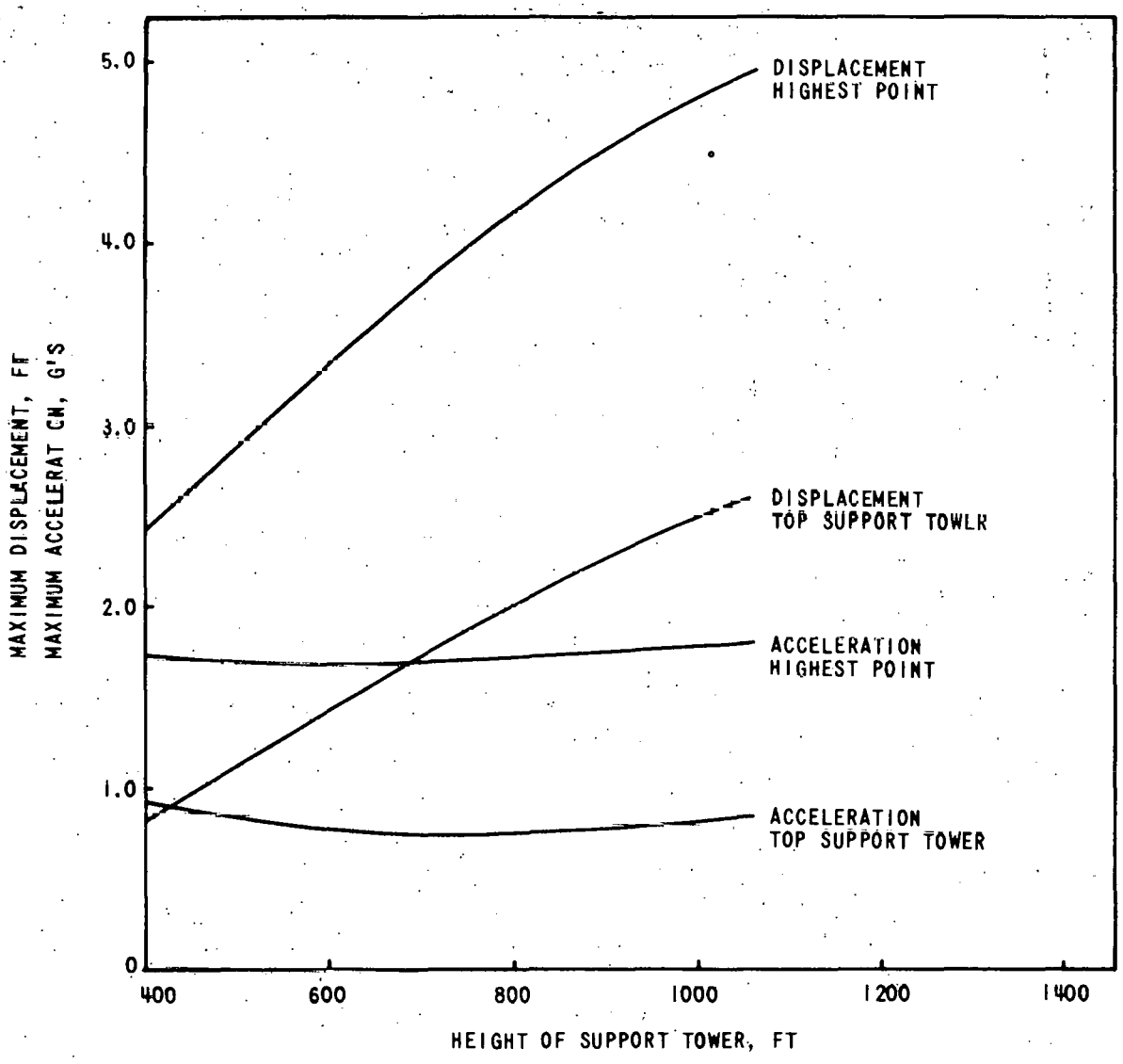

Figure 13. Maximum Accelerations and Displacements as a Function of Support Tower Height

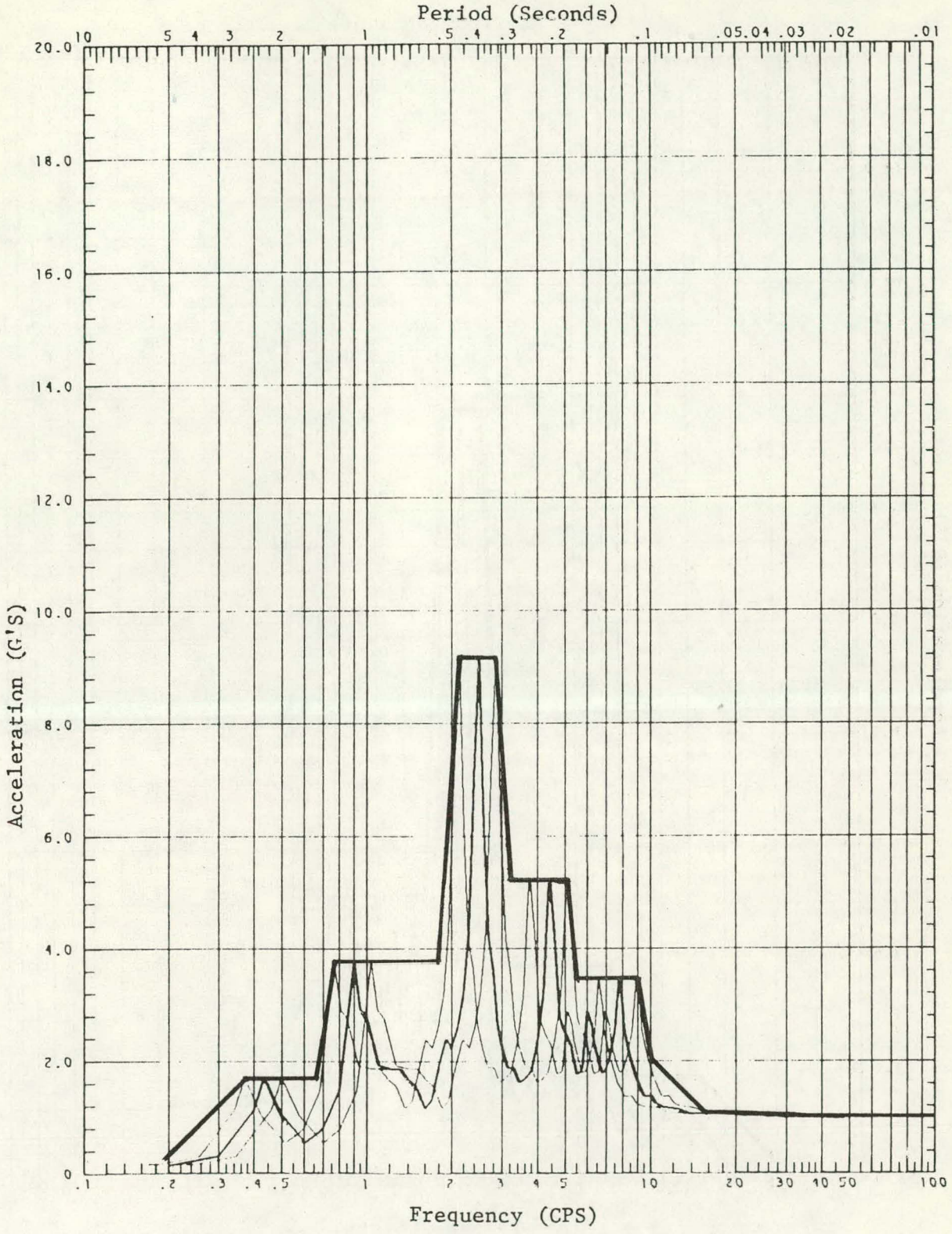

Figure 14. Equipment Response Spectrum at Pilot Plant Elev. 390

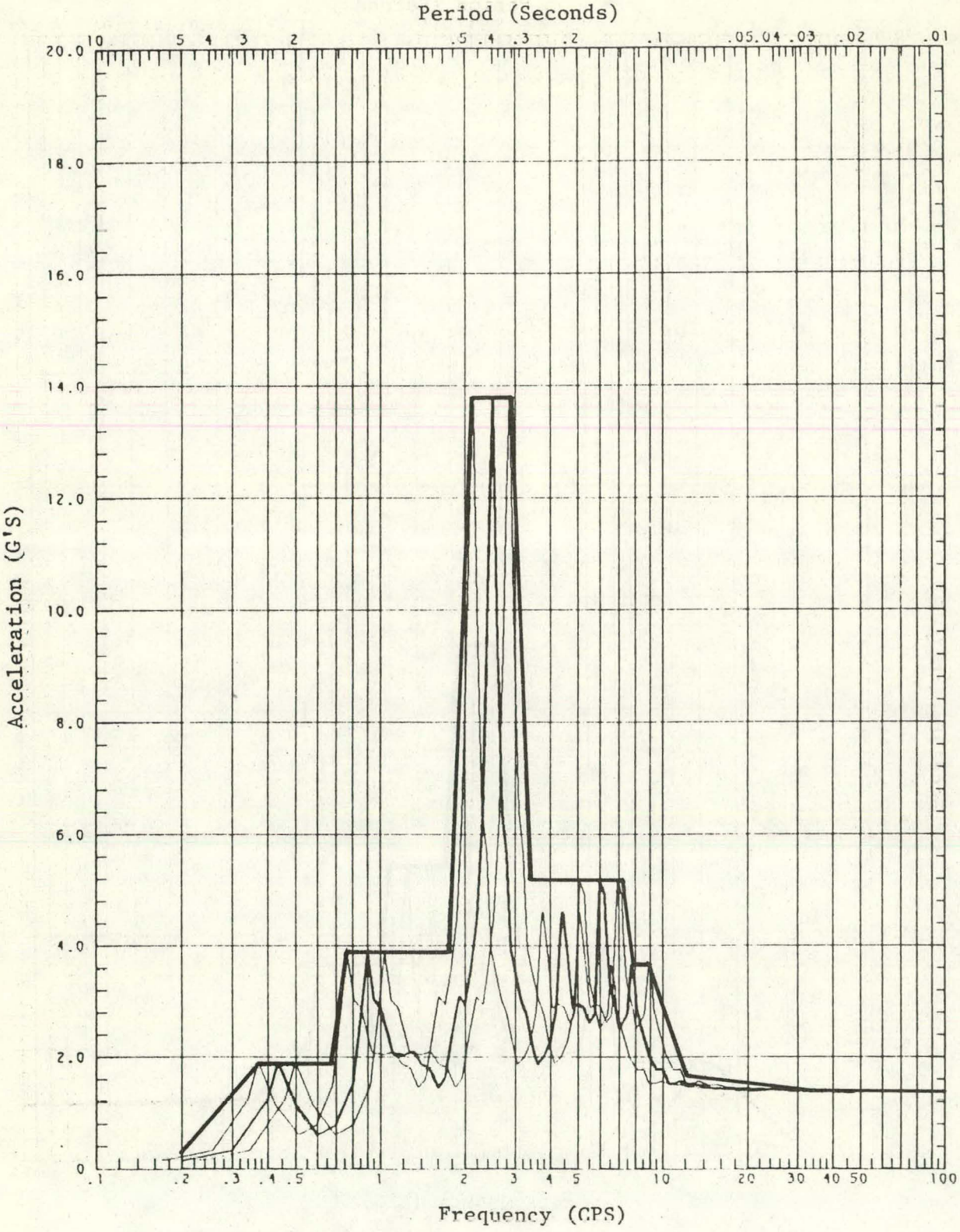

Figure 15. Equipment Response Spectrum at Pilot Plant Elev. 410

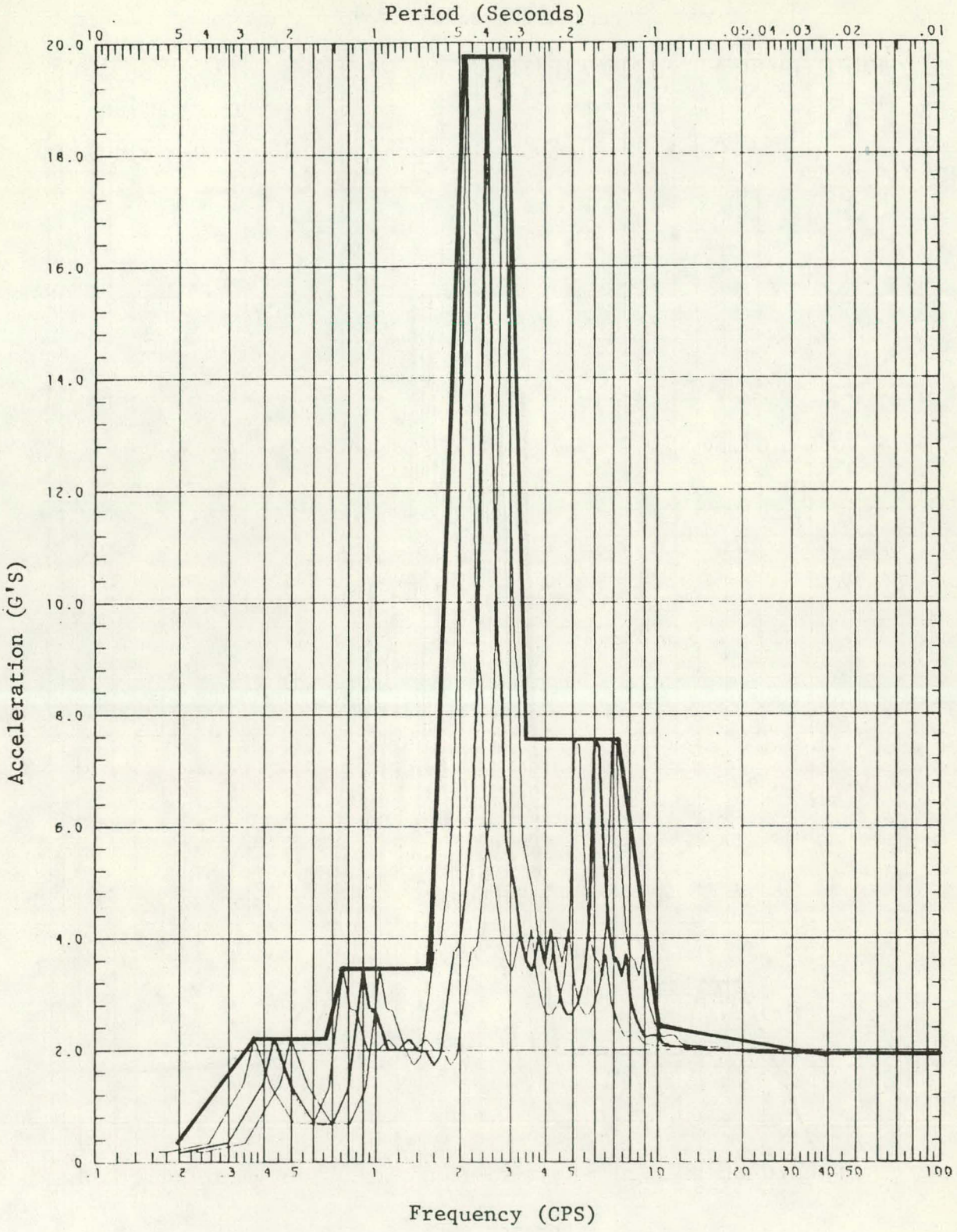

Figure 16. Equipment Response Spectrum at Pilot Plant Elev. 431

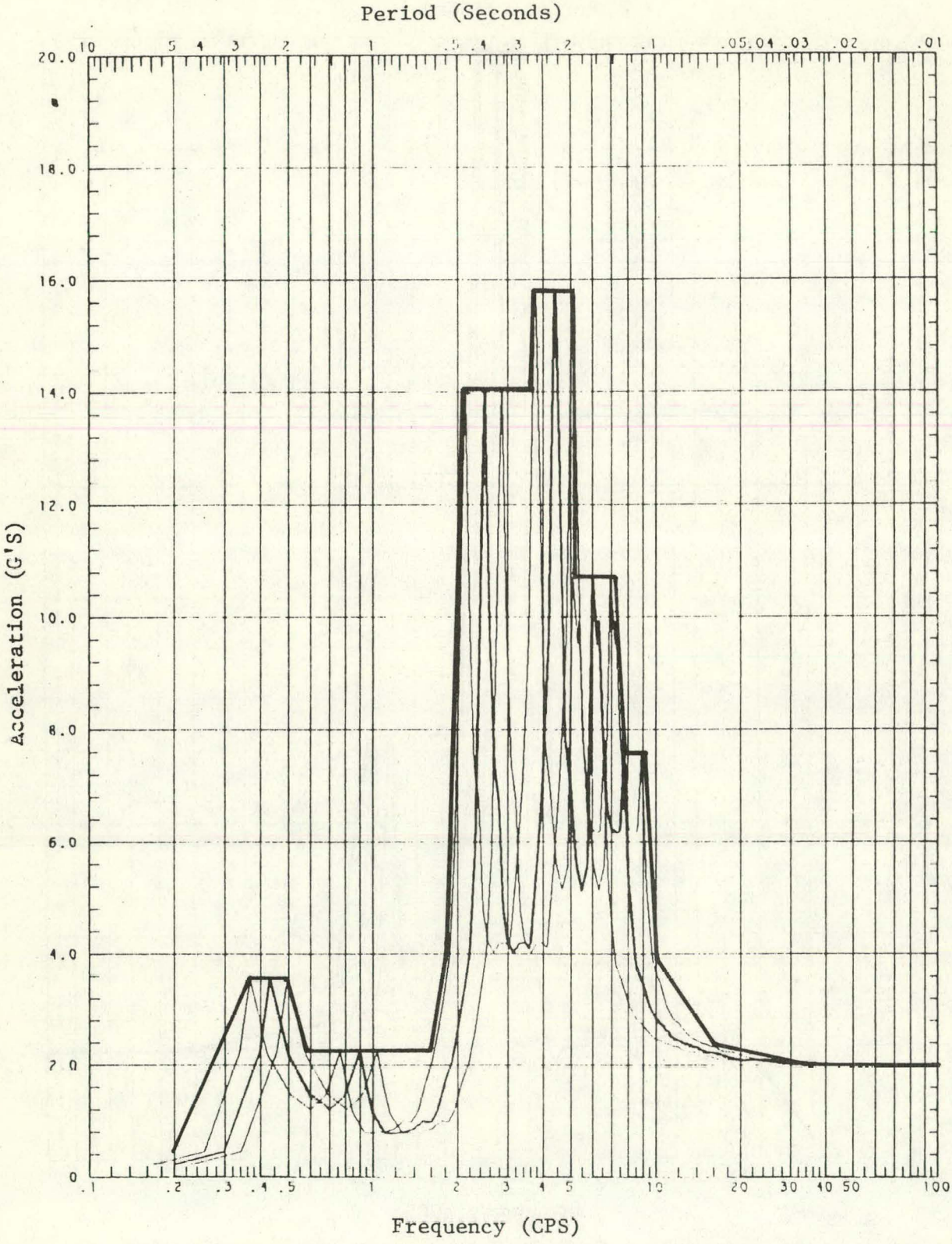

Figure 17. Equipment Response Spectrum at Pilot Plant Elev. 475

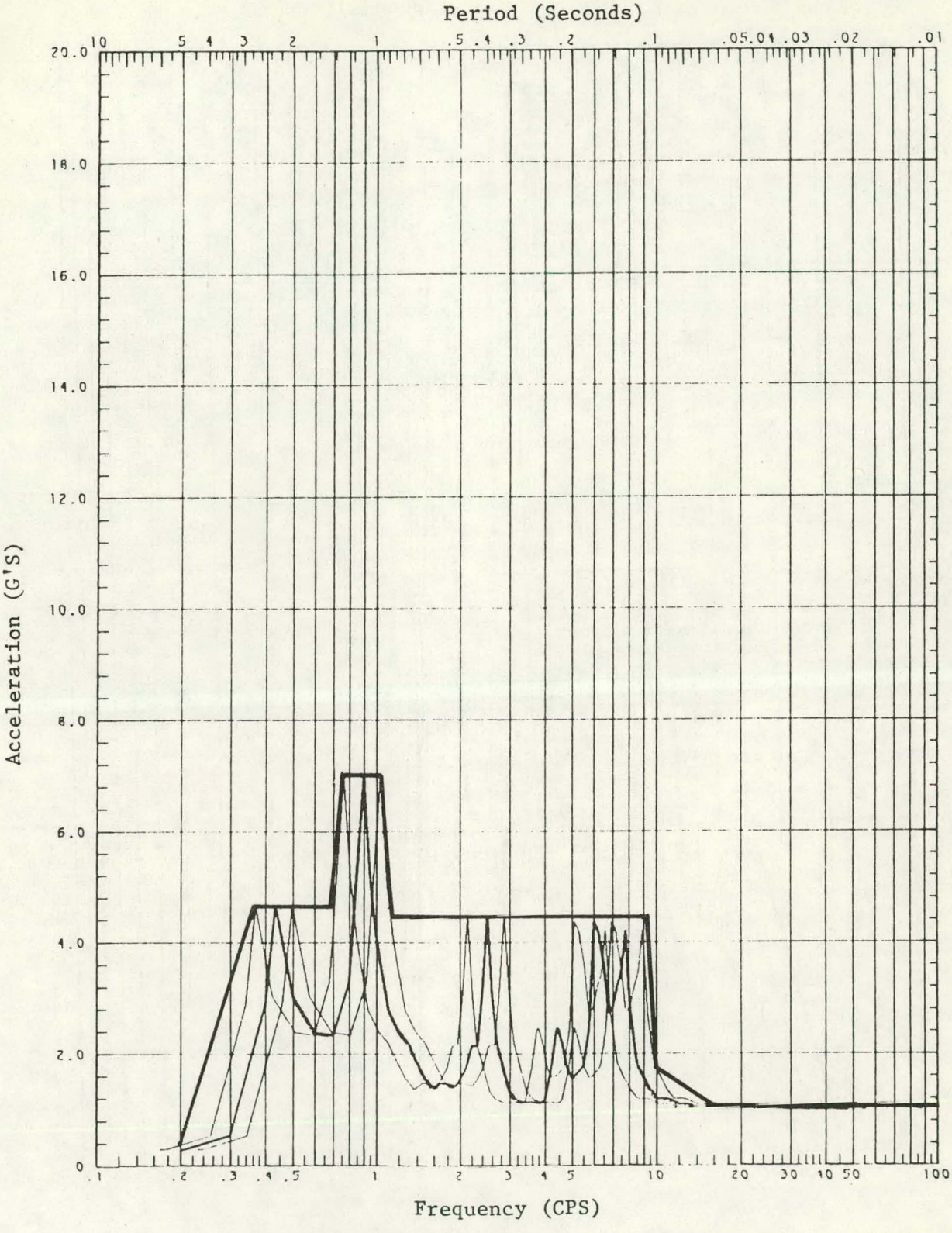

Figure 18. Equipment Response Spectrum at Pilot Plant Elev. 503

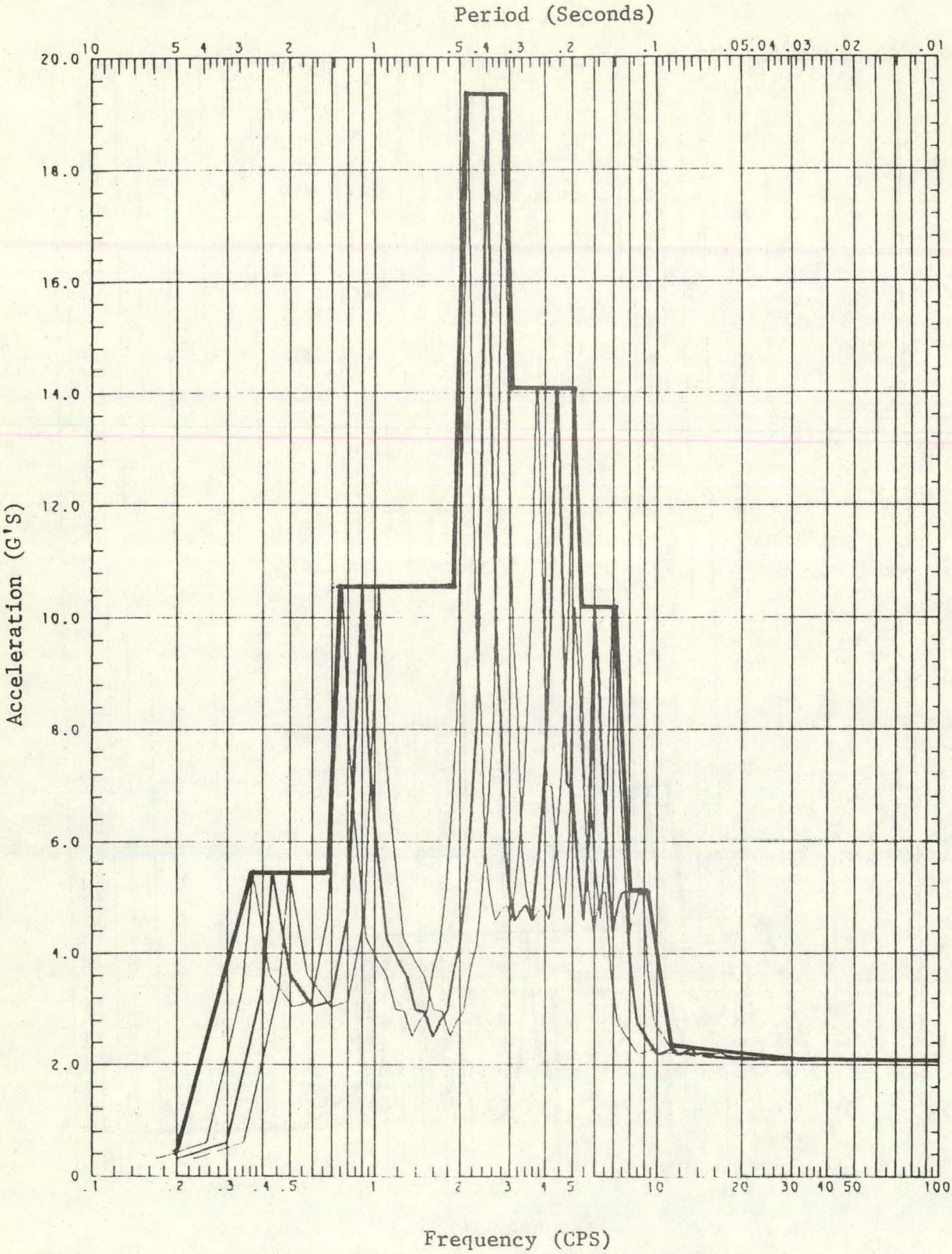

Figure 19. Equipment Response Spectrum at Pilot Plant Elev. 523

APPENDIX F

DRAWINGS S1001 THROUGH S1004

DRAWINGS A1001 THROUGH A1006

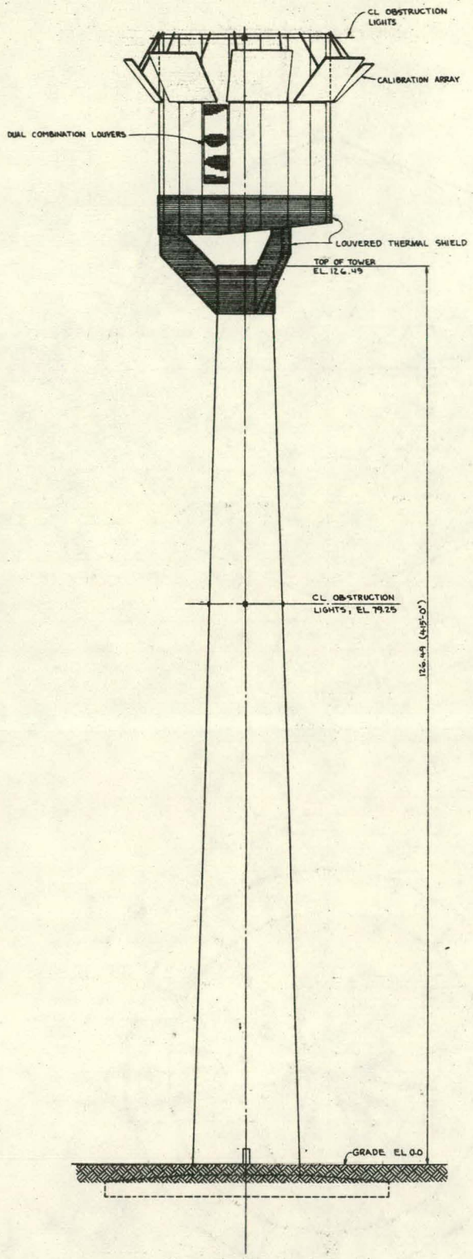

EAST ELEVATION
SCALE = 1:250

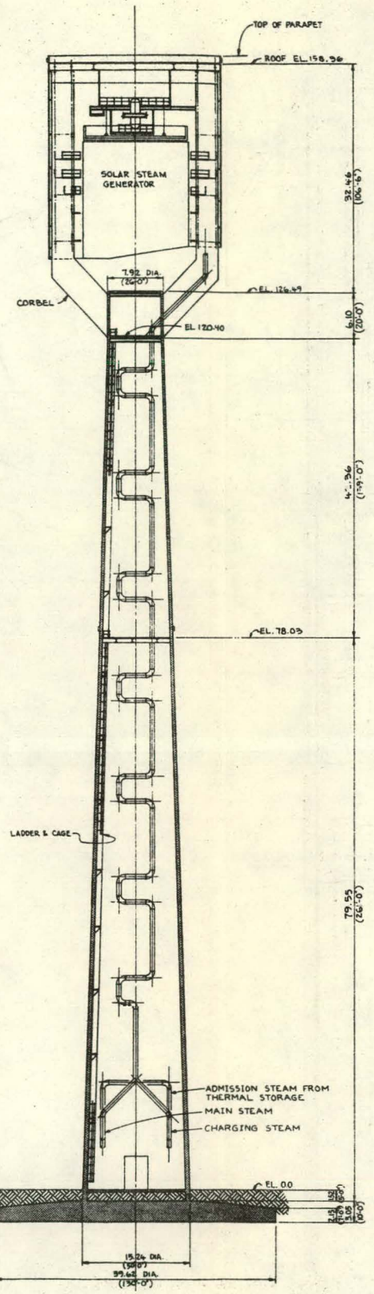

SECTION 1
SCALE = 1:250

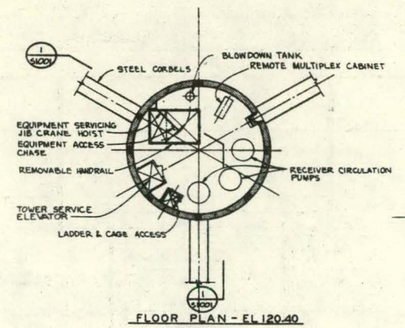

FLOOR PLAN - EL 120.40
SCALE = 1:100

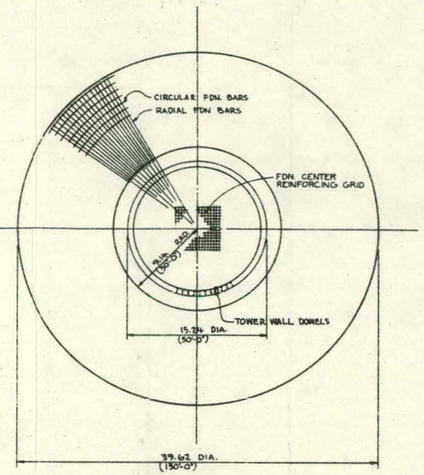

FOUNDATION PLAN
SCALE = 1:200

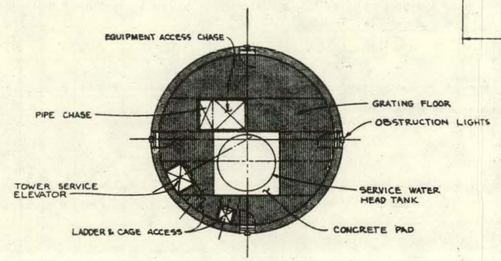

FLOOR PLAN - EL 78.03
SCALE = 1:100

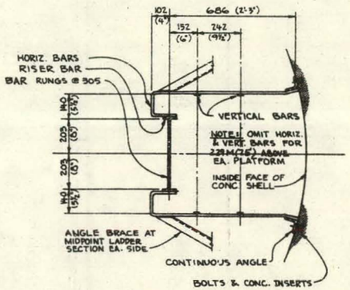

INSIDE LADDER & CAGE DETAIL
SCALE = 1:10 (IN MILLIMETERS)

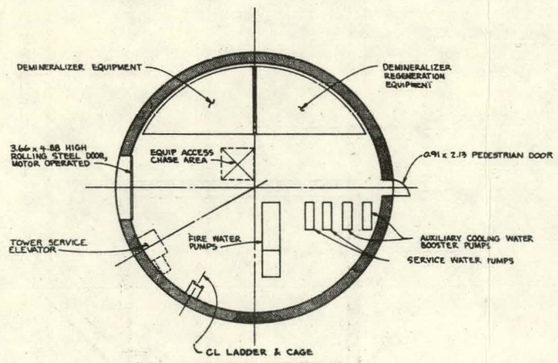

FINISH GROUND FLOOR PLAN - EL 0.0
SCALE = 1:100

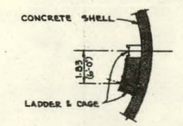

TYPICAL REST PLATFORM
SCALE = 1:100

SCALE IN METERS
SCALE IN MILLIMETERS
SCALE: AS NOTED

NOT TO BE USED FOR CONSTRUCTION

BLACK & VEATCH CONSULTING ENGINEERS
PROJECT 7021

ENERGY RESEARCH AND DEVELOPMENT ADMINISTRATION
10 MWe SOLAR PILOT PLANT
RECEIVER TOWER AND FOUNDATION

S1001

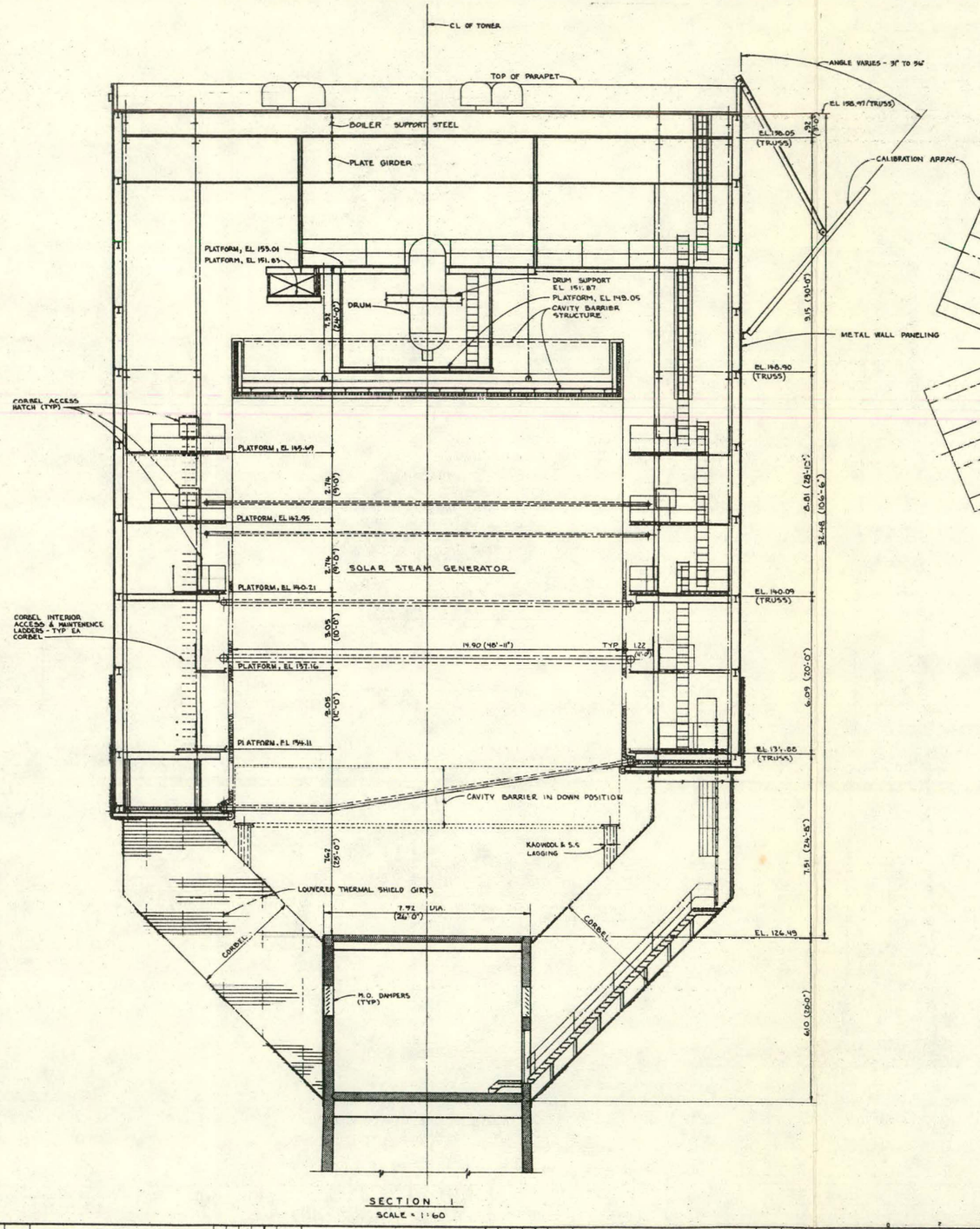

SECTION 1
SCALE = 1:60

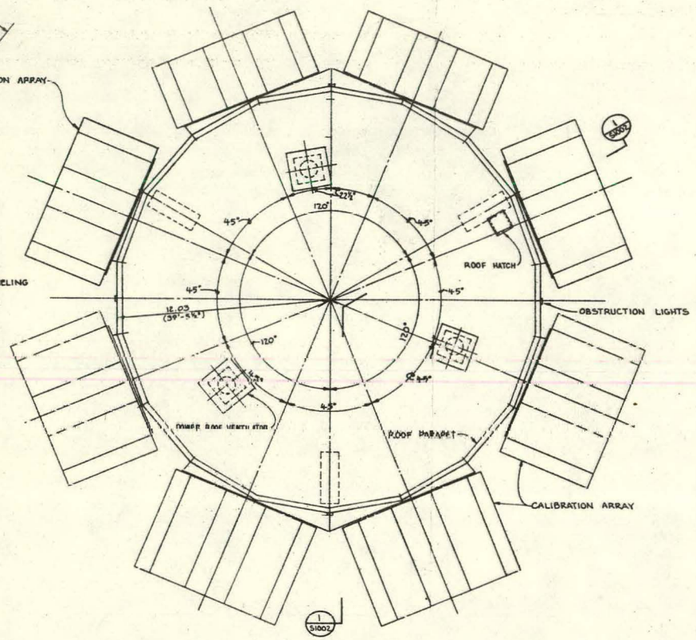

ROOF PLAN
SCALE = 1:100

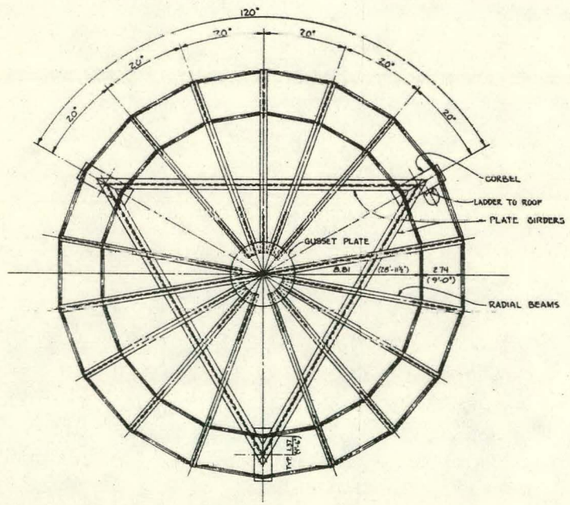

ROOF FRAMING AND BOILER SUPPORT STEEL PLAN-EL 158.97
SCALE = 1:100

NO	DATE	REVISIONS	DRWN	CK	AGC	APP

1:60 SCALE IN METERS
1:100 SCALE IN METERS
SCALE: AS NOTED

NOT TO BE USED FOR CONSTRUCTION
DATE OF ISSUE

BLACK & VEATCH CONSULTING ENGINEERS
PROJECT 7021

ENERGY RESEARCH AND DEVELOPMENT ADMINISTRATION
10 MWe SOLAR PILOT PLANT
RECEIVER HOUSING

SDV DWG NO. S1002 REV.

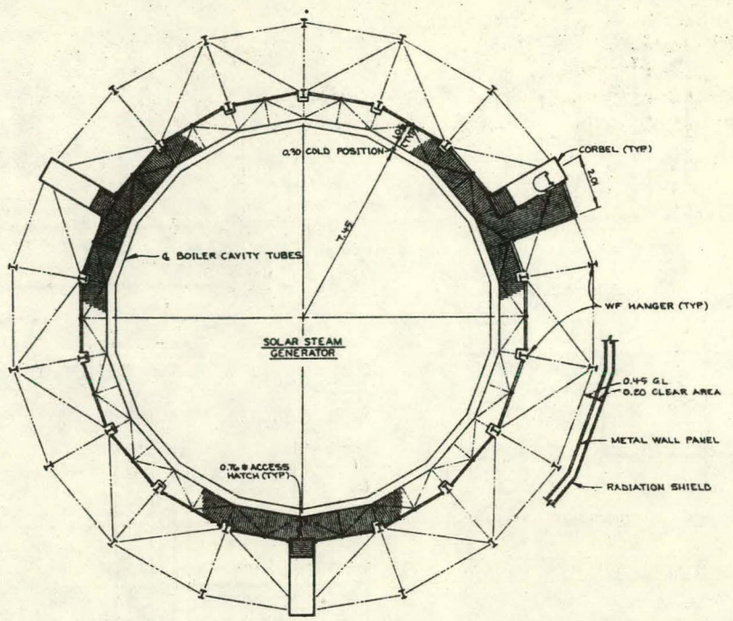

ACCESS PLATFORM EL. 134.11 & EL. 137.16 (SIMILAR)

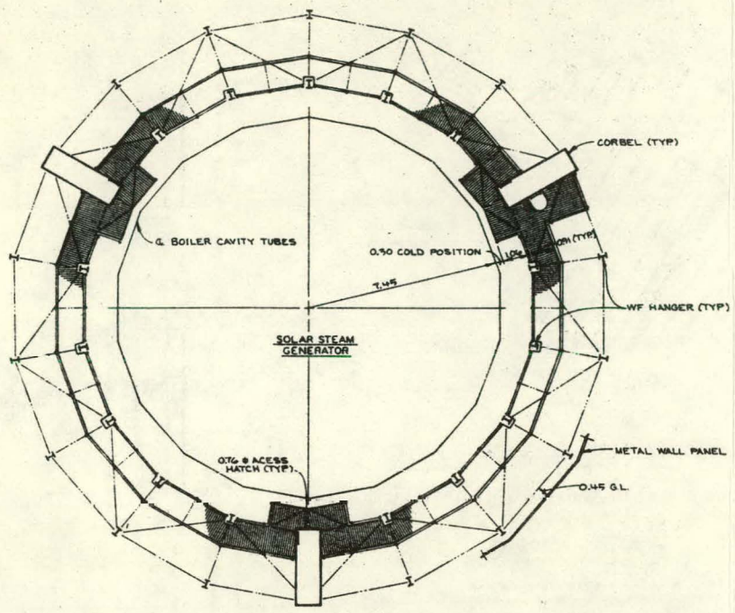

ACCESS PLATFORM EL. 140.21

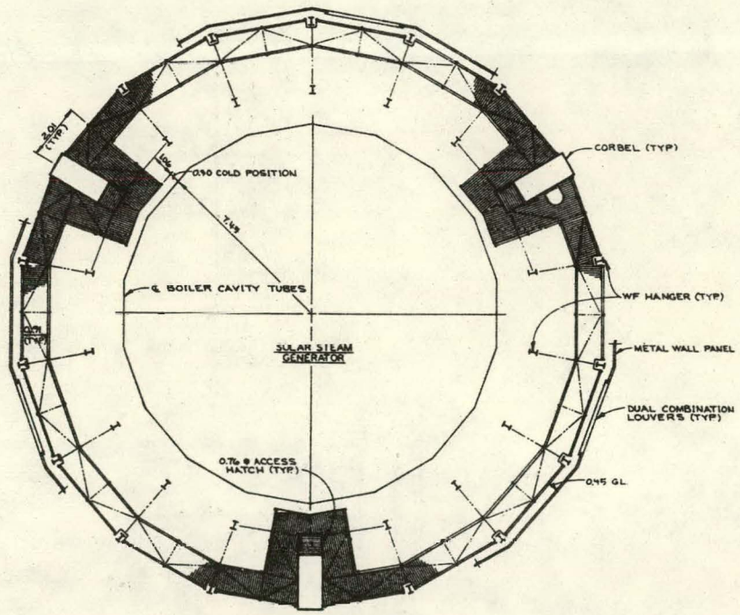

ACCESS PLATFORM EL. 142.95 & EL. 145.69 (SIMILAR)

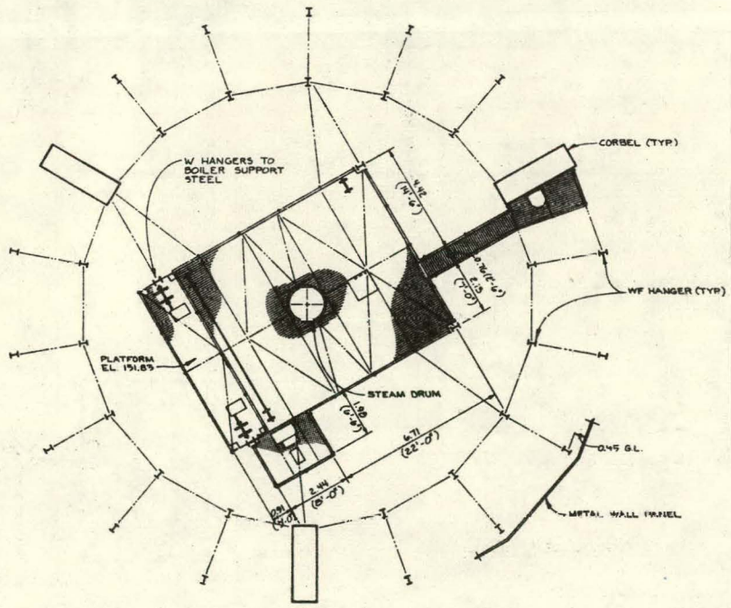

ACCESS PLATFORM EL. 153.05

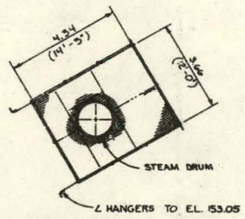

ACCESS PLATFORM EL. 149.08

NOT TO BE USED FOR CONSTRUCTION

SCALE: IN METERS

BLACK & VEATCH CONSULTING ENGINEERS

PROJECT 7021

ENERGY RESEARCH AND DEVELOPMENT ADMINISTRATION
10 MWe SOLAR PILOT PLANT

ACCESS PLATFORMS

S1003

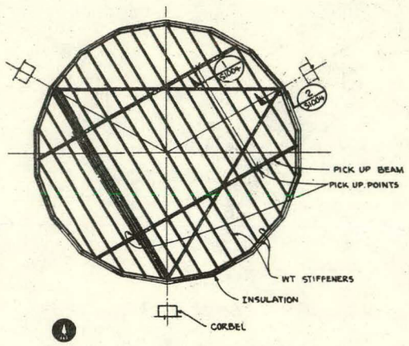

PLAN-CAVITY BARRIER STRUCTURE
SCALE = 1:100

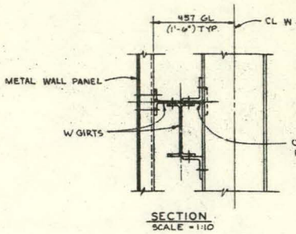

SECTION
SCALE = 1:10

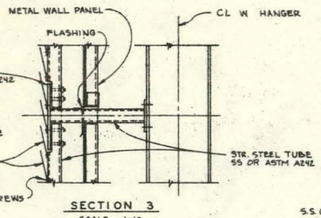

SECTION 3
SCALE = 1:10

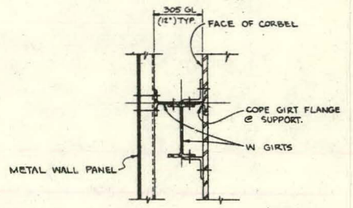

SECTION
SCALE = 1:10

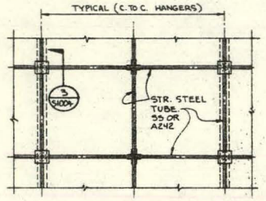

ELEVATION
SCALE = 1:50

TYPICAL GIRT DETAILS AT RECEIVER HOUSING

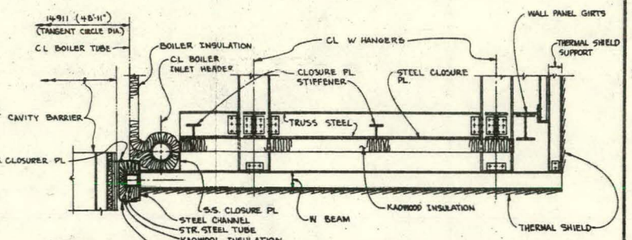

TYPICAL RECEIVER HOUSING BOTTOM CLOSURE DETAIL
SCALE = 1:20

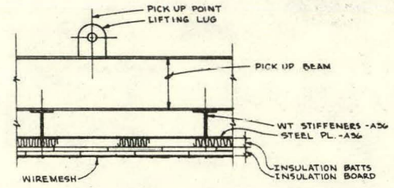

SECTION 1
SCALE = 1:10

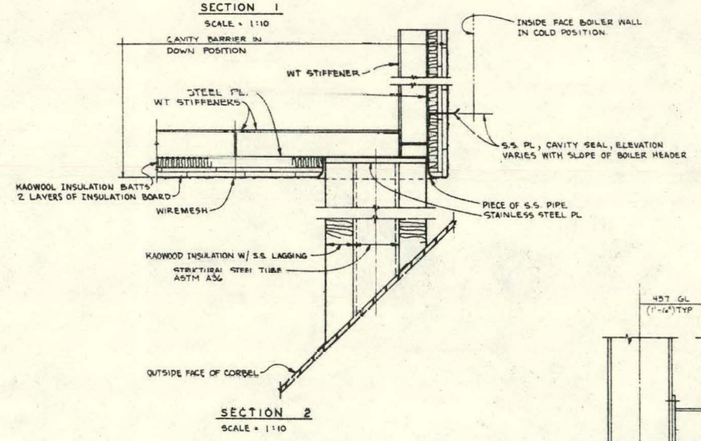

SECTION 2
SCALE = 1:10

CAVITY BARRIER SECTIONS

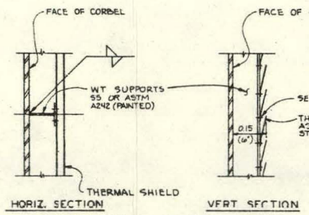

TYPICAL THERMAL SHIELD SUPPORT DETAILS AT CORBELS

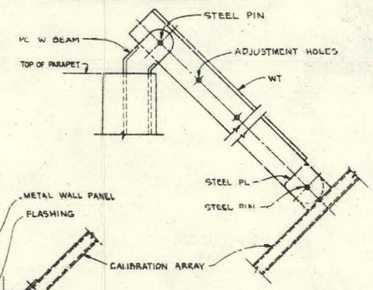

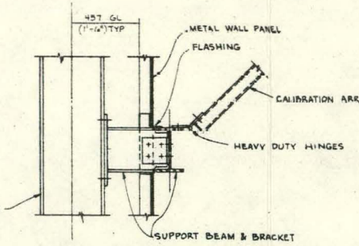

TYPICAL CALIBRATION ARRAY SUPPORT DETAILS
NO SCALE

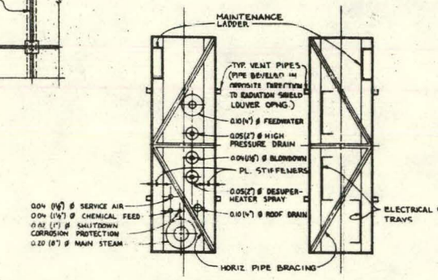

NORTHWEST CORBEL NORTHEAST CORBEL

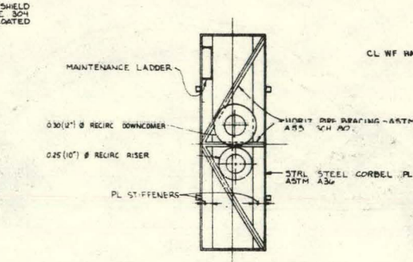

SOUTH CORBEL

TYPICAL SECTIONAL PLANS THRU CORBELS
SCALE = 1:25

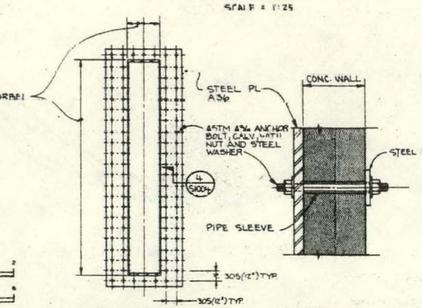

SECTIONAL ELEVATION
SCALE = 1:50

SECTION 4
SCALE = 1:10

TYPICAL CORBEL CONNECTION TO CONC. TOWER

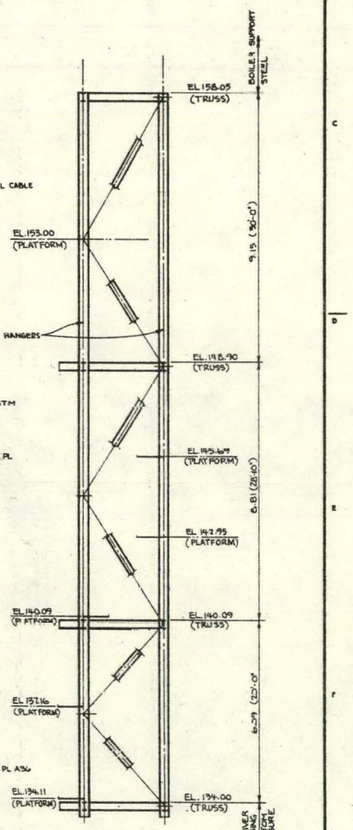

TYPICAL DETAIL OF TRUSS HANGERS
SCALE = 1:60

1:25 SCALE IN METERS 0 1 2
1:100 SCALE IN METERS 0 2 4 6
1:60 SCALE IN METERS 0 2 4
1:50 SCALE IN METERS 0 1000 2000 3000 4000
SCALE IN MILLIMETERS 0 500 1000 1500
1:20 SCALE IN MILLIMETERS 0 200 400 600 800
1:10

SCALE: AS NOTED

NO. DATE REVISIONS DWN. CK. ACC. APP.

NOT TO BE USED FOR CONSTRUCTION
DATE OF ISSUE

BLACK & VEATCH CONSULTING ENGINEERS
PROJECT 7021

ENERGY RESEARCH AND DEVELOPMENT ADMINISTRATION
10 MWe SOLAR PILOT PLANT
RECEIVER TOWER
SECTIONS AND DETAILS

B&V DWG NO. S1004 REV.

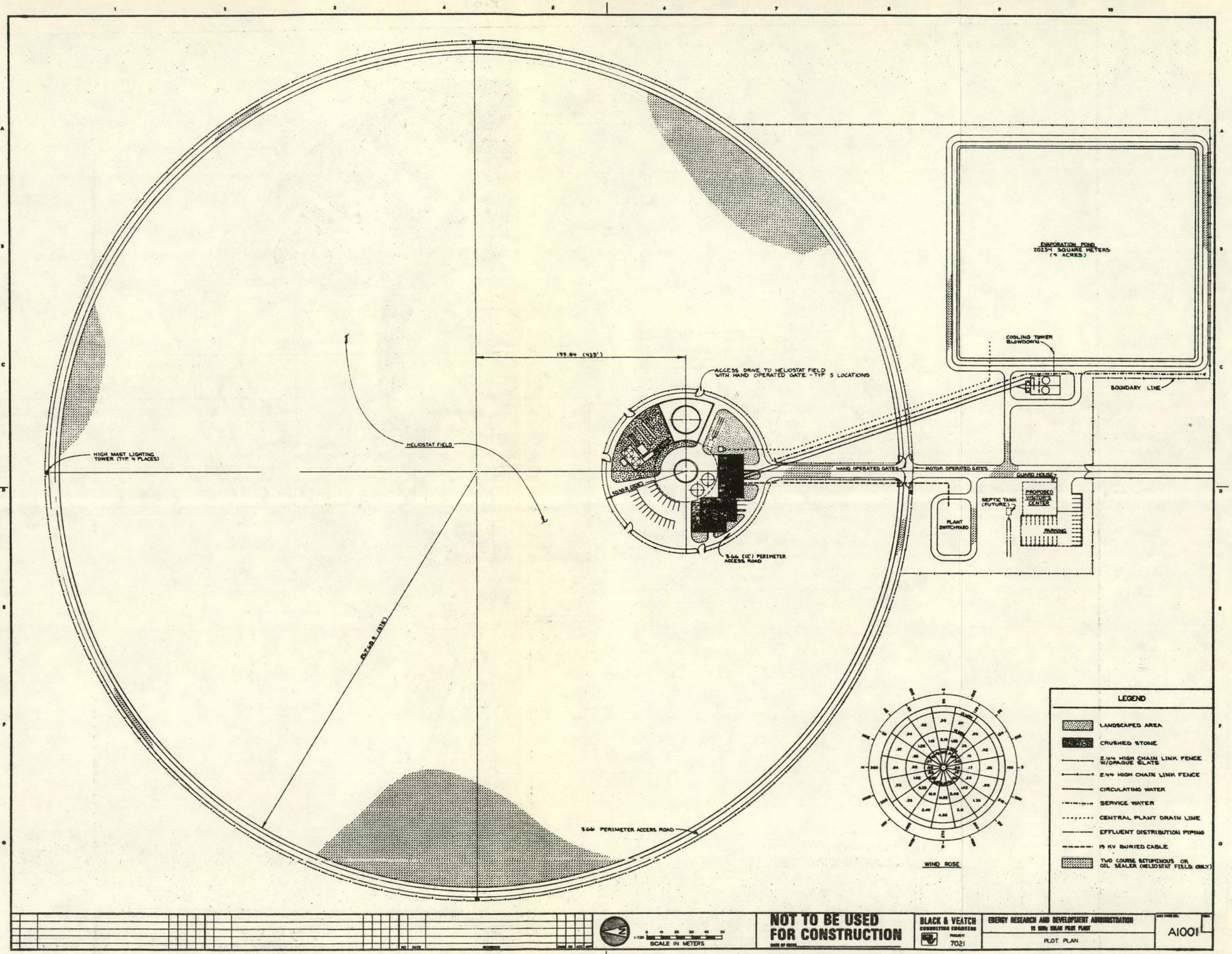
EVAPORATION POND
20254 SQUARE METERS
(5 ACRES)
COOLING TOWER BLOWDOWN
BOUNDARY LINE
199.84 (439')
ACCESS DRIVE TO HELIOSTAT FIELD WITH HAND OPERATED GATE - TYP 5 LOCATIONS
HELIOSTAT FIELD
HIGH MAST LIGHTING TOWER (TYP. 4 PLACES)
HAND OPERATED GATES
MOTOR OPERATED GATES
GUARD HOUSE
SEPTIC TANK (FUTURE)
PROPOSED VISITOR'S CENTER
PARKING
PLANT SWITCHYARD
9.66 (32') PERIMETER ACCESS ROAD
9.66 PERIMETER ACCESS ROAD
WIND ROSE
LEGEND
LANDSCAPED AREA
CRUSHED STONE
2.44 HIGH CHAIN LINK FENCE W/OPAQUE SLATE
2.44 HIGH CHAIN LINK FENCE
CIRCULATING WATER
SERVICE WATER
CENTRAL PLANT DRAIN LINE
EFFLUENT DISTRIBUTION PIPING
15 KV BURIED CABLE
TWO COURSE BITUMINOUS OR OIL SEALER (HELIOSTAT FIELD ONLY)
SCALE IN METERS
NOT TO BE USED FOR CONSTRUCTION
BLACK & VEATCH CONSULTING ENGINEERS
PROJECT 7021
ENERGY RESEARCH AND DEVELOPMENT ADMINISTRATION
10 MWe SOLAR PILOT PLANT
PLOT PLAN
A1001

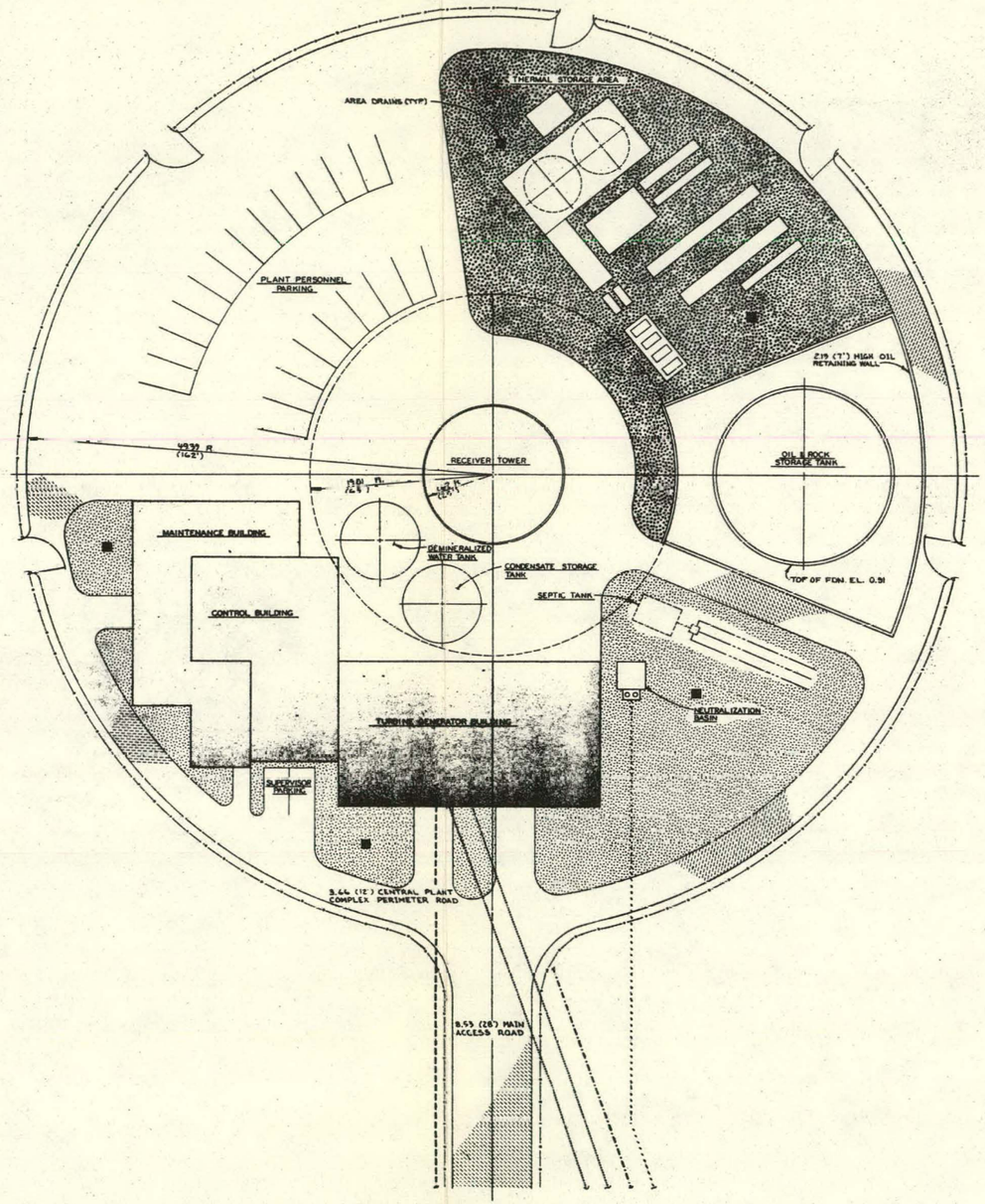

SCALE IN METERS

NOT TO BE USED FOR CONSTRUCTION

BLACK & VEATCH CONSULTING ENGINEERS

PROJECT 7021

ENERGY RESEARCH AND DEVELOPMENT ADMINISTRATION
10 MWe SOLAR PILOT PLANT
SITE ARRANGEMENT

DWG NO. A1002 REV.

RECEIVER SUPPORT TOWER

FILTER A.H.U.

FILTER A.H.U.

MAINTENANCE & MACHINE SHOP

BATTERY ROOM

CHEMICAL STORAGE AREA

CHEM. FEED EQUIP.

RELAY CABINET

INVERTERS

RELAY ROOM

CHEMICAL WORK BENCH

CONDENSATE POLISHER EQUIP.

UP

WATER QUALITY PANEL

WOMENS RESTROOM

TOOL ROOM

ELEC SHOP

SECONDARY UNIT SUBSTATION

CONDENSATE PUMPS

CONDENSER

FEEDWATER HEATERS

FEEDWATER BOOSTER PUMPS

AUXILIARY FEEDWATER PUMP

MAIN FEEDWATER PUMPS

PIPE CHASE

AUXILIARY COOLING WATER PUMPS

AUXILIARY COOLING WATER HEAT EXCHANGERS

AIR DRYERS

AIR COMPRESSORS

MEN'S LOCKERS, SHOWER & REST ROOM

MOTOR CONTROL CENTER PT & SURGE CUBICLE

GENERATOR BREAKER

4160 V SWITCHGEAR & AUXILIARY TRANSFORMER

NEUTRAL GROUNDING ENCLOSURE

MISC. DRAINS RECIEVER

EHC CABINET

ACCESS

OFFICE

RECEPTION

EXCITATION SWGR

CONDENSER EXHAUSTERS

TURBINE LUBE OIL RESERVOIR AND DRAIN TANK

TURBINE LUBE OIL COOLERS

CONDENSER TUBE REMOVAL AREA

LUNCH ROOM

KITCHEN

STORAGE AREA

CONFERENCE ROOM

PARTIAL PLAN AT EL. 3.05

NOT TO BE USED FOR CONSTRUCTION

DATE OF ISSUE

BLACK & VEATCH CONSULTING ENGINEERS

PROJECT 7021

ENERGY RESEARCH AND DEVELOPMENT ADMINISTRATION

10 MWe SOLAR PILOT PLANT

PLANT ARRANGEMENT

GROUND FLOOR EL. 0.0

DRW DWG NO. A1003

REV.

SCALE IN METERS

SCALE: 1/8" = 1'-0"

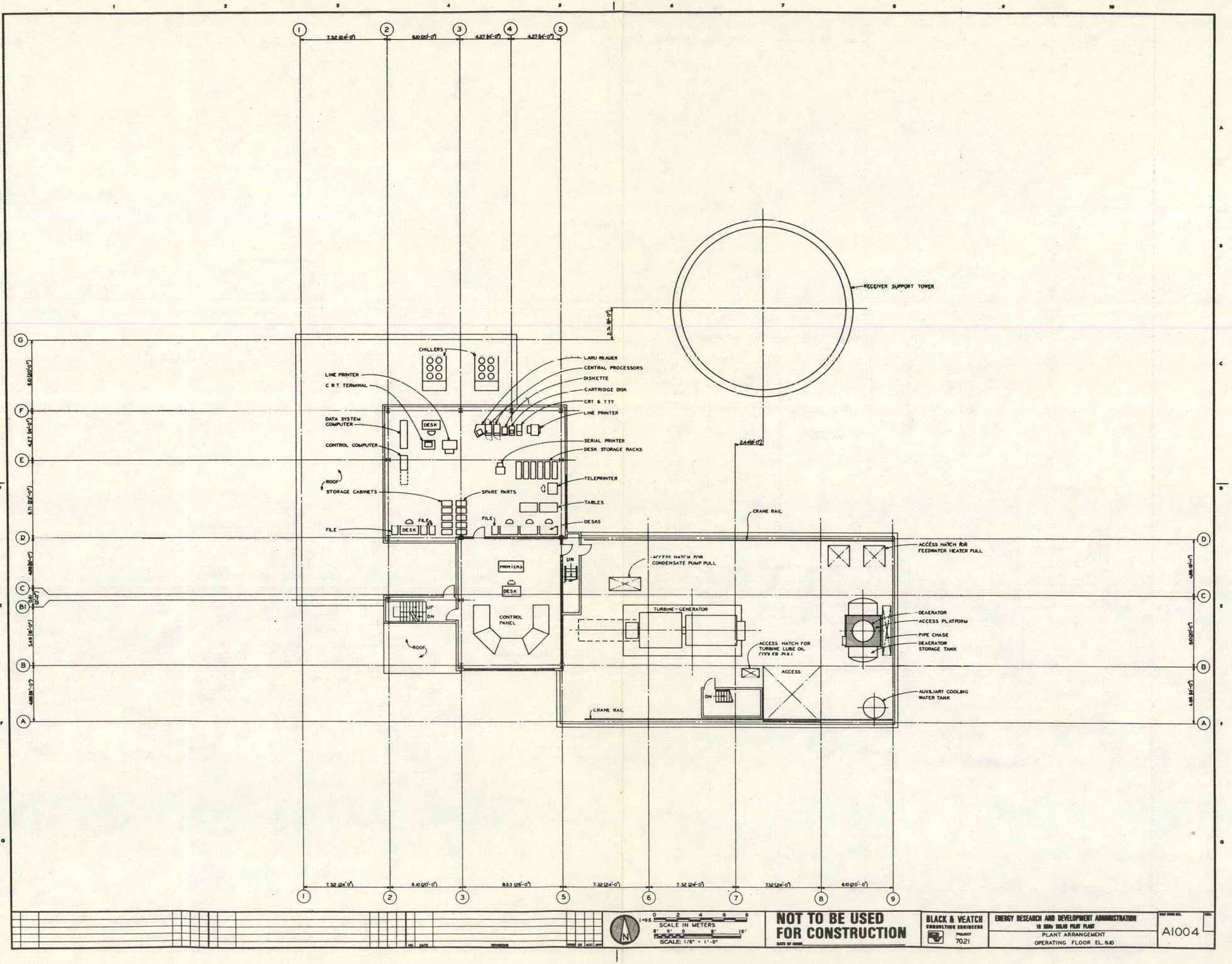
RECEIVER SUPPORT TOWER
CHILLERS
LAMU REALIER
CENTRAL PROCESSORS
DISKETTE
CARTRIDGE DISK
CRT & TTY
LINE PRINTER
LINE PRINTER
C R T TERMINAL
DATA SYSTEM COMPUTER
DESK
CONTROL COMPUTER
SERIAL PRINTER
DESK STORAGE RACKS
TELEPRINTER
ROOF
STORAGE CABINETS
SPARE PARTS
TABLES
DESKS
FILE
FILE
DESK
FILE
DESK
PRINTERS
DESK
UP
DN
CONTROL PANEL
ROOF
UP
CRANE RAIL
ACCESS HATCH FOR FEEDWATER HEATER PULL
ACCESS HATCH FOR CONDENSATE PUMP PULL
TURBINE-GENERATOR
DEAERATOR
ACCESS PLATFORM
PIPE CHASE
DEAERATOR STORAGE TANK
ACCESS HATCH FOR TURBINE LUBE OIL COOLER PULL
ACCESS
DN
AUXILIARY COOLING WATER TANK
CRANE RAIL
7.32 (24'-0")
6.10 (20'-0")
8.53 (28'-0")
7.32 (24'-0")
7.32 (24'-0")
7.32 (24'-0")
6.10 (20'-0")
SCALE IN METERS
SCALE: 1/8" = 1'-0"
NOT TO BE USED FOR CONSTRUCTION
BLACK & VEATCH CONSULTING ENGINEERS
PROJECT 7021
ENERGY RESEARCH AND DEVELOPMENT ADMINISTRATION
10 MWe SOLAR PILOT PLANT
PLANT ARRANGEMENT
OPERATING FLOOR EL. 6.10
A1004

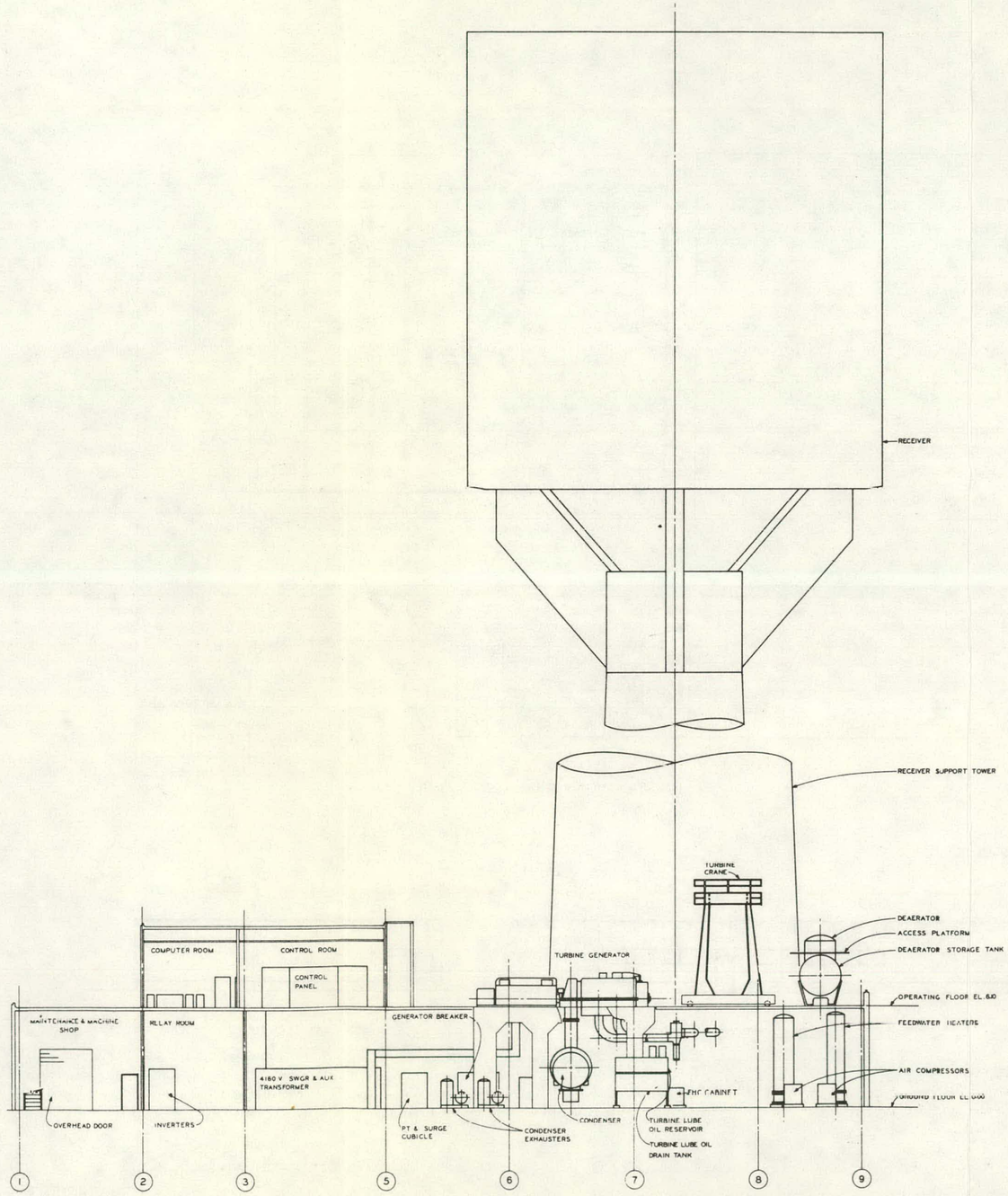

1"=96'

SCALE IN METERS

SCALE: 1/8" = 1'-0"

NOT TO BE USED FOR CONSTRUCTION

DATE OF ISSUE

BLACK & VEATCH
CONSULTING ENGINEERS
PROJECT 7021

ENERGY RESEARCH AND DEVELOPMENT ADMINISTRATION
10 MWe SOLAR PILOT PLANT
PLANT ARRANGEMENT
SECTIONAL ELEVATION

DRAWING NO. A1005

REV.

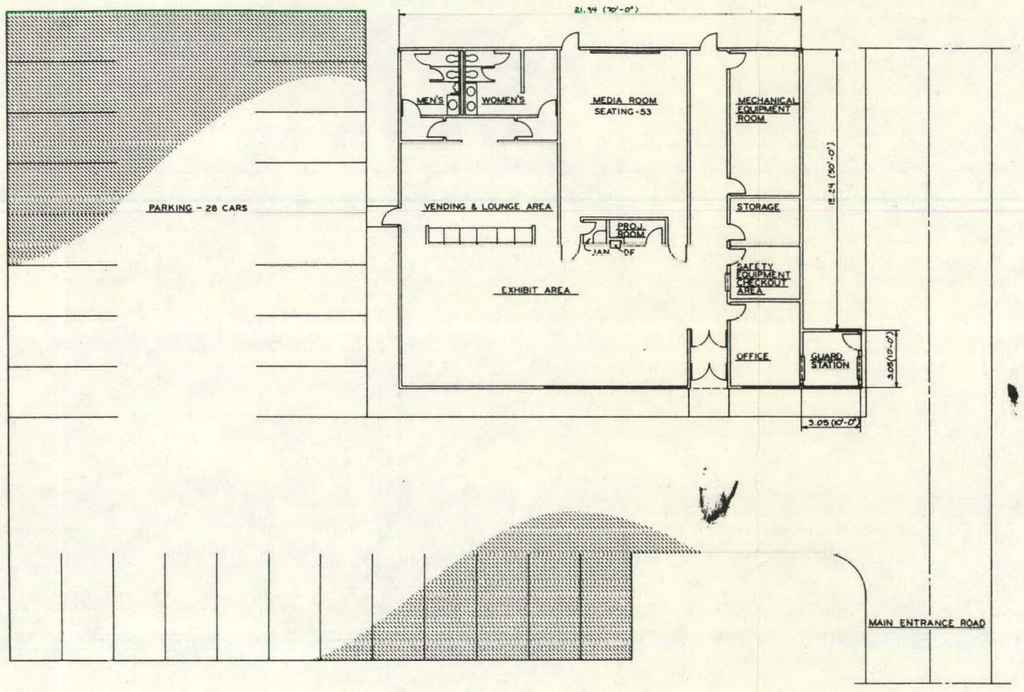

VISITOR'S CENTER & GUARD STATION - PLAN

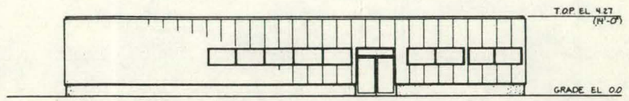

SOUTH ELEVATION

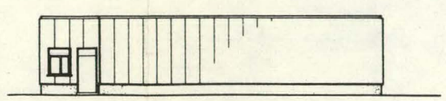

EAST ELEVATION

1:96 SCALE: SCALE IN METERS

NOT TO BE USED FOR CONSTRUCTION

BLACK & VEATCH CONSULTING ENGINEERS PROJECT 7021

ENERGY RESEARCH AND DEVELOPMENT ADMINISTRATION
10 MWe SOLAR PILOT PLANT
PROPOSED VISITOR'S CENTER
PLAN & ELEVATIONS

A1006

APPENDIX G
GLOSSARY

Symbol	Description	Units
E	Modulus of elasticity	MPa (ksi)
h	Height from the bottom of the steam generator cavity	m (ft)
H	Total steam generator cavity height	m (ft)
h_{ATT}	Enthalpy of the spray flow entering the attemperator $h_{ATT} = f(P_{ATT}, T_{ATT})$	kJ/kg (Btu/lbm)
h_{FW}	Enthalpy of feedwater entering the drum $h_{FW} = f(P_{FW}, T_{FW})$	kJ/kg (Btu/lbm)
h_g	Enthalpy of saturated steam exiting the $h_g = f(P_D)$	kJ/kg (Btu/lbm)
h_{S1O}	Enthalpy of superheated steam at the primary (first stage) superheater outlet	kJ/kg (Btu/lbm)
h_{S2I}	Enthalpy of superheated steam at the attemperator exit entering the secondary (second stage) superheater	kJ/kg (Btu/lbm)
h_{S2O}	Enthalpy of superheated steam at the secondary superheater outlet	kJ/kg (Btu/lbm)
I_{XX}	Moment of inertia	mm^4 (in^4)
IR	Infrared	
M	Thermal moment	mm-N (in-lbf)
n	Number of superheater tubes	
r_o	Outside tube radius	mm (in)
P_{ATT}	Pressure of the spray water to the attemperator	MPa (psia)
P_{FW}	Pressure of the feedwater to the drum	MPa (psia)
P_{S1O}	Pressure of the primary superheater outlet	MPa (psia)
P_{S2I}	Pressure at the secondary superheater inlet	MPa (psia)
P_{S2O}	Pressure at the secondary superheater outlet	MPa (psia)
ΔP	Pressure drop	kPa (psi)
Q_B	Absorbed heat input into the boiler section	MW (Btu/hr)

Symbol	Description	Units
Q_{S1}	Absorbed heat input into the primary superheater section	MW (Btu/hr)
Q_{S2}	Absorbed heat input into the secondary superheater section	MW (Btu/hr)
S_a	Allowable amplitude of the alternating stress component	MPa (ksi)
S_M	Design stress intensity	MPa (ksi)
T_{ATT}	Temperature of spray water to the attemperator	°C (°F)
T_{bulk}	Bulk fluid temperature	°C (°F)
T_{FW}	Temperature of feedwater to the drum	°C (°F)
T_m	Mean metal temperature	°C (°F)
T_{OD}	Tube metal temperature at outside diameter	°C (°F)
T_S	Superheater average steam temperature	°C (°F)
T_s	Local steam temperature	°C (°F)
T_{S1O}	Primary superheater outlet temperature	°C (°F)
T_{S2I}	Secondary superheater inlet temperature	°C (°F)
T_{S2O}	Secondary superheater outlet temperature	°C (°F)
T(X)	Temperature as a functionof X	°C (°F)
W_{ATT}	Attemperator spray flow rate	kg/min (lbm/hr)
W_{FW}	Feedwater flow rate	kg/min (lbm/hr)
W_S	Steam flow rate exiting the steam generator	kg/min (lbm/hr)
W_τ	Superheater total tube weight	kg (lbm)
α	Absorptivity	
α	Coefficient of thermal expansion	mm/mm °C (in/in °F)
ϵ	Emissivity	
σ	Thermal stress	MPA (ksi)
σ_ϕ	Tangential (hoop) stress	MPa (ksi)
σ_ℓ	Longitudinal stress	MPa (ksi)
σ_r	Radial stress	MPa (ksi)
σ_x	Stress in x direction (refer to Figure 3-50)	MPa (ksi)

Symbol	Description	Units
ϕ_A	Absorbed heat flux	kw/m^2 ($Btu/hr\ ft^2$)
ϕ_I	Incident heat flux	kw/m^2 ($Btu/hr\ ft^2$)

LIST OF ABBREVIATIONS AND ACRONYMS

ACI	American Concrete Institute
AISC	American Institute of Steel Construction
ANSI	American National Standards Institute
ASME	American Society of Mechanical Engineers
ASTM	American Society for Testing and Materials
AWS	American Welding Society
B&V	Black & Veatch
Bldg	Building
Btu	British thermal units
$Btu/hr-ft^2$	British thermal units per hour per square foot
C	degrees Centigrade
CL	center line
cm	centimeters
cu yd	cubic yards
DF	drinking fountain
DIA.	diameter
EGS or EPGS	Electrical Generation Subsystem
EL.	elevation

LIST OF ABBREVIATIONS AND ACRONYMS (Continued)

EPA	Environmental Protection Agency
ERDA	Energy Research and Development Administration
F	degrees Fahrenheit
FAA	Federal Aviation Administration
FDN	foundation
fpm	feet per minute
ft	feet
ft^2	square feet
g	gravitational acceleration
gal	gallons
GALV	galvanized
GEN	generator
GL	girt line
gpd	gallons per day
gpm	gallons per minute
HP	high pressure
Hz	Hertz
ID	inside diameter
in.	inches
IP	intermediate pressure
kg/s	kilograms per second
kPa	kilopascals
ksf	kips per square foot
ksi	kips per square inch
kV	kilovolts
kW	kilowatts
kWh	kilowatt-hour
kW/m^2	kilowatts per square meter
lb/hr	pounds per hour
m	meters

LIST OF ABBREVIATIONS AND ACRONYMS (Continued)

misc.	miscellaneous
MO	motor operated
MPa	megapascals
mph	miles per hour
MW	megawatts
MWe	megawatts (electric)
NPSH	net positive suction head
NRC	Nuclear Regulatory Commission
OSHA	Occupational Safety and Health Act
P	pressure
PL	plate
psi	pounds per square inch
psia	pounds per square inch absolute
psig	pounds per square inch gage
psf	pounds per square foot
RAD.	radius
SCE	Southern California Edison
SEAOC	Structural Engineers Association of California
SH	superheater
SRE	Subsystem Research Experiment
SS	stainless steel
STR	structural
T	temperature
TOP	top of parapet

LIST OF ABBREVIATIONS AND ACRONYMS (Continued)

TYP	typical
UBC	Uniform Building Code
V	volts
W	wide flange